AI Solutions for Maintenance Decision Support in Railway Infrastructure

Phusakulkajorn, W.

DOI
10.4233/uuid:77765019-ab29-43f2-94fb-42b115a5d186

Publication date
2025

Document Version
Final published version

Citation (APA)
Phusakulkajorn, W. (2025). *AI Solutions for Maintenance Decision Support in Railway Infrastructure*. [Dissertation (TU Delft), Delft University of Technology]. https://doi.org/10.4233/uuid:77765019-ab29-43f2-94fb-42b115a5d186

Important note
To cite this publication, please use the final published version (if applicable).
Please check the document version above.

AI Solutions for Maintenance Decision Support in Railway Infrastructure

AI Solutions for Maintenance Decision Support in Railway Infrastructure

Dissertation

for the purpose of obtaining the degree of doctor
at Delft University of Technology
by the authority of the Rector Magnificus, prof. dr. ir. T.H.J.J. van der Hagen,
chair of the Board for Doctorates
to be defended publicly on
Wednesday 26 March 2025 at 15:00 o'clock

by

Wassamon PHUSAKULKAJORN

Master of Philosophy in Applied Mathematics,
University of Manchester, UK
Born in Songkla, Thailand

This dissertation has been approved by the promotors.

Composition of the doctoral committee:

Rector Magnificus,	Chairperson
Prof. dr. Z. Li	Delft University of Technology, *promotor*
Dr. A.A. Núñez Vicencio	Delft University of Technology, *promotor*
Independent members:	
Prof. dr. ir. R.P.B.J. Dollevoet	Delft University of Technology, the Netherlands
Prof. dr. ir. B.H.K. De Schutter	Delft University of Technology, the Netherlands
Prof. dr. D. Sáez Hueichapan	Universidad de Chile, Chile
Prof. dr. I. Škrjanc	University of Ljubljana, Slovenia
Dr. ir. A. Zoeteman	ProRail

Printed by: Gildeprint

Cover by: Cover art is created using pictures from https://www.freepik.com/.

ISBN 978-94-6384-707-0

An electronic version of this dissertation is available at
https://repository.tudelft.nl/

To Martin, for his love and sacrifices.

CONTENTS

SUMMARY

Artificial intelligence (AI) is a field that has been increasingly and successfully applied to solve practical problems in the railway infrastructure domain for over two decades. AI has been employed to enhance the reliability of railway infrastructure, ensuring smooth railway operations and services. Despite its success, AI solutions for the entire railway system still need to be tailored to local conditions and further optimised with field domain knowledge. This underscores the need for further AI developments to achieve a truly intelligent railway infrastructure.

This dissertation comprises six chapters. Chapter 1 presents an introduction to the research. Chapter 2 comprehensively reviews AI methodologies used in railway infrastructure. The review indicates that some components of the railway infrastructure have limited AI deployment and open challenges. This PhD research addresses three challenges: 1) to improve the detection of early-stage defects in rails and components such as fasteners, 2) to provide insight into massive unlabelled railway data, and 3) to integrate information from multiple monitoring technologies for accurate health assessment. These challenges are addressed in Chapters 3, 4, and 5 through the proposal of new AI solutions.

Chapter 3 addresses the challenge of detecting rail surface defects at early development stages using axle box acceleration (ABA) measurements. Spiking neural networks (SNNs) offer the ability to handle temporal and spatiotemporal patterns through their unique mechanism of processing data as discrete events or spikes. Therefore, a methodology based on SNN is proposed to tackle the challenge. Additionally, the signal transmission in SNNs, occurring as trains of spiking events, resembles the pattern of an ABA signal, where each spike represents an abrupt change in ABA response at squats, further motivating the selection. The proposed method utilises a simple SNN architecture with time-varying weights and no hidden layers. The SNN is trained using a method that combines genetic algorithms, k-fold cross-validation, and multi-start backpropagation to optimise hyperparameters and weights. Demonstrated by real-field measurements from Dutch and Swedish railways, the proposed methodology effectively captures subtle changes in the responses of light squats in ABA signals. It significantly enhances the detection accuracy of light squats from the traditional methods, which are 78-85%, to more than 93% using a simpler network architecture. The success in squat detection is attributed to the use of time-varying weights that allow variations in synaptic weights. Furthermore, the proposed method provides interpretability. The internal behaviours of spike responses, postsynaptic and membrane potentials highlight a correspondence with a high-frequency band between 1000-2000 Hz of the detection problem of squats.

Chapter 4 addresses the challenge when high-frequency vibration signals are obtained in new environments where prior knowledge or reference information

about infrastructure conditions is unavailable or very limited. To tackle the challenge, this chapter proposes an unsupervised representation learning methodology to automatically capture and extract characteristic features of dynamic responses that reflect the conditions of rail infrastructures. This method employs a collaborative optimisation process that synchronises empirical mode decomposition (EMD) with a convolutional autoencoder (CAE). The EMD level is tuned to remove noise while preserving effective vibration responses. The CAE is trained using demodulated signals that are considered normal to generate representations that ensure reconstruction quality and differentiate between normal and abnormal conditions. The effectiveness of this approach is demonstrated using a Gaussian mixture model. Applied to validated ABA data for rail defect detection and train-borne LDV data for rail fastener monitoring, the proposed method outperforms other variants of autoencoder-based models and the wavelet-based CAE in accurately identifying the conditions. It achieves an average improvement of 16% with the ABA data and 21% with the LDV data.

Chapter 5 addresses the limitations of individual monitoring technologies and presents a data fusion framework to predict railway infrastructure health using multiple monitoring technologies. The framework addresses missing data through spatio-temporal interpolation and enhances predictive accuracy with a hybrid neural network. The proposed framework is showcased to enable a more frequent evaluation of transition zone health by integrating multiple monitoring technologies, including track geometry, interferometric synthetic aperture radar (InSAR), and ABA measurements. A spatio-temporal interpolation approach is employed to fill in missing InSAR data. Then, hybrid neural models are evaluated to predict track longitudinal levels, including a hybrid convolutional neural network (CNN) with gated recurrent units (GRU) network and a hybrid CNN with a long short-term memory (LSTM) network. The prediction relies on a fusion of historical and interpolated data from InSAR and the ABA measurements. Subsequently, a novel key performance index (KPI) based on the predicted track longitudinal levels is proposed, facilitating more frequent assessments due to the regularity of InSAR and ABA data. The framework effectively detects track irregularities early, even before the next measurement of track geometry profiles. This offers predictive insights that can guide decisions regarding the timing and locations for essential track maintenance.

These chapters collectively underscore the potential of AI to support decisions in the maintenance of railway infrastructure, ultimately enhancing the maintenance of large-scale railway infrastructure. Chapter 6 concludes the dissertation with recommendations for future research and practice.

SAMENVATTING

Kunstmatige intelligentie of Artificial intelligence (AI) is een vakgebied dat al meer dan twee decennia steeds vaker en succesvoller in het spoor wordt toegepast om praktische problemen op te lossen. Het wordt ingezet voor verbetering van de betrouwbaarheid van de spoorweginfrastructuur, zodat onderhoud en dienstregelingen soepel verlopen. Ondanks dit succes moeten AI-oplossingen voor het gehele spoorwegsysteem nog steeds worden afgestemd op de lokale omstandigheden en verder worden geoptimaliseerd met technische domeinkennis uit het veld. Dit onderstreept de noodzaak van verdere ontwikkelingen op het gebied van AI in het spoor om een echt intelligente railinfrastructuur te bereiken.

Dit proefschrift bestaat uit zes hoofdstukken. Hoofdstuk 1 geeft een inleiding op het onderzoek. Hoofdstuk 2 beschrijft een diepgaande review van AI-methodologieën die reeds worden gebruikt in de spoorweginfrastructuur. Uit deze review blijkt dat voor bepaalde onderdelen van de spoorweginfrastructuur het gebruik van AI nog altijd beperkt is en er op dit vlak dus uitdagingen zijn die moeten worden aangepakt. Dit promotieonderzoek richt zich op drie uitdagingen: 1) het verbeteren van de detectie van defecten in rails en componenten zoals bevestigingsmiddelen in een vroeg stadium, 2) het bieden van inzicht in enorme hoeveelheden niet-gelabelde data, en 3) het integreren van informatie van meerdere monitoringtechnologieën voor een nauwkeurige beoordeling van de conditie van de spoorweginfrastructuur. Deze uitdagingen worden behandeld in de hoofdstukken 3, 4, en 5 door de introductie van nieuwe AI-oplossingen.

Hoofdstuk 3 is gericht op het vraagstuk over het in een vroeg stadium detecteren van het ontstaan van defecten in het rijoppervlak van rails met behulp van axle box acceleration (ABA)-metingen. Spiking neural networks (SNNs) zijn kunstmatige neurale netwerken die natuurlijke neurale netwerken beter simuleren en zo de mogelijkheid bieden om temporele en spatiotemporele patronen te verwerken via een uniek datamechanisme voor discrete toestanden of spikes. Vandaar dat een op SNN gebaseerde methodologie wordt voorgesteld om de uitdaging van detectie van genoemde raildefecten aan te pakken. Daarnaast vertoont de signaaloverdracht in SNNs - die plaatsvindt als reeksen van spiking-gebeurtenissen – gelijkenis met het patroon van een ABA-signaal, waarbij elke spike een abrupte verandering in de ABA-respons bij squats vertegenwoordigt, hetgeen een onderbouwing is van de selectie van SNN. De voorgestelde methode maakt gebruik van een eenvoudige SNN-architectuur met tijdsafhankelijke waarden en geen verborgen lagen. De SNN wordt getraind met een methode die genetische algoritmen, k-fold cross-validation en multi-start backpropagation combineert om hyperparameters en waarden te optimaliseren. Zoals met metingen in de Nederlandse en Zweedse railinfrastructuur is aangetoond, registreert de voorgestelde methodologie effectief subtiele veranderingen

in de reacties van beginnende of lichte squats in ABA-signalen. In vergelijking met de bestaande methodieken voor verwerking van ABA-data leidt deze methodologie met een eenvoudigere netwerkarchitectuur tot een aanzienlijke verbetering van de detectienauwkeurigheid tot meer dan 93%, tegen 78-85% voor de bestaande methodieken. Het succes in squat-detectie wordt toegeschreven aan het gebruik van tijdsafhankelijke waarden die variaties in synaptische waarden mogelijk maken. Bovendien biedt de voorgestelde methode interpreteerbaarheid. Het interne gedrag van spike-reacties, postsynaptische- en membraanpotentialen laten een overeenkomst zien met een hoogfrequentieband tussen 1000-2000 Hz van het detectieprobleem van squats.

Hoofdstuk 4 behandelt het vraagstuk over hoogfrequente trillingssignalen die worden verkregen in nieuwe omgevingen waar voorkennis of referentie-informatie over de staat van de infrastructuur ontbreekt of zeer beperkt beschikbaar is. Om dit vraagstuk aan te pakken, wordt in dit hoofdstuk een unsupervised representation learning methodology voorgesteld om automatisch karakteristieke kenmerken van dynamische reacties , die de staat van de railinfrastructuur weerspiegelen, vast te leggen en te extraheren. Deze methode maakt gebruik van een collaboratief optimalisatieproces dat de empirische mode decompositie (EMD) synchroniseert met een convolutional auto-encoder (CAE). Het EMD-niveau wordt aangepast om ruis te verwijderen terwijl daadwerkelijke trillingsreacties behouden blijven. De CAE wordt getraind met gedemoduleerde signalen die als basis worden beschouwd voor het genereren van representaties die de kwaliteit van reconstructie waarborgen en daarbij onderscheid maken tussen normale en abnormale condities. De effectiviteit van deze benadering wordt aangetoond met behulp van een Gaussian-mengmodel. Toegepast op zowel gevalideerde ABA-data voor raildefectdetectie als op data van railbevestigingsmonitoring, afkomstig van een op een trein gemonteerde Laser Doppler Vibrometer (LDV), overtreft de voorgestelde methode andere varianten van auto-encoder-gebaseerde modellen en de wavelet-gebaseerde CAE in het nauwkeurig bepalen van de condities van rails en de bevestigingen. De methode bereikt een gemiddelde verbetering van 16% met de ABA-gegevens en 21% met de LDV-gegevens.

Hoofdstuk 5 gaat in op de beperkingen van afzonderlijke monitoringtechnologieën en introduceert een datafusiekader om de conditie van de spoorweginfrastructuur te voorspellen met behulp van deze verschillende monitoringtechnologieën. Het kader zorgt daarmee voor een oplossing voor ontbrekende gegevens door middel van spatio-temporele interpolatie en verbetert zo de voorspellende nauwkeurigheid met een hybride neuraal netwerk. De meerwaarde van het voorgestelde kader wordt aangetoond door een frequentere evaluatie van de toestand van transitiezones mogelijk te maken door de integratie van meerdere monitoringtechnologieën, waaronder spoorgeometrie, Interferometrische Synthetic Aperture Radar (InSAR) en ABA-metingen. Een spatio-temporele interpolatiebenadering wordt gebruikt om ontbrekende InSAR-gegevens in te vullen. Vervolgens worden hybride neurale modellen geëvalueerd om de longitudinale spoorniveaus te voorspellen, inclusief een hybride convolutioneel neuraal netwerk (CNN) met gated recurrent units (GRU) netwerk en een hybride CNN met een long short-term memory (LSTM) netwerk. De voorspelling is gebaseerd op een fusie van historische - en geïnterpoleerde

gegevens van InSAR en de ABA-metingen. Vervolgens wordt een nieuwe key performance indicator (KPI) voorgesteld op basis van de voorspelde longitudinale spoorniveaus, wat meer frequente beoordelingen mogelijk maakt dankzij de regelmatige beschikbaarheid van de InSAR- en ABA-gegevens. Het kader detecteert effectief en vroegtijdig geometrische afwijkingen in het spoor, zelfs vóór de volgende reguliere meting van spoorgeometrieprofielen. Dit biedt voorspellende inzichten die richting geven aan besluitvorming over de selectie van locaties en de planning van noodzakelijk spooronderhoud.

De hoofdstukken benadrukken het potentieel van AI voor ondersteuning van het besluitvormingsproces over onderhoud van het spoor, waarmee uiteindelijk het onderhoud van grootschalige railinfrastructuur verbetert. Hoofdstuk 6 besluit het proefschrift met aanbevelingen voor gebruik van de geïntroduceerde methoden in de praktijk en de uitvoering van toekomstig onderzoek.

1

INTRODUCTION

It all starts with an Introduction.

1

1.1. MOTIVATION

RAILWAY infrastructures are complex and large-scale systems. Railway infrastructures are characterised by dynamics that vary over time and across different locations. Temporal changes are primarily due to continuous use, degradation, and maintenance activities, while spatial variations arise from the variability of dynamics at various locations, such as railway tracks at bridges, tunnels, stations, and curves, compared to straight tracks. Despite some local periodic features like sleeper spacing, the track structure parameters are often unique to each location. Moreover, the functionality of railway infrastructure is influenced by stochastic factors like weather conditions. All of these make it a dynamic, continuous, distributed, and stochastic system. This inherent complexity highlights the need for innovative, intelligent methods tailored to address practical and localised challenges in railway infrastructure.

Effective management of railway infrastructure necessitates an approach that considers the underlying connections between infrastructure, society, and the environment. Research in railway infrastructure is inherently multidisciplinary. To address fundamental questions in this field, it is crucial to understand not only the physical behaviours (such as structural and mechanical responses) but also the limitations of various mathematical modelling techniques, the potential of state-of-the-art measurement technologies (including vibration, images, and laser scanning), and the available maintenance technologies. Additionally, we must account for the influence of stochastic variables like weather and reliability, the human factors related to both users and workers, and the complex relationships between railway governance and contractual agreements. The unique nature of railway infrastructure challenges at different locations and times presents numerous opportunities to develop innovative solutions using AI. These AI solutions can capture the essential characteristics of the infrastructure and address issues that traditional methods fail to resolve. By exploring the current practices and technologies used in railway infrastructure monitoring and maintenance, we can identify the areas where AI can further contribute to the specific challenges in railway infrastructure that need to be addressed. This PhD research focuses on AI-based solutions for decision support to improve and facilitate monitoring and maintenance decisions.

1.2. OVERVIEW OF RAILWAY INFRASTRUCTURE MONITORING AND MAINTENANCE

Health condition monitoring and maintenance play a vital role in ensuring the safety, availability, and reliability of services and in prolonging the life span of railway infrastructures. Early detection and preventive maintenance of possible failures before they occur have shown great potential for cost savings [1, 2]. The continuous monitoring of critical components has not only increased the level of safety but drastically increased the availability of the infrastructure, as early warning systems allowing to include the repairs or replacement of these components during the routine maintenance slots. This section provides an overview of railway infrastructures, condition monitoring, and maintenance.

1.2.1. RAILWAY INFRASTRUCTURES

Railway infrastructure can be categorised into four key groups: track system, catenary system, civil structures, and track substructures, as illustrated in Figure 1.1. The track system is the backbone of railway infrastructure. The track system comprises several critical components such as rails, sleepers, fasteners, ballast, switches and crossings (turnouts), as depicted in Figure 1.1(a). The catenary system is essential for electrified railways, supplying electrical power to trains. Examples of components in the system include contact wires, catenary cantilevers, pantographs, masts and poles, as depicted in Figure 1.1(b). Civil structures encompass the non-track elements of railway infrastructure. Examples of components in the system are culverts, viaducts, tunnels, and bridges, as depicted in Figure 1.1(c). The track substructure provides the foundational support for the track system. Examples of components in the system include sub-ballast, soil, and embankment, as depicted in Figure 1.1(d). Each of these groups plays a vital role in the overall integrity and functionality of railway infrastructure.

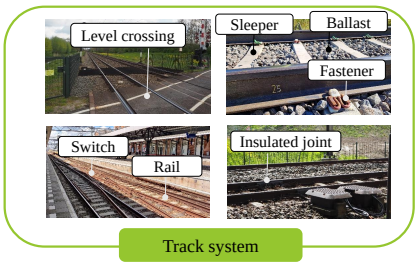

(a) Track system.

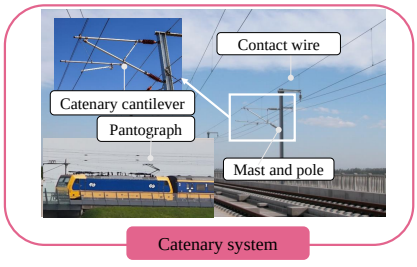

(b) Catenary system.

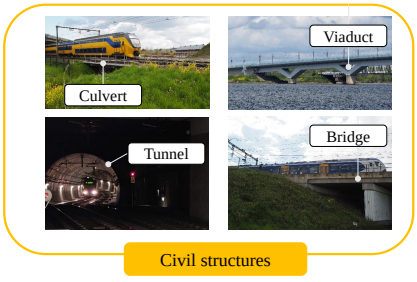

(c) Civil structures.

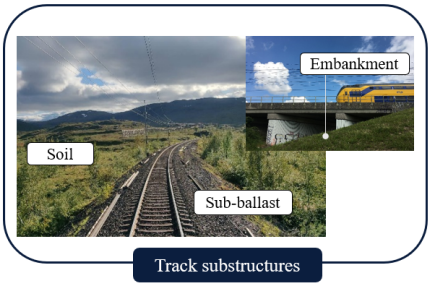

(d) Track substructures.

Figure 1.1: Groups of railway infrastructures.

1.2.2. RAILWAY INFRASTRUCTURE MONITORING

With the developments in sensors and information technology, health conditions in railway infrastructure can be continually assessed using information obtained from

track-side measurements, onboard measurements, and remote sensing technologies. Track-side measurements employ point-sensor technologies such as acceleration sensors, strain gauges, temperature sensors, and ground penetrating radar. The measurements are typically installed at critical locations. This results in the local coverage of responses. Given the large scale of the railway infrastructure, it is not always feasible to fully instrument railway lines spanning thousands of kilometres with a large number of sensors. The costs associated with these sensors, including expenses related to devices, labour, and power supplies, can be prohibitive. Moreover, full instrumentation is often unnecessary as onboard systems can effectively collect data. Additionally, some onboard monitoring techniques have not yet been standardised. Therefore, significant efforts are required from the railway industry to define their robust integration with existing systems and ensure efficient data analysis.

Onboard measurement systems have been used in continuous monitoring frameworks. These systems use sensors such as accelerometers and laser Doppler vibrometers to acquire data related to the conditions of railway infrastructure during train operations. This method provides information about the behaviours and conditions of rail infrastructures over many kilometres in a single run, facilitating large-scale monitoring. However, onboard monitoring techniques require robust integration with existing systems and efficient data analysis. This is essential due to the massive volume of data generated that covers each track position with a very short signal duration for critical locations that require special attention. These data contain a variety of dynamic and transient responses that vary significantly along the track and are affected by noise. Additionally, adapting these systems for use in passenger trains presents challenges, such as distinguishing global responses from those specific to individual components, like substructures. Addressing these challenges remains an ongoing research in the field.

Remote sensing technologies, such as satellite-based methods utilising global navigation satellite system (GNSS) and interferometric synthetic aperture radar (InSAR), are also employed for railway infrastructure monitoring. These technologies enable real-time displacement monitoring of structures such as bridges and detecting hazards such as landslides along railway embankments. While satellite data provides valuable insights, challenges remain in achieving the required resolution and accuracy for specific railway applications.

1.2.3. RAILWAY INFRASTRUCTURE MAINTENANCE

Preserving and enhancing the condition of railway infrastructures requires effective maintenance strategies, comprising four primary strategies detailed as below.

CORRECTIVE MAINTENANCE

Corrective maintenance refers to the maintenance activities performed to identify, isolate, and rectify a fault or defect that has already occurred in a system, thereby restoring it to its proper working condition. This type of maintenance is reactive in nature, meaning it takes place after a problem has been detected

rather than preventing issues before they arise. While it can lead to downtime and unsafe situations from unexpected failures, corrective maintenance is the simplest maintenance strategy to implement.

PREVENTIVE MAINTENANCE

Preventive maintenance refers to an approach to maintaining railway infrastructure by performing regular, scheduled inspections, and routine repairs to ensure proper functioning, early detection of defects and failures, and to extend the lifespan of assets. This approach aims to identify and address potential issues before they escalate into significant problems, thereby reducing downtime, improving safety, and optimising operational efficiency. The replacement or repair of components in preventive maintenance is based on predefined time intervals or usage metrics. However, this method may not capture all problems that arise between scheduled maintenance activities. For example, preventive grinding might also remove healthy rail top layer. Traditionally, preventive maintenance does not utilise predictive models, meaning updates on robustness and predictive accuracy are not explicitly considered.

PREDICTIVE MAINTENANCE

Predictive maintenance is a maintenance strategy that uses data analysis tools, machine learning, and AI techniques to detect anomalies and predict failures before they occur. The goal of predictive maintenance is to support maintenance activities and minimise unexpected breakdowns by relying on continuous monitoring and analysis of infrastructure conditions. This approach depends heavily on predictive models, which can be affected by uncertainty in parameters, noise, and drastic changes in operational conditions, potentially hindering predictive accuracy and informed decision-making. Implementing predictive maintenance requires significant initial investment in advanced data analysis tools, machine learning, and AI technologies. Additionally, specialised expertise is required to interpret data and maintain predictive systems.

PRESCRIPTIVE MAINTENANCE

Prescriptive maintenance is an advanced maintenance strategy that not only predicts failures. It also aims to identify the root causes of problems and propose design changes to eliminate the issues. Prescriptive maintenance comprises information from diagnosis, prognosis to maintenance decision-making. It combines field domain knowledge and know-how, data analytics, machine learning, and expert knowledge to offer actionable insights and optimal recommendations on actions to prevent or mitigate failures, thereby optimising maintenance schedules and resources more effectively. In prescriptive maintenance, component health information should represent a trend, and a major focus is on analysing the root cause of abnormal behaviour, not just the symptoms. However, the successful implementation of prescriptive maintenance in railway infrastructure requires the development of new AI solutions. This includes solutions from defect detection, root-cause identification,

classification, and prediction of degradation patterns to decision-making supporting maintenance planning. A higher level of specialised expertise is also required to interpret the recommendations and implement the suggested actions, which can be more challenging and resource-intensive than predictive maintenance.

Overall, corrective maintenance is crucial for addressing unexpected issues and ensuring the continued safe and efficient operation of railway systems. It complements preventive and predictive maintenance strategies by tackling problems that cannot be foreseen and preventively managed. Preventive, predictive, and prescriptive maintenance are condition-based strategies that heavily rely on advancements in monitoring technology to provide information about the current health condition of railway infrastructures.

1.3. SELECTED CHALLENGES FROM RAILWAY INFRASTRUCTURES

Monitoring of railway infrastructures has the potential to support the management of their performance and maintenance strategies. Yet, how to respond to the daily detection of faults poses another problem for inframanagers due to limited resources, short closure times, lack of alternative routes, and the standards that rely on time-based inspection. Additionally, databases constructed from continuous data monitoring become larger over time, which poses a challenge to their transmission, storage, and analytics. For instance, when using onboard axle box acceleration systems and laser Doppler vibrometers, an open challenge is how to migrate such high-frequency sampling data onto any cloud and database due to the limitation of the existing communication bandwidth. Data pre-processing and on-premise analytics can be options to reduce the amount of data. Further, new standards are still required when using ABAs and LDVs and when dealing with multiple measurement sources and new sensing technologies, e.g., satellite data. Further discussion about the detailed challenges in railway infrastructures is elaborated in Chapter 2. In this dissertation, some challenges addressed in the literature are selected for this PhD research. The selected challenges include the detection of rail surface defects called squats at their early development stage, insufficient labelled data for supervised model training, and information fusion of various monitoring technologies. Detailed information about the selected challenges is elaborated as follows.

1.3.1. DETECTION OF RAIL SQUATS AT EARLY DEVELOPMENT STAGE

Squats are short-wave surface defects and one type of rolling contact fatigue of railway rails [1–7]. Rail squats are critical to detect and manage because they can lead to increased maintenance costs, reduced rail life, and potential safety hazards. However, detecting squats, particularly for light squats, with high accuracy is challenging. Some possible underlying reasons are the following. First, light squats are anomalies with a low percentage of appearance in monitoring data. Some light

squats are difficult to find via visual inspections (or even impossible when these are still not visible to human eyes), making the labelling process difficult. Second, the response of light squats in ABA signals appears suddenly and has a very short duration. For example, at a light squat of 8 mm in wavelength with a measurement speed of 110 km/hr, the duration of its response can be 0.26 milliseconds. Third, the response of light squats in ABA signals is affected by the variability of the railway track parameters and measurement conditions. For example, different dynamic responses occur at squats on top or in between sleepers, thermite welds, flash welds, joints, crossings, transition zones, etc. Last and most importantly, the frequency components of light squats are slightly different from those of healthy rails, with subtle characteristics occurring dominantly at high frequencies. Early detection significantly reduces the maintenance cost of tracks because severe squats can lead to the replacement of the track section, while light squats can be effectively treated by grinding. Therefore, this PhD research considers using AI to improve the detection accuracy of rail squats, particularly light squats, based on ABA measurements, thereby enhancing the effectiveness of rail degradation control.

1.3.2. INSUFFICIENT LABELLED DATA FOR SUPERVISED MODEL TRAINING

Supervised methods, such as deep learning, require extensive labelled data to ensure high performance. However, for railway infrastructures, collecting accurate and verified labelled samples of high-quality faulty and healthy states from thousands of kilometres of rail lines is extremely difficult, costly, and time-consuming. Regarding class information for defects, often few labelled data are available due to the lack of historical data with sufficient quality and localisation. Likewise, health data are difficult to label because of their variants of behaviour at different locations; in particular, rails are affected by local track dynamics and different operational conditions and stochastic variables. In addition, there is no established standard or threshold to evaluate the level of health conditions based on onboard measurements such as LDVs and ABAs. Beyond the need for standardised evaluation methods for all railway components, there are components like embankments that remain particularly challenging. Existing studies do not clearly demonstrate that these onboard measurements accurately capture their dynamic behaviours and reflect their true health conditions. Consequently, we need further research on the fundamental analysis of dynamic responses to better understand and assess their health under varying conditions. Therefore, data from healthy infrastructure are abundant, whereas defective ones are few. As a result, data used for training AI models are seriously imbalanced, and labelled data are insufficient.

Rolling stock can be equipped with high-frequency vibration sensors to continuously monitor rail infrastructures and detect defects. These moving sensors measure at high speeds and sampling frequencies, generating a massive amount of data that covers each track position with very short signal durations. These data contain a variety of dynamic and transient responses that vary significantly along the track and are affected by noise. Using moving vibration sensors poses an additional challenge as this leads to a large amount of unlabelled and noisy data, complicating the extraction of dynamic responses for effective anomaly detection.

Hence, this PhD research considers using AI to automatically extract characteristic features of dynamic responses that reflect the conditions of rail infrastructures in an unsupervised manner.

1.3.3. INFORMATION FUSION OF VARIOUS MONITORING TECHNOLOGIES

Railway infrastructures are complex and highly nonlinear. They involve different assets and can be affected by various anomalies. Several advanced technologies are employed in railway infrastructure monitoring, each offering unique advantages for specific purposes. Thus, detecting failures and maintaining the structure requires multiple measurement systems. Typical monitoring systems used for railway infrastructures employ eddy current and ultrasonic tests, vibration measurements of wheel and rail using accelerometers, videos, and track geometry recording [8, 9]. Depending on traffic tonnage and maximum line speed, measurement frequencies and data processing requirements can differ substantially among technologies.

Employing multiple systems to monitor railway infrastructure performance indicates the need to deal with heterogeneous data. The information about defects obtained by a single source can easily show trends; however, it is limited by the nature of the measurement itself. Assessing transition zone conditions, for example, heavily depends on the measurement frequency and the density of data gathered. A more frequent measurement is essential to enhance forecasts and insights into the evolution over time and assess severe events, allowing better maintenance strategic plans. High-density measurements are essential for detecting track irregularities along transition zones. The more frequent measurements from satellites offer the advantage of tracking transition zone conditions over time and assessing significant events on a global scale. In a complementary manner, data obtained from ABA measurements excel at capturing local dynamic responses. Currently, ABA measurements occur less frequently because the system is still on the path towards standardisation, and it is required to be effectively installed in passenger trains. Additionally, track geometry is a standardised measurement used in various railway companies. While its quality is guaranteed with accuracy and resolution, track geometry does not capture locations with a poor dynamic train-track interaction. Recognising the complementary nature of these measurements, this PhD research considers using AI for the fusion of track geometry, InSAR, and ABA measurements to assess transition zone conditions with a more frequent evaluation.

1.4. RESEARCH OBJECTIVES AND QUESTIONS

This PhD research proposes AI solutions to support maintenance decisions in railway infrastructure. Specifically, the research covers three key challenges of rail surface defect detection at early development stages based on ABA measurements, unsupervised representation learning from high-frequency moving vibration sensors, and the fusion of information from different monitoring technologies. The primary objective is to leverage AI to transform monitoring data into actionable insights, thereby supporting maintenance planning for railway infrastructure. The key research question guiding this research is:

"How can AI be adopted so that maintenance in a large-scale railway infrastructure is improved?"

Specifically, the thesis aims to respond to the following sub-research questions:

1. How successful are AI developments in addressing railway infrastructure problems?
2. Can an SNN-based methodology improve the detection accuracy of rail squats, particularly light squats, based on ABA measurements?
3. How can we effectively extract, in an unsupervised manner and from high-frequency moving vibration sensing, representations that characterise dynamic behaviours of rail infrastructures?
4. How can a hybrid neural model exploit information from track geometry measurements, InSAR measurements, and ABA measurements to assess transition zone conditions with a more frequent evaluation?

1.5. RESEARCH SIGNIFICANCE

Upon completion, this dissertation offers several benefits to researchers and engineers in academia and the railway industry:

1.5.1. SCIENTIFIC CONTRIBUTIONS

- Through a comprehensive review, this dissertation provides considerations and discussions on the challenges and the need for new intelligent methods to bridge the gaps between industrial applications and new AI developments. This information can help researchers and engineers in academia and industry visualise trends and develop benchmarks tailored to the specific needs of railway infrastructures.
- An SNN-based methodology is presented for detecting rail squats, particularly light squats. This method utilises a simple network architecture with time-varying weights and no hidden layers to address the complex spatiotemporal problem of early squat detection. A global optimisation approach is adopted for the SNN training process, incorporating a genetic algorithm for hyper-parameter search based on cross-validation and backpropagation to adjust time-varying weights with multi-starts. The process relies on SpikeProp and an update rule that accounts for the time-varying characteristics of the weights.
- A utilisation of spike responses, postsynaptic potentials, and membrane potentials is presented to provide a new explainable way for squat detection that relies on ABA signals. Visual explanations from these internal spike behaviours can be used to identify a correspondence with the physical problem.

- An unsupervised representation learning methodology is proposed to automatically extract features that characterise the dynamic behaviours of rail infrastructures from noisy, short-duration monitoring data obtained from moving high-frequency sensors at different locations.

- A collaborative optimisation process between empirical mode decomposition and a convolutional autoencoder is proposed to generate representations that demonstrate reconstruction quality and differentiate between rail infrastructures under normal and abnormal conditions.

- To demonstrate the applicability and performance of the proposed unsupervised representation learning method for monitoring rail infrastructures, two field measurements with different targeted components, sensor types, and operational conditions are considered: one for monitoring rail defects using an ABA and the other one for rail fasteners using a train-borne LDV.

- Multiple monitoring data, including track geometry measurements, InSAR measurements, and ABA measurements, are utilised for assessing the health of railway transition zones.

- A spatio-temporal interpolation approach is introduced to impute missing InSAR data, while hybrid neural models are proposed to fuse information from InSAR and ABA data to predict missing track longitudinal levels.

- A novel key performance index based on InSAR and ABA measurements is proposed to assess the health of railway transition zones.

1.5.2. SOCIETAL CONTRIBUTIONS

- Enhance the safety of railway infrastructure: this minimises delays and disruption through more reliable infrastructure as a result of condition-based maintenance procedures at a large scale.

- Reduce cost in maintenance: early warning through automatic condition monitoring and condition-based maintenance improve the effectiveness of maintenance activities.

- Reduce cost in railway operation: early information about anomalies, e.g., rail surface defects, will help operators adjust their schedules to the current situation.

- Lastly, and most importantly, provide technological solutions to strengthen rail transport: this helps to achieve sustainable development goals, with the potential for significant advancements in transportation systems across diverse national contexts.

1.6. DISSERTATION OUTLINE

The outline of this dissertation is illustrated in Figure 1.2. Chapter 1 presents an introduction to the PhD research. Chapter 2 comprehensively reviews AI methodologies developed and integrated into railway infrastructure and provides insights into the challenges for successful implementation in the railway industry. Chapter 3 focuses on an improvement of rail squat detection using the spiking neural network (SNN) with time-varying weights relying on ABA measurements. Research presented in Chapter 4 involves an unsupervised representation learning methodology to capture dynamic responses of rail infrastructures using monitoring data obtained from high-frequency moving vibration sensors. Chapter 5 presents a framework that enables a more frequent evaluation of transition zone health by integrating multiple monitoring technologies, including track geometry measurements, InSAR, and ABA. Chapter 6 concludes the dissertation with recommendations for future research and practice.

1

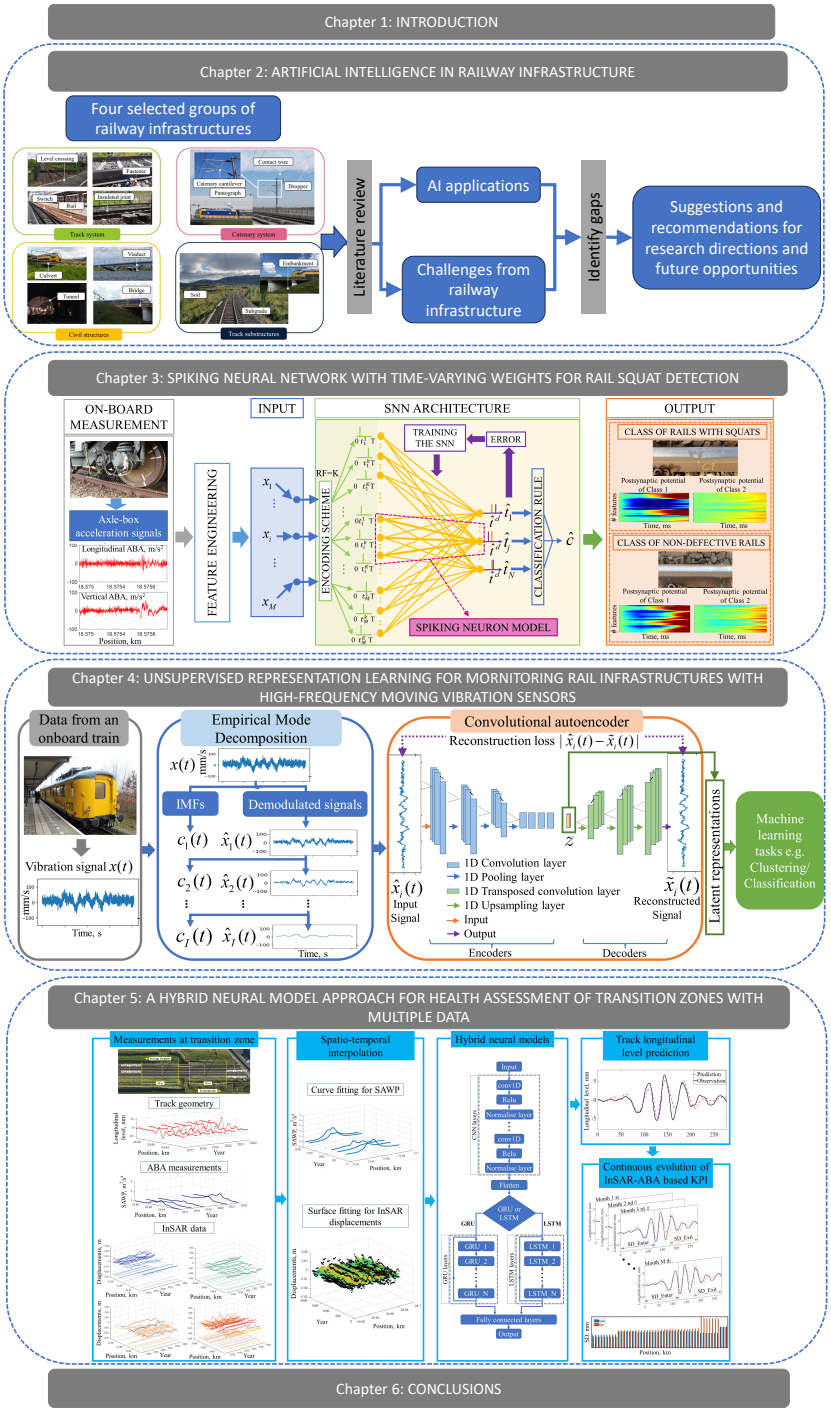

Figure 1.2: Dissertation outline.

2

ARTIFICIAL INTELLIGENCE IN RAILWAY INFRASTRUCTURE

The railway industry has the potential to make a strong contribution to the achievement of various sustainable development goals, by an expansion of its role in the transportation system of different countries. To realize this, complex technological and societal challenges are to be addressed, along with the development of suitable state-of-the-art methodologies fully tailored to the particular needs of the wide variety of railway infrastructure types and conditions. Artificial intelligence (AI) methods have been increasingly and successfully applied to solve practical problems in the railway infrastructure domain for over two decades. This chapter proposes a review of the development of AI methods in railway infrastructure. First, we present a survey limited to selected journal papers published between 2010 and 2022. Bibliographical statistics are obtained, showing the increasing number of contributions in this field. Then, we select key AI methodologies and discuss their applications in the railway infrastructure. Next, AI methods for key railway components are analyzed. Finally, current challenges and future opportunities are discussed.

This chapter is an award-winning paper published in Phusakulkajorn, W., Núñez, A., Wang, H., Jamshidi, A., Zoeteman, A., Ripke, B., Dollevoet, R.P.B.J., De Schutter, B., Li, Z., Artificial intelligence in railway infrastructure: Current research, challenges, and future opportunities, Intelligent Transportation Infrastructure, liad016, pp. 1–24, 2023.

2.1. Introduction

Industrial sectors have been increasingly limiting the use of fossil fuel consumption. However, transport sectors still struggle to significantly reduce CO_2 emissions. With the current technological progress, the road sector cannot cope with the challenge despite the environmental standards and the development and steady improvement of alternative fuel vehicles [10]. Increasing rail usage in the modal share between rail and road transport is envisioned as an important strategy when developing greener and more sustainable societies [11]. In some countries, this can be achieved by equipping more regions with new railway networks and infrastructures. In other countries where railway infrastructure is already densely used, increasing the effectiveness of their operations, the level of satisfaction of users, and the optimal use of resources are major challenges.

By 2030, rail sectors in Europe aim to reduce CO_2 emissions for passenger and freight transport by 30% from 1990. However, more regions equipped with railway tracks and more intense use of the infrastructure imply higher degradation rates and a higher likelihood of facing disruptions. As trains run on the track, the quality of railway infrastructure gradually deteriorates over time. When this deterioration is not under control, it can cause disastrous events, e.g., broken rails, train derailment, etc [12]. Thus, railway infrastructure must be kept in acceptable condition under all sorts of different scenarios of degradation mechanisms, considering the most updated knowledge about the particular types of failures in all the components and their consequences. Further, in highly used networks, disruption might affect many passenger and freight transports. Thus it is crucial to not only prevent safety issues but to keep the trust of users in the reliability of services so that rail users do not shift to other transportation modes [13].

Generally, railway assets can be grouped into two main types: the infrastructures and the rolling stock. Railway infrastructures include tracks, tunnels, bridges, and catenary systems. Rolling stock refers to assets that can move on a railway network, and examples are locomotives, passenger coaches, and freight cars. Common problems affecting these assets can include failures with origin in the usage of infrastructure components (such as rail defects), failures in the rolling stock (such as door opening failures), and events due to exogenous factors such as third parties (e.g., collisions with persons at stations and non-authorized/trespassing people on railway properties) and weather conditions (such as flooding). The railway industry has been dealing with those problems mostly by relying on traditional approaches. Still, some examples from the industry about the use of artificial intelligence (AI) in railway applications have been reported. Just to mention some, there are monitoring systems of the infrastructures powered by AI to monitor the status of bridges, tunnels, switches, and energy systems. Other reported examples of sensing technologies enhanced by AI include line-scan sensors and cameras from passenger trains, and fiber optic acoustic sensors to detect rail and wheel defects, trespassers, and level crossings. AI-based algorithms relying on wayside train monitoring systems have been developed for damage detection of pantographs, wheels, and brake blocks. Furthermore, AI has also been exploited for robust rail logistic planning. However, the use of AI in railway environments is not yet the standard. This

indicates that further developments are needed before reaching a maturity level to be ready to implement reliable solutions under a large variety of infrastructures. While the current developments in the industry are interesting to analyze as they give indications on the acceptance level of AI solutions, in this chapter, we focus on the advancements in AI solutions reported in journal publications. Our target is to provide an overview of developments and discuss gaps and future opportunities that can support understanding the use of AI technologies in railway infrastructure.

Our review primarily focuses on publications dealing with four selected groups of railway infrastructures as illustrated in Figure 2.1. The selected groups comprise railway track (rails, welds, joints, switches, fastening systems, ballast, crossings, and sleepers), railway catenary (catenary and pantograph), railway civil structures (tunnels, bridges, viaducts, culverts), and railway substructures (subgrade, soil, and embankments). The reason is that these infrastructures form the foundation for safety, quality and reliability of services, and long-term costs. Moreover, by proactively identifying and addressing degradation-related failures, risks can be minimized and a safe railway systems can be ensured. Therefore, the focus is on their failures arising from degradation and usage. Rolling stock, railway signaling, and operations are excluded from our review. Interested readers in other railway topics are referred to other recent reviews such as [14–17].

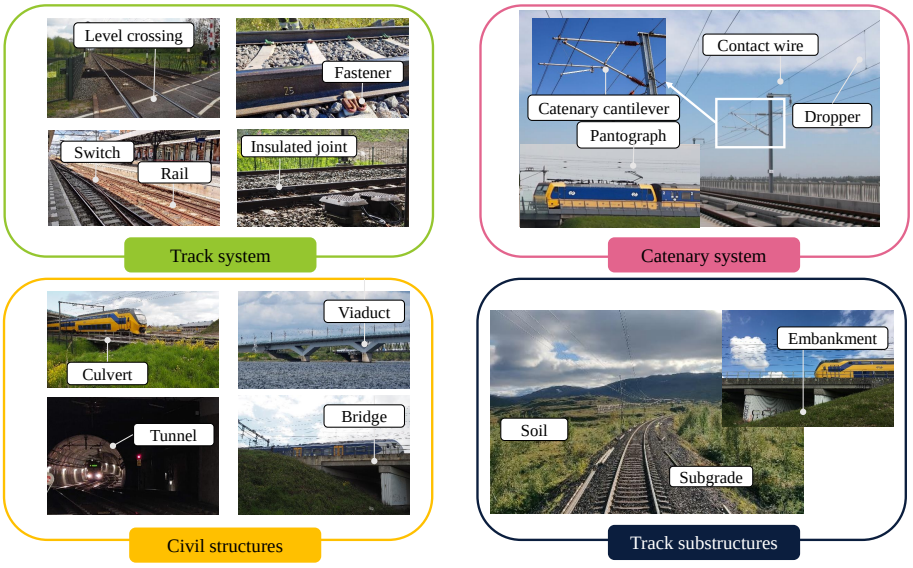

Figure 2.1: Illustration of the four selected groups of railway infrastructures considered in this work: track system, catenary system, civil structures, and track substructures.

Railway infrastructure is a highly complex distributed parameter system. In other words, the dynamic characteristics of the railway infrastructure change over time and space. The changes over time refer mainly to the consequences due to its continuous

usage, degradation processes, and human interventions such as maintenance. The changes over space refer to the fact that governing dynamics are different per location; for instance, railway tracks at bridges, tunnels, stations, and curves behave differently than straight tracks. Although the railway infrastructure can also be seen as a line structure with some components presenting a sort of local periodicity (such as the sleeper spacing), the substructure and structure track parameters are unique at each location. Additionally, the railway infrastructure is subject to various sources of stochasticity that can affect its functionality, such as weather conditions. Thus, the railway infrastructure is a dynamic, continuous, distributed, and stochastic system that is fundamentally challenging, and from where the need to develop new intelligent methods that can be tailored to practical solutions at a local level naturally appears.

The optimal use of railway infrastructure requires holistic approaches to its management that explicitly include the complex interlinks among infrastructure, society, and the environment. Railway infrastructure research is inherently multidisciplinary. Answering fundamental questions in this field requires not only knowledge of its physical responses (structural, mechanical, etc.). We also need to understand the limitations of selected mathematical modeling approaches, the capabilities of state-of-the-art measurement technologies (vibration, images, laser, etc.), the maintenance technology available, the behavior of stochastic variables (weather, reliability, etc.), the inclusion of the human aspects regarding users and workers, and the complex interlinks between railway governance and contracts, etc. It appears that the problems associated with railway infrastructure are unique to different places and times. This opens up many opportunities to develop a variety of new intelligent solutions to capture the essential characteristics of the infrastructure and to provide solutions that traditional methods cannot truly provide.

Health condition monitoring and maintenance play a vital role in ensuring the safety, availability, and reliability of service simultaneously and in prolonging the life span of the infrastructure. Early detection and preventive maintenance of possible failures before they occur have shown great potential for cost savings [18, 19]. The continuous monitoring of critical components has not only increased the level of safety but drastically increased the availability of the infrastructure, as early warning systems allow to include the repairs or replacement of these components during the routine maintenance slots. Therefore, the railway industry and researchers from various countries have been developing integrated and robust approaches to continuously monitor and maintain railway infrastructures [20–24]. With the developments in sensors and information technology, health conditions in railway infrastructure get monitored continually by using sensors installed in the rolling stock (e.g., rail and pantograph monitoring), in areas adjacent to the track (e.g., switch engine monitoring), and crowd sensing (e.g., with mobile phones that measure vibrations, temperature, pressure, etc.). Monitoring of railway systems has the potential to support the management of their performance. Yet, how to respond to the daily detection of faults poses another problem for inframanagers due to limited resources, short closure times, lack of alternative routes, and the standards that rely on time-based inspection. Additionally, databases constructed

from continuous data monitoring become larger over time, which poses a challenge to their transmission, storage, and analytics. For instance, when using onboard axle box acceleration systems and laser Doppler vibrometers, an open challenge is how to migrate such high-frequency sampling data onto any cloud and database due to the limitation of the existing communication bandwidth. To reduce the amount of data, data pre-processing and analytics on-premise can be an option. Further, new standards are still required when dealing with multiple measurement sources and new sensing technologies, e.g., satellite data. All in all, the railway industry and academia have been working to address these challenging issues in which further cooperation can unlock the best solutions and overcome these barriers to the adoption of AI.

Thus, advanced railway networks, in essence, require standardization and governance for big data management and analytics to monitor the infrastructure condition and control life cycle costs adequately [14, 25]. In the literature, sophisticated data management for data storage and analytics has proven to enable the development of better railway maintenance solutions. This is because big data analytics enables asset managers to switch from reactive maintenance towards predictive maintenance [26]. The literature on data analytics [27–29] shows that artificial intelligence (AI) is increasingly popular in various domains as it allows automation in decision support tools by linking data with decisions and enabling asset-specific and whole system behavior analyses. This chapter focuses on AI applications in railway infrastructure, including technologies, methods, and models in AI that have been published concerning monitoring, diagnosis, prognosis, detection, classification, and maintenance. The paper is structured as follows. In the next section, we conduct a bibliographical analysis to identify the most used and promising AI methodologies in the field of railway infrastructure. Then, we discuss how these methods have been adapted to railway environments for tackling different challenges. Given the dense literature, we describe a few selected characteristic examples of these AI methods and railway applications. Finally, we discuss open challenges and opportunities for the development of AI in the asset management of railway infrastructures.

The chapter is structured as follows. In the next section, we conduct a bibliographical analysis to identify the most used and promising AI methodologies in the field of railway infrastructure. Then, we discuss how these methods have been adapted to railway environments to tackle different challenges. Given the dense literature, we describe a few selected characteristic examples of these AI methods and railway applications. Finally, we discuss open challenges and opportunities for the development of AI in the asset management of railway infrastructures.

2.2. BIBLIOGRAPHICAL ANALYSIS

Artificial intelligence (AI) refers to developing computer systems and machines that can replicate or simulate human cognitive abilities. AI involves the creation of algorithms and models that allow computer systems and machines to understand natural language, to recognize patterns, to solve problems, to make decisions, and to

adapt to new situations. AI has been deployed in railway applications for decades. Some of the first works reported in the literature of railways that explicitly mention AI in the eighties are in the fields of diesel-electric locomotives using expert systems [30] and derailment analysis [31]. For neural networks, the first applications reported in the early nineties were in traffic management [32] and rail defects using ultrasonic images [33], among others. Nowadays, AI plays an essential role in analyzing characteristics of complex railway measurements and in identifying relevant patterns amongst an abundance of information. Many intelligent systems relying on AI technologies have been developed and integrated into railway infrastructure to tackle problems arising from its usage and natural degradation mechanisms. To select these topics, a first broad bibliographical search was conducted from where the more prominent fields and recent trends were selected, including neural networks, metaheuristics, regression (supervised), probabilistic graphical models, fuzzy logic, clustering (unsupervised learning), and transfer learning.

The bibliographical search is conducted over papers published within the context of AI and railway infrastructure. We consider the track system, catenary-pantograph system, civil structures, and substructure. Papers about rolling stock, railway signaling, and operations are excluded from the analysis. The review aims at papers in scientific journals considering both article and review types of documents. The publication years considered are from 2010 to 2022. Only papers in English and the engineering subject area are included (which will leave out papers at the interfaces with other domains). Scopus is chosen as the citation database, and the precise search terms are considered in conjunction with the generic words to capture most documents of our interest. The search terms are incorporated into three groups as presented in Table 2.1.

2.2.1. PAPER RETRIEVING PROCESS

The search is restricted to fields in the article title, abstract, and keywords. As shown in Table 2.1, the wildcard “asterisk” is employed to include plurals and spelling variants. Likewise, the double quote, “ ”, is used to search for vague phrases in which symbols are ignored. To search for papers using AI methodologies in railway infrastructure, the associated search terms from Group 1, Group 2, and Group 3 are all joined with the “AND” operator. Once the primary search is done, the results are manually verified to check whether some of the most well-known publications in the different fields are included in their respective lists. Next, the potential search results are assessed by considering criteria described in Table 2.2. Upon completing the literature retrieval process, the papers are analyzed and grouped based on the aims and approaches of this review. Table 2.3 summarises the search results of each related area. We understand particular papers might have been excluded from the search engine, or some unrelated papers that mention the keywords in the abstract might fall in the selection. With our manual check, we found that the number of these cases was minimal, and the trends are representative enough to draw some general analysis.

Table 2.1: Search terms for retrieving publications.

Group	Related area	Identified search terms
1	Railway infrastructure	rail* AND (catenary OR pantograph OR “rail" OR track* OR ballast* OR weld* OR joint* OR switch* OR turnout* OR fasten* OR “level crossing*" OR sleeper* OR tunnel* OR bridge* OR viaduct* OR culvert* OR subgrade* OR substructure OR soil OR embankment)
2	Railway applications	monitoring OR diagnos* OR prognos* OR detect* OR predict* OR classif* OR maintenance
3	AI	“computational intelligen*" OR “artificial intelligen*" OR “big data" OR “machine learning" OR “deep learning" OR “computer vision" OR probabilistic* OR bayesian OR markov OR “belief network" OR “transfer learning" OR “domain adaptation” OR clustering OR k-mean OR regression OR “neural network" OR convolution* OR encoder OR heuristic* OR fuzzy OR “particle swarm" OR “genetic algorithm" OR evolution*

Table 2.2: Inclusion criteria.

Criterion	Description
1	Only papers in track systems, catenary system, civil structures, and substructures.
2	Only papers in monitoring and maintenance.
3	Only papers that focus on using AI.
4	Papers in railway signalling, rolling stock, and operations are excluded.

Table 2.3: Summary of the search results.

Group	Related area	No. of papers
1 & 2	Railway infrastructure	17,393
3	AI	4,284,974
1 & 2 & 3	AI in railway infrastructure	3,465

2.2.2. BIBLIOGRAPHICAL ANALYSIS

The quantitative analysis assisted in identifying 3,465 papers. These are illustrated in Figure 2.2 in which an overview of research trends observed from the number of publications by year from 2010 to 2022 is given. As expected, research with AI applications in this field has gained popularity over the last twelve years. Between 2010 and 2017, the number of publications per year rose slightly from 95 papers to 208 papers. The number of publications expanded significantly after 2017. This made the overall number of publications after 2017 approximately two times greater than that between 2010-2017. This increasing trend over the past five years indicated the need and demand for AI technology developments in the railway infrastructure

domain.

Next, the current progress of AI applications in rail infrastructure is overviewed based on the AI methodologies elaborated in the previous section. Figure 2.3 illustrates the utilization trend of each AI methodology for railway infrastructures. It can be seen that the four most commonly used methods in rail infrastructure are neural networks, metaheuristics, PGM, and regression. The total amount of publications using the neural network-based method was the biggest.

A breakdown of the relative utilization of the AI categories over the years is also shown in Figure 2.3. It can be seen that the utilization trend of the neural network-based method shot up in 2017. This made the neural network-based method the most deployed in 2022. For other AI categories, their utilization trend progressed similarly over the past decade. However, a slight drop was observed in the research trend using fuzzy-based methods. Note that no publications about railway infrastructure that employ transfer learning have been found before 2018. Its upsurge of interest was noticed after 2018.

An overview of the AI research share for railway infrastructure systems is presented in Figure 2.4. AI has been employed the most in track systems, whereas less attention has been paid to catenary and substructure systems. To obtain insight into the share of AI in railway infrastructure research, a comparison between the number of publications using AI and without AI is exhibited in Figure 2.5 per selected railway component. To retrieve the relevant AI papers per component, the associated search terms from the selected railway component from Group 1, all railway applications from Group 2, and all AI methodologies from Group 3, shown in Table 2.1, are all joined with the “AND” operator. In this figure, the analysis of viaducts and culverts is included with bridges, the analysis of substructures includes soil, and wheels are included due to wheel-rail dynamics. Even though rails, wheels, and bridges are the top three components that have received the highest attention in research, their proportion of AI research papers is less than that of catenary and pantographs. Substructures and embankments have received the least attention in research, and their proportion of AI research is also lower than the other components. Further discussions on the underlying reasons that prevent the use of AI methodologies for these components will be given later.

Figure 2.6 presents the distribution of AI methodologies across the four groups of railway infrastructure. Unlike the retrieval process of Figure 2.5, the search terms for Figure 6 were more restricted to the selected AI methodology. Without including general terms of AI, this resulted in the number difference between Figure 2.5 and Figure 2.6 due to particular papers being excluded from the search engine. However, the analysis is to draw some general trends. Based on this, some insightful findings are drawn:

1. For all four groups of railway infrastructures, neural networks, meta-heuristics, PGMs, and regressions are the most commonly used methodologies.

2. Among the four groups, neural networks dominate the catenary system with a share of 55%. The track system follows with a 34% share, while civil structures and substructures account for 27% and 22%, respectively. In contrast, transfer

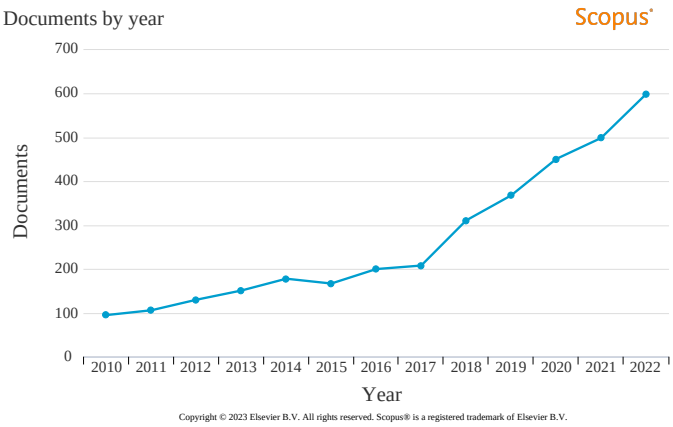

Figure 2.2: AI research trend in railway infrastructures.

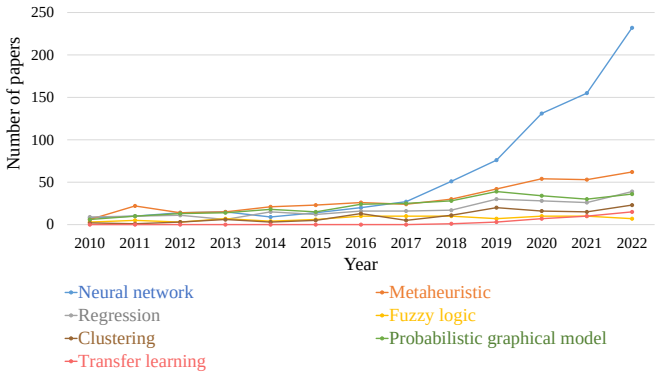

Figure 2.3: Utilisation trend of each AI methodology for railway infrastructures.

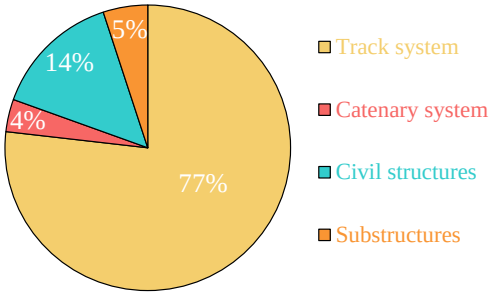

Figure 2.4: An overview of the AI research share across railway infrastructure systems.

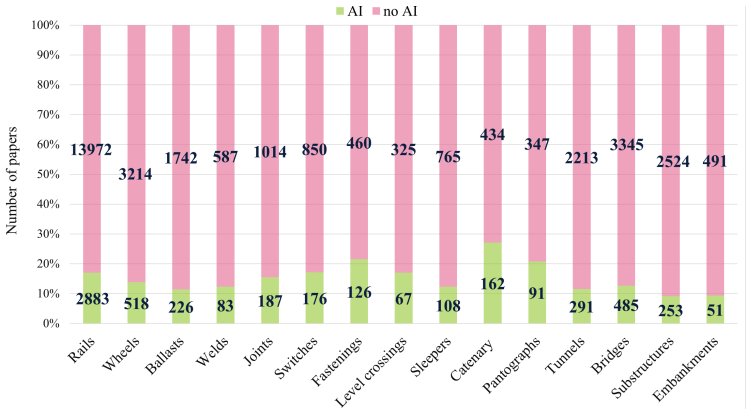

Figure 2.5: The proportion of AI research papers per component. NB: one research paper can include multiple railway components.

learning exhibits limited applicability, constituting only a 1% share in both the track system and civil structures.

3. All the selected AI methodologies have been adopted to tackle issues in railway track system and civil structures.

4. Not all the selected AI methodologies have been adopted to tackle issues in every component of the railway track system, catenary system, and substructures. There was no deployment of transfer learning in some components of the track system, the catenary system, and substructures, whereas transfer learning has been applied to civil structures. Railway welds and joints are examples that researchers have not used transfer learning for the track system.

5. Even though regression was widely used amongst other railway components, there was no publication (to the best of our knowledge) about those methods in research for fasteners. Likewise, no research was conducted on fasteners using fuzzy logic.

6. There were limited numbers of AI methodologies applied to embankments. To the best of our knowledge, AI research was conducted using only methodologies from neural networks, metaheuristics, PGMs, and regression. There was no deployment of clustering, fuzzy logic, or transfer learning for embankments.

In Figure 2.7, the recent development of the selected AI methodologies in 2023 is presented across the four groups of railway infrastructure, and a summary is given as follows:

1. Within the context of the track system, railway researchers tend to focus more intently on rails, wheels, and ballasts, with comparatively less attention

to welds and fastenings. Similar to the AI developments observed in the preceding years, all the selected AI methodologies have been applied within the group and the utilization of neural networks is more prevalent than those of the other methodologies. Transfer learning is the least popular method, and its applications remain absent in welds and joints in 2023.

2. Within the context of the catenary system, the utilization of transfer learning remains unexplored. A number of research is distributed equally between catenary and pantographs, using predominantly methods stemming from neural networks. As of 2023, there exists no research employing fuzzy logic within the catenary system.

3. The development trend of the selected AI methods in civil structures is similar to the catenary system. Nonetheless, all the selected AI methodologies have found their applications within civil structures. Notably, there exists research employing transfer learning in the context of bridges, but such applications have yet to extend to tunnels.

4. The recent trend of AI method development in substructures also shares similarities with that of the catenary system. Notably, the utilization of neural networks is less than metaheuristics in embankments, and employment of transfer learning is still missing.

2.3. AI IN RAILWAY INFRASTRUCTURE

Beyond a safe railway operation, multiple aspects have to be taken into account by the inframanager and railway operators. For instance, to minimize passenger and freight delay, to maximize the capacity at which they can operate their networks, to maximize the reliability of the infrastructure, and to do all of these at minimum costs. Further, societal and environmental impacts also have to be addressed. To achieve those targets, the infrastructure needs to be reliable. This can be achieved by proper maintenance strategies that can be used for requirements of new designs when tackling root cause problems or new maintenance procedures over a lifecycle that also considers the interlinks between replacements and recycling processes. This is the so-call prescriptive maintenance. It is a new maintenance concept emerging in the railway industry along with the development of business globalization. Similar to the other maintenance concepts, prescriptive maintenance comprises information from the diagnosis and prognosis and maintenance decision-making. Its goal is also to intelligently monitor, predict, and optimize the performance of railway infrastructure. In prescriptive maintenance, component health information should represent a trend, and a major focus is on analyzing the root cause of abnormal behavior, not just the symptoms. However, the successful implementation of prescriptive maintenance in railway infrastructure requires the development of new AI solutions. This includes solutions from defect detection, root-cause identification, classification, and prediction of degradation patterns to decision-making supporting maintenance planning. Following is a narrative literature review to offer insights into the use of AI methodologies in railway infrastructure.

2.3.1. Railways and neural networks

Neural networks are non-linear models that can be used to capture the dynamics of complex systems. Their architecture/model structure is based on layers, namely the input layer, hidden layer, and output layer. Each layer comprises interconnected processing units (called neurons) to uncover the underlying patterns or relationships within a dataset. Neural networks can be constructed 1) with different topologies in which connections between processing units can be designed differently, 2) with different input signals in which input neurons can accept continuous or binary values, 3) with different internal state dynamics, and 4) with different learning processes to perform certain tasks. Contrary to multiple-layer neural networks, typically considered as shallow networks, deep neural networks consist of many layers commonly ranging from several tens to more than hundreds. They are designed to automatically learn and extract representations from raw input data. Deep learning, with its emphasis on deep architectures and hierarchical representation learning, has been developed and gained much attention from researchers to leverage the capabilities of neural networks for feature transformation and extraction in big data environments. Examples of neural networks are multilayer perceptron, artificial neural network, spiking neural network, graph neural network, radial basis function network, residual neural network, convolution neural network, and recurrent neural network. Interested readers in the field of neural networks are referred to review papers such as [34, 35], and recent reviews such as [36–38].

Much of modern technology is based on big data environments with highly inherent complex relationships between dependent and independent variables. In railway infrastructure, both neural networks and deep neural networks have found their applications for various railway infrastructure components, e.g., rails [39], catenary [40, 41], tracks [42–46], fasteners [44, 47], tunnels [48], turnouts [49], and bridges [50]. The existing applications of neural networks focus, among others, on detection [39–44, 47, 50, 51], prediction [45, 46, 48, 49], and decision-making [39, 43]. In the railway industry, there have been various applications of neural networks and deep learning to detect defects and anomalies and to diagnose and prognose of railway infrastructures including rails, level crossings, switches, welds, catenary and pantographs.

In the research topic of detection, the challenge is to achieve complete automation of defect detection at the early stages [40–42, 50]. Algorithms based on deep convolutional neural networks (DCNNs) are predominantly utilized in railway fault inspection and detection [39–43, 47]. This is due to the capabilities of DCNNs and the popularity of vision-based inspection. Dealing with vision-based data, intensive research has been devoted to alleviating problems concerning image quality acquired from inspection systems [40, 42, 44, 47, 51].

To deal with the visual complexity of defects and the similarity between the component and background, Kang et al. [40] and Chen et al. [47] proposed methodologies based on DCNNs. Many modules were considered in developing the detection system, including component localization and defect detection. In the component localization module, object detection algorithms employed were the single shot multibox detector, You-Only-Look-Once, a region convolutional neural

network (R-CNN), and fast R-CNN. Besides a fully convolutional Network used in [47], a deep multitask neural network integrating both a deep material classifier and a deep denoising autoencoder into its architecture was introduced in [40] to accomplish simultaneous segmentation and defect detection. To obtain better high-speed performance in detection, Zhang et al. [44] proposed a novel structured light method based on motion image to assist a feed-forward neural network for an inspection of moving objects.

For prediction, neural networks are mainly selected due to their universal approximation capabilities for non-linear systems, self-adaptation, and the precision of their predictions. Some of the algorithms utilized within the area of railway prediction are neural networks trained with back-propagation [45], multi-layer perceptrons [46, 48], multi-valued neural network [49], and several other algorithms. Multilayer feedforward neural networks based on multi-valued neurons (MLMVN) proposed by Fink et al. [49] were applied to predict reliability and degradation based on time series. This research demonstrated that the MLMVN developed good results for multi-step ahead predictions and did not show accumulating errors.

Jamshidi et al. [39] and Oukhellou et al. [43] presented a framework using a neural network to detect faults. A data-fusion technique based on Bayesian probability theory was considered afterward to combine the outputs from a neural network in order to make a final decision on the detection and localization of a fault in the system. The Dempster–Shafer theory was considered in [43] while Bayesian inference was considered in [39]. The Dempster–Shafer theory provides a convenient framework for handling imprecision and uncertainty in decision problems regarding the presence and location of a fault.

2.3.2. RAILWAYS AND REGRESSION

Regression and AI typically build models based on a labeled set of data examples and predict a certain data characteristic. For instance, the regression models can be used to evaluate new data, which will tend to provide a prediction as the examples provided in the database. A new data point with a high similarity measure to a data point in the dataset indicates the best match to predict a certain output [52]. Examples of regression algorithms are logistic regression, ridge regression, linear regression, stepwise regression, ordinary least-square regression, multivariate adaptive regression, principal component regression, partial least-square regression, and project pursuit regression. For recent review papers on regression, readers are referred to [53, 54]. Regression has been widely employed in rail infrastructure due to its simplicity. Based on our review, regression has been used for association, prediction, and assessment.

For association, examples of algorithms are Bayesian regression [55], logistic regression [56], auto-associative kernel regression [57], locally weighted regression [57], partial least squared regression [58], etc. Chen et al. [57] employed an auto-associative kernel regression to explicit mapping relationships between the remaining useful life and health indexes to provide a reliable and effective RUL estimation. Sysyn et al. [58] employed principal component analysis and partial least squares regression to show a significant statistical relationship between a change

in the dynamic response of a railway crossing and the rolling surface degradation during the life cycle of the crossing.

For prediction, Wang et al. [55] employed Bayesian regression, a generalized linear regression method, for probabilistic assessment of crack-alike rail damage using acoustic emission monitoring data. This was developed based on a nonparametric approach in the context of Bayesian inference with the combined use of Bayesian regression and Bayes factor. To forecast the degradation of track geometry, Cardenas-Gallo et al. [56] proposed an ensemble classifier based on deterioration, regression, and classification. In regression, a binary logistic regression model was employed to predict how the future state of a particular defect is described by the independent variables.

Regression-based methods have also found their applications in feature extraction and selection in railway infrastructure. A multivariate regression analysis with feature selection and extraction techniques contains many popular methods like stepwise regression, ridge and lasso regression, principal components analysis [58], partial least squares regression [58], proper orthogonal decomposition [59], and locally weighted regression [57], etc. Azam et al. [59] developed a framework to detect damage under operational conditions in railway truss bridges. Before using an ANN to detect damage, the proper orthogonal decomposition was employed to categorize responses to different load patterns of trains near a bridge in their work. In [58], principal components analysis and partial least squares regression were two feature extraction methods applied to determine the rolling surface degradation during the life cycle of a crossing. To reduce the noise interference, the extracted features and the combined health indicators are all smoothed using the locally weighted regression in [57].

2.3.3. RAILWAYS AND METAHEURISTICS

Metaheuristics are strategies that guide the search for near-optimal solutions to an optimization problem. Convergence to a global optimum is not guaranteed, yet statistical analysis shows that these techniques can systematically get close to a global optimum. Their performance is rather problem-specific, but their fundamentals can be applied to a broader class of problems. Their search techniques range from local-search to global-search-based procedures, such as population-based approaches. Examples of metaheuristic algorithms are differential evolution, evolutionary computation, particle swarm optimization (PSO), genetic algorithms (GA), and ant colony optimization. For recent review papers on metaheuristics, readers are referred to [60–62].

In recent years, metaheuristics have been applied to various railway infrastructures, e.g., welds [18], bridges [63–67], tracks [68, 69], rails [70–73], catenary and pantograph [74, 75]. According to our survey, applications of metaheuristics lie within model updating [63, 65–67, 69] and optimization in structural design [64, 71–74], maintenance [18, 44, 70, 76], and operations and control [75].

In structural health monitoring and safety assessments, the Finite Element Method (FEM) is the standard tool for modeling the structural behavior of railway infrastructures. However, the FEM cannot accurately represent the dynamic

characteristics of a structure due to a wide range of simplifying assumptions. To achieve a more suitable finite element model of the structure [65, 67, 77], calibration, a.k.a. model updating, on uncertain parameters in the model with new measurements is typically needed. This aims at minimizing the relative difference between analytical predictions and experimental measurements. GA and PSO are two optimization techniques widely used for this purpose. GA is a search and optimization technique inspired by the process of natural selection and genetics. PSO, on the other hand, is inspired by the collective behavior of bird flocking or fish schooling, where particles adjust their position based on their own experience and the experience of their neighboring particles. With its simplicity and trustworthy evaluations, GA has been used in [63, 65, 67] to enhance assessment performance. In [63], Tran-Ngoc et al. employed GA to update the unknown model parameters for a railway bridge. Costa et al. [67] proposed an iterative method based on GA to minimize the differences between numerical and experimental modal responses of a stone masonry arch railway bridge. Ribeiro et al. [65] described the finite element model updating of a bowstring-arch railway bridge based on experimental modal data using an iterative procedure with GA.

As GA usually takes more time to converge towards a global optimum, PSO has been employed by researchers to find the global optima of the problem. Qin et al. [66] applied the kriging model and PSO for the dynamic model updating of bridge structures using the higher vibration modes under large-amplitude initial conditions. Tran-Ngoc et al. [63] employed PSO to minimize the discrepancies between the experimental and the numerical results. A comparison between applying PSO and GA was also studied in their work. The results showed that the PSO algorithm provided better accuracy, and it reduced the computational time compared to GA. For model updating, Shen et al. [69] employed PSO and proposed a fusion strategy that directly infers the stiffness of the rail pad and the ballast from measured frequency response functions based on Gaussian process regression. It was demonstrated that their fusion method outperformed the PSO method in terms of accuracy and time efficiency.

Metaheuristics have also been applied for structural design optimization. GA is the most widely used technique within this area based on our literature search results. Sgambi et al. [64] proposed a method based on the combined application of GA and FEM to design a complex long-span suspension bridge. In [72], GA was used to optimize the rail profile on the Stockholm underground to alleviate a problem with rolling contact fatigue without consequent issues with wear and noise. Li et al. [73] proposed a hybrid method to design a challenging railway alignment for topographically complex mountainous regions. The hybrid approach uses a bidirectional distance transform and GA. Even though this hybrid method improved the performance of GA and solved the challenging problems concerning topographically complex mountainous regions, it was computationally more expensive than the other existing methods. In addition, differential evolution is another technique used in [74, 78]. In [74], differential evolution was used to define the regressive function and to determine the optimum values for stable current collection performance of the pantograph for a high-speed train. In [78], the railway

track Health monitoring system employed a dynamic differential evolution algorithm for identifying defects in railway tracks. In [79], Harris hawks optimization with PSO-based mutation were used for predicting soil consolidation parameter. In [80], the performance of the Grey Wolf optimization, PSO, and GA were compared for the estimation of railway track parameters. Their results showed that the Grey Wolf optimization performed the best in most of the used tested cases.

The information provided by the metaheuristic-based methodology can be used to support the decision for maintenance. Typically, most optimization solutions in railway infrastructures have focused on single-objective problems. To schedule the maintenance crew for freight rail optimally, Gorman et al. [76] adopted three techniques (mixed integer programming, constraint programming, and GA) and compared them. The results showed that the mixed integer programming network formulation showed the most potential for quickly finding quality solutions among the techniques used. Zhang et al. [68] developed an enhanced GA approach to deduce the optimal scheduling for the maintenance work of railway tracks in the UK. In the enhanced GA, they employed various additional techniques, e.g., orthogonal experimental design to initialize the population, roulette selection to generate a population for the next generation of solutions, and the differential evolution operator to perform the variation process. Moreover, the selection was executed on the pooled solutions from both the parent and the newly generated offspring to guarantee that the best solution was not disregarded.

However, in railway maintenance optimization, focusing on a single objective is not always valid. In the structural health monitoring context, sometimes two or more failures often occur simultaneously. It is thus necessary to consider all related goals as bi-or multi-objective functions to be optimized. These objectives make it challenging to find a single solution that optimally satisfies all of them simultaneously. Evolutionary Multiobjective Optimization (EMO) is a computational optimization technique that aims to solve problems with multiple objectives.

In the maintenance context, reliability, life-cycle costs, and sometimes environmental costs are to be considered. Such optimization concerns multiple objectives and searches for solutions in the global Pareto-optimal region, where solutions cannot be reallocated to make one objective better off without making at least one of the others worse off. This is to achieve solutions that are separated from one another to the maximum possible extent to form the trade-off surface in the objective space [70]. Various multi-objective methods have been employed to obtain multiple Pareto optimal solutions. Generally, two classes can be distinguished: genetic algorithm-based [18, 70, 71, 75] and evolutionary algorithm-based approach [18]. In [18, 70, 71, 75], multi-objective optimization was handled by a fast nondominated sorting genetic algorithm (NSGA). In [75], NSGA2 was used to optimize both the contact force and the consumption of the energy supplied by the control force for the design process and control of the catenary–pantograph system. In [71], Choi et al. adopted NSGA2 to minimize both the wear and fatigue of a wheel with consideration for derailment, lateral force, vehicle overturning, and vertical force generated during motion along a curved track. The research objectives of Caetano [70] was to support an informed decision that considered not only the railway track

life-cycle cost but also the track occupation. Nunez et al. [18] also performed multi-objective optimization to identify the set of all Pareto optimal solutions that formed the trade-off surface between performance and maintenance cost for rail welds in a regional railway network. In their work, a multi-objective optimization tool from Matlab was used, and the algorithms ARMOEA, NSGA2, SPEA2, GrEA, RSEA, and VaEA, were compared. It was shown that SPEA demonstrated superiority among other algorithms for their proposed maintenance decisions optimization problem, at least when the number of integer decision variables was not extremely large.

2.3.4. RAILWAYS AND PROBABILISTIC GRAPHICAL MODELS

A probabilistic graphical model (PGM) expresses relationships between variables based on graphic architectures. It operates to provide an intuitive framework for representing uncertainty using probability distributions [81]. PGMs can be divided into two classes, i.e., Bayesian models and Markov models [82]. Examples of algorithms within PGMs are Naïve and non-Naïve Bayesian, Bayesian (belief) network, Hidden Markov model, Markov models, and Averaged one-dependence estimator. For recent review papers on PGMs, readers are referred to [83, 84].

PGMs have been applied for various railway infrastructures, e.g., railway bridges [85–87], catenary [88], turnouts [89, 90], rails [39], tracks [91]. They are considered a powerful tool for anomaly quantification in the presence of uncertainty. There has been a growing interest in applying PGMs to fault diagnosis and prognosis in railway systems. In particular, they offer solutions to damage detection, predicting the future conditions of railway infrastructures, identifying causality inference, and providing a learning mechanism that can be adaptive over time.

For railway infrastructures, it happens that multiple failure events cannot be identified and the probability of failure cannot be reached quantitatively by event tree and fault tree analysis [90]. Many researchers have then proposed methods based on the Bayesian network to identify the probability and the underlying root cause of failures in railway infrastructures through various basic principles and inference algorithms. Generally, the systematic Bayesian networks are developed in three steps; 1) variable selection, 2) structural design of the Bayesian network, and 3) parameter learning. Wang et al. [89] proposed a Bayesian network for weather-related failure prediction in railway turnout. In the Bayesian network development, they first selected variables that related to weather and failures. An entropy minimization-based method was presented to discretize model variables in order to reduce the input type and to capture better performance. In the second step, they designed the structure of the Bayesian network by learning from real data combined with expert experience. Lastly, in parameter learning, the Bayesian network was transferred into a noisy independence of causal influence model and took advantage of learning the conditional probabilities using a noisy MAX model to overcome the parameter learning problem from small data sets. Monte Carlo simulations were also employed to determine with greater accuracy the mean and the confidence interval for weekly estimations of failures. Dindar et al. [90] employed a Bayesian network to analyze the probability of train derailments caused by extreme

weather patterns on railway turnouts. They followed the same steps as in [89] but employed fuzzy probability using Buckley's confidence interval-based method to allow for gathering more information than just a single confidence interval or just a point estimate in the last step of the Bayesian network development. As opposed to [89, 90], Imran Rafiq et al. [85] proposed a dynamic Bayesian network to model the variation in the bridge condition with time. In a dynamic Bayesian network, the Bayesian model is connected to its successive 'time slices' through temporal links to form a time-varying model, while the Bayesian network model discussed in [89, 90] serves as a 'snapshot' model to estimate the railway infrastructure condition based on its constituent element conditions at a given point in time. Markov chain principles were employed to quantify the transitional probabilities in [85].

PGMs are computationally efficient in updating the model when new information regarding the condition state of any variable becomes available. Neves et al. [87] proposed a PGM-based method to update an ANN model for damage detection of railway bridges. In their work, a Gaussian process was employed to statistically analyze the distribution of the errors using the predicted acceleration errors obtained from the developed ANN. This was to define the detection threshold for the system, allowing the determination of the probability of true and false detection events. Finally, probability-based expected cost, as a function of the chosen threshold, was proposed based on the theorem of Bayes to update the model. To infer some stiffness properties of the ballast and subsoil from measurements carried out on the railway bridge, considering uncertain seasonal effects, Gonzales et al. [86] also employed Bayesian updating of a 3D finite element model with Markov-Chain Monte Carlo sampling to determine posterior distributions of the uncertain stiffness properties in the warm and cold states of the bridge.

Another typical application of PGMs is for analysis of the risk factors correlated with failures in railway systems. Jamshidi et al. [39] proposed a failure risk assessment framework based on the PGM for analyzing the rail surface defects called squats. The proposed framework aimed to estimate the probability of rail failure based on the growth and severity of rail squats. In their work, defect severity and growth analysis were performed via an N-step ahead prediction model using data measured by ultrasonic detection. To assess model uncertainty and robustness for stochastic data behaviors, the Bayesian inference model was employed to estimate the failure probability. Andrade et al. [91] used a hierarchical Bayesian model to handle the spatial correlations of the deterioration rates and the initial qualities for consecutive track sections. With a hierarchical Bayesian model, the predictive model for the degradation of railway track geometry was improved based on the deviance information criterion.

Furthermore, a Markov random field model was developed in [88] for image segmentation in order to facilitate automatic fault detection for the loose strands of the isoelectric line in the catenary system. This work employed the Markov random field model to provide a link between the uncertainty description and prior knowledge in their work. They showed that detection accuracy was improved with the use of Markov random field.

2.3.5. RAILWAYS AND FUZZY SYSTEMS

Fuzzy logic can deal with ambiguity. While traditional logic allows a proposition to be either true or false, in fuzzy logic, a proposition has a degree of truth, ranging from being completely true to completely false. A formulation based on fuzzy logic is defined by multi-valued logic where the value of a variable can be any real number between, but not limited to, 0 and 1. The applications of fuzzy logic-based methodology often lie within solving a problem with uncertainties, vagueness, or imprecision [81]. Examples of fuzzy logic methods are type1- type2-fuzzy logic, Takagi-Sugeno fuzzy inference system, Mamdani fuzzy inference system, fuzzy C-means, and adaptive network-based fuzzy inference system. Interested readers in fuzzy logic are referred to review papers such as [92–95].

The applications of fuzzy logic-based methods often lie within the problem of prediction and decision under uncertainties or vagueness. Examples of their applications for railway infrastructures are detection, risk assessment, and decision support [96–100].

For detection problems within a railway environment, false alarms are one of the biggest issues that create financial losses in the railway industry [96]. False alarms are generated when the system detects a non-existent obstacle or does not detect an existent obstacle. Techniques utilized to alleviate the problem include, e.g., the design of the sensor used, the conditions in which the sensor is working, and the signal processing that is carried out by the system, Garcia et al. [96] employed a Mamdani fuzzy controller to weigh the certainty of the existence of objects given by a multisensory system to inform the monitoring system about the existence of obstacles. Hussain et al. [99] also employed a fuzzy logic-based method to deal with such uncertain circumstances in detecting adhesion and its changes under different wheel-rail contact conditions.

As detection and diagnosis systems can facilitate the decision-making process, much attention has been paid to improving the reliability of such systems by using fuzzy logic-based methods. As numerous circumstances threaten safety and operations in railway infrastructures, it is necessary to consider key performance indicators (KPIs) affecting the health conditions of railway infrastructures over time. Under the stochasticity of operational conditions, fuzzy logic-based methods have been adopted to assess the dynamics of threats. Within this context, Jamshidi et al. [97] and Li et al. [100] proposed a technique stemming from fuzzy logic. To assess the dynamic of water inrush in the progressive process of tunnel construction, Li et al. [100] employed a fuzzy evaluation method to quantitatively analyze the risk level of factors concerning both geological condition and construction situation. Jamshidi et al. [97] presented a fuzzy Takagi–Sugeno interval model to predict squat growth over time under different possible scenarios and under different maintenance decisions. Moreover, a Mamdani fuzzy expert system was used to calculate a single KPI to conclude the dynamics of the deterioration of railway tracks.

In addition to railway safety and operations, there are increasing requirements concerning riding comfort. As railway tracks deteriorate over time and maintenance becomes expensive, Metin et al. [98] presented a fuzzy logic controller to ensure that the vibration responses are within permissible limits. In their work, the

performance of the fuzzy logic controller was compared with the conventional proportional integral derivative controller. The results showed that the fuzzy logic controller demonstrated superiority in active vibration control and increased passenger comfort. Other notable AI techniques applied in catenary systems using fuzzy logic are [101–105].

2.3.6. RAILWAYS AND CLUSTERING

Clustering is a technique for partitioning a set of objects into different data groups. The procedure is done so that objects in the same cluster are more similar than those in other clusters. Further, different clusters are preferred to contain rather different samples. Thus, clustering methods require selecting an appropriate measure and an objective function that minimizes the within-cluster variation and maximizes the between-cluster variation. Different measures result in different clusters. Examples of clustering algorithms are k-means, k-nearest neighbor, self-organizing maps, mixture of Gaussian models, and hierarchical clustering. Interested readers in the field of clustering are referred to review papers such as [106–108].

Various applications in the area of railway monitoring and maintenance have been found using clustering methodologies. For monitoring, clustering can be employed to detect and assess damage in railway infrastructures. Cardoso et al. [109] proposed a clustering technique to uncover hidden patterns in monitoring data. A hierarchical clustering algorithm was applied to modal parameters and used to perform automated modal identification in railway bridges. Unlike [109], Cury et al. [110] proposed a novel technique based on symbolic data analysis for providing a clustering of different structural states in which the number of states is not known a priori and has to be determined. The symbolic clustering methods considered in [110] included hierarchy-divisive methods, dynamic clustering, and hierarchy-agglomerative schemes. The results highlighted the large capability of the symbolic data analysis methods to provide clusters of different structural behaviors in railway bridges. Both hierarchy-divisive and dynamic cloud methods demonstrated better results compared to those obtained by using the hierarchy-agglomerative method.

Clustering-based methodologies have been applied to support decisions for the optimal planning of maintenance of railway infrastructures. Within this context, Cirovic et al. [111], Su et al [19], and Peng and Ouyang [112] presented a clustering technique to determine groups of maintenance jobs and groups of railway assets that can be treated within either the allocated time slots or budget allowance. In [111], Cirovic et al. proposed a technique based on fuzzy clustering to define the optimal strategy which supports the choice of level crossings for installing safety equipment in Serbian railway. These criteria were used to form a set of data for training the adaptive neuro-fuzzy network. In [19], Su et al. solved a mixed integer linear programming problem to obtain the resulting optimal clusters of railway components that were treated within the allocated maintenance time slots. This was to determine the trade-off between traffic disruption and the total setup cost associated with each maintenance slot while guaranteeing that the total duration of the resulting maintenance slots was no less than the estimated maintenance

time. In [112], F. Peng and Y. Ouyang also employed a mixed-integer mathematical programming model in the form of a vehicle routing problem with side constraints to classify track maintenance jobs into projects. The algorithm framework of job clustering considered in their work included a constructive greedy heuristic, a local search heuristic, and a feasibility heuristic.

2.3.7. RAILWAYS AND TRANSFER LEARNING

Transfer learning-based methods are developed to tackle problems concerning limited labeled data in supervised learning. The knowledge from one or multiple tasks (the source domain) is expected to transfer to other related but different ones (the target domain). The transfer scenarios can be divided into two categories, i.e., transfer in the identical machine and transfer across different machines [82]. The latter is also known as domain adaptation, where differences between feature spaces and label spaces are allowed, e.g., transferring knowledge from railway track to railway catenary. For recent review papers on transfer learning, readers are referred to [113, 114].

The existing supervised AI learning algorithms manifest a relatively advanced performance in different railway engineering applications. Their fruitful performance relies extensively on sufficient training data and high-dimensional balanced datasets [40, 42, 43]. Otherwise, imbalance and insufficient labeled datasets can impair the ability of, e.g., the classification algorithms. For railway engineering, the amount of monitoring data collected from railway infrastructures, especially defective samples, cannot generally be collected in a short time to obtain balanced datasets for network training under different operating conditions [115–118]. To alleviate this issue, increasing attention has been paid to developing algorithms based on the transfer learning approach. It refers to the concept of transferring the knowledge of the pre-trained model to other related but different ones. The transfer scenarios can be developed using other AI methodologies such as CNN [115, 116], deep learning [117, 118], and AdaBoost [115, 119].

Zhong et al. [115] and Chen et al [116] proposed a transfer learning approach based on CNN. In [116], a multi-layer CNN was employed in which the low-level layers of a model were pre-trained on large audio data for feature extraction. Next, the acoustic-specific features were transferred to train the high-level layers by using acoustic emission monitoring data for condition assessment of the rail structure. To overcome the problem of a limited amount of defective data, Zhong et al. [115] proposed an improved algorithm based on the Faster R-CNN algorithm to build a transfer learning model in defect localization.

Based on deep learning, Zhong et al. [115] also introduced an algorithm based on a generative adversarial network to construct defect detection models by using only normal samples. Yao et al. [117] employed a generative adversarial network to generate additional fault samples in order to balance and train the data sets. Residual Network was developed for fault diagnosis and classification of track fasteners, and the extended data set was used for group training and validation. With generative adversarial network and residual network, the results showed that the fault detection accuracy of rail fasteners did not impair when using a serious shortage of fault

data. In [118], Zhuang et al. employed firstly extended Haar-like features to extract effective features of cracks on railway ties and fasteners. Secondly, a cascading classifier ensemble was developed by integrating individual cascading classifiers built via the LogitBoost algorithm with a bootstrap aggregation. However, the framework proposed in [118] could not identify patterns that were not included in the training dataset.

Among transfer learning algorithms, the Adaboost algorithm is one of the most widely used tools to overcome the problem of insufficient training data. The core idea of AdaBoost is to iteratively train the weak learning algorithm, whose predictive performance is lower, for the same data set and integrate them into a strong learning algorithm, whose predictive performance is higher. Lin et al. [119] employed AdaBoost to relate catenary fault frequency with meteorological conditions. In their work, only a small number of training samples were classified correctly by each weak classifier chosen from the single decision tree. The AdaBoost algorithm was adopted to adjust the weights of misclassified samples and weak classifiers and train multiple weak classifiers. Finally, the weak classifiers were combined to construct a strong classifier for the final prediction.

Transfer learning can be applied to a pre-trained model of any type and transfer learning alone particularly deals with the issue when the amount of available data for the target task is limited. However, the combination of transfer learning with other neural network architectures (such as recurrent neural networks, and convolutional neural networks) can lead to hybrid models that leverage the strengths of different approaches, providing more accurate solutions for railway problems. Furthermore, when multiple neural networks are trained independently, the knowledge of the pre-trained models can be aggregated by using transfer learning in an ensemble setting and can be adapted to different railway networks or different environments. The combination of transfer learning with neural networks can potentially lead to improved performance, generalization, and robustness. In [120], the concept of transfer learning was applied to deep convolutional neural networks for multi-category damage image classification recognition of high-speed rail reinforced concrete bridges. The results showed that the approach reduced the training time of the neural network models and led to lower generalization errors. In [121], deep transfer learning and graph neural networks were proposed for the health assessment of high-speed rail suspension systems. Using transfer learning in an ensemble setting to combine transferable features in the source domain, the shortage problem of labeled data in the real operating condition was alleviated as the initial hyper-parameters of the model in the target domain were obtained from the pre-train model in the source domain.

2.3.8. Discussion

Table 2.4 presents the potentials of the selected AI methodologies for applications in railway infrastructure and their limitations. Based on these, some insightful findings are:

- Neural networks require further adaptations to describe real-world physical

interpretation due to their black-box characteristic. Having a black box model that is not guaranteed to perform under new unexpected conditions makes the users and rail operators concerned about the use of the model predictions. Based on the review in this section, it is observed that several works have applied neural networks in combination with regression [48, 50] and other soft-computing techniques, e.g., support vector machine [51], decision tree [43], and fuzzy [39] to provide more explainability about the correlation between model behaviors and the physical problem.

- It was observed that researchers have developed hybrid models combining two (or more) AI techniques to perform a specific task. Examples of combing AI methods are 1) meta-heuristics-based method with neural network-based method [73, 87], 2) PGM-based method with neural network-based method [39, 43], 3) regression-based method with PGM-based methods [55, 56], etc. The use of a combination of methods has the potential to improve overall performance when these methods are complementary to each other. For instance, global optimization approaches can potentially find parameters of neural networks that better fit an objective function. However, when different methods solve a similar task, a major emphasis on the analysis of the consensus between these methods is needed.

- Deep learning concerns multiple layers of computational units in which the actual optimization of the whole structure is a highly non-convex problem. They contain a huge amount of parameters and, in some cases, more than millions of parameters which results in long computation time to find a near-optimal solution. Moreover, large labeled datasets, preferably balanced, are required to train deep learning models. Despite these shortcomings, interest in these methods has increased in view of the rather impressive results from other fields. To alleviate the issues and make its advantages more pronounced, transfer learning is employed to help retrain the trained deep learning models to perform a similar task. This not only reduces computational effort but also the amount of training data for deep learning.

- PGMs and fuzzy logic have received a growing interest for applications in fault prognosis due to their powerful capability to deal with the presence of vagueness, uncertainty and solving inference problems [39, 85, 89–91]. However, there are several sources of uncertainty, e.g., measurement data, model structure and parameters, and different data behavior from future operational conditions. These uncertainties propagate over time and the existing models have to be updated when new information regarding the health condition of any variable becomes available. Most existing models are computationally inefficient in updating. Based on our review, however, limited work has been found to address such a problem for railway infrastructure.

2.4. Challenges from railway infrastructure

State-of-the-art intelligent solutions show good generalization capabilities to solve problems from different fields. Some particular challenges from railway infrastructures prevent direct exploitation of the existing state-of-the-art methodologies, as will be highlighted in a sequel. Consequently, their successful application in the field of railway infrastructure requires designing and developing methodologies to capture the particular and challenging characteristics of railway infrastructure.

2.4.1. Insufficient and imbalanced data for model training

For railway infrastructure, conventional supervised methods, particularly deep learning, require a large amount of labeled data available for learning to guarantee their performance. However, collecting accurate and verified labeled samples of high-quality faulty and healthy states from thousands of km of rail lines is extremely difficult, costly, and time-consuming. Regarding class information for defects, often few labeled data are available due to the lack of historical data with sufficient quality and localization. Likewise, healthy data are difficult to label because of their variants of behavior at different locations; in particular, rails are affected by local track dynamics and different stochastic variables. Sometimes, there is no standard/threshold to evaluate the level of health conditions. For instance, an embankment is one of the areas in railway infrastructure that require further study. Furthermore, in some railway infrastructure, obtaining a wide variety of class information for defects is extremely difficult. Therefore, data from healthy infrastructure are abundant, whereas defective ones are few. As a result, the data used for training AI models are seriously imbalanced, and labeled data are insufficient.

2.4.2. Training AI models with complex railway data

Railway infrastructures are complex and highly nonlinear. They involve different assets and can be affected by various anomalies. Detecting failures and maintaining the structure requires multiple measurement systems. Most of the information about the condition of the infrastructure is collected with inspection systems. Typical systems in the industry include eddy current, ultra-sonic, vibration measurements between wheel and rail using accelerometers, video images and track geometry recording vehicles [8, 9]. Depending on track tonnage, the number of trains passing by the track, and maximum line speed, data measurement frequencies and data processing requirements can differ substantially. Thus, selecting a proper AI methodology must account for the nature of the railway components and their inherent dynamics. There is a significant interdependency between railway track-related assets, not only in functionality but also in using anomaly detection algorithms or maintenance planning. For example, a track video scan [122–125] allows the asset manager to capture the health condition of different track components, e.g., fasteners, switches, and sleepers [126–131]. However, video image-based measurements can only capture anomalies in the track structure when they are visible. This means that early-stage anomalies in rail (invisible ones) or

vertical irregularities in the track cannot be detected effectively using only video cameras. Using together images and other sources of data, such as axle box acceleration (ABA) measurements, track geometry, or eddy current and ultrasonics, can provide a more integrated assessment of the track condition. ABA measurements can detect light squats [132, 133], which occur at frequency bands up to 2.5 kHz with train speeds of about 100 kilometers per hour [134]. New technologies, such as a Laser Doppler Vibrometer sensor, can also provide continuous monitoring along a railway line, and they can measure with frequency sampling that goes higher than the order of MHz. Thus, continuous monitoring of hundreds of kilometers with the latest technologies creates a better overview of the current track condition, but at the expense of creating a huge volume of data and a very high dimensionally problem from which key features are to be extracted to represent the data effectively. In this case, developing ultra-fast AI solutions, also considering edge computing [135], could support addressing these challenges.

In addition to the characteristics of the railway infrastructure, the most suitable AI method can be determined based on the nature of the measurement data. Measuring data can vary from an unorganized and semi-organized data structure to a fully organized structure. Measured data collected by human operators, e.g., track information and historical operational activities, usually are fully structured or semi-structured. On the contrary, advanced anomaly detection systems contain a massive sampling pool and high complexity as they are high-dimensional and nonlinear that require additional methodologies for preprocessing, including noise removal, feature extraction, and selection.

Employing multiple systems to monitor railway infrastructure performance indicates the need to deal with heterogeneous data. The information about defects obtained by a single source can easily show trends; however, it is limited by the nature of the measurement itself. When different data types are exploited to extract information and to provide additional information about the same defect, we have the risk that the data sources are not containing complementary information for data analytics. That is when the physical understanding of the advantages and limitations of the different monitoring systems is not included. Different systems might provide different detection reports that appear to contradict each other. Thus, new AI solutions to deal with heterogeneous data can also support the development of holistic approaches to integrate railway information and make the decision-support models more robust. In addition to the integration of information, data alignment from different measurement trains on a track is another challenge. A robust optimization model is needed to correct positional errors of inspection data from heterogeneous measurements [136].

2.4.3. TRAINING AI MODELS FOR MAINTENANCE PURPOSES

Railway infrastructures are dynamic, stochastic, and distributed parameter systems that change critical parameters over different locations and times. Moreover, their failures have complex characteristics that result from multiple incidents involving different causalities and uncertainties affecting their functionality, e.g., operational conditions, maintenance activities, weather conditions, traffic loads, the geometry of

the infrastructure, and the properties of construction materials [137, 138]. Therefore, it is crucial to have an accurate remaining useful life and degradation pattern estimation. An early prediction may result in over-maintenance, and a late prediction could lead to catastrophic failures. Consequently, the existing degradation models for rails have to be updated when new information regarding the health condition of any variable becomes available. However, some models may not be computationally efficient in updating. New models and techniques are needed to alleviate the issue.

To estimate remaining useful life or degradation patterns, many existing models rely on handcrafted features representing degradation processes caused by those factors. The feature selection/extraction often requires domain knowledge and expertise about common causes leading to system degradation. For instance, the location or type of rail surface defects may cause different degradation patterns. The dependency on a large variability of datasets and experimental tests in large railway infrastructures presents a challenge for training in prognostic models. Research in certain applications uses data from run-to-failure tests, from which the labels can be derived [139]. For railway applications, it is impossible to conduct such tests. To accurately determine the associated remaining useful life and degradation pattern at every time step for railway infrastructure, the threshold of its failure must be defined. Therefore, some experiential knowledge is needed. For instance, a rail is deemed reliable when the size of rail surface defects achieves a threshold of a certain length [39]. As such, condition-based maintenance strategies have to systematically improve to capture new situations and to perform better under new conditions, e.g., when facing new challenges from more intensive use of the infrastructure, climate change, and harsh environmental conditions.

Railway infrastructure systems are also large-scale due to various reasons. Firstly, railway infrastructure often involves many basic components distributed over various kilometers of railway tracks. Further, a railway line can cover a long distance (e.g., over 250 km) with defects that have a size in the order of centimeters (e.g., squats) which their locations are distributed over the whole infrastructure [19]. This causes the maintenance optimization problem to become large and intractable. Obtaining an exact resolution of each plan along the prediction horizon is time-consuming and leads to the large-scale optimization problem [140]. Secondly, maintenance operations over the whole prediction horizon might change when performing maintenance optimization based on a rolling horizon under real-life conditions. That is, long-term maintenance plans might continuously change according to new predictions and new operation plans. Consequently, the flexibility in the maintenance contracts to include adaptive plans and methods for learning from these plans can be supported with new AI methodologies. Lastly, and most importantly, incorporating the inherent characteristics of the railway system gives rise to a complex nonlinear model that becomes too large and complex to solve efficiently and that leads to a high computational burden [141]. For these, the amount of information needed to guarantee the proper operation and the high computational burden of solving problems for such complex and large-scale systems present challenges in research concerning AI. The difficulties include stack overflow and long computation time, and a very challenging-to-obtain set of optimal solutions

due to the irregular shape of the resulting Pareto fronts.

2.4.4. BARRIERS FOR AI DEPLOYMENTS IN THE RAILWAY INDUSTRY

Many stakeholders are interrelated within the railway industry. However, they are conservative and usually resist the changes introduced by the digitalization of railway infrastructure, as these can affect the way they worked before. Likewise, the lack of understanding of AI used and the reliability of the results are barriers to the adoption of new methods, especially with regard to safety requirements. Without effective cybersecurity, rail operators cannot be assured of securing their data and information. Consequently, business resources cannot be consolidated, and data are scarce with limited access.

Other aspects that prevent the successful implementation of AI in railway infrastructures also include a lack of standards, traceability, and interpretability of results using complex AI methodologies, particularly neural networks. Results and their implications for the safety of railway infrastructure provided by AI are often difficult to understand. As the infrastructure manager is responsible for his assets and has to ensure the required safe operation, the physical explanation of the problem and the causality are crucial for preventing failures. Failing to provide such information prevents the exploitation of AI methodologies for decision support systems.

Even though there are more applications of AI methodologies in the railway industry, some projects did not have a continuation. The reasons are, firstly and importantly, lack of budget. Secondly, digitalization is not complete and accurate. The railway industry tends to be conservative, and for some inframanagers, the documentation is mainly paper-based. Dynamical models used are primarily in 2D and digital maps of the asset positions are partly not available. This creates a problem of allocating failures when the location of railway infrastructures is not accurate and precise. Therefore, AI developments are needed to check and improve localization accuracy in order to obtain reliable data in the future. Lastly, system integration requires a proper understanding of the system hazards and associated risks. Proper integration of a new system into the current operating system requires to be done in a smooth way and without interrupting the service. Moreover, how to implement AI in real operations is another challenge.

2.5. RESEARCH DIRECTIONS AND FUTURE OPPORTUNITIES

The challenges discussed previously create a need to develop new intelligent methods based on AI that should be tailored to the particularities of railway infrastructures. This section presents research directions and future opportunities for railway infrastructure. As the use of AI is not yet standardized and their solutions are mostly not traceable and interpretable, implementing AI solutions only serves as a decision-support for railway infrastructure managers at the moment. Humans are still required to make final decisions. We have not yet reached the point of having fully automated AI capable of making final decisions.

Based on our literature review and our view, research directions and future opportunities for railway infrastructure given in Subsections 2.5.1 - 2.5.7 are conceivable as there exist current developments in academia. However, further validations in different environments/network lines and standardizations are still needed before reaching a maturity level to be ready for real implementation in the railway industry.

It is noteworthy that some research directions are relatively difficult to achieve in the upcoming years within the context of railway infrastructure. Given the rapid pace of technological development and advancements, making such conclusive judgments about the feasibility and ease of potential research directions in the near future for railway infrastructures is complex and subjective. Therefore, the discussion only serves as an informative and advantageous resource for the readers. Drawing from our perspective, these are transformers (see Section 2.5.8), metaverse (see Section 2.5.9), and emerging technologies such as blockchain technology (see Section 2.5.10). This is because their adoption and implementation are hindered by the unique challenges and characteristics of the railway infrastructures. For instance, many railway infrastructures and systems have been in place for decades. They may have been designed and built using outdated technologies and standards. Introducing new technologies often requires retrofitting or replacing existing infrastructure, which can be expensive, time-consuming, and disruptive. Moreover, integrating new technologies like transformers or blockchain requires careful consideration of how these technologies will interact with existing systems and processes. A skilled workforce with expertise is also required for implementing and maintaining advanced technologies like transformers, metaverse-related solutions, and blockchain where railway organizations may lack the necessary expertise and resources.

2.5.1. Hybrid models

Hybrid models are promising and have the potential to offer more competitive AI and machine learning models with high performance. Hybrid models refer to a combination of multiple methods or techniques to solve a particular problem. They are developed not only to improve overall performance via their advantages but also to alleviate the limitations of the methods. The models can be constituted by combining 1) different AI methods, 2) human experts and AI methods, 3) physical-based methods or other traditional methods and AI methods, or 4) a mixture of AI, human experts, and physical-based models. Tailoring hybrid models to railway infrastructure applications requires in-depth knowledge of the particularities of the problem and a particular focus on the interfaces between the methods. For example, the performance of probabilistic models in prognosis can be impaired by the accumulating error from using results obtained from diagnosis models based on deep learning. Then, a combination of AI-based models with human-expert or physical-based knowledge is required. In catenary systems, it was mentioned in [142] that, despite the fruitful outcomes of using AI for catenary systems, the growing dependency on data has led to underutilized knowledge of physics accumulated in the past decades. However, the use of AI for catenary systems seldom exploits the physical knowledge to improve the resulting performances. It has been

demonstrated that PGMs such as Bayesian networks can consider the underlying physics in inspection data using tailored features [143]. Likewise, hybrid multi-scale models can also capture degradation mechanisms for various components involved in the maintenance process while considering some parameters and dynamics determined by data-based approaches. As the methods explicitly include the physical/mechanical characteristics of the infrastructure, the link between data and the physical infrastructure system can be explainable. This helps to improve the interpretability of AI methodologies, particularly neural networks. Therefore, it can be foreseen that AI applications will be even more powerful when combined with knowledge from other approaches. Hybrid models will allow researchers in railway engineering to enhance model effectiveness and get better solutions for railway problems. Moreover, combining AI-based models with human-expert or physical-based knowledge is expected to increase exploitation and reduce resistance to the use of AI in the railway industry.

2.5.2. LEARNING METHODOLOGIES

Learning methodologies are crucial to improving performance based on current and previous experiences systematically. AI methods have been used to learn from current data and performance. However, learning can be continuous based on previous experiences and mistakes. For example, defects that were not detected on time or maintenance decisions that were not correctly prioritized. Learning mechanisms (such as deep reinforcement learning) allow us to systematically include ways to improve our perception and decision mechanism continuously. Learning methodologies provide practical answers to how railway infrastructures 1) can perceive their condition, 2) can make optimal and timely decisions, and 3) can keep learning to improve their performance over time systematically. For these, three promising approaches to learning methodologies are highlighted as follows:

DEEP LEARNING

Deep learning has shown the capability to extract highly complex abstractions from different data types and achieved great success in many applications. It is foreseen that deep learning has opened up an opportunity to step beyond the capabilities of a human operator. Deep learning provides a promising direction for big data analytics for assessment and prediction using a tremendous amount of railway data. With the help of deep learning, inspections of railway infrastructures can be fully automated, which fully or partially replaces traditional manual testing and visual inspections. Moreover, computational intelligence methods for expert system design can support railway infrastructure assessment in real time. For instance, in [144], deep learning relying on image-based data that can capture the vibrations of pantograph-catenary interactions and the health conditions of catenary-supporting structures was employed to simultaneously monitor the health condition of catenary components, including contact wires, messenger wires, droppers, and up to 12 types of supporting components. In [40, 41, 47, 88, 145–154], deep learning was also employed for defect detection and achieved satisfactory results in imaging data.

Likewise, recent deep learning-based approaches have significantly demonstrated their capability to fuse information for multi-sensor condition data, including the fusion of static, moving, and crowd-based sensing technologies [43, 104]. Various fusion techniques using deep learning algorithms have been proven to assist in learning features from multiple signal sources simultaneously and effectively [57]. However, choosing data representations of fused data plays a fundamental role in designing data fusion algorithms. As a result, how to integrate information from multiple data sources and then make a more robust deep learning algorithm is another challenging task for railway infrastructure. In addition to data-based deep learning approaches, physics-informed neural networks [155, 156] have recently emerged as another promising approach for solving problems based on mathematical physics models of railway infrastructures with a small amount of data.

Transfer learning

Within the concept of transfer learning, we can benefit from existing pre-trained models in various ways. Firstly, statistically similar datasets of identical structures can be leveraged to replace the requirement of augmenting a training dataset, especially when some of the actual measurement data are difficult to obtain. In [157], it showed that transfer learning allows the CNN model trained in one domain to the use in other domains where training data are lacking. In [116], transfer learning was employed for evaluating structural conditions of rail in a progressive manner by using acoustic emission monitoring data and knowledge transferred from an acoustic-related database. Secondly, transfer learning has shown its potential to relax the prerequisite for training a deep learning architecture containing up to millions of model parameters. This allows computation time to be reduced, and this facilitates online monitoring of railway infrastructure systems. Thirdly, transfer learning can be used to adapt to work under new conditions where the models have not yet been tested/trained. Due to the impossibility of acquiring training data that represent all operating conditions and fault types, transfer learning is beneficial to make use of information between units or between models. In [158–160], transfer learning was shown to be able to train models that are robust to newly encountered conditions. This resulted in an improvement in the model performance on the target task. Therefore, transfer learning should be further explored in the field of railway infrastructure, where we aim to apply knowledge from a different railway network to the monitoring and decision-making processes in another network. With transfer learning, intelligent sensing and decision support systems can improve over time.

Deep reinforcement learning

Deep reinforcement learning (DRL) refers to a broad group of learning techniques that emulate how living beings learn by trying actions and learning from successes and failures [161]. Its learning process is experience-driven, and its efficiency is enhanced by trial and error to optimize the cumulative reward. In DRL, labeled data are not required, which is beneficial when mainly unlabeled data are available. DRL has shown the potential to handle the dynamic and complex nature of physical problems where solutions to new problems can be adjusted and utilize experience

and knowledge learned from solving old problems. For instance, an algorithm developed for track component A can be applied to track component B even though they might be at the same usage level, track tonnage, or environmental situation. In [162], a DRL approach was developed to refine the localization of fasteners in the catenary support to improve an automatic looseness detection method based on deep learning. With state-of-the-art methods, the learning process can be fast and efficient. DRL is also capable of modeling complex stochastic environments and handling relatively high-dimensional problems. It can be used to optimize maintenance and renewal planning by considering cost-effectiveness and risk reduction over a planning horizon and taking into account predictive and condition-based maintenance tasks, as well as time, resource, and engineering constraints [163]. However, DRL has not experienced many key developments compared to deep learning. Research on its application to solve problems related to renewal and maintenance planning for railway infrastructure is still limited. As DRL is relatively new to railway infrastructure, its adaptation to solve railway problems has many open challenges, e.g., a major difficulty is data recorded at different monitoring times that is required to train this sort of network. In addition to data-based deep learning approaches, recent advances in physics-informed neural networks have emerged as another promising approach for solving problems based on mathematical physics models of railway infrastructures with a small amount of data.

All in all, by including perception, decision, and learning, the railway infrastructures can be emulated as a living being from where each methodology will contribute to creating its digital brain. However, learning methodologies for railway infrastructures have still been relatively limited.

METAHEURISTICS

Heuristic optimization is a promising approach for decision-making in railway infrastructure systems. For example, one typical characteristic of maintenance strategies in railways (such as grinding and tamping) is that relaxing strong assumptions of simple models leads to the formulation of more realistic and complex problem formulations. This may create a need for nonlinear relationships between variables which gives rise to a mixed-integer nonlinear optimization problem, especially when discrete decisions are present in a problem. To deal with challenges in maintaining large-scale railway infrastructures, hierarchical and distributed optimization-based methods can be considered. A significant challenge is to speed up the solution of the optimization problems by partitioning and coordination between reduced-size subproblems. Most decomposition-based approaches work by decomposing the large-scale multi-objective optimization problem into multiple single-objective subproblems based on a set of weight vectors. Then, the subproblems can be solved cooperatively in, e.g., an evolutionary algorithm framework. Stochastic optimization for decisions in rail systems explicitly includes the effect of different sources of stochasticity and uncertainty, such as in measurements, loading conditions, infrastructure parameters, and external factors, including climate/weather. Multi-objective decision-based methods for dynamic

decision support tools in railway infrastructure systems help find different solutions, typically to quantify trade-offs between cost reduction and performance. But they can include punctuality, efficiency, robustness, safety, sustainability (recycling/disposal), energy consumption, etc.

2.5.3. DIGITAL TWINS

When only limited data are available and they are imbalanced, transfer learning, on the one hand, can be considered to alleviate the issues arising from using small datasets to train machine learning models. On the other hand, it is crucial to have a sufficient amount of data. When it is not possible to collect real data, particularly data related to rare events, e.g., failures or defects, using synthetic data is an option. A digital twin can be a good candidate for that.

Digital twins are a conceptual framework for interconnecting a physical system and its digital representations [164]. Digital twins are created by capturing and integrating various data types from sensors, devices, and other sources, including physical models. The purpose is to gain deeper insights into the physical entities they represent. Digital twins allow us to emulate future scenarios of the consequences. This helps us with risk assessment and decision-making to prepare for and mitigate the impact of rare events. Within this context, an open challenge that needs to be addressed is an effective method to generate synthetic data representing the total variation of the expected railway operating conditions.

In [165], a building information model (BIM) was used to photo-realistically simulate severe structural damage in a synthetic computer graphics environment. In [166], a deep learning-integrated digital twin model was developed to establish an interoperable functionality and to develop typologies of models described for autonomous real-time interpretation and decision-making support for the architecture, engineering and construction sector. By applying the concept of digital twins to railway infrastructure, railway companies can cut costs, modernize workflows, and increase efficiency and performance. Digital twins allow companies to offer new services such as remote monitoring, real-time diagnostics, predictive maintenance, and automated operations. With a combination of various sensors throughout the whole infrastructure, information can be immediately analyzed by AI and big data to plan maintenance actions proactively. This can avoid incidents or delay and improve safety and operational efficiency.

While digital twins bring numerous opportunities to the railway industry, they present challenges in their implementation. To successfully implement digital twins in railway infrastructure, sufficient data need to be available for properly calibrating digital twins. Moreover, a new mindset of rail operators and authorities must be developed; they must promote cooperation, share data, and consolidate business resources. Also, business models need to be changed, and, most importantly, financial investments and a strategy to tackle cyber threats are required [167].

2.5.4. MULTIDISCIPLINARY RESEARCH FOR HOLISTIC APPROACH

Railway infrastructure research is inherently multidisciplinary. Answering fundamental questions in the field requires knowledge from different fields. Combined with AI, some of the emerging fields related to resilience engineering, climate change, cyber security, etc., are essential for solving open research questions. For example, AI research related to an embankment requires knowledge of geosciences, railway engineering, and computer sciences, among other fields. Without knowledge sharing and research collaborations, the essential physics and dynamics of the infrastructures cannot be studied efficiently. When considering the whole life cycle of the railway infrastructure, environmental and social impacts add more dimensions. This requires a holistic approach to analyze different aspects of the overall life cycle cost to evaluate the system's environmental, economic, and social performance. For instance, the study in [168] showed that the operation and maintenance phases are responsible for most emissions, with electricity consumption being the primary contributor. Energy costs were identified as the main contributor (92%) to the overall life cycle cost, and reducing these costs could help lower the system's total cost. The social impact assessment in [168] revealed that the urban transportation industry has strong connections with consumers, workers, the local community, and society. Even though new AI technologies can be employed to assist learning, they can extract valuable insights, patterns, or relationships from the data without human dependency. When no historical data is available, physical models are needed. In the field of railway infrastructure, 3D dynamic models are widely used as they offer dynamics and physical interpretation of the systems. However, when it comes to a complex non-static problem, e.g., soil [169, 170], a new dynamical model and sensing technologies are needed. The lack of historical data and efficient higher-dimensional dynamic models results in less research on some railway components, e.g., substructures and embankments. However, this also opens up opportunities for AI approaches in the areas with few data when the available physical knowledge can be included.

2.5.5. VALIDITY OF THE DATA

Many existing studies developed AI methodologies using training data under specific environments and operating conditions. Ultimately, we aim to develop innovative solutions that can facilitate the work of infra managers so they can focus on other critical challenges. To ensure the robustness, generalization, and efficacy of the new methodologies, the validity of the data sources and field validations are required. It's essential to regularly and continuously assess and measure the impact of data to ensure they deliver tangible results that meet the needs of rail operators. Accurate and reliable data serves as the foundation for making informed decisions. For example, can we trust the decision driven by the data we use to train the model? Moreover, more controlled field measurements and shared case studies should be provided so that the researchers can validate and compare the performance level of their models developed with the state-of-the-art methods in the field of railway infrastructures.

2.5.6. INTEROPERABILITY OF THE DATA

In the railway industry, data interoperability appears to be a significant challenge in delivering AI-based solutions. Its problem is how to convert and integrate the data between different systems, e.g., the data coming from the APIs of different customers. Each API has its own way of working. Having compatibility among software is thus critical to facilitate the use of AI. A data standard is also required to enable the available interactions between heterogeneous formats and systems.

2.5.7. CLOUD INFRASTRUCTURES

Digitalization in railway infrastructures generates a large volume of real-time data as many devices and sensors are used to monitor the assets. This data can provide insights into the health conditions of the monitored assets, and this enables predictive maintenance. To derive actionable insights in real-time, cloud infrastructures need to be invested and leveraged. With such big data, the communication network and the adoption of 5G technology are required. A petabyte-scale Internet of Things and edge data to the cloud must be agile. The adoption of edge computing is required for the use of machine learning and AI algorithms to help manage the infrastructures in near real-time.

2.5.8. TRANSFORMERS

Transformer models refer to a specific type of deep learning networks. They are designed with large encoder and decoder blocks based on a self-attention mechanism which represents the key innovation that allows transformers to selectively focus on different parts of the input sequence [171]. Instead of relying on sequential processing, transformers process the entire input sequence in parallel. Before transformers arrived, users had to train neural networks with large labeled datasets that were costly and time-consuming to produce. By finding patterns between elements mathematically, transformers eliminate that need. Even without pre-training on large datasets, transformer-based models are more robust to generalization [172]. Therefore, transformer models have opened up another technique to tackle insufficient and imbalanced railway data. This allows more researchers in railway engineering to conduct research with machine learning without facing issues arising from the training data. However, transformer models themselves can contain trillion parameters, e.g., Google's Switch Transformer has 1.6 trillion parameters [173]. This poses another challenge in training transformer models that require further research.

2.5.9. METAVERSE

Metaverse is a concept referring to a virtual world where users can interact with each other and computer-generated environments in real time. The concept of the metaverse often involves a combination of technologies such as virtual reality (VR), augmented reality (AR), artificial intelligence (AI), blockchain, and other emerging technologies, e.g., robotics and drones. Even though the metaverse is currently used for entertainment and gaming, it has the potential to be applied in the railway industry.

By using technologies that are equipped with cameras, IoT devices, and sensors that collect real-time data from instrumented railway infrastructure, data obtained can be analyzed by AI and can be used to create virtual environments. Many aspects of real fieldwork that transcend physical limitations can be created. For instance, to create a virtual environment from information collected in areas that are difficult to access and risky to humans. This enables railway infra managers to conduct virtual inspections, identify issues, explore, analyze, and optimize various aspects of the railway infrastructure, e.g., design, operation, and maintenance. However, applying the metaverse in railway infrastructure is still an emerging concept, and its full potential is yet to be explored.

2.5.10. EMERGING TECHNOLOGIES

Several emerging technologies can contribute to improving the reliability of railway infrastructure. Examples include blockchain technology, robotics, and drones. Blockchain technology can enhance the reliability of the supply chain management process in the railway industry. It can provide transparent and tamper-resistant records of the origin, maintenance history, and certification of critical components, ensuring the integrity and reliability of the infrastructure. Robots and drones, equipped with cameras and sensors, can be used to regularly inspect railway tracks, bridges, tunnels, and other infrastructure components. They can provide detailed visual data and collect information in areas that are difficult to access and risky to humans. In addition to the aforementioned trends, further potential technologies can include web3, cryptocurrencies, nonfungible tokens, natural language processing, 5G or 6G technology, conversational AI Humans, etc. These emerging technologies have the potential to revolutionize the railway industry by improving reliability, safety, minimizing various types of risks, and enhancing the overall performance of the railway infrastructure. However, their use cases and implementation will depend on technological advancements, industry requirements, and regulatory considerations on planning and integration with existing systems.

2.6. CONCLUSION

This chapter reviews some AI methodologies developed and integrated into railway infrastructures to tackle problems arising from its usage and natural degradation mechanisms. The methods focused on in this chapter are neural networks, metaheuristics, regressions, probabilistic graphical models, clustering, fuzzy logic, and transfer learning. Based on our survey of journal papers on Scopus, they have shown great promise for various applications in railway infrastructure. Not only at a research level but many of these AI and ML applications have also been implemented in the railway industry, in which the extent of their implementations varies across different railway operators and regions. Despite their success, the use of AI methodologies exhibits certain limitations that pose challenges for a successful implementation in the railway industry. Some considerations and discussions about the challenges and the need for new intelligent methods are presented in this chapter to bridge the gaps between industrial applications and new AI developments.

Researchers in academia and industry can exploit the information from our paper to visualize trends and to develop benchmarks of problems and methods tailored to the particularities of railway infrastructures. Finally, we aim with this chapter to also inform the railway industry about the overview of technological advances in the field of AI, so even more innovative use cases and applications can emerge in the near future. In addition to the enthusiasm surrounding the implementation of AI in railway infrastructure, it is imperative to prioritize economic efficiency and feasibility. For instance, the existing maintenance and operational protocols rely on predefined rule sets, which would necessitate modifications when incorporating solutions provided by AI technologies. Consequently, alongside technological advancements, a fundamental redesign of inspection, monitoring, and maintenance procedures becomes essential.

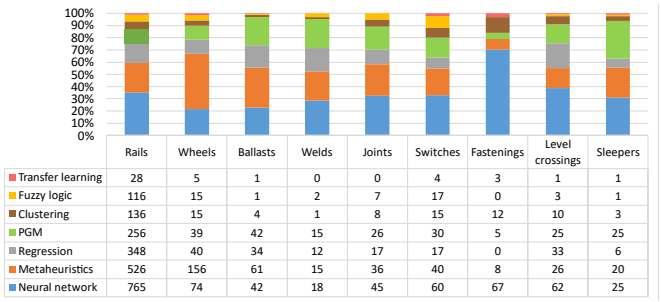

	Rails	Wheels	Ballasts	Welds	Joints	Switches	Fastenings	Level crossings	Sleepers
Transfer learning	28	5	1	0	0	4	3	1	1
Fuzzy logic	116	15	1	2	7	17	0	3	1
Clustering	136	15	4	1	8	15	12	10	3
PGM	256	39	42	15	26	30	5	25	25
Regression	348	40	34	12	17	17	0	33	6
Metaheuristics	526	156	61	15	36	40	8	26	20
Neural network	765	74	42	18	45	60	67	62	25

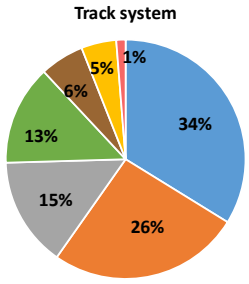

(a) Across track system.

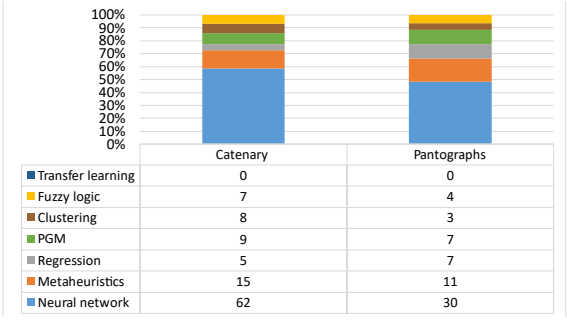

	Catenary	Pantographs
Transfer learning	0	0
Fuzzy logic	7	4
Clustering	8	3
PGM	9	7
Regression	5	7
Metaheuristics	15	11
Neural network	62	30

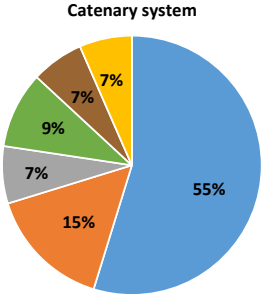

(b) Across catenary system.

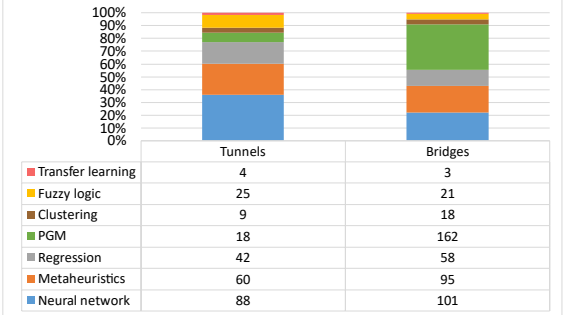

	Tunnels	Bridges
Transfer learning	4	3
Fuzzy logic	25	21
Clustering	9	18
PGM	18	162
Regression	42	58
Metaheuristics	60	95
Neural network	88	101

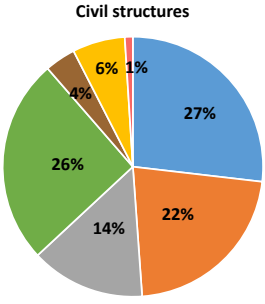

(c) Across civil structures.

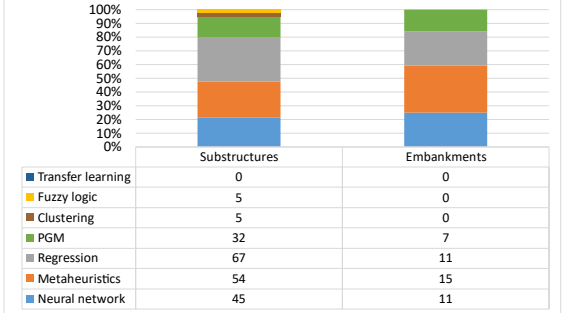

	Substructures	Embankments
Transfer learning	0	0
Fuzzy logic	5	0
Clustering	5	0
PGM	32	7
Regression	67	11
Metaheuristics	54	15
Neural network	45	11

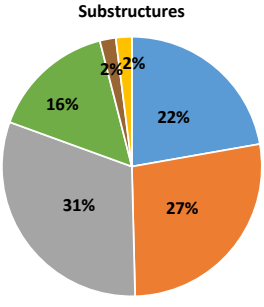

(d) Across substructure system.

Figure 2.6: Distribution of the selected AI methodologies across the four groups of railway infrastructures. NB: one research paper can include multiple AI methodologies.

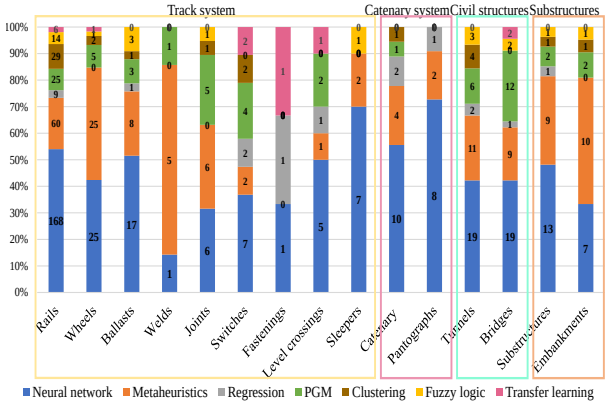

Figure 2.7: Development of the selected AI methodologies in 2023.

Table 2.4: Summary of potentials and limitations of selective AI methodologies.

AI methods	Tasks	Achievements	Limitations	Papers discussed in this work
Neural network	detection, association, prediction, decision support	capability to deal with non-linear and complex relationships between dependent and independent variables with high precision of the predictions	long training process to determine the optimal network and lack of interpretability	[39, 40, 47] [41–43] [44–46] [48–50] [51]
Regression	association, prediction, assessment	ability to provide an explicit mapping relationships between variables with physical meaning	non-competitive accuracy compare to other AI methods	[55–57] [58, 59]
Meta-heuristic	FE model updating, design optimization, and maintenance optimization	ability to provide optimal solution to problems concerning either single or multiple objectives.	long computation time to find optimal solution	[18, 63, 64] [65–67] [68–70] [71–73] [74–76] [78–80]
PGM	detection, prediction, identify causality inference	powerful tool for dealing with situation in the presence of uncertainty, and solving inference problems	rely on a high-quality training dataset and often suffer from the curse of dimensionality.	[85–87] [88–90] [39, 91]
Fuzzy logic	detection, assessment, control	ability to produce fuzzy rules for problems with uncertainty	highly dependent on human knowledge and expertise, and have to regularly update the rules.	[96–98] [99, 100]
Clustering	detection, assessment,	ability to discover hidden patterns in datasets without providing labelled data	inability to perform if there exists a mixture of clusters with different characteristics	[19, 109, 110] [111, 112]
Transfer learning	detection, prediction	capability to deal with imbalance and insufficient labeled datasets	inability to deal with situations when health information are unrelated.	[115–117] [118, 119]

3

SPIKING NEURAL NETWORK WITH TIME-VARYING WEIGHTS FOR RAIL SQUAT DETECTION

Axle box acceleration (ABA) measurements can be used for continuously monitoring rail infrastructure and detecting rail surface defects such as squats. However, accurately detecting squats is challenging due to their short-duration responses and low occurrence in ABA signals, particularly for light squats that exhibit subtle ABA responses. To address this challenge, we propose using a spiking neural network (SNN) with time-varying weights to enhance the detection accuracy of rail squats based on ABA measurements. Our approach employs a simple SNN architecture without hidden layers, trained using a method that combines genetic algorithms, k-fold cross-validation, and multi-start backpropagation to optimise hyperparameters and weights. The proposed methodology demonstrates competitive accuracy compared to other state-of-the-art SNN-based methods on UCI benchmarks for both binary and multi-class nonlinear problems. Part of the advantages of the methodology due to the use of SNN include higher efficiency with a simpler architecture that reduces computational times while achieving effective spatiotemporal pattern detection. As shown by real-field measurements from Dutch and Swedish railways in anomaly detection, it effectively captures subtle changes in light squat defect responses in ABA signals and achieves a detection accuracy of 100% for severe squat defects and over 93% for light squat defects. Furthermore, we show that the spike responses, postsynaptic potentials, and membrane potentials can be used as a new way to explain and analyse the ABA signals. The proposed method using time-varying weights highlights a correspondence with the physical problem and offers an ability to capture sudden and subtle changes in the responses, which is crucial, particularly for detecting defects in their early stages.

This chapter has been submitted for publication as: Phusakulkajorn, W., Hendriks, J.M., Li, Z., Núñez, A., Spiking Neural Network with Time-Varying Weights for Rail Squat Detection, under review

3.1. INTRODUCTION

SQUATS are short-wave surface defects and one type of rolling contact fatigue on railway rails [1–7]. Figure 3.2 illustrates examples of surface defects from a railway line in Sweden and the Netherlands. The severity of squats can be classified into light, moderate, and severe [134]. Early detection and assessment of all types of squats are crucial for planning maintenance operations [24, 174, 175].

(a) Sweden

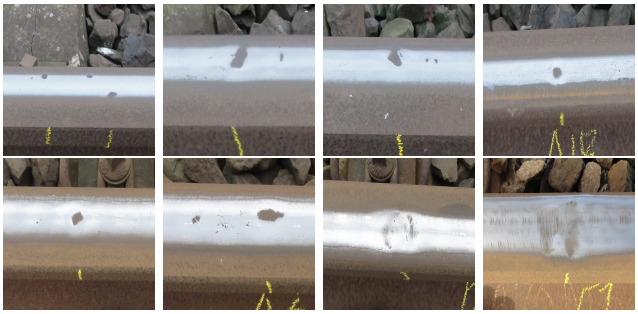

(b) The Netherlands

Figure 3.1: Rail surface defects from different countries.

Rail maintenance typically considers grinding and replacement. In the case of light squats with minor cracks, grinding has the potential to remove them completely from the rail surface [176]. When squats become severe, a degradation of the track structure is experienced, and rail breaks can eventually occur. For severe squats, rail replacement is more suitable as multiple grinding passages might not entirely remove them, leading to the re-appearing of the defect due to residual damages. As grinding is more cost- and performance-effective than rail replacement, the early and accurate detection and management of squats are needed.

Various measurement technologies have been used for the detection of squats, for example, ultrasonic [39], eddy current [177], guided waves [178], image processing [40–42], axle box acceleration (ABA) [3, 47, 97, 134], among others. In the literature, light squats can be detected using ABA measurements with accuracy between 78% to 85% [3, 134]. Using vertical and longitudinal ABA signals in conjunction with

noise-reduction techniques in [3], 100% of severe squats were detected, while 85% of small rail surface defects were found. For the automatic detection method proposed in [134], the detection accuracy was 100% for severe squats but 78% for light squats. As approximately 15-22% of light squats are not detected using traditional methods, we consider using neural networks to increase performance in this work.

In the literature, deep learning neural networks have been utilised to detect squats [179–181]. In [179], the performance of small, medium, and large DCNNs for detecting squats using video images were compared. The results demonstrated that a large DCNN model was needed to detect light squats with 64.4% accuracy. In [180], a deep convolutional neural network (DCNN) was proposed to detect squats using video images correlated to the corresponding ABA signals. This approach detected 96.9% of visible squats. In [181], the proposed unsupervised method based on convolutional variational auto-encoder achieved a hit rate of 100% for light squats using ABA measurements under a simulated vehicle-track environment. However, in practice, the detection accuracy of light squats is not 100% due to their complex spatiotemporal patterns, which are challenging for current detection methods to capture.

Spiking neural networks (SNNs), considered the third generation of neural networks [182], offer the ability to handle temporal and spatiotemporal patterns through their unique mechanism of processing data as discrete events or spikes. The potential applications of SNNs span various fields such as biomedical science and mechanical engineering [183–191]. To explore their capability in railway application further, this chapter proposes using SNNs for detecting rail squats due to their capability in capturing spatiotemporal patterns. Additionally, the signal transmission in SNNs, occurring as trains of spiking events, resembles the pattern of an ABA signal, where each spike represents an abrupt change in ABA response at squats, further motivating their use in this application.

SNNs have been designed with many network parameters [192–197]. On the one hand, having many hidden layers and nodes allows biological plausibility and higher accuracy. On the other hand, having many parameters poses the issue that SNNs are more difficult to train and their evaluation can be computationally costly. Railway infrastructures are inherently large-scale, with variations that depend on time and track location (spatial dependency) and stochastic systems. Additionally, rail squat detection technologies rely on high-frequency monitoring data. Thus, a less computationally expensive model that meets online detection requirements and facilitates decision-making is preferred.

Employing SNNs without hidden layers or hidden nodes has been considered in the literature to reduce computational efforts. In [198] and [199], efficient algorithms for networks with no hidden layer were presented. In both works, the algorithms outperformed the existing SNNs with more complex network architecture in terms of both accuracy and computational cost when testing with benchmarks from the UCI machine learning repository for both binary and multiple classes. The contribution from [198] and [199] has opened up an opportunity to find a well-balanced trade-off between computational effort and accuracy for SNNs. Therefore, instead of using large network architecture, this work uses simple network architecture with no

hidden layers to solve a complex spatiotemporal problem presented in early squat detection. The main contributions of this chapter are:

1. An SNN-based methodology with time-varying weights is proposed to detect rail surface defects, e.g., squats, of varying severity levels, using ABA measurements. This method aims to improve the detection accuracy of light squats, which present challenges due to their subtle, short-duration responses and typically a low percentage of appearance in ABA signals compared to healthy rails. Instead of using large network architecture, this work uses simple network architecture with no hidden layers to solve a complex spatiotemporal problem presented in early squat detection.

2. A global optimisation approach is considered for the training process, incorporating a genetic algorithm to search for hyper-parameters based on cross-validation and backpropagation to adjust time-varying weights with multiple starts.

3. A utilisation of spike responses, postsynaptic potentials, and membrane potentials is presented to provide an explainable way for squat detection that relies on ABA signals. Visual explanations from these internal spike behaviours are presented to identify a correspondence with the physical problem.

The rest of this chapter is outlined as follows. Section 3.2 provides background knowledge of rail squats and SNNs. Section 3.3 introduces the problem of squat detection and the proposed framework, while the feature engineering is elaborated in Section 3.4. Section 3.5 presents the proposed SNN-based methodology. Section 3.6 presents a sensitivity analysis of hyper-parameters of our methodology and the comparative study with the state-of-the-art SNNs using UCI benchmarks. In Section 3.7, the capability of our SNN-based methodology to solve a complex spatiotemporal problem presented in squat detection based on ABA measurements is compared with other methods. The explainability of the methodology for squat detection is also elaborated in this section. This chapter is concluded in Section 3.8.

3.2. BACKGROUND KNOWLEDGE

3.2.1. RAIL SQUATS

(a) Severe squat. (b) Moderate squat. (c) Light squat.

Figure 3.2: Illustration of rail squats with different severity levels.

A rail squat is a type of rail surface defect that arises from rolling contact fatigue (RCF). It is characterised by local plastic deformation on the rail top surface. The direct cause is excessive dynamic wheel–rail contact force. Contributing factors to their occurrence include increased axle loads and traffic density, different maintenance policies, deteriorating track quality, new materials for wheels and rails, and the use of stiffer concrete sleepers [200].

Severe, moderate, and light squats are classifications of rail squats distinguished by their wavelengths and the frequency characteristics of wheel–rail dynamic interactions, which can be measured by ABA systems. Figure 3.2 illustrates squat classifications in which Figures 3.2(a), 3.2(b), and 3.2(c) show an example of a severe, moderate, and light squat, respectively. Severe squats are the largest and deepest defects among the three categories, with lengths typically ranging more than 50 millimetres [97]. Severe squats generate pronounced, high-amplitude vibrations with distinct frequency characteristics between 200-400 Hz [134]. The larger the severe squats, the greater the risk of derailment. Moderate squats are smaller than severe squats, with lengths ranging between 30-50 millimetres [97]. They cause rail vibrations with the same frequency band as the severe squats, though less pronounced amplitudes. Light squats are the smallest and shallowest defects among the three categories, often representing the initial or early stages of rail squats. Their lengths range between 8-30 millimetres [97]. The characteristic frequency bands for light squats are between 200–400 Hz and 1000–2000 Hz [134]. If left untreated, light squats can develop into more severe defects. However, some small defects can be worn away through natural wear.

Rail squats are critical to detect and manage because they can lead to increased maintenance costs, reduced rail life, and potential safety hazards. However, detecting squats, particularly for light squats, with high accuracy is challenging. Some possible underlying reasons are the following. First, light squats are anomalies with a low percentage of appearance in monitoring data. Some light squats are difficult to find via visual inspections (or even impossible when these are still not visible to human eyes), making the labelling process difficult. Second, the response of light squats in ABA signals appears suddenly and has a very short duration. For example, at a light squat of 8 mm in wavelength with a measurement speed of 110km/hr, the duration of its response can be 0.26 milliseconds. Third, the responses of light squats in ABA signals are affected by the variability of the railway track parameters and measurement conditions. For example, different dynamic responses occur at squats on top or in between sleepers, thermite welds, flash welds, joints, crossings, transition zones, etc. Last and most importantly, the frequency components of light squats are slightly different from those of healthy rails, with subtle characteristics occurring dominantly at high frequencies. Therefore, advanced detection methods are essential for identifying these defects early and accurately.

3.2.2. SPIKING NEURAL NETWORKS

A spiking neural network (SNN) is brain-inspired and is a class of neural networks that more closely mimic the functioning of biological brains compared to traditional neural networks [182]. Unlike the other two generations, inputs of SNNs are

encoded into temporal information represented as trains of spiking events rather than numeric values.

SPIKING NEURON MODELS

The core component of an SNN is spiking neurons. They communicate with each other by generating and propagating electrical pulses known as action potentials or spikes. The likelihood of a spike generation depends on the types of synaptic inputs, i.e., excitatory or inhibitory. Excitatory inputs enhance the likelihood of a neuron firing a spike, whereas inhibitory inputs decrease this likelihood. The dynamics of a spiking neuron are characterised by its membrane potential, which evolves according to the excitatory and inhibitory inputs it receives from presynaptic neurons. When the membrane potential reaches a certain threshold, the neuron generates one or more spikes. As a result, the internal potential of each neuron has to be computed for a continuous duration of time to obtain the precisely timed patterns of spikes [192, 195]. Producing a continuous time-encoded output and connecting to other neurons, SNNs offer an ability to deal with temporal and spatiotemporal patterns.

The most widely used model to describe the dynamics of the spiking neurons is the leaky integrate-and-fire (LIF) neuron model. The LIF model integrates incoming spikes until the membrane potential $v(t)$ reaches a threshold v_{th}, at which point the neuron fires (emits a spike) and resets its potential. The dynamics of the LIF model are described by the following formula [201]:

$$\tau_{\text{m}} \frac{dv(t)}{dt} = -(v(t) - v_{\text{rest}}) + I_{\text{exc}}(t) - I_{\text{inh}}(t), \tag{3.1}$$

$$\text{if } v(t) \geq v_{\text{th}}, \text{ then } v(t) \leftarrow v_{\text{rest}} \text{ and emit a spike,}$$

where τ_{m} is the membrane time constant, v_{rest} is the resting potential, $I_{\text{exc}}(t)$ and $I_{\text{inh}}(t)$ are the excitatory and inhibitory currents, respectively. More spiking neuron models can be found in [202].

INFORMATION TRANSMISSION AND PROCESSING

Synapses in SNNs are the connections between neurons, where the presynaptic neuron sends signals and the postsynaptic neuron receives them. When a presynaptic neuron fires, a spike is transmitted to another neuron across synapses, in which synaptic weights play a crucial role as they determine the strength and impact of these transmitted spikes on the postsynaptic neuron. The postsynaptic neuron then responds to the incoming spike from multiple presynaptic neurons by integrating the signal into its membrane potential and generating spikes when the potential exceeds a certain threshold. In SNNs, information processing relies on the precise timing of these spikes, enabling efficient computation. The event-driven nature of SNNs allows for asynchronous processing [203], where neurons fire only when necessary, potentially reducing power consumption and enhancing response times compared to traditional neural networks [203, 204]. These properties make SNNs particularly well-suited for applications requiring real-time processing and energy efficiency [182, 203, 204].

LEARNING

Synaptic plasticity plays an important role in reaching the high-level performance of SNNs. It is the process of learning and adjusting the synaptic weights to perform a given task. Various approaches have been proposed to adjust the synaptic weights. The spike-timing-dependent plasticity (STDP) is an approach based on a bio-inspired formulation of synaptic plasticity. The STDP updates synaptic weights in an unsupervised manner based on dependencies between presynaptic and postsynaptic spikes. Learning algorithms developed based on the STDP are, for instance, Tempotron [194], SWAT [196], ReSuMe [197], TMM-SNN [205], SEFRON [198], and reward-modulation spike-timing-dependent plasticity (R-STDP) [206]. The SWAT, TMM-SNN, and R-STDP algorithms successfully implemented the classification of multi-layer feed-forward SNNs, while the Tempotron, ReSuMe, and SEFRON algorithms were successful for a single-layer SNN. Another approach for training SNNs considers the backpropagation algorithm [207]. In the case of SNNs, the discontinuity mechanism between the internal state potential and the response of spiking neurons prevents the direct use of backpropagation. In [192], the SpikeProp deployed backpropagation with the assumption that a piece-wise linear function can approximate the internal potential at an infinitesimal time around the instant of neuronal firing. The learning rule of SpikeProp has been successfully extended from single to multiple spikes to enhance the training performance of SNNs [193, 195, 208–212].

Inspired by [198], the SNN in this chapter is designed with time-varying weights and contains no hidden layers. We use the SpikeProp to deal with the discontinuity when a spike is fired. Then, backpropagation is used to adjust time-varying weights by including an additional term that captures the variations over time in the update rule of the weights. Multi-starts are considered, and a genetic algorithm is employed to search for the optimal hyper-parameters based on cross-validation.

3.3. SQUAT DETECTION PROBLEM

The detection of squats using ABA measurements can be considered a classification problem. This problem assumes availability of training samples $\mathscr{H}_D = \{(\mathbf{x}^{(d)}, c^{(d)}), d = 1,\dots,D\}$ in which an input $\mathbf{x}^{(d)} \in \mathbb{R}^M$. and its class label $c^{(d)} \in \mathbb{N}$ are required. Assigning a respective class label for ABA measurements at rails is a tedious and time-consuming process. Additionally, when dealing with squats at an early stage of their development, multiple data sources are required to confirm their existence and it is common to rely on field observation which is prone to human error. Moreover, it is difficult to obtain class information for defective and healthy samples because early squats can be invisible to the human eye or video cameras. Also, rails are affected by local infrastructure conditions, local railway track dynamics, and different stochastic variables. In this chapter, labelling was carried out by human domain experts and was verified by fieldwork.

To obtain an estimator of the mapping between measured ABA signals at rails and their class label, an SNN-based methodology is proposed. Figure 3.3 illustrates the framework of early detection of rail squats considered in this chapter. It

comprises two main parts: the feature engineering to obtain the representations of the measured ABA signals at rails (see 3.4) and the spiking neural network-based methodology that classifies whether or not a given rail segment contains squats. The latter part is detailed in Section 3.5.

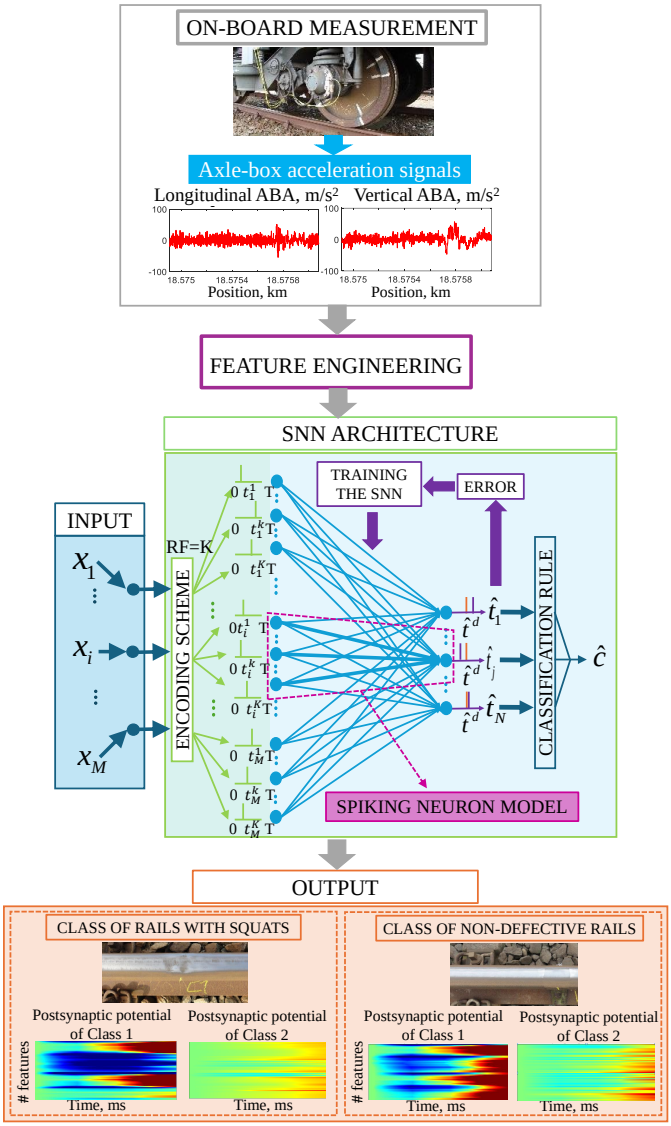

Figure 3.3: The framework of spiking neural network with time-varying weights for detecting rail squats.

3.4. FEATURE ENGINEERING

Figure 3.4 presents the processes of feature engineering considered in this work. The original acceleration signals of each rail sample are first pre-processed by means of wavelet analysis with the Morlet function to realise the frequency content of the rail dynamics. A moving standard deviation is proposed to extract representative features for ABA measurements in the frequency domain. Then, data are represented by concatenating representative features from vertical and longitudinal ABAs.

3.4.1. WAVELET ANALYSIS

To analyse the frequency content of the signal, we employ wavelet analysis due to its independence between the window size and the time–frequency representation. The continuous wavelet transform (CWT) is a time–frequency analysis tool in which the observed function is multiplied by a group of shifted and scaled wavelet functions. To achieve computational feasibility, we discretised the CWT and the wavelet coefficient $W_n(s)$ at a discrete wavelet scale $s>0$ and time index n are defined as [134]:

$$W_n(s) = \sum_{n'=0}^{N-1} a_{n'} \psi^{\star}\left(\frac{(n'-n)\,\delta_t}{s}\right), \tag{3.2}$$

where a_n is a time series with a time step of δ_t; $n' = 0,\ldots,N-1$ is the time shift operator where N is time window of the signal; $\psi^{\star}$ is a family of wavelets deduced from the mother wavelet by different translations and scaling; $\star$ indicates a complex conjugate. In this chapter, we consider the Morlet function for the mother wavelet. The Morlet function is defined as:

$$\psi_0(\eta) = \pi^{-1/4} e^{i\omega_0\eta} e^{-\eta^2/2}, \tag{3.3}$$

where ψ_0 is a nondimensional frequency. The power spectrum of a wavelet transform is defined as the square of the wavelet coefficients, i.e.,

$$\left|W_n^2(s)\right|. \tag{3.4}$$

Note that the frequency scale s obtained from our wavelet analysis has logarithmic spacing. This is due to the adjustable length of each wavelet. At higher frequencies, the length is shorter. Thus, higher frequencies have a larger bandwidth and are spaced further apart than lower frequencies. In this work, we select 113 wavelet scales as they provide a good trade-off between computational time for the wavelet analysis and the SNN and representation of the responses of rail dynamics at defects.

3.4.2. FEATURE EXTRACTION USING MOVING STANDARD DEVIATION

For a vector of the wavelet power spectrum at a wavelet scale s, $\mathbf{W}(s) = \left[\left|W_1^2(s)\right|,\ldots,\left|W_N^2(s)\right|\right] \in \mathbb{R}^{1\times N}$, the moving standard deviation $\mathbf{Z}(s) = [z_1(s), \ldots, z_q(s),\ldots,z_Q(s)] \in \mathbb{R}^{1\times Q}$ of $\mathbf{W}(s)$ is obtained by calculating a standard deviation over a sliding window of length k across the N neighbouring elements of $\mathbf{W}(s)$. When k is odd, the window is centred about the element in the current position. When k is even, the window is centred on the current and previous elements. The window

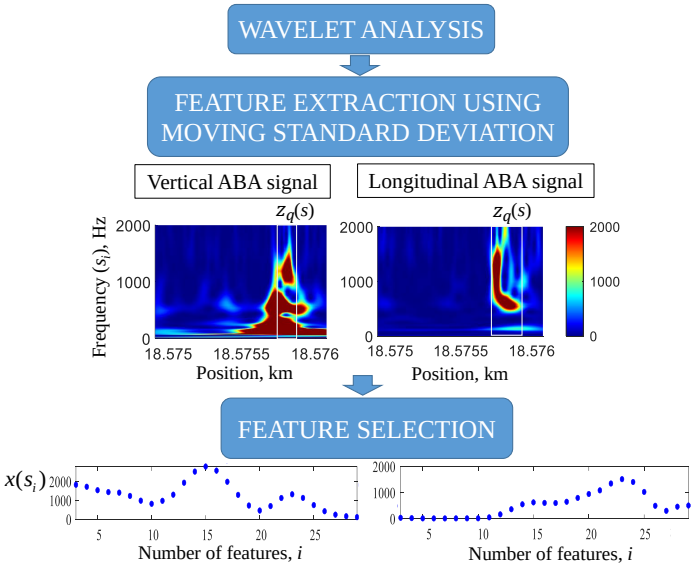

Figure 3.4: Steps in feature engineering.

size is automatically truncated at the endpoints when there are not enough elements to fill the window, i.e., $Q = (N - k + 1)$. When the window is truncated, the standard deviation is taken over only the elements that fill the window. Mathematically, the moving standard deviation $\mathbf{Z}(s)$ of the sliding window of length k is expressed as:

$$z_q(s) = \sqrt{\frac{\sum_{i=q}^{q+k-1}\left(\left|W_i^2(s)\right| - \bar{W}(s)\right)^2}{k-1}}; q = k, \ldots, Q, \tag{3.5}$$

where $\bar{W}(s)$ is the mean of $\left[\left|W_q^2(s)\right|, \ldots, |W_{q+k-1}^2(s)|\right]$. The representative feature at each frequency scale s, $x(s)$, is then obtained by:

$$x(s) = \max_q z_q(s). \tag{3.6}$$

In this chapter, a sensitivity analysis is performed to obtain the appropriate length of sliding windows, k, that is used to extract features from ABA signals in the vertical and longitudinal directions. With the length window k moving along a rail line as shown in Figure 3.4, variation of the energy contents can be realised. In this work, these energy contents along distances provide temporal characteristics of a rail, whereas the energy contents across different frequencies are regarded as spatial characteristics of a rail. Using (3.6), these temporal pieces of information are embedded per frequency. When considering a certain range of frequencies, their corresponding temporal information forms one-dimensional frequency-based features that serve as inputs that provide spatiotemporal characteristics of rail defects to an SNN.

3.4.3. FEATURE SELECTION

To represent the dynamic of rails, we follow [134], and we select the wavelet scales where most of the physical responses of squats are observed, that is, in the range between 200–2000 Hz as:

$$\mathbf{x} = \{x_i = x(s_i); s_i \in [200, 2000]\}. \tag{3.7}$$

Considering ABA signals from both vertical and longitudinal directions [3], particularly longitudinal ABA increases the detection of light squats, a total of 54 frequency-based features are used to represent the dynamic of rails in this chapter. For further research, it is interesting to explore a combination of data-based and physics-based approaches to determine the optimal resolution for the methodology. While the current study uses bands chosen in logarithmic ranges, alternative partitioning or other frequency-based features could be of interest for effective detection.

3.5. SPIKING NEURAL NETWORK WITH TIME-VARYING WEIGHTS METHODOLOGY

The SNN-based methodology consists of five main aspects: the temporal spike encoding scheme, the spiking neuron model, the network architecture, the methodology used to train the SNN, and the classification rule.

3.5.1. ENCODING SCHEME

For a given input $\mathbf{x} = [x_1, \ldots, x_i, \ldots, x_M]^T \in [0,1]^M$, each feature x_i must be converted into spike events. In this chapter, we consider the most used population rank encoding scheme to convert information into spike events [213]. Unlike time-to-first spike encoding, which uses the precise timing of the first spike, and rate encoding, which uses the firing rate, population rank encoding represents information based on the pattern of neuron activation rather than the timing order or firing rate alone.

In this chapter, the scheme uses overlapping Gaussian receptive field neurons to encode each input feature x_i into spike times. The firing strength of the i^{th} input feature $r_k(x_i)$ emitted by the Gaussian receptive field neuron k is defined as [199]:

$$r_k(x_i) = \exp \frac{-(x_i - \delta_k)^2}{2\sigma^2}, \tag{3.8}$$

$$\delta_k = \frac{2k-3}{2(K-2)}, \tag{3.9}$$

and

$$\sigma = \frac{1}{\gamma} \cdot \frac{1}{K-2}, \tag{3.10}$$

where K represents the number of receptive field neurons (given by the number of populations with different Gaussian receptive fields), and γ the overlap constant, the

centre δ_k and the width σ of the Gaussian function are defined according to the range of the input features.

Therefore, each feature x_i is converted into K presynaptic spikes of firing strength $[r_1(x_i),\ldots,r_K(x_i)]^T$ using (3.8). The associated firing times $\mathbf{t}_i = \left[t_i^1,\ \ldots, t_i^K\right]^T \in [0,T]^K$ of the feature x_i are obtained by linearly distributing $r_k(x_i)$, $k=1,\ldots,K$ into the presynaptic spike time interval of $[0,T]$ ms.

3.5.2. SPIKING NEURON MODEL

In this chapter, a spiking neuron model based on the leaky-integrate-and-fire model [214] is adopted, as illustrated in Figure 3.5. Our SNN is designed with time-varying synaptic weights, $w_{ij}^k(t) \in [0,T]$, to connect between the presynaptic neurons associated with the k^{th} spike time, t_i^k, of the input feature x_i and the postsynaptic neuron j.

A postsynaptic potential $S_{ij}^k(t)$ of the output neuron j at time t is determined as the product of the spike response of the presynaptic spike t_i^k, $\epsilon\left(t-t_i^k\right)$, and the time-varying synaptic weight $w_{ij}^k(t)$ evaluated at $t=t_i^k$, $w_{ij}^k\left(t_i^k\right)$, which is mathematically expressed as [198]:

$$S_{ij}^k(t) = w_{ij}^k\left(t_i^k\right)\cdot\epsilon\left(t-t_i^k\right). \tag{3.11}$$

A membrane potential $v_j(t)$ of the output neuron j is defined as the summation of a postsynaptic potential $S_{ij}^k(t)$ over the input spikes of $\mathbf{x}$, $\mathbf{t}_i = \left[t_i^1,\ldots,t_i^K\right]^T$. A membrane potential $v_j(t)$ is expressed as [198]:

$$v_j(t) = \sum_{i=1}^{M}\sum_{k=1}^{K} S_{ij}^k(t) \tag{3.12}$$

$$= \sum_{i=1}^{M}\sum_{k=1}^{K} w_{ij}^k\left(t_i^k\right)\cdot\epsilon\left(t-t_i^k\right), \tag{3.13}$$

$$\epsilon(t) = \begin{cases} 0 & \text{if } t\le 0, \\ \dfrac{t}{\tau}\exp\left(1-\dfrac{t}{\tau}\right) & \text{if } t>0, \end{cases} \tag{3.14}$$

where τ is the time constant of the spiking neuron.

The neuron fires a postsynaptic spike when the membrane potential reaches the firing threshold Λ. The postsynaptic firing time $\hat{t}_j$ is defined as:

$$\hat{t}_j = \left\{t \mid v_j\left(\hat{t}_j\right) \ge \Lambda\right\}. \tag{3.15}$$

At the postsynaptic firing time $\hat{t}_j$, the membrane potential of the neuron j is defined as:

$$v_j\left(\hat{t}_j\right) = \sum_{i=1}^{M}\sum_{k=1}^{K} w_{ij}^k\left(t_i^k\right)\cdot\epsilon\left(\hat{t}_j-t_i^k\right), \tag{3.16}$$

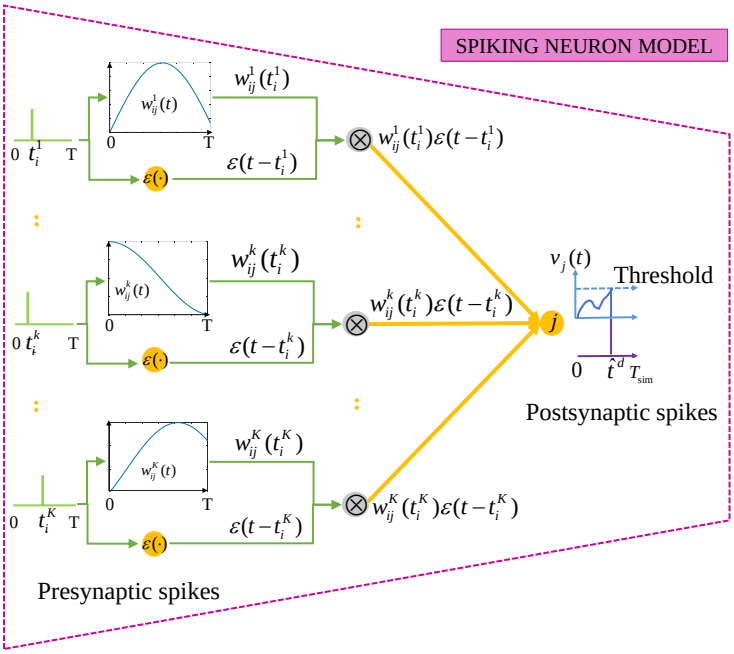

Figure 3.5: The spiking neuron model.

where $\hat{t}_j$ lies in the postsynaptic spike time interval of $[0, T_{\text{sim}}]$ ms. The parameter T_{sim} represents the simulation time used for the internal potential to reach the threshold of the neuron. Its value can be set differently [198], and it is a problem-dependent parameter.

3.5.3. SPIKING NEURAL NETWORK ARCHITECTURE

This chapter considers a two-layered fully connected feedforward SNN with no hidden layers and no hidden nodes, as illustrated in Figure 3.3. For K receptive field neurons, an input $\mathbf{x}$ is encoded into the presynaptic input spike time $\mathbf{t} = [\mathbf{t}_1, \ldots, \mathbf{t}_M]^T \in [0, T]^{M \times K}$, in which the number $K \times M$ determines the number of input neurons for our SNN architecture. An output neuron is designed to associate with one of the N classes. Therefore, the network architecture comprises N output neurons. This architecture is referred to as $K \times M{:}N$ and constitutes a total of $K \times M \times N$ time-varying synaptic weights to determine.

3.5.4. TRAINING THE SNN

For the proposed SNN, three groups of parameters are defined: a group of given parameters, a group of hyper-parameters, and a group of initial synaptic weights and synaptic weights. The first group contains parameters that are assumed given as in [198]. The parameters and their associated value are encoding-related parameters

with $K = 6$ and $\gamma = 0.7$, the presynaptic spike interval $T = 3$ ms, and the postsynaptic spike interval $T_{\text{sim}} = 4$ ms. A time resolution of 0.01 ms is considered for all synapses in the network.

To obtain the value of parameters of the second and the third group, an SNN-based methodology is proposed as illustrated in Figure 3.6. To obtain parameters as close to optimal global ones as possible, three main steps considered in the methodology include 1) hyper-parameter tuning with a genetic algorithm (GA), 2) weight initialisation with multi-starts and 3) weight updating with a backpropagation algorithm including the effects of the time dependency of the weights in the update rule.

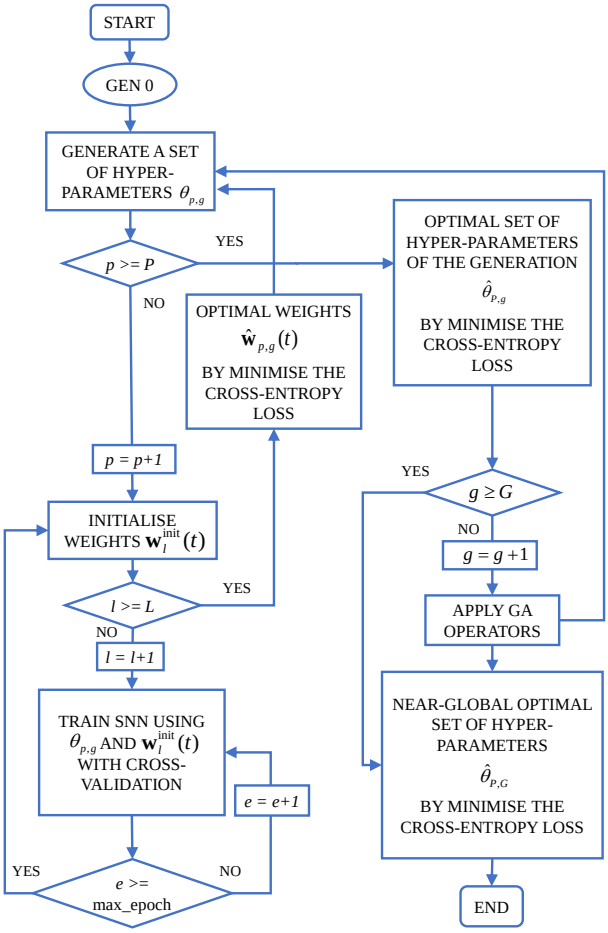

Figure 3.6: Schematic diagram of the SNN training.

HYPER-PARAMETER TUNING WITH GA

To achieve a near-global optimal set of hyper-parameters, $\hat{\theta}$, we perform a genetic algorithm considering the number of individuals, $p \in \{1,\dots,P\}$ and the number of generations, $g \in \{1,\dots,G\}$. The hyper-parameters tuned by a GA include the time-varying weight kernel ($\sigma \in [0.05, 0.55]$) [198], the desired postsynaptic firing time $\left(\hat{t}^d \in [0, T_{\text{sim}}]\right)$, the time constant of spike response function ($\tau \geq T$), and learning rate of weight update (η). The time constant of the spike response function is set to be greater than T as only a single spike is allowed from the output neuron. The maximum value of τ is considered to be 4 ms as a higher value of τ results in difficulty in raising the potential toward the threshold. The range of each hyper-parameter shown in Table 3.1 is determined to search for a good classification of all benchmarks.

Table 3.1: A range of the hyper-parameters considered for classification.

Hyper-parameter	Range	Search step size
$\hat{t}^d$	[0.05,3.5]	0.05
σ	[0.05,0.55]	0.05
η	[0.0001,0.001]	0.00005
τ	[3.0,4.0]	0.01

Throughout the evolution process of the GA, individuals of each generation, $\theta_{p,g}$, are obtained via the process of crossover and mutation. The two parents are chosen randomly from the whole population of the present generation. Then, two off-springs are bred by swapping the tails of their two parents at a random crossover point. The tuning parameters of GA are selected by default in the toolbox. A sensitivity analysis can be conducted to determine a reasonable number of generations and individuals.

Using a given set of hyper-parameter values $\theta_{p,g}$, the SNN is trained using the multi-start and cross-validation strategy to obtain the optimal set of time-varying weights $\hat{\mathbf{w}}_{p,g}(t)$. Then, the different P combinations of hyper-parameter values are computed and evaluated to find the near-global optimal set of hyper-parameters of the generation g, $\hat{\theta}_{P,g}$. Finally, the set of hyper-parameter values $\hat{\theta}_{P,g}, g = 1,\dots,G$ that achieves the best solution is selected as the set of hyper-parameters, $\hat{\theta}_{P,G}$.

WEIGHT INITIALISATION WITH MULTI-STARTS

For a given $K \times M$ input spike times and the corresponding N output synaptic neurons, the total number of $K \times M \times N$ synaptic weights are initialised by the uniformly distributed random numbers between 0 and 1. We limit the range of the initial synaptic weights to make sure that all neurons fire within the simulation time in the first epoch of network training. These initial weights are then distributed over the time interval by employing (3.23) to obtain time-varying weights, $\mathbf{w}^{\text{init}}(t) = \left\{ w_{ij}^{k,\text{init}}(t); k = 1,\dots,K, i = 1,\dots,M, \quad j = 1,\dots,N \right\}$. In this chapter, the training process of the synaptic weights are repeated according to the multiple sets of initial weights $\{\mathbf{w}_l^{\text{init}}(t); l = 1,\dots,L\}$, in which L is the number of multi-starts.

TIME-VARYING WEIGHTS UPDATING WITH BACKPROPAGATION

Using encoding, each input $\mathbf{x}$ gets a unique spike representation $\mathbf{t}$. For a given set of hyper-parameter values $\theta_{p,g}$ and an initial set of time-varying weights $\mathbf{w}_l^{\text{init}}(t)$, the predicted postsynaptic output spike times, $\hat{\mathbf{t}}^a$, are obtained. Then, the error ($\mathscr{L}$) obtained at the output neurons between the predicted and the desired spike time is used to update the synaptic weights between the i^{th} presynaptic and the j^{th} postsynaptic neurons.

In our approach, the time-varying weights are updated by using SpikeProp as proposed in [192] and a back-propagation update rule that includes the effect of time in the weights. For epoch e, the synaptic weights, $w_{ij}^{k,e}(t)$ at a single time instance $t = t_i^k$ is adjusted by:

$$\Delta w_{ij}^{k,e}\left(t_i^k\right) = -\eta \frac{\partial \mathscr{L}}{\partial w_{ij}^{k,e}\left(t_i^k\right)}. \tag{3.17}$$

where η is the learning rate and the sum squared error ($\mathscr{L}$) is used as a measure of the discrepancy between the desired and the predicted postsynaptic spike times. As $\hat{t}_j$ is a function of v_j, which depends on the weights w_{ij}^k at time instance t_i^k, the derivative on the right-hand part of (3.17) can be expanded to:

$$\frac{\partial \mathscr{L}}{\partial w_{ij}^{k,e}\left(t_i^k\right)} = \frac{\partial \mathscr{L}}{\partial \hat{t}_j}\left(\hat{t}_j^a\right) \frac{\partial \hat{t}_j}{\partial v_j\left(\hat{t}_j\right)}\left(\hat{t}_j^a\right) \frac{\partial v_j\left(\hat{t}_j\right)}{\partial w_{ij}^{k,e}\left(t_i^k\right)}\left(\hat{t}_j^a\right). \tag{3.18}$$

As given in [192], the first and the third derivative terms can be expressed coordinatewise for $j = 1, \ldots, N$ as:

$$\frac{\partial \mathscr{L}}{\partial \hat{t}_j} = \hat{t}_j^a - \hat{t}^d, \tag{3.19}$$

$$\frac{\partial v_j\left(\hat{t}_j^a\right)}{\partial w_{ij}^{k,e}\left(t_i^k\right)} = \epsilon\left(\hat{t}_j^a - t_i^k\right), \tag{3.20}$$

and, the second derivative term can be obtained by following [192] as:

$$\frac{\partial \hat{t}_j}{\partial v_j\left(\hat{t}_j\right)}\left(\hat{t}_j^a\right) = \frac{-1}{\partial v_j\left(\hat{t}_j\right)/\partial \hat{t}_j}\left(\hat{t}_j^a\right) = \frac{-1}{\partial v_j\left(\hat{t}_j^a\right)/\partial \hat{t}_j^a}. \tag{3.21}$$

Considering the denominator, we have

$$\begin{aligned}\frac{\partial v_j\left(\hat{t}_j^a\right)}{\partial \hat{t}_j^a} &= \frac{\partial}{\partial \hat{t}_j^a}\left(\sum_{i=1}^{M}\sum_{k=1}^{K} w_{ij}^{k,e}\left(t_i^k\right)\cdot\epsilon\left(\hat{t}_j^a - t_i^k\right)\right)\\ &= \sum_{i=1}^{M}\sum_{k=1}^{K} w_{ij}^{k,e}\left(t_i^k\right)\frac{\partial\epsilon\left(\hat{t}_j^a - t_i^k\right)}{\partial \hat{t}_j^a}\\ &= \sum_{i=1}^{M}\sum_{k=1}^{K} w_{ij}^{k,e}\left(t_i^k\right)\epsilon\left(\hat{t}_j^a - t_i^k\right)\left(\frac{1}{\hat{t}_j^a - t_i^k} - \frac{1}{\tau}\right).\end{aligned} \tag{3.22}$$

Substituting (3.22) into (3.21), the second derivative term is obtained. Hence, the error gradient at the postsynaptic spike time of an output neuron j at $t = \hat{t}_j$ is obtained using (3.19), (3.20), and (3.21).

Next, we include short-term plasticity by distributing the long-term plasticity over a specific time interval. Following [198], a Gaussian distribution is chosen as the modulating function. Therefore, $\Delta w_{ij}^{k,e}\left(t_i^k\right)$ at single time instance t_i^k is embedded into a Gaussian distribution such that a time-varying function $\Gamma_{ij}^{k}(t)$ is described as:

$$\Gamma_{ij}^{k,e}(t) = \Delta w_{ij}^{k,e}\left(t_i^k\right)\cdot\exp\left(\frac{-\left(t - t_i^k\right)^2}{2\sigma^2}\right), \tag{3.23}$$

where σ is the efficacy update range. The use of the exponential function to describe time-varying features of synaptic weights is followed from [198] to achieve biological plausibility. It is described in [215, 216] that neural behaviour and learning processes in the human brain involve changes in synaptic potential that follow exponential decay or growth patterns. While exponential functions are often employed to model these temporal dynamics, an evaluation of the impact of different time-varying functions can be interesting.

Hence, the update rule of time-varying synaptic weights for the synapse connected between the presynaptic neuron i and the postsynaptic neuron j is:

$$w_{ij}^{k,e+1}(t) = w_{ij}^{k,e}(t) + \Gamma_{ij}^{k,e}(t), e = 1,\ldots,E, \tag{3.24}$$

in which E denotes the maximum number of training epochs used for a simulation.

Note that (3.24) is used to obtain the weight parameters for each cross-validation fold. To obtain the optimal set of time-varying weights, k-fold cross-validation is considered to train and test the SNN with k different portions of the dataset. Then, the optimal set of time-varying weights is obtained by minimising the cross-entropy loss.

3.5.5. CLASSIFICATION RULE

In this chapter, the transmission types are ruled by the time-to-first spike coding scheme. Our output neuron can emit only once and its output associated with class j is the first postsynaptic spike time $\hat{t}_j$. For a problem with N classes, the

classification rule to predict the class label from the postsynaptic spike times $\hat{\mathbf{t}} = [\hat{t}_1, \ldots, \hat{t}_j, \ldots, \hat{t}_N]^T$ for an input $\mathbf{x}$ is defined as follow:

$$\hat{c} = \arg\min_j \hat{t}_j. \tag{3.25}$$

3.6. COMPARATIVE STUDY USING UCI BENCHMARKS

In this section, we perform a sensitivity analysis of hyper-parameters and evaluate the classification performance of the proposed SNN-based methodology using UCI benchmarks.

3.6.1. SENSITIVITY ANALYSIS

The Iris dataset is considered as a showcase for sensitivity analyses of the number of individuals and generations used in GA and a number of multi-starts. The Iris dataset contains 3 classes of 50 instances each [217]. Each class refers to a type of iris plant which are Iris Setosa (class 1), Iris Versicolour (class 2), and Iris Virginica (class 3). There are 4 input features for each instance: sepal length, sepal width, petal length, and petal width. In total, 75 instances are used for training and 75 instances are used for testing.

After the normalisation, each input feature is encoded by an array of six different one-dimensional Gaussian receptive fields. The network architecture for the Iris dataset, therefore, consists of 24 input neurons and 3 output neurons, referred to as 24:3. We followed the procedure presented in Figure 3.6 to obtain the parameters that better fit the Iris dataset. The number of epochs considered in the analysis is 100 epochs which shows to be sufficient for the training.

NUMBER OF MULTI-STARTS

For the network architecture of 24:3, a total number of 72 synaptic weights are initialised and distributed over the time interval $[0,3]$ ms. Given a set of hyper-parameters $\theta = \{\hat{t}^d = 0.95, \sigma = 0.30, \eta = 0.00045, \tau = 3.30\}$, we investigate the proposed SNN-based methodology in terms of classification accuracy when considering different numbers of multi-starts. Considering $l = 10, 20, \ldots, 90, 100$ and repeating the experiments ten times, Figure 3.7 shows that the classification accuracy is distributed between 94.54% and 98.67%. It is observed that the higher the number of multi-starts, the lower the variance and the higher the average classification accuracy. However, there is a trade-off between the computational time and the use of a higher number of multi-starts.

HYPER-PARAMETER VARIATION

To understand the effect of the hyper-parameters in the SNN architecture, classification accuracy as a function of some hyper-parameters is presented in Figure 3.8. It is observed that when the value of $\hat{t}^d$ increases, the obtained classification accuracy tends to decrease. The same trend is also observed for the variation of η and τ, whereas the obtained classification accuracy is enhanced by

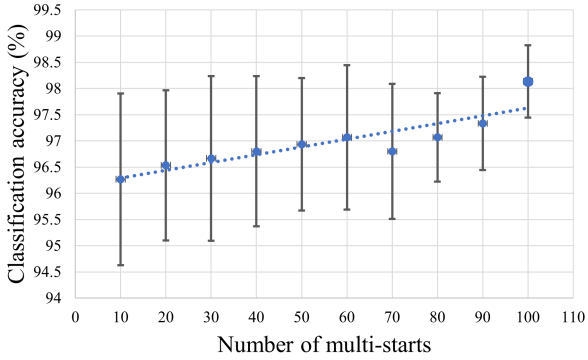

Figure 3.7: The effect of the number of multi-starts.

decreasing their value. For the value of σ, higher classification accuracy can be achieved by increasing its value. Furthermore, it is observed that the proposed methodology is sensitive to the variations of $\hat{t}^d$ more than the variation of other hyper-parameters.

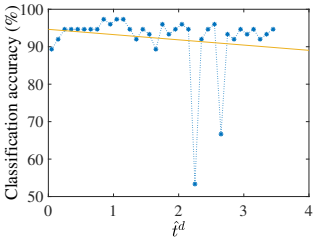

(a) Vary $\hat{t}^d$: $\sigma = 0.30, \eta = 0.00045, \tau = 3.30$.

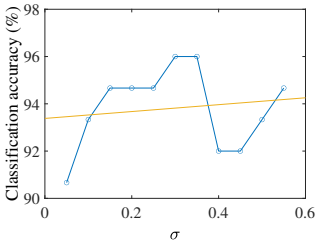

(b) Vary σ : $\hat{t}^d = 0.95, \eta = 0.00045, \tau = 3.30$.

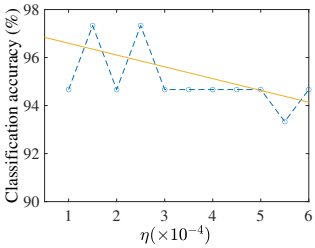

(c) Vary η : $\hat{t}^d = 0.95, \sigma = 0.30, \tau = 3.30$.

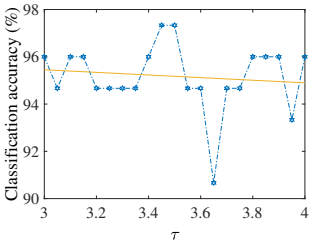

(d) Vary τ : $\hat{t}^d = 0.95, \sigma = 0.30, \eta = 0.00045$.

Figure 3.8: Effect of hyper-parameter variation for the SNN-based methodology – the Iris dataset.

NUMBER OF INDIVIDUALS AND GENERATIONS IN GENETIC ALGORITHM

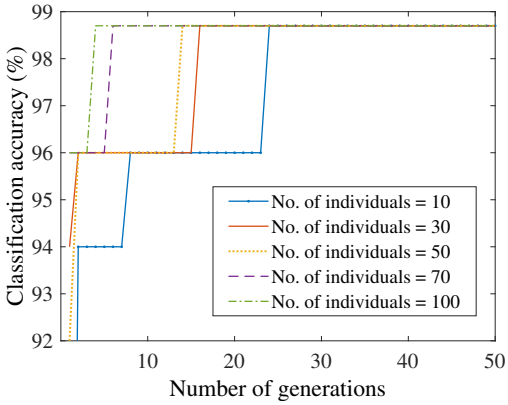

Figure 3.9: The evolution of the classification accuracy for the best individual in a generation. The plot shows the classification accuracy at the last epoch (=100).

Following the procedure in Figure 3.6 with the number of multi-starts set to 60, we perform a sensitivity analysis for the number of individuals and generations in GA to obtain a set of hyper-parameters, $\hat{\theta}$, for the Iris dataset. We consider the numbers of individuals, $p \in \{1,\dots,P\}, P = \{10,30,50,70,100\}$ and the number of generations, $g \in \{1,\dots,G\}, G = 100$. Figure 3.9 illustrates that the classification accuracy increases as the number of generations increases. Moreover, it is demonstrated that a larger population size can significantly improve accuracy using fewer generations. This observation allows understanding the effect of the GA parameters to obtain the hyper-parameter setting considering the Iris dataset. However, a GA expends more memory and more computational time in finding a solution for a large population size. Therefore, a compromise between accuracy and computational effort is to be considered for a reasonable trade-off.

3.6.2. PERFORMANCE

First, the performance of the SNN-based methodology is examined using four benchmarks from the UCI machine learning repository [217]. Each UCI benchmark dataset presents unique challenges such as imbalanced classes, small sample sizes, high dimensionality, nonlinear separability, and noisy data [217]. These datasets have been widely used to benchmark proposed methods in several studies [196, 198, 199]. The datasets are described in Table 3.2. To solve the classification problems, our SNN is trained by following the procedure in Figure 3.6. The tuned hyper-parameters are the time-varying weight kernel (σ), the desired postsynaptic firing time ($\hat{t}^d$), the time constant of spike response (τ), and the learning rate of weight update (η).

Table 3.3 presents the optimal set of hyper-parameters and the corresponding classification accuracy for each benchmark obtained from our proposed SNN-based methodology. By setting the hyper-parameters as described, Table 3.3 shows that

Table 3.2: A description of benchmark datasets from the UCI machine learning repository.

Dataset	Feature	No. of Class	No. of Instances	
			Training	Testing
Liver disorders	6	2	170	175
Breast cancer	9	2	350	333
Ionosphere	33	2	175	176
Iris	4	3	75	75

Table 3.3: The optimal set of hyper-parameter values and the corresponding classification accuracy for UCI benchmarks obtained from the proposed SNN-based methodology.

Benchmark	Hyper-parameter				Accuracy (%)				Epoch
					Training		Testing		
	$\hat{t}^d$	σ	η	τ	Max	Avg	Max	Avg	
Liver disorders	3.48	0.52	0.00015	3.09	95.4	91.8	75.6	70.2	100
Breast cancer	0.20	0.50	0.00080	3.45	96.5	96.3	98.8	98.7	100
Ionosphere	1.90	0.25	0.00010	3.00	100.0	99.5	97.7	94.3	100
Iris	0.95	0.30	0.00045	3.30	100.0	100.0	98.7	96.5	100

the classification accuracy for both training and test sets achieves more than 90% for Breast cancer, Ionosphere, and Iris datasets. The highest averaged accuracy is 100% and 98.7% for training and test sets, respectively. The obtained performance demonstrates the effectiveness of the proposed methodology in addressing the mentioned challenges in each dataset. However, it initially encountered poor performance on the liver disorder dataset, achieving only 67% accuracy. After the proposed global optimisation approach is employed to fine-tune network parameters, the liver disorder dataset accuracy is improved by 3.5% and overall performance is enhanced. Consequently, our methodology outperformed other methods like SpikeProp, SWAT, and SEFRON, as shown in Table 3.4.

3.6.3. COMPARISON WITH OTHER SNN METHODS

Our methodology is compared with state-of-the-art SNNs. Three learning algorithms with larger SNN architecture, e.g. SpikeProp [192], SWAT [196] and TMM-SNN [205], and two learning algorithms with a simple SNN architecture (without hidden layers and nodes), e.g. SEFRON [198] and WOLIF [199] are selected. To quantify the advantages of the proposed global optimisation approach, a comparison of our methodology both with and without the use of GA is also included. For our methodology without the GA, the hyper-parameter values as suggested in [198] are used. However, our learning rate is set to 0.001 in order to increase the probability of convergence [192, 195]. The comparative analysis considers the evaluation of averaged classification accuracy, the number of epochs used in each method, and the average training time used per epoch. Note that the training time reported for

Table 3.4: Performance comparison with the other SNN methods.

Dataset	Method	Architecture	Avg. accuracy (%)		No. of Epoch	Training time (s)
			Training	Testing		
Liver disorders	SpikeProp [192]	37:15:2	71.5	65.1	3000	11.36
	SWAT [196]	36:468:2	74.8	60.9	500	93.04
	TMM-SNN [205]	36:5:8:2	74.2	70.4	442	4.16
	WOLIF [199]	19:1	81.9	**80.3**	500	-
	SEFRON [198]	37:1	91.5	67.7	100	1.1637
	SNN with time-varying weights without GA	36:2	89.5	67.8	100	0.4401
	SNN with time-varying weights with GA	36:2	**91.8**	70.2	100	0.4401
Breast cancer	SpikeProp [192]	64:15:2	97.6	97.0	1500	16.07
	SWAT [196]	54:702:2	96.5	95.8	500	278.87
	TMM-SNN [205]	54:2:8:2	97.4	97.2	70	17.75
	WOLIF [199]	28:1	97.8	97.0	500	-
	SEFRON [198]	55:1	98.3	96.4	100	1.3202
	SNN with time-varying weights without GA	54:2	**98.9**	97.2	100	0.7225
	SNN with time-varying weights with GA	54:2	96.3	**98.7**	100	0.7225
Ionosphere	SpikeProp [192]	199:25:2	89.0	86.5	3000	27.30
	SWAT [196]	198:2574:2	86.5	90.0	500	503.79
	TMM-SNN [205]	204:23:34:2	98.7	92.4	246	25.17
	WOLIF [199]	100:1	94.4	90.6	500	-
	SEFRON [198]	199:1	97.0	88.9	100	2.1686
	SNN with time-varying weights without GA	198:2	97.1	91.5	100	0.8147
	SNN with time-varying weights with GA	198:2	**99.5**	**94.3**	100	0.8147
Iris	SpikeProp [192]	50:10:3	97.4	96.1	1000	9.01
	SWAT [196]	16:208:3	95.5	95.3	500	34.77
	TMM-SNN [205]	24:4:7:3	97.5	**97.2**	94	1.41
	WOLIF [199]	13:1	94.1	95.1	500	-
	SNN with time-varying weights without GA	24:3	99.6	95.3	100	0.2626
	SNN with time-varying weights with GA	24:3	**100**	96.5	100	0.2626

the SpikeProp, SWAT, TMM-SNN, and SEFRON is obtained from [198, 218], while the computational time for our methodology with and without GA is conducted in MATLAB 2021b using a 64-bit operating system with Windows 10 OS in a CPU with 4 cores, 16 GB memory, and 3.6 GHz speed. For a fair comparison, we reproduce the computational time of SEFRON on our hardware and calculate the performance ratio of the computational time for SEFRON between our hardware and the one used in [198, 218]. Then, we use the SEFRON as an intermediary to estimate computational time for other methods on our hardware through the performance ratio.

It is shown in Table 3.4 that the SpikeProp, SWAT, and TMM-SNN require many hidden neurons to achieve a testing accuracy above 85% on Ionosphere, Breast cancer, and Iris benchmarks, whereas our method achieves comparable performance with fewer neurons. Consequently, the larger SNN architectures of those methods result in significantly higher computational time used per training epoch compared to our method. In the case of Ionosphere dataset, the SpikeProp algorithm achieves 89% training accuracy and 86.5% testing accuracy using 25 hidden nodes and 3000 epochs, taking 27.3 seconds per epoch. In contrast, our methodology achieves a significantly higher training accuracy of 99.5% and testing accuracy of 94.3%, using

no hidden nodes, significantly fewer epochs, and lower computational time per epoch. For the difficult binary classification problem of Liver disorders, our method requires fewer epochs, fewer neurons, and less computational time to achieve similar accuracy to the TMM-SNN. This indicates that the time-varying weight SNN, trained using our proposed methodology, achieves performance comparable to that of an SNN with a larger network architecture while requiring less computational time. Notably, when the GA is not utilised, there is a noticeable decline in performance. This underscores the importance of our proposed global optimisation approach in determining the network parameters and highlights its significant contribution to the effectiveness of our method.

Compared with the WOLIF in which its network is designed with constant weights and without hidden layers, both of our method configurations (with and without the GA) use a lower number of epochs to achieve higher accuracy for Ionosphere, Breast cancer and Iris benchmarks. With the global optimisation using GA, our method demonstrates approximately 2% improved accuracy on average from the WOLIF. However, the WOLIF demonstrates the highest accuracy in Liver disorders dataset among the methods. The training time for the WOLIF is not available and, therefore, is not included in the table.

Compared to SEFRON on benchmarks for Liver disorders, Breast cancer, Ionosphere, our proposed SNN-based methodology achieves higher classification accuracy regardless of the use of a GA. With the same number of epochs and a similar architecture, our method also consumes less training time per epoch. This improvement indicates that backpropagation can effectively train an SNN with time-varying weights, offering higher classification accuracy with lower computational cost compared to the STDP-based learning rule. Additionally, when our method employs global optimisation using GA, it achieves an average accuracy improvement of approximately 5% over SEFRON. Note that the SEFRON cannot directly be tested using the Iris benchmark as the network is applicable only for binary classification due to the use of a single output neuron, whereas we employed more output neurons.

3.7. SPIKING NEURAL NETWORK-BASED METHODOLOGY WITH SQUAT DETECTION

With its promising performance on classification, this section presents the applicability of an SNN with time-varying weights having no hidden layers and our proposed methodology to solve a complex spatiotemporal problem presented in squat detection.

3.7.1. MEASUREMENTS

Data used in this chapter were obtained from multiple ABA measurements mounted on a measuring train in a track section measured at almost constant speed in a range between 100 and 110 km/hr. The sampling frequency of the ABA measurements was 25.6 kHz. The information was acquired from accelerometers installed in both

longitudinal and vertical directions and from the left and the right wheels of the leading and trailing wheelsets [3, 134]. We repeated the measurements and both are used in the analysis.

The ABA measurements and field validation campaigns were conducted in 1) the track between Zwolle and Meppel, the Netherlands and 2) the track between Luleå and Narvik, Sweden. The measurements captured responses from healthy rails, welds, insulated joints, switches, and squats (light and severe). Our measurements are labelled according to observations and fieldwork. The locations of insulated joints, welds, and switches are known. The responses of insulated joints and switches are removed from the analysis as their locations are known and their degradation mechanisms have particular characteristics that are possible to analyse. As squats can initiate from welds, our analysis includes the responses of welds for both welds with squats and welds without visible squats.

3.7.2. IMPLEMENTATION DETAILS

A sensitivity analysis on the length of the ABA signals used is performed for both measurements. For the measurements from the Netherlands, the analysis suggests that using the ABA signals covering a distance of 78 cm yields the best predictive performance in terms of detection accuracy for the particular measurements of light squats considered in this case study. This performance is obtained with the sliding window of length equals to the distance of 8 and 4 centimetres for the vertical and longitudinal ABA signals, respectively. For the measurements from Sweden, the analysis suggests using the ABA signals covering a distance of 100 cm with the sliding window of length equals to the distance of 10 and 5 centimetres for the vertical and longitudinal ABA signals, respectively.

For each case study, the SNN is trained to classify whether or not a given rail segment contains squats. Therefore, our problem consists of a class of non-defective rails, referred to as Class 1, and a class of rails with squats, referred to as Class 2. For Class 1, the samples include rails at welds and healthy rails, whereas Class 2 includes rail samples with light and severe squats. For the Dutch case study, the dataset contains a total of 944 rail samples, of which 824 samples are labelled as non-defective rails and 120 samples are labelled as rails with squats. For the Swedish case study, the dataset contains a total of 1222 rail samples, of which 1068 samples are labelled as non-defective rails and 154 samples are labelled as rails with squats. In railway applications, labelled data are limited due to the complexity of the labelling process. For instance, the correct label of one defect, particularly for early-stage defects, requires an analysis of locations and a confirmation from multiple data sources because of their subtle development and these early-stage defects are frequently overlooked by human observers or video cameras. Additionally, railway tracks involve hundreds of kilometres, and fieldwork has limited access. Moreover, diverse local infrastructure conditions, track dynamics, and stochastic variables make the labelling process more difficult. As a result, assigning class labels is a laborious and time-consuming process. For the model training, each of the datasets is divided into the training and test sets with the ratio of 70:30, and 10-fold cross-validation is performed, in which 90% of the training set is used to train the SNN and the other

10% are used for validating the trained model. The trained model is then tested with the holdout test set to evaluate its performance for squat detection.

3.7.3. IMBALANCED DATASET

Conventional supervised methods rely extensively on balanced datasets between classes to guarantee their performance. In some railway infrastructures, it is extremely difficult to obtain a wide variety of class information for defects. That is the case when the inframanager conducts preventive grinding campaigns. In the cases reported in this chapter, the dataset used for training our model is imbalanced; that is, examples of healthy rails are abundant. Moreover, not only defects but healthy data are also difficult to label. This is because of different rail behaviours at different locations, the time-varying characteristic of railway infrastructure conditions and various different stochastic variables.

To deal with the situation of imbalanced data, clustering can be exploited to construct the balanced data set by reducing the number of the majority classes [219–222] or oversampling the minority classes [223, 224]. Transfer learning is another approach that researchers use to transfer learned parameters from a domain of balanced datasets to another one whose datasets are imbalanced [115–119, 225]. To show the effect of the imbalanced dataset on the performance of our method, a sensitivity analysis is done by considering different percentages of faulty data in the training set. By reducing the number of the healthy class, we consider five different percentages of faulty samples: 1) 13%, 2) 17%, 3) 25%, 4) 50%, and 5) 67%. To obtain model performance, we follow the feature engineering described in Section 3.4 and obtain the 54 frequency-based representations of the measured ABAs at rails. After encoding these features into spikes, the SNN architecture for this problem constitutes $54 \times 6 = 324$ input nodes and 2 output nodes. Following our SNN-based methodology (see Figure 3.6), Figure 3.10 reports an averaged classification performance obtained from the training set of each case. It is observed that detection accuracy for defects improves when a higher percentage of defective samples is included in the training set. However, for this experiment, total classification accuracy and detection accuracy for healthy samples degrade as the model is trained with an insufficient amount of data.

3.7.4. RESULTS

Firstly, the capability of our SNN-based methodology to solve the problem of squat detection is compared with other methods using ABA measurements from the Netherlands in terms of detection accuracy and computational cost. Then, we show its applicability in a railway line from Sweden. For both case studies, we follow the datasets described in section 3.7.2.

EVALUATION METRICS

The effectiveness of the proposed methodology is assessed based on the following metrics:

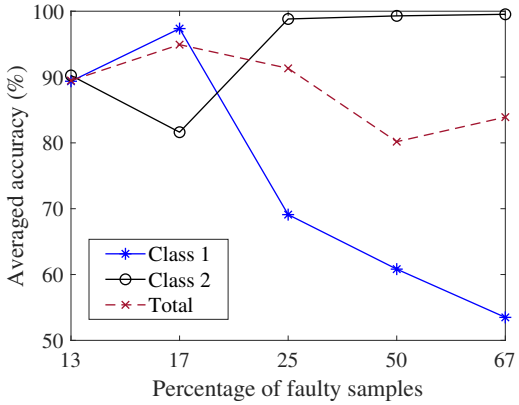

Figure 3.10: Effect of the percentage of faulty samples in the training set.

$$\text{Specificity} = \frac{TN}{TN+FP}, \tag{3.26}$$

$$\text{Recall} = \frac{TP}{TP+FN}, \tag{3.27}$$

$$\text{Precision} = \frac{TP}{TP+FP}, \tag{3.28}$$

$$\text{F1-score} = \frac{2 \times \text{Precision} \times \text{Recall}}{\text{Precision} + \text{Recall}}, \tag{3.29}$$

$$\text{FA} = \frac{FP}{TP+FP}, \tag{3.30}$$

where true positives (TP) are the number of correctly classified defects, false positives (FP) are the number of normal samples classified as defects, and False Negatives (FN) are the number of misclassified defects. Specificity is a metric for the detection accuracy of non-defective rails (Class 1), while Recall is a metric for the detection accuracy of defective rails (Class 2). FA denotes false alarm or false positive rate.

CLASSIFICATION PERFORMANCE AND COMPUTATIONAL COST

Following our SNN-based methodology (see Figure 3.6), the optimal set of hyper-parameter values for the Dutch railway line is: $T = 3$, $T_{\text{sim}} = 4$, $\hat{t}^d = 2.46$, $\sigma = 0.21$, $\eta = 0.000248$, and $\tau = 3.44$. By setting the hyper-parameters as described, the experimental results show that our SNN-based methodology yields an accuracy of 93.12% for non-defective rails (Specificity) and 97.14% for squat detection (Recall). The methodology can detect 100% of severe squats and 95.83% of light squats. It achieves the highest F1-score at 79.07% with an FA of 33.33%. Figure 3.11a) shows an example of predictions for the Dutch railway line. The length showcased here is

1.03 km, with 30 locations of squats reported. Our method predicts 42 locations of squats, of which 29 locations are correct, one squat location is missed, and 13 locations are false alarms. The field validation has indicated that these false alarms are at welds. With the high magnitude of ABA responses, the method classified them as defects. Further research is needed to differentiate welds from defects directly from ABA responses. Still, the location of welds can be registered in advance by inframanagers and verified with other measurement sources. Thus, welds can be excluded from the analysis of the detection of isolated defects. An example of a false alarm is given and discussed in Section 3.7.6.

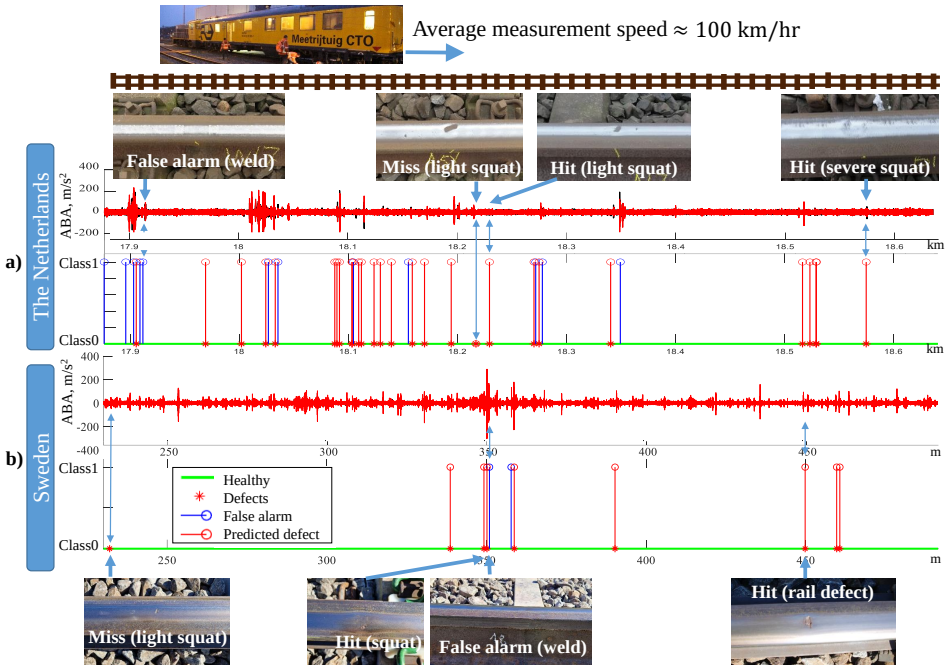

Figure 3.11: Detection of rail squats.

In order to justify its applicability of squat detection, the performance of our method is compared with a wavelet-based method [134], support vector machine (SVM), and neural network-based methods. SVM is included as it has a simple architecture. For the NN-based methods, Gated Recurrent Unit (GRU) and artificial NN (ANN) are selected. Although more layers can be used to increase the predictive performance of the models, GRU and ANN are designed with a single hidden layer to showcase a comparison with our SNN which contains no hidden layers. To evaluate the performance of the SNN with time-varying weights and no hidden layer, a comparison with the SEFRON [198] and a constant weights version of our method is also presented.

For the wavelet-based method presented in [134], the scale-averaged wavelet power (SAWP) was proposed to detect squats in which an empirical constant C related to

the mother wavelet and a constant threshold are chosen to maximise the hit rate and reduce the number of false alarms. In this chapter, the constant C is optimized and set to 35 and the same threshold of 0.5 m^2/s^4 is used to detect squats. For the other methods, the same implementation details described in Section 3.7.2 are followed and sensitivity analysis of hidden nodes used is performed.

Table 3.5 presents the comparative results of a squat detection obtained from the selected methods. It can be seen that all the methods achieve reasonable accuracy for non-defective rails (Class 1). For the detection accuracy of squats (Class 2), particularly light squats, SNN-based approaches, including SEFRON, SNN with constant weights, and SNN with time-varying weights, demonstrate higher accuracy. Among these, our SNN-based method achieves the highest detection accuracy for squats, particularly light squats. This benefit comes from its ability to produce time-encoded outputs that resemble the continuous scanning of ABA measurements.

The wavelet-based method can detect approximately 80.0% of light squats. This is consistent with the results reported in Molodova,Li in which light squats can be detected using ABA measurements with accuracy between 78% to 85%. The SVM and NN-based methods using a single hidden layer demonstrate similar detection accuracy for light squats. Their accuracy is less than 60.0%. Among all the methods, the SVM shows the lowest percentage of false alarms. Even though our SNN-based method produces more false alarms than the SVM, our SNN-based methodology has shown an ability to capture subtle changes in the responses of light squats in ABA signals using simple network architecture. Additionally, our method achieves a significantly higher F1-score, indicating a superior balance between precision and recall. Compared with the SEFRON, an SNN with the time-varying weights trained by our methodology achieves 8.3% higher accuracy for the detection of light squats but produces 2.6% more false alarms. Moreover, the comparison with the constant weights demonstrates that SNN with the time-varying weights trained by our methodology has improved accuracy in solving the complex spatiotemporal pattern presented in the light squat detection problem.

Table 3.6 presents a comparison of the computational time, measured as the average time taken to complete one epoch, for our SNN-based methodology and other methods using ABA measurements from the Netherlands. Our method outperforms the others in terms of computational efficiency. Despite having a single hidden layer, the NN-based methods, i.e., GRU and ANN, require the most time per epoch due to the complexity of their network structures. Among the simpler architectures, SVM consumes more computational time than both SEFRON and our method. The SNN-based methods require less computational time, highlighting their efficiency by utilising temporal information instead of numeric values. Notably, our method is faster than SEFRON, underscoring the effectiveness of using back-propagation over the STDP learning approach.

For the measurements from Sweden, the optimal set of hyper-parameters used in its SNN model is: $T = 3$, $T_{\text{sim}} = 4$, $\hat{t}^d = 0.4$, $\sigma = 0.1$, $\eta = 0.00085$, and $\tau = 3.76$. By setting the hyper-parameters as described, our SNN-based methodology can be used to detect squats in a railway line from Sweden with an accuracy of 95.65% with 8.33% false alarm rate. Figure 3.11b) illustrates the selected portion from the Swedish

Table 3.5: Comparative results of our SNN-based methodology with other methods using the ABA measurements from the Netherlands.

Method	Architecture	Detection accuracy (%)				Precision (%)	F1-score (%)	FA (%)
		Class 1 (Spec.)	Class 2 (Recall)	Light squats	Severe squats			
- Wavelet-based method Molodova	-	87.87	85.71	79.17	100.0	50.0	63.16	50.0
- SVM with non-linear RBF kernel	-	98.38	60.00	45.83	90.91	84.0	70.0	16.00
- GRU	54:150:2	85.00	68.57	58.33	90.91	80.0	73.85	20.00
- ANN	54:450:2	77.50	68.57	58.33	90.91	72.72	70.59	27.27
- SEFRON [198]	324:1	95.14	91.43	87.50	100.0	69.23	72.97	30.77
- SNN with constant weights	324:2	93.12	88.57	83.33	100.0	64.58	74.69	35.42
- SNN with time-varying weights	324:2	93.12	97.14	95.83	100.0	66.67	79.07	33.33

Table 3.6: Comparison of computational time obtained from our SNN-based methodology and other machine learning methods using the ABA measurements from the Netherlands.

Method	Architecture	Avg. time per epoch (s)
SVM with non-linear RBF kernel	-	25.2488
GRU	54:150:2	145.6138
ANN	54:450:2	34.0459
SEFRON [198]	324:1	4.2244
SNN with time-varying weights	324:2	1.9222

railway line with a length of 0.3 km, where 10 locations of squats are reported. The model has detected 12 locations of squats, of which 10 locations are correct, one location is missed, and 2 locations show as false alarms. Similar to the performance obtained for the Netherlands results, the Swedish railway line data demonstrate the applicability of our SNN-based methodology for rail squat detection. Similar to the measurements from the Netherlands, the locations of false alarms are at welds that are not in a good condition.

3.7.5. SCALABILITY

This section evaluates the scalability of the proposed SNN-based methodology as data complexity increases. The railway data from the Netherlands is exploited and the data complexity is reflected through increased dimensionality and utilisation of training data from both the time and time-frequency domains. Detecting rail squats from high-dimensional time-domain ABA signals can be challenging due to significant variability in dynamic behaviours at different track locations, which are affected by local properties of rail infrastructures and changing operational conditions of trains. Incorporating a longer signal length includes more variability of dynamic behaviours, complicating the analysis. Consequently, time-domain analysis can be more sensitive to variations, which may obscure important patterns related to rail squat dynamics. Therefore, the effect of increased data complexity on performance is investigated through five cases with different feature dimensions. The first three cases address data complexity in the frequency domain by selecting

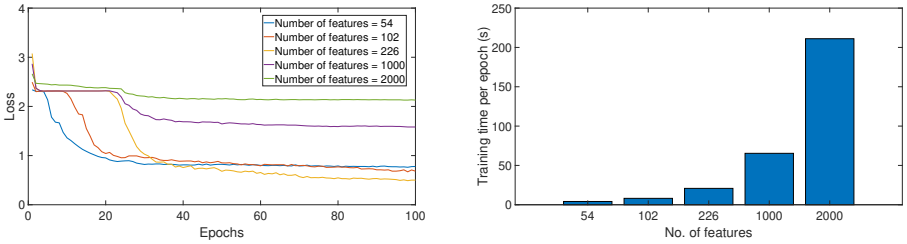

(a) (b)

Figure 3.12: Effect of data dimensions on the performance of our SNN-based method in terms of a) convergence rate over 100 epochs and b) computational time.

three different frequency ranges to describe ABA signals: 200-2000 Hz resulting in 54 features, 50-4000 Hz resulting in 102 features, and the full frequency range resulting in 226 features. These frequency-based features are obtained as described in Section 3.4. The last two cases focus on the temporal aspect reflected by different rail segment lengths. In these cases, we simulate scalability by increasing the length of the time series corresponding to feature dimensions of 1000 and 2000. The simulations are repeated 10 times, and the performance of the method is evaluated in terms of convergence and computational efficiency across varying complexities. The reported values represent the average results from these ten repetitions.

Figure 3.6 illustrates that both the computational time and the convergence rate of the proposed SNN-based methodology are affected as the dimensionality of the data increases. For 54 and 102 features, the convergence is relatively fast, with loss decreasing rapidly within the first 20 epochs and stabilising thereafter as seen in Figure 3.12(a). When the number of features increases to 226, the convergence rate slows slightly compared to 54 and 102 features. However, the loss still reduces to a low value, demonstrating that the method can handle moderate increases in dimensionality without significant degradation in performance. The training time per epoch for 54, 102, and 226 features remains relatively low, with a slight increase as the number of features rises from 54 to 226, as shown in Figure 3.12(b). However, when the feature dimension is significantly increased to 1000 and 2000, the convergence rate is notably slower, resulting in higher loss values. Moreover, the training time per epoch escalates dramatically, as depicted in Figure 3.12(b). This indicates that while the method can still learn from high-dimensional data, the increased complexity from using time-domain features impairs its efficiency and effectiveness.

3.7.6. EXPLAINABILITY FOR REPRESENTATION LEARNING

Researchers have been working on developing models with a good balance between explainability and accuracy [226–228]. To achieve the explainability of squat detection, wavelet analysis is typically employed due to its direct physical

interpretation. However, due to multiple sources of variability in the ABA responses, its accuracy is inferior to NN-based models (see Section 3.7.4). On the other hand, even though using NN-based models can achieve high accuracy, they are blackboxes and their prediction under new measurement conditions can be unreliable and not explainable.

To address the explainability of squat detection using SNN, we investigate 1) how well the SNN learns the data representations, 2) how the decision of the SNN is obtained, and 3) how the representative features learned by our methodology are favourable for early squat detection. Measurements from the Dutch railway are used as a showcase.

VISUALISATION OF OUR FEATURES USING T-SNE

For demonstration purposes, we perform a t-Distributed Stochastic Neighbor Embedding (t-SNE) of the representative features in three dimensions using the Euclidean distance metric. Figure 3.13 shows the cluster assignments obtained with our SNN-based methodology. The visualisation demonstrates a minimal overlap between the class of non-defective rails (blue) and the class of rails with squats (yellow) in the three represented dimensions. As features that are close in the high-dimensional feature space are also close in the three t-SNE represented dimensions, it infers that a reasonably good separation of clusters is given by our method. This supports that the SNN learns well the represented data.

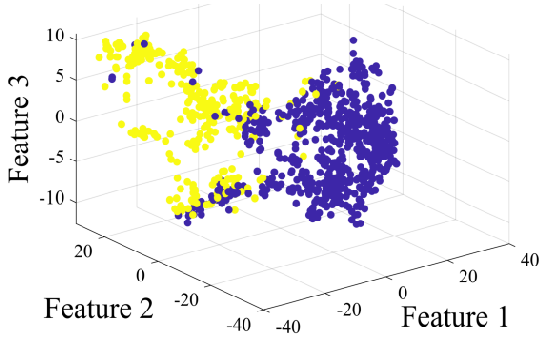

Figure 3.13: The three-dimensional t-SNE embedding of the representative features for our SNN-based methodology. The class of non-defective rails is illustrated in blue and the class of rails with squats is illustrated in yellow.

VISUALISATION OF REPRESENTATION LEARNING

Figure 3.14 illustrates the time-varying weights for Class 1 and Class 2 after learning with our methodology. It is seen that the values of the synaptic weights inside box A fluctuate as time varies. In box B, the synaptic weights for Class 1 switch in sign from negative to positive. The same behaviours are also observed for Class 2 but

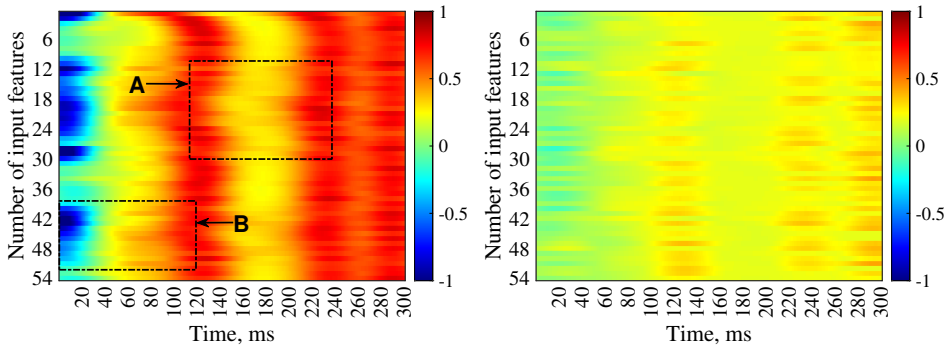

(a) Class 1. (b) Class 2.

Figure 3.14: Visualisation of the time-varying synaptic weights from the input layer to the output layer after learning with our method for squat detection.

with small variation. The key characteristic that allows the variations in the synaptic weights is the use of an exponential decay function, as defined in (3.23). The exponential function plays an important role in controlling the weight variations, $\Delta w_{ij}^{k,e}\left(t_i^k\right)$, with the parameter σ determining the range of influence over time. This dynamic adjustment allows the method to effectively track changes in synaptic weights within a specific time window. Consequently, the variations in synaptic weights facilitate both excitatory and inhibitory postsynaptic potentials depending on the timing of presynaptic spikes t_i^k. Without the exponential decay function, the weights remain constant over time. This results in inferior performance compared to using time-varying weights, as evidenced by the results in Table 3.5. Therefore, the success in squat detection is attributed to the implementation of the exponential function within the time-varying weight framework.

To provide information about which input features have contributed to the respective decision of the SNN-based methodology, the postsynaptic potentials for Class 1 and Class 2 are evaluated over the simulation time using the time-varying synaptic weights of the corresponding class and the spike response in order to determine the membrane potentials of the corresponding class. In the following, we illustrate how different representations of rail dynamics affected the performance of the detection of squats. The colour mapping of the postsynaptic potentials is symmetric around 0 (green), from dark-blue (strong inhibitory) to dark-red (strong excitatory). The change in sign from positive to negative reveals that our SNN can capture both excitatory and inhibitory states within a single synapse.

Figures 3.15 and 3.16 demonstrate a correct detection of a weld and a light squat by our SNN-based methodology. It is observed in Figures 3.15 (see D and F) and 3.16 (see H and J) that, for both Class 1 and Class 2, the excitatory postsynaptic potentials or positively activated parts of the SNN (red) increase towards the end of the simulation time. However, the excitatory postsynaptic potentials of Class 2 increase relatively slower than Class 1.

To determine the membrane potential of each class at a time instance, the excitatory postsynaptic potentials are compensated with the inhibitory postsynaptic potentials. If the measured ABA signals are at squats, their corresponding membrane potential of Class 2 has to cross the threshold (represented by the dotted red line) and emit the first spike. This infers that the membrane potential of Class 1 has to be weaker positively activated (lower amplitude) than that of Class 2 at the output spike time.

From our observations, the inhibitory postsynaptic potentials or deactivated parts of the SNN (blue) appear to influence the decision. It is shown that the inhibitory postsynaptic potentials in Figure 3.16 (see I) are more pronounced and remain deactivated towards the end of the simulation time in Class 1, compared to those in Figure 3.15 (see E). The final membrane potential of Class 1 in Figure 3.16 is then weaker positively activated than that in Figure 3.15. Therefore, the measured ABAs in Figure 3.16 are classified as a rail at squats.

Figure 3.17 provides an analysis of rail responses measured by ABAs at a weld that are misclassified by our SNN-based methodology. It is observed that the inhibitory postsynaptic potentials are more pronounced towards the end of simulation time in Class 1 as shown in Figure 3.17 (see L). The wrong behaviour of inhibitory postsynaptic potentials in Class 1 is a possible reason that leads to misclassification.

EXPLANATION OF THE REPRESENTATIVE FEATURES

Figures 3.15 and 3.16 show that the spike response of the encoded input features from different classes are different. The response of all input spikes from the ABA signals of non-defective rails increases uniformly over the simulation time, as illustrated in Figure 3.15 (see C). In contrast, Figure 3.16 (see G) shows that there are input spikes from the measured ABA signals at squats whose response increases dominantly. These input spikes are representative features from both vertical and longitudinal ABA signals that are associated with the high-frequency band between 1000-2000 Hz. According to [3], this frequency band is a frequency characteristic of light and severe squats. When making a decision, the features from this band are informative for evaluating squats. Figure 3.17 (see K) assures the finding as the wrong behavior of the spike responses leads to misclassification. This infers that our representative features are favourable for early squat detection as the variation of energy of light squats in the high-frequency band is more pronounced using an SNN.

3.7.7. DISCUSSION

The proposed SNN-based methodology achieves an improvement in the detection accuracy of light squats. However, it still suffers from misclassification from the measured ABA signals at non-defective rails into the class of rails with squats. At these non-defective rails with false detection, it is observed that our method provides consistent squat predictions in signals with different measurements. For instance, squats are predicted by our method in the signals of all wheels from the left and the right rails with the first measurement, whereas squats are predicted in the signals of all wheels from the left rail and in the signals of one out of two wheels from

the right rail with the second measurement. This suggests that there might be some invisible rail defects located at these healthy rails. Further experiments can be conducted at those rails where a false detection is shown.

Further improvement on the false negative and positive rates is needed because they have an impact on maintenance costs. New methods that can support reducing the uncertainties coming from the labelling process are needed. As the presence of invisible defects is highly affected by the labelling process, having historical information allows investigating the complete time evolution of a defect, from the moment it was first detected by the system until the latest stage of its evolution. This can be obtained using the advancement of ABA measurements in which accelerometers can be mounted on operational trains and multiple measurements can be easily conducted over the same track and over different time periods.

Moreover, our SNN-based methodology has exhibited difficulty in differentiating between the ABA responses of welds and squats. An underlying reason for the misclassification is that a weld and a squat can be located in close proximity in certain rail sections. Consequently, the rail response of squats influences the measured ABAs at welds. Additionally, welds can be healthy (with ABA signals resembling healthy rail) or suffer from degradation (with ABA signals resembling local defects). This poses a challenge for our method to distinguish by using solely ABA measurements. Still, the location of welds is known, and they are visible, so they can be obtained and verified with measurement campaigns and technology such as video images. As monitoring data of rail health conditions are also available in other formats, e.g. images, our future research will use these monitoring data as well. Therefore, the fusion of information obtained from different data types will be studied to provide not only more accurate early detection of rail surface defects but also fewer false alarms.

Even though the frequency characteristics of squats in ABA signals are consistent and typically appear in a frequency band of 200-2000 Hz for the train speed of 100 km/hr, making the method potentially applicable across different railway systems, variations in environmental conditions, infrastructure layouts, and operational characteristics can affect signal prominence. For example, lower loads and speeds produce less pronounced responses. To ensure generalisation, careful adaptation is required. This includes preprocessing and filtering to denoise and enhance signal prominence, and adjusting model parameters with new data to minimise false alarms and ensure accurate detection across different systems.

3.8. CONCLUSIONS

This chapter proposes a spiking neural network with time-varying weights using no hidden layers and its training methodology based on backpropagation. Testing on four UCI benchmarks, the accuracy obtained from our SNN-based methodology is competitive to other state-of-the-art SNNs when dealing with nonlinear classification problems for not only binary but also multiple classes. Using field measurements from the Netherlands and Sweden, the results from a squat detection have shown that our method is applicable of solving a complex spatio-temporal problem in

railway. We have improved the detection accuracy of light squats from the traditional methods which is of 78-85% to more than 93%. Furthermore, our method can be used to provide interpretability. The spike responses, postsynaptic potentials, and membrane potentials have offered an explainable way to analyse the ABA signals. These internal spike behaviours highlight a correspondency with high frequency band between 1000-2000 Hz of the detection problem of squats and offer an ability to capture subtle changes in the responses. Despite its success, the effectiveness of our SNN-based methodology can be affected by factors such as class imbalance, noise levels, and uncertainty in distinguishing subtle behaviours, such as rail dynamics. Future research can consider enhancing the robustness and effectiveness of the SNN-based methodology in handling these data characteristics by explicitly including possible stochasticity in the objective function and the robust parameters in the design.

Compared to current state-of-the-art methods, the SNN-based approach excels in situations with limited training data and complex spatiotemporal problems. These advantages arise because SNNs process data as discrete events (spikes) and capture information through spike timing patterns. Additionally, the proposed SNN incorporates time-varying weights, allowing the variations in the synaptic weights as time varies. This capability allows SNNs to model temporal sequences and dynamic behaviours where the timing and sequence of events are critical, such as in rail squat detection. The use of a global optimisation approach for determining network parameters further enhances the performance of our method as the approach helps in mitigating overfitting and avoiding local minima. However, the proposed SNN-based methodology has limitations. The SNN is not explicitly designed to address class imbalance, noise, and uncertainties. However, it is interesting for further research to analyse how explicitly the SNN can tackle these issues and evaluate its performance compared to the existing methods, such as generative-based, probabilistic, and transfer learning methods. Understanding these limitations is essential for optimising the application of the proposed method and improving its performance and robustness across various datasets and conditions. Additionally, a hybrid approach that combines those state-of-the-art methods with SNNs could further enhance performance in jointly tackling issues presented in the problems.

3.9. FUTURE RESEARCH DIRECTION

Further research lines can include a technique to alleviate the issue of imbalanced dataset and the adaptations for using SNN considering multiple measurements from different sources and data types. An evaluation of the impact of different time-varying functions can be considered. The use of fuzzy interval methods is being explored to explicitly capture uncertainties from the training process, so to better understand the behaviour of an SNN-based classifier when dealing with rail data. In addition, advancements in machine learning, signal processing, and railway engineering can enhance the development of rail defect detection techniques [132]. For instance, deep learning models, such as convolutional neural networks (CNNs),

can enable autonomous feature extraction, alleviating reliance on expert knowledge and improving detection accuracy. Applying transfer learning techniques can help models adapt to new conditions by using knowledge learned from different railway networks. This allows for defect detection in environments where models have not been previously trained or tested. Implementing advanced denoising algorithms can enhance the detection of subtle defects by improving the signal-to-noise ratio. This makes it easier to identify and address issues in their early stages. Deploying high-frequency sensors, such as ABAs, on operational trains can enable continuous monitoring of rail infrastructure, enhancing detection capabilities and predictive maintenance. Incorporating additional monitoring data sources and measurements can be considered with the development of data fusion techniques to enhance the accuracy and reliability of rail defect detection.

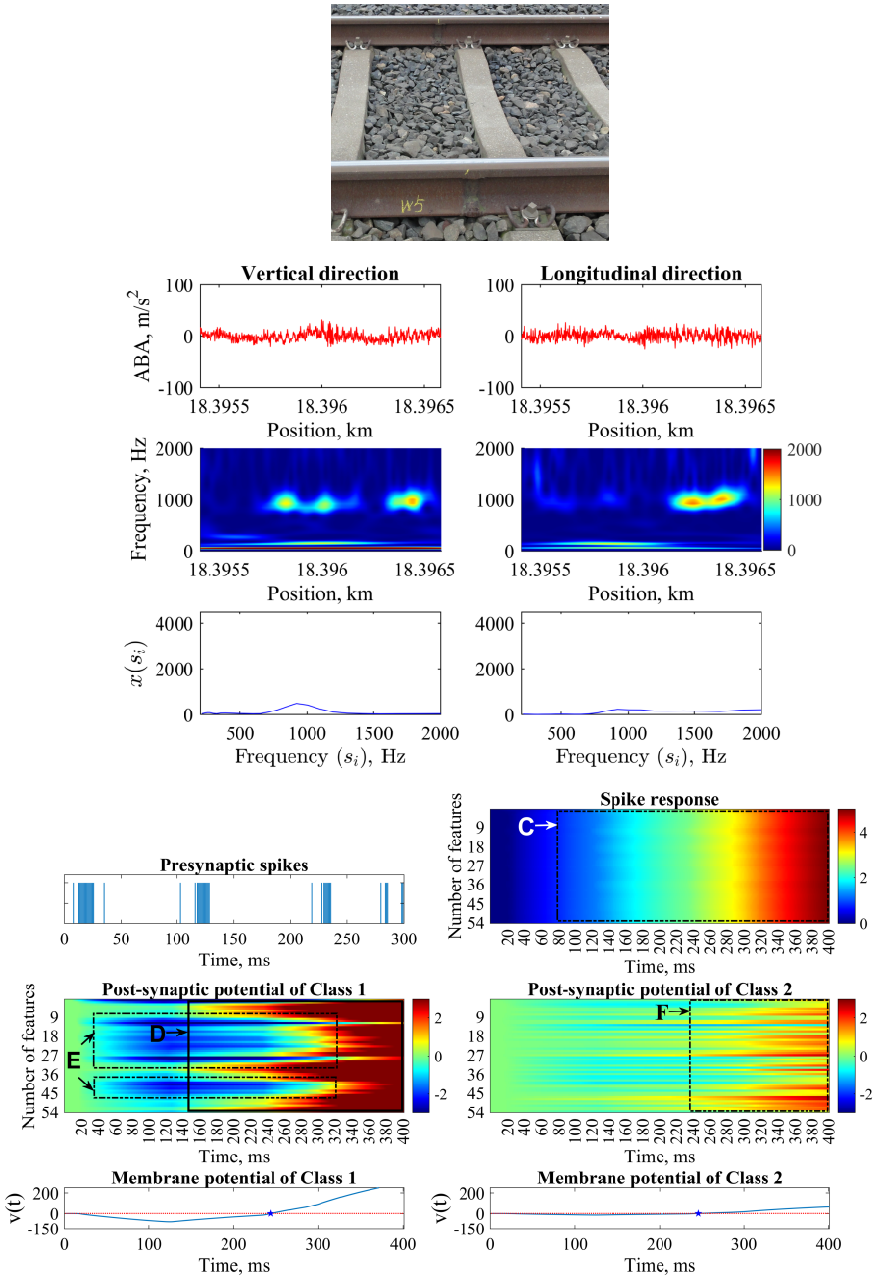

Figure 3.15: Visualisation of correctly classified ABA responses at a weld by the SNN-based methodology. In the membrane potential graphs, the blue line represents the membrane potential $v(t)$. The red dotted line indicates the threshold for neuron firing. When the membrane potential crosses this threshold, the neuron fires a postsynaptic spike, which is marked by blue star symbols on the graph.

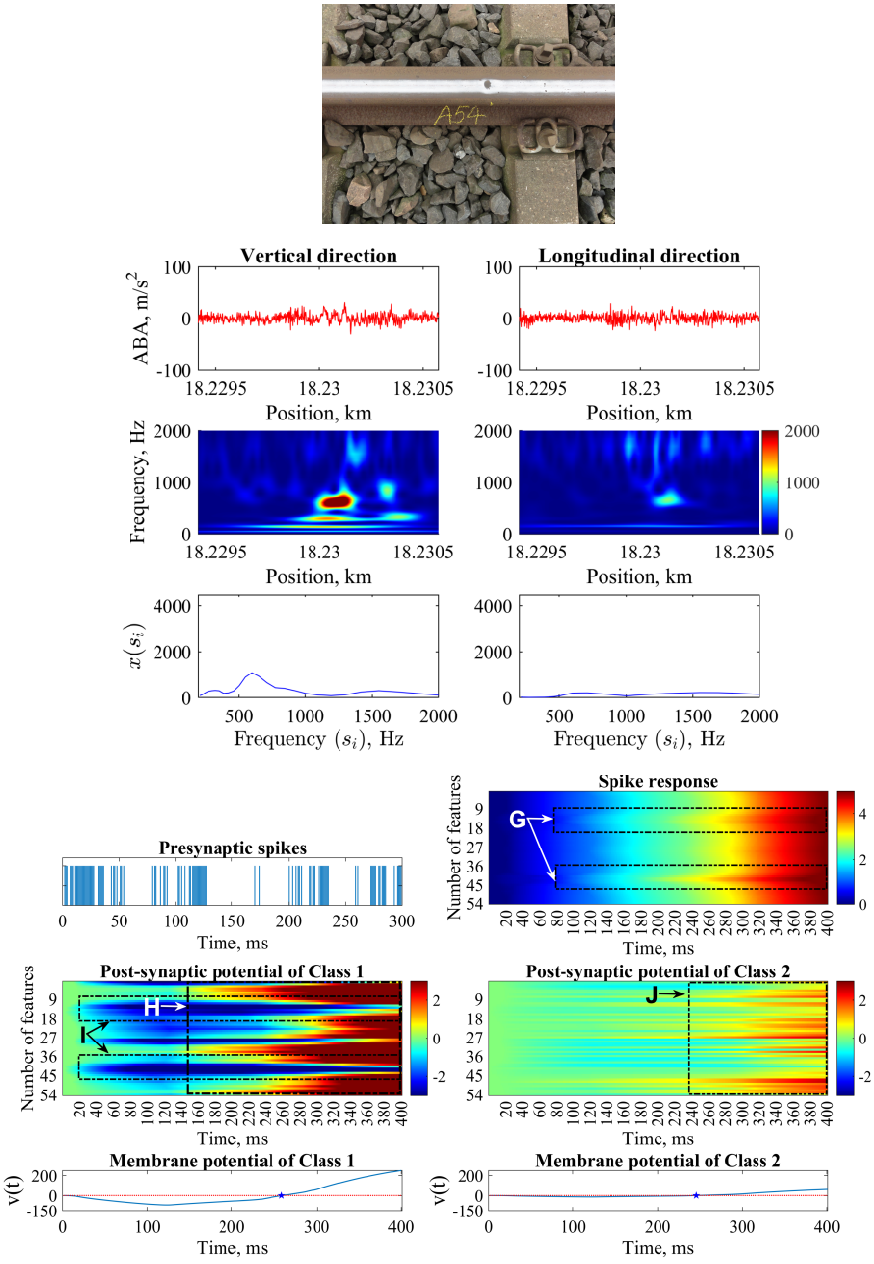

Figure 3.16: Visualisation of correctly classified ABA responses at a light squat by the SNN-based methodology. In the membrane potential graphs, the blue line represents the membrane potential $v(t)$. The red dotted line indicates the threshold for neuron firing. When the membrane potential crosses this threshold, the neuron fires a postsynaptic spike, which is marked by blue star symbols on the graph.

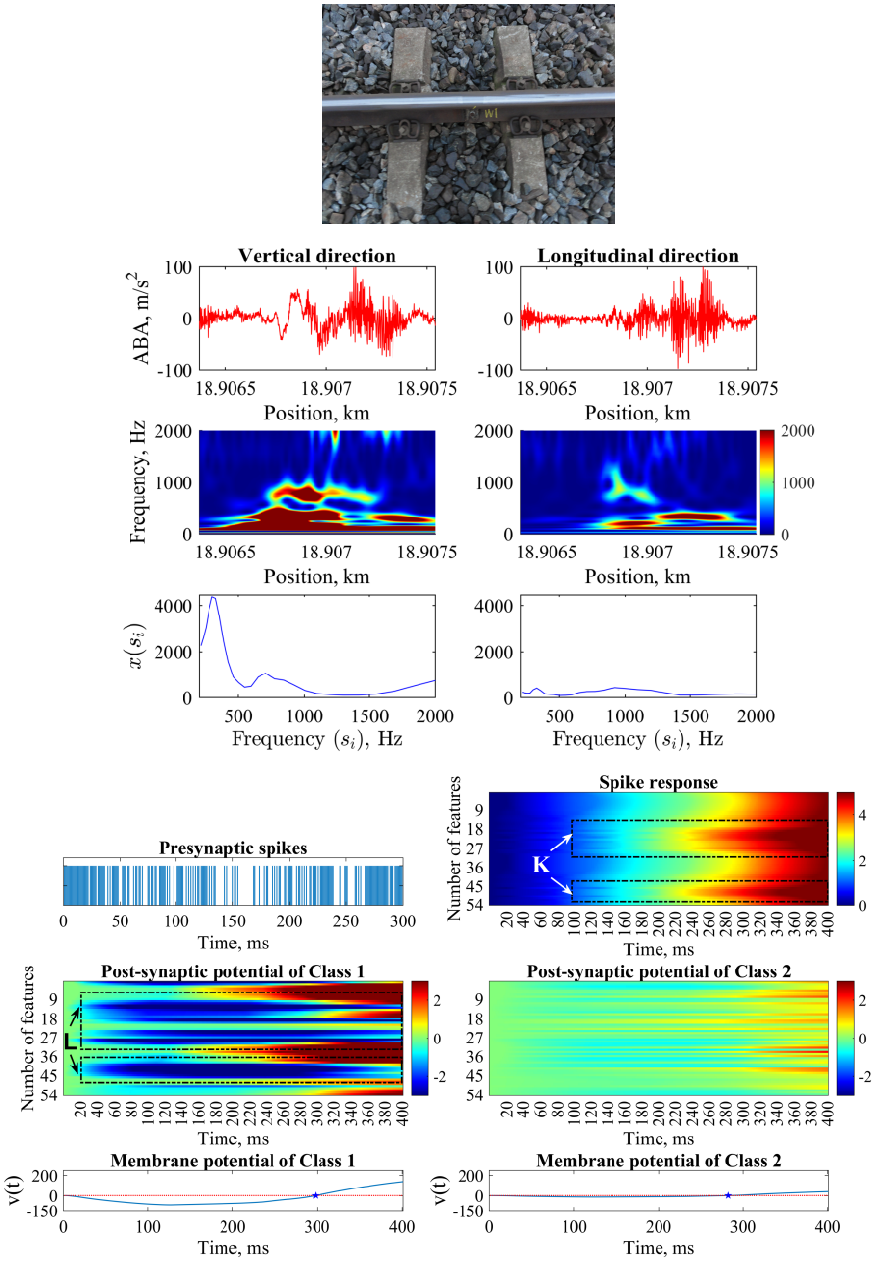

Figure 3.17: Visualisation of misclassified ABA responses at a weld by the SNN-based methodology. In the membrane potential graphs, the blue line represents the membrane potential $v(t)$. The red dotted line indicates the threshold for neuron firing. When the membrane potential crosses this threshold, the neuron fires a postsynaptic spike, which is marked by blue star symbols on the graph.

4

Unsupervised Representation Learning for Monitoring Rail Infrastructures with High-Frequency Moving Vibration Sensors

Nowadays, rolling stock can be equipped with high-frequency vibration sensors to continuously monitor rail infrastructures and accurately detect defects. These moving sensors generate a massive amount of data that contains multiple local transient dynamic responses with short signal duration. These responses are affected by noise and strong variations across different locations, complicating the identification of the dynamic responses. This leads to a complex and large amount of unlabeled data. This chapter proposes an unsupervised representation learning methodology to automatically capture the dynamic responses of rail infrastructures and provide insights into the underlying characteristics of their conditions. It aims for exploratory purposes, which allows the analysis of vibration signals in new operating environments where previous data about rail infrastructure health conditions are unavailable. A collaborative optimization process that synchronizes the empirical mode decomposition (EMD) with the parameters of a convolutional autoencoder (CAE) is presented. The CAE is trained on demodulated signals at each EMD level considering normal condition data to generate representations that ensure reconstruction quality and effectively differentiate between normal and abnormal conditions. In this chapter, a Gaussian mixture model is used to showcase the effectiveness of the learned

This chapter has been submitted for publication as: Phusakulkajorn, W., Zeng, Y., Li, Z., Núñez, A., Unsupervised Representation Learning for Monitoring Rail Infrastructures with High-Frequency Moving Vibration Sensors.

representations for rail infrastructures. Applied to validated axle box acceleration data for rail defect detection and train-borne laser Doppler vibrometer data for rail fastener monitoring, our method outperforms other variants of autoencoder-based models and the wavelet-based CAE in accurately identifying the conditions. It achieves an average improvement of 16% with ABA data and 21% with LDV data.

4.1. INTRODUCTION

STRUCTURAL health monitoring plays a pivotal role in ensuring the safety and integrity of rail infrastructures. Through the development of various sensing technologies and data analytics techniques, defects can be detected timely, thus allowing corrective and predictive maintenance to prevent catastrophic accidents. The collection and analysis of data further enable the digitalization of railway transportation systems. Among various monitoring technologies, vibration-based monitoring is an effective approach to characterize a wide range of dynamic behaviors and properties of rail infrastructures [229–233].

Vibration-based monitoring can be implemented by distributing sensors on rail infrastructures and measuring their vibrations induced by moving train loads, such as in [234, 235]. Distributed sensors can record structural vibrations at different locations over time, thus providing rich data for parameter estimation and health assessment. Numerous methods have been developed to analyze such signals, including signal processing methods [236, 237] and machine learning methods [238]. However, it is cost-prohibitive to apply distributed sensors to large-scale transportation systems, such as railway lines spanning thousands of kilometers.

Vibration-based monitoring of rail infrastructures with sensors on trains in operation is gaining increasing prominence. In [239–243], accelerometers are utilized, while in [244–246], vibrometers are employed to monitor various components and properties of railway track structures. In [247, 248], smartphones are used for evaluating the quality of railway tracks. These technologies enable the dynamic behaviors at different locations of an infrastructure to be measured in a single run, which is highly preferred for large-scale monitoring. These technologies generally pursue monitoring under the operational speed and load of the rail network to avoid disturbance to train traffic and capture structural response under realistic loading conditions.

Compared to the use of distributed sensors, vibration-based monitoring with moving sensors poses several challenges for data analysis and anomaly detection. The first challenge is significant variability in dynamic behaviors at different locations, which is affected by local properties of rail infrastructures and changing operational conditions of trains. For example, Fig. 4.1 depicts a portion of a vibration signal measured by an axle box accelerometers (ABA). This signal contains rail dynamics that vary along the track, which are evident by the vibration patterns of the weld and surface defects, highlighted as examples in the figure. Additionally, the green boxes in the figure represent the ABA signals from nearby locations that exhibit significantly different amplitudes in their frequency contents. This variability across large-scale infrastructures complicates the identification of anomalies, necessitating advanced techniques to isolate them.

The second challenge arises from the need to segment signals for high-resolution localization of defects. This segmentation process results in short-duration signal fragments. For instance, when a train travels at a speed of 100 km/h, it covers a distance of 1 meter in 36 milliseconds. As train speed increases, the time duration over a specific distance decreases accordingly. A shorter duration of the signals makes it more difficult to achieve accurate and reliable defect detection because less

information is available within the segment. Therefore, a high sampling frequency is necessary to capture the variations of dynamic behaviors within these signals, resulting in an increased number of data points within a given distance. For example, ABA data are collected with a high sampling frequency of 25.6 kHz in [134], while the sampling frequency of a train-borne laser Doppler vibrometer (LDV) is 102.4 kHz in [244]. This generates large volumes of data with short durations and high frequencies, requiring effective and efficient methods to process them.

The third challenge concerns disturbances and noise from multiple sources, including vehicle vibrations, track irregularities, and measurement noise. Fig. 4.2 shows an example of the train-borne LDV signal measured on rail fasteners where severe noise is observed. The major source is the speckle noise due to the drastic change of speckle patterns as the laser spot scans the rough surfaces [249]. The speckle noise deteriorates the quality and usability of LDV signals. It obscures the actual vibration patterns of defects and anomalies, making it difficult to detect accurately. The mitigation of noise and disturbances is achieved with specialized filtering algorithms in [245, 249].

The last challenge involves fuzziness in distinguishing between different dynamic behaviors. For instance, when dealing with defects at the early stage of their development, their responses in ABA signals are subtle and slightly different from those of healthy rails, as seen from the dynamic responses of the small defect in Fig. 4.1. These responses may not be apparent to human inspectors or traditional detection methods. As a result, many samples fall within the ambiguous boundaries between normal and abnormal conditions. These samples complicate the labeling process and yield a substantial amount of unlabeled data, hindering the use of supervised learning.

Conventionally, the above challenges are addressed by crafting data analysis methods based on the knowledge and experience of experts in the physics of targeted structures and defects, such as [245, 250]. However, with the increasing volume of data, diversity of objects, and complexity of features, manual judgement becomes less efficient, robust, and reliable. Alternatively, the advancement of unsupervised learning has the potential to fill this gap [132].

Several unsupervised learning approaches have been developed to analyze vibration data from distributed sensors, such as t-distributed stochastic neighbor embedding (t-SNE) [251, 252], principal component analysis [253], K-means clustering [252], tensor clustering [254], one-class support vector machine [255], and self-organizing maps [256]. Deep learning has gained attention in addressing such problems in recent years, and various auto-encoder (AE) variants have been developed for feature learning. In [257–261], convolutional autoencoder (CAE) is exploited in feature extraction and fault detection based on vibration signals. In [262], an expectation-maximization algorithm with an adversarial autoencoder was used in feature extraction for rotating machinery fault diagnosis. In [263], a one-dimensional residual convolutional autoencoder was proposed in which residual learning played a role in feature learning on 1-D vibration signals for gearbox fault diagnosis. In [264], an unsupervised feature learning method for machinery health monitoring was proposed using a generative adversarial networks model. In [265–267], a

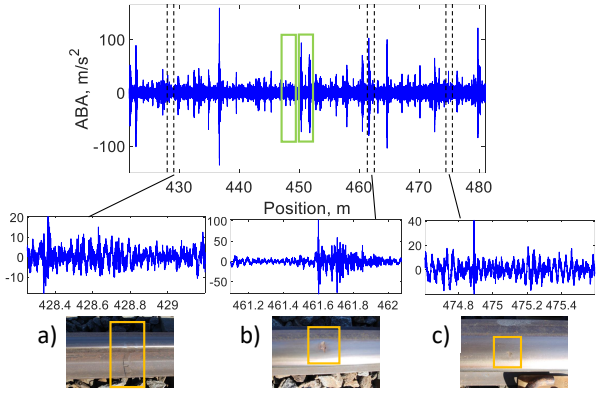

Figure 4.1: Example of a raw ABA signal containing various rail dynamics: a) weld, b) squat, and c) small defect.

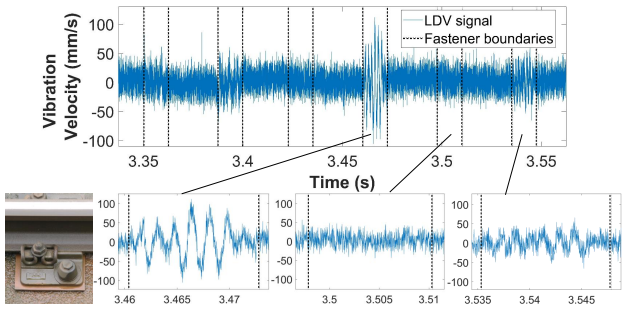

Figure 4.2: Example of a raw LDV signal containing severe noise.

method based on sparse filtering, an unsupervised two-layer neural network, was proposed for fault feature learning from mechanical vibration signals. However, all the aforementioned research focuses on vibration data measured by distributed sensors. Given the challenges mentioned above, there is a very limited amount of unsupervised learning methods developed to handle vibration data from moving sensors.

Therefore, this chapter develops an unsupervised representation learning methodology to extract features characterizing the dynamic behaviors of rail infrastructures measured by high-frequency moving vibration sensors. The methodology employs a collaborative optimization process that synchronizes empirical mode decomposition (EMD) with the parameters of a CAE. EMD plays a fundamental role in this method based on its advantage of adaptively separating different frequency characteristics without the need for predefining each frequency range [240, 268]. EMD offers the possibility to explore dynamic behaviors over a broad frequency band while reducing the disturbance of measurement noise. The

CAE then extracts features from vibration signals to characterize these dynamic behaviors automatically. The latent features learned from the collaborative process of EMD and CAE ensure reconstruction quality and distinguish between normal and abnormal behaviors. This facilitates various analyses, including dimensionality reduction, classification, clustering, and supports anomaly detection by identifying deviations from the normal behavior pattern. The key contributions of this work are summarized as follows:

- An unsupervised representation learning methodology is proposed to automatically extract features that characterize dynamic behaviors of rail infrastructures from vibration data that is noisy and short-duration obtained from high-frequency moving sensors at different locations.
- A collaborative optimization process between EMD level and the parameters of CAE is proposed for a generation of representations that demonstrate reconstruction quality and can differentiate between rail infrastructures under normal and abnormal conditions.
- Two field measurements with different targeted components, sensor types, and operational conditions are used to demonstrate the applicability and performance of the proposed methodology for monitoring rail defects using an ABA and rail fasteners using a train-borne LDV.

The rest of the chapter is as follows. Section 4.2 presents fundamental knowledge of the methodology used. Section 4.3 presents problem formulation and the proposed framework. In Section 4.4, the proposed unsupervised representation learning methodology is elaborated. Section 4.5 describes the real-world applications used to showcase the methodology. The comparison of the proposed methodology with different models from the literature and discussions are presented in Section 4.6. The paper is concluded in Section 4.7.

4.2. Fundamental knowledge

4.2.1. Empirical mode decomposition

The EMD has been pioneered by Huang et al. [269] for adaptively representing nonlinear and non-stationary signals. For a given signal $x(t)$, EMD decomposes $x(t)$ into a series of intrinsic mode functions (IMFs), denoted as $c_i(t)$, where $i = 1, 2, \ldots, I$ and I is the total number of IMFs, and a residual $r_i(t)$ [270]. The EMD algorithm, referred to as the sifting process, iteratively extracts IMFs based on the local maxima and minima of the signal. At the end of the EMD process, the original signal $x(t)$ can be expressed by a sum of IMFs and a residual component as [271]:

$$x(t) = \sum_{i=1}^{I} c_i(t) + r_I(t). \tag{4.1}$$

4.2.2. CONVOLUTIONAL AUTOENCODER

A CAE is a type of autoencoder architecture that combines convolutional layers with an autoencoder model [272, 273]. It aims at unsupervised learning of a lower-dimensional representation from higher-dimensional data. The CAE network comprises three main parts: encoder, latent representation, and decoder. The encoder and decoder are designed using convolutional layers and can have several hidden layers, making a deep CAE.

Given an input signal $x(t)$ and let denote the output of the l^{th} convolutional layer as z_l, where l ranges from 1 to L, in which L is the number of convolutional layers designed in the encoder. The output of the encoder z_L is a latent representation of the input data $x(t)$, typically with reduced dimensions. The decoder takes the latent representation z_L and aims to reconstruct the original input $x(t)$. The decoder consists of a stack of transposed convolutional layers. Let denote the output of the k^{th} transposed convolutional layer as u_k, where k ranges from 1 to the number of transposed convolutional layers K. The output of the decoder $u_K = \tilde{x}(t)$ is the reconstructed version of the input data $x(t)$. Mathematically, the process of encoding and decoding in a CAE is given as follows:

$$z_l = \sigma\big(w_l * z_{l-1} + b_l\big), \tag{4.2}$$

$$u_k = \sigma\big(v_k * u_{k-1} + e_k\big), \tag{4.3}$$

where $*$ denotes the convolution operation, σ denotes an activation function, w_l and b_l are the weights and biases of the l^{th} convolutional layer, v_k and e_k are the weights and biases of the k^{th} transposed convolutional layer.

4.3. PROBLEM FORMULATION AND THE PROPOSED FRAMEWORK

Let $x_a(t) = a(p(t))$ denote acceleration signals from ABA and $x_v(t) = v(p(t))$ denote velocity signals from LDV obtained from a positioning system at track position $p(t)$ and at time instance t. For simplicity, we will represent these signals collectively as $x(t)$ throughout the rest of the chapter.

For a vibration signal $x(t)$ obtained from a moving sensor collected with sampling frequency f Hz and measuring speed $s(t)$ m/s, this work assumes segmenting the signal $x(t)$ into a set $\mathscr{D}$ of M smaller segments containing β datapoints. The set $\mathscr{D}$ is mathematically expressed as:

$$\mathscr{D} = \Big\{ x_m(t) \;\Big|\; t = t_{(m-1)\phi+1}, \ldots, t_{(m-1)\phi+\beta}, \Big\}_{m=1}^{M}, \tag{4.4}$$

where $x_m(t)$ denote the m^{th} segment corresponding to the time instances between $t_{(m-1)\phi+1}$ and $t_{(m-1)\phi+\beta}$ with time duration $\zeta_m = t_{(m-1)\phi+\beta} - t_{(m-1)\phi+1}$ and ϕ is the number of datapoints used as a step size for moving the segment.

The signal segmentation can be done to allow overlapping, meaning $\phi < \beta$. A sensitivity analysis can also be considered to identify the appropriate time duration ζ_m suitable for the data analysis task. This is due to a need to balance between

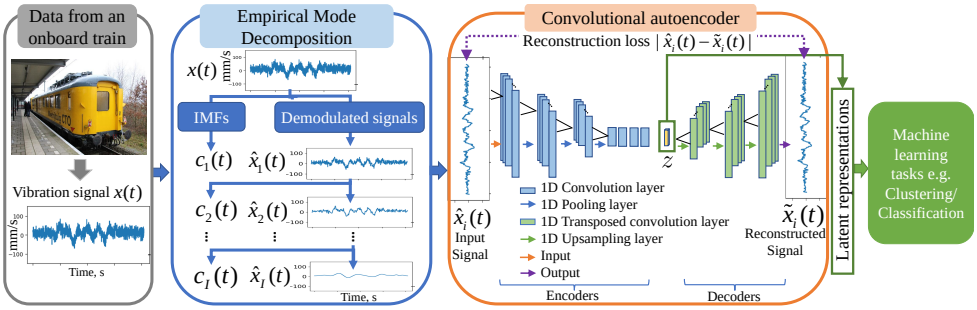

Figure 4.3: Framework for unsupervised representation learning.

4

accommodating the characteristic response length and capturing sufficient detail for the detection and localization of the targeted rail infrastructure. Given a targeted rail infrastructure r, let t_{b_r} and t_{e_r} be the starting and ending time of its dynamic response, and $\tau_r = t_{e_r} - t_{b_r}$ be the duration of this response. Additionally, let t_{α_r} represent an additional time duration used to capture extra responses. The appropriate segment length can be determined by minimizing the datapoints β contained within each segment while finding an optimal t_{α_r} that ensures the segments cover the critical dynamic response duration τ_r. This optimization process can be formalized into the objective function and constraints as follows.

$$\min_{\beta, t_{\alpha_r}} \zeta_m(\beta) \tag{4.5}$$

subject to, $\forall r \in \mathbb{Z}^+$,

$$2t_{\alpha_r} + \tau_r \leq \zeta_m(\beta), \forall m = 1, \ldots, M, \tag{4.6}$$

$$\left[t_{b_r} - t_{\alpha_r}, t_{e_r} + t_{\alpha_r}\right] \subseteq \left[t_{(m-1)\phi+1}, t_{(m-1)\phi+\beta}\right], \exists m. \tag{4.7}$$

Unsupervised representation learning aims at autonomously extracting useful features that capture key characteristics of data without labels. This technique generally involves a reconstruction process relying on learning representations from data with normal behaviors/conditions to capture their common and essential features. In alignment with this principle, this chapter introduces a hard threshold for identifying some normal samples from the unlabeled data. This hard threshold allows the reconstruction process to function without requiring a complete and pure dataset of normal data. Instead, it allows part of normal data to be utilized and even some ambiguous abnormalities to be included. This approach eliminates the need for extensive collections of purely normal data. The flexibility in data acquisition aligns with the unsupervised learning paradigm, which does not rely on prior input from experts or extensive fieldwork.

For a given hard threshold λ, this chapter considers a set $\mathcal{N} \subseteq \mathcal{D}$ containing samples most likely with normal conditions for representation learning. The set $\mathcal{N}$ is obtained as:

$$\mathcal{N} = \left\{ x_n(t) \in \mathcal{D} \;\middle|\; C\big(x_n(t), \lambda\big) \right\}_{n=1}^{N}, N < M, \tag{4.8}$$

where C is a specified condition for a selection of normal samples.

As vibration signals from moving sensors contain various disturbances and noise, this work employs EMD to decompose $x_n(t) \in \mathcal{N}$ into several IMFs. Each IMF represents an oscillatory mode embedded within the signal, with different levels of IMFs capturing different high-frequency components and noise inherent in the signal. The residual signal represents the part of the signal that cannot be effectively decomposed into the IMFs of the respective level. It typically consists of low-frequency components and trends of the signal. This chapter considers the residual signal at various levels $r_i(t), i = 1, 2, \ldots, I$, to extract representations inherent in the normal data. This approach resembles multi-level denoising, as the noise components are removed at various levels. In this context, these residual signals are referred to as demodulated signals as they are the signals from which the cumulative sum of IMFs up to level i has been extracted from the original signal. Let $\widehat{N}_i$ be a set of demodulated signals at level i, then the demodulated signal $\hat{x}_{n,i}(t)$ at level i within this set is expressed as:

$$\hat{x}_{n,i}(t) = x_n(t) - \sum_{j=1}^{i} c_j(t). \tag{4.9}$$

The EMD method allows for a separation of noise and extraction of meaningful representations from the vibration signals. Therefore, this chapter considers learning a representation of $\mathcal{N}$ through the demodulated signals in $\widehat{\mathcal{N}}$.

For the reconstruction process at each EMD level i, an autoencoder model $F_i = D_i \circ E_i$ is developed such that the encoder E_i encodes the demodulated signals $\hat{x}_{n,i}(t) \in \widehat{\mathcal{N}_i}$ into a lower-dimensional latent representation space $z_{n,i}(t)$. Then, the decoder D_i decodes it back to the original space, yielding the reconstructed data $\tilde{x}_{n,i}(t)$ from its representation. The reconstruction process is mathematically expressed as:

$$\tilde{x}_{n,i}(t) = F_i(\hat{x}_{n,i}(t)) = D_i(E_i(\hat{x}_{n,i}(t))), \tag{4.10}$$

in which

$$z_{n,i}(t) = E_i(\hat{x}_{n,i}(t)), \tag{4.11}$$

$$\tilde{x}_{n,i}(t) = D_i(z_{n,i}(t)). \tag{4.12}$$

This chapter proposes a methodology to collaboratively train the EMD and reconstruction for generating discriminative and informative representations. Fig. 5.3 illustrates the proposed unsupervised representation learning framework, consisting of three main parts. The first part utilizes EMD to remove the disturbance and noise and preserve the vibration pattern in the learning data, resulting in the demodulated signals. The second part uses a CAE model to implement representation learning from the demodulated signals based on the reconstruction technique. The final part applies the learned representations to various data analysis tasks. This step demonstrates the practical utility of the extracted features for further analysis, such as anomaly detection.

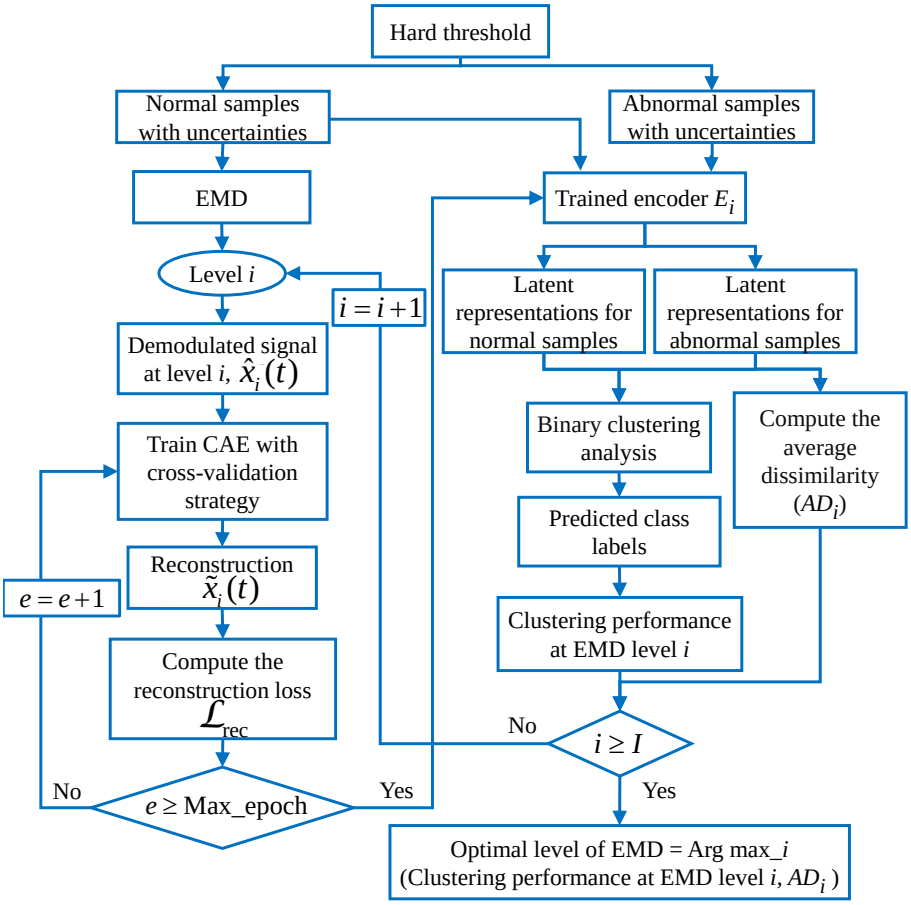

Figure 4.4: Workflow of the proposed methodology.

4.4. Proposed Methodology

Fig. 4.4 illustrates the workflow of the collaborative method proposed in this chapter. The method involves, firstly, signal denoising via EMD described in (4.9), secondly, identification of a corresponding autoencoder model defined in (4.10), (4.11), and (4.12) that allows mapping input signals onto the latent representation such that the reconstruction loss is minimized, and, lastly, an identification of the optimal EMD level of (4.9) for anomaly detection of rail infrastructures via binary clustering.

For a given hard threshold, consider a set of vibration data $\mathscr{D} = \left\{x_m(t)\right\}_{m=1}^{M}$ and a set of normal data $\mathscr{N} = \left\{x_n(t)\right\}_{n=1}^{N}$. We define a set of abnormal data $\mathscr{N}'$ as a subset of $\mathscr{D}$ that remains after removing the data present in $\mathscr{N}$. This set $\mathscr{N}'$ contains

abnormal data, including data with uncertain abnormalities, in which it is defined as

$$\mathscr{N}' = \mathscr{D} - \mathscr{N} = \left\{ x'_k(t) \in \mathscr{D} \;\middle|\; x'_k(t) \notin \mathscr{N} \right\}_{k=1}^{N'}.$$

For a given EMD level i and the corresponding set of demodulated signals $\widehat{\mathscr{N}_i} = \{\hat{x}_{n,i}(t)\}_{n=1}^{N}$, the reconstruction technique is considered to train CAE relying on learning representations from $\widehat{\mathscr{N}_i}$ to capture its common and essential features. Then, the CAE is trained on $\widehat{\mathscr{N}_i}$ to obtain the latent representation by minimizing a loss function that measures the discrepancy between the input data and its reconstruction. In this work, a loss function is defined as a combination of mean squared error (MSE), $\mathscr{L}_{\text{MSE}}$, and KL divergence, $\mathscr{L}_{\text{KL}}$, as our reconstruction loss, $\mathscr{L}_{\text{rec}}$, and it is expressed as:

$$\mathscr{L}_{\text{rec}} = \mathscr{L}_{\text{MSE}} + \mathscr{L}_{\text{KL}}, \tag{4.13}$$

where

$$\mathscr{L}_{\text{MSE}} = \frac{1}{N} \sum_{n=1}^{N} \left(\hat{x}_{n,i}(t) - \tilde{x}_{n,i}(t) \right)^2, \tag{4.14}$$

$$\mathscr{L}_{\text{KL}} = -\frac{1}{2} \sum_{j} \left(1 + \log(\sigma_j^2) - \mu_j^2 - \sigma_j^2 \right) + \frac{1}{2} \sum_{j} \left(\log(\sigma_{\text{prior}}^2) - 1 - \frac{\sigma_j^2}{\sigma_{\text{prior}}^2} + \frac{\mu_j^2}{\sigma_{\text{prior}}^2} \right),$$

where N is the number of normal samples, μ_i and σ_i are, respectively, the mean and standard deviation of the distribution of the latent representation z along the j^{th} dimension, μ_{prior} and σ_{prior} are the mean and standard deviation of the prior distribution, in which its value can be obtained from a standard Gaussian distribution, i.e., $\mu_{\text{prior}} = 0$ and $\sigma_{\text{prior}} = 1$.

The trained CAE allows us to obtain an encoder E_i developed with respect to the EMD level i, which is used to generate the respective embedded representation $z_{n,i}(t)$. This chapter considers a binary clustering task to identify the optimal EMD level that provides the discriminative representation between normal and abnormal conditions of rail infrastructures. The Gaussian Mixture Models (GMM) are employed to showcase clustering, chosen for their robustness to initialization compared to k-means [274]. In this chapter, the GMM is trained to provide two clusters using a dataset containing normal and abnormal samples. By following Fig. 4.4, a trained encoder E_i encodes normal and abnormal samples into the respective representations. Then, class labels are predicted and compared with those from the specified hard threshold to assess clustering performance. The training process is repeated according to the total number of IMFs. Based on the clustering performance achieved for all the EMD levels, we identify the optimal level as the one that yields the highest clustering performance. Algorithm 1 presents a pseudo-algorithm detailing the steps involved in the proposed collaborative optimization.

The effectiveness of the proposed methodology is evaluated based on its performance in representation learning and clustering. The performance of representation learning is measured via a signal reconstruction and a generation of discriminative features to distinguish between normal and abnormal conditions.

Algorithm 1 Collaborative optimization procedure

Input: Normal set ($x(t) \in \mathcal{N}$) and its labels (Y) obtained from a hard threshold, abnormal set ($x'(t) \in \mathcal{N}'$) and its labels (Y') obtained from a hard threshold, the maximum number of IMFs (I)
Output: Optimal level of EMD (i_{opt}), clustering performance, dissimilarity between $\mathcal{N}$ and $\mathcal{N}'$
Initialize EMD level $i \leftarrow 1$
repeat
  // Step 1: EMD on $x(t) \in \mathcal{N}$
  $\hat{x}_i(t) \leftarrow H_i(x(t))$ %IMF at level i
  Initialize number of epoch $e \leftarrow 1$
  repeat
    // Step 2: CAE Training on $\hat{x}_i(t) \in \widehat{\mathcal{N}_i}$
    Train CAE using cross-validation on $\hat{x}_i(t)$
    $\tilde{x}_i(t) \leftarrow D_i(E_i(\hat{x}_i(t)))$ % Reconstruction at level i
    Compute reconstruction loss $\mathscr{L}_{\text{rec}}(\hat{x}_i(t), \tilde{x}_i(t))$
    $e \leftarrow e + 1$
  until $e \geq$ Maximum epoch
  // Step 3: Obtain Latent Representations
  $E_i \leftarrow$ Trained encoder at level i
  $\hat{x}'_i(t) \leftarrow H_i(x'(t))$ %EMD on $x'(t) \in \mathcal{N}'$
  Latent representations for normal samples: $z_i(t) \leftarrow E_i(\hat{x}_i(t))$
  Latent representations for abnormal samples: $z'_i(t) \leftarrow E_i(\hat{x}'_i(t))$
  // Step 4: Binary Clustering Analysis
  Perform binary clustering on $z_i(t)$ and $z'_i(t)$
  Obtain predicted class labels $\widehat{Y}_i$ and $\widehat{Y}'_i$
  Compute clustering performance at EMD level i
  // Step 5: Compute Average Dissimilarity
  Compute average dissimilarity $AD_i(z_i(t), z'_i(t))$
  $i \leftarrow i + 1$
until $i > I$
// Step 6: Determine Optimal EMD Level
$i_{\text{opt}} \leftarrow \text{argmax}_i \left(\text{clustering performance at level } i, \text{average dissimilarity at level } i\right)$
return Optimal level of EMD i_{opt}, clustering performance, average dissimilarity =0

The former aspect is quantitatively assessed through the reconstruction loss, $\mathscr{L}_{\text{rec}}$, defined in (4.13). To assess the effectiveness of the method in generating discriminative features, we measure the dissimilarity between normal and abnormal samples obtained from clustering analysis, in which an average dissimilarity (AD) is exploited for this purpose. It is calculated from the average distance across all pairs of normal and abnormal samples. In this chapter, an Euclidean distance metric is considered. A greater dissimilarity indicates a greater distinction between the normal and abnormal samples. The average dissimilarity based on the Euclidean distance is expressed as:

$$AD_i(z_{n,i}(t), z'_{k,i}(t)) = \frac{1}{N \cdot N'} \sum_{n=1}^{N} \sum_{k=1}^{N'} \sqrt{\sum_{j=1}^{\beta'} (z_{n,i}(t_j) - z'_{k,i}(t_j))^2}, \tag{4.15}$$

where $z_{n,i}(t_j)$ and $z'_{k,i}(t_j)$ denote the j^{th} dimension of the latent representation at the EMD level i of the n^{th} normal and k^{th} abnormal sample. The total number of normal and abnormal samples are denoted by N and N', respectively, and β' is the number of dimensions of the latent representation.

Compared against labels obtained from the hard threshold, the clustering performance is assessed in terms of precision, recall, and F1 score, which are expressed as:

$$\text{Precision} = \frac{TP}{TP + FP}, \tag{4.16}$$

$$\text{Recall} = \frac{TP}{TP + FN}, \tag{4.17}$$

$$\text{F1-score} = \frac{2 \times \text{Precision} \times \text{Recall}}{\text{Precision} + \text{Recall}}, \tag{4.18}$$

where, in the context of anomaly detection, true positives (TP) are the number of correctly classified abnormalities, false positives (FP) are the number of normal samples classified as abnormalities, and False Negatives (FN) are the number of abnormalities classified as normal.

4.5. CASE STUDIES

To demonstrate the proposed methodology, we present two case studies from field measurements conducted on operational rail lines in Sweden and the Netherlands. In the two case studies, different track components are monitored using different sensing technologies applied on different operational conditions.

4.5.1. CASE 1: MONITORING RAIL SURFACES WITH ABA

ABA is a measurement technology that utilizes accelerometers attached to the axle boxes of moving trains to measure dynamic responses due to wheel-rail contact. Rail component conditions and defects can be assessed by examining deviations

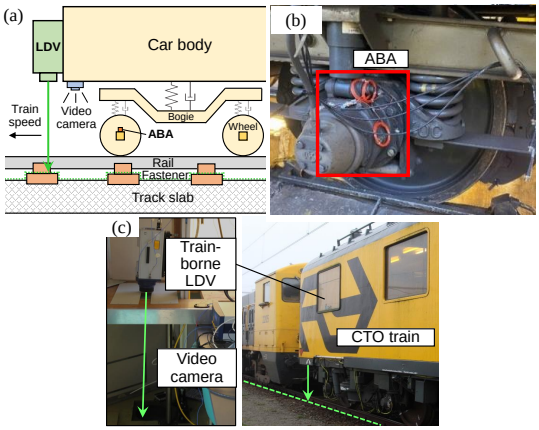

Figure 4.5: Train-borne sensing technology. (a) Illustration; Implementation of (b) ABA measurement in Sweden and (c) train-borne LDV on the TU Delft CTO measurement train in the Netherlands.

in their responses. ABA has been successfully tested in various countries to assess the conditions of various railway components, e.g., fasteners, rails, insulated joints, transition zones, and crossings [134, 241, 250, 275]. This chapter uses ABA technology to monitor rail surfaces and applies the proposed unsupervised representation learning for anomaly detection, where the method learns the normal behavior from the ABA data and helps detect abnormalities for further inspection.

Fig. 4.5 illustrates a setup of the ABA measurement system. The ABA data used in this chapter are collected from the Iron Ore line between Luleå, Sweden, and Narvik, Norway. It is a single-track line with passenger-freight mixed traffic and heavy axle load (up to 31 t). This chapter acquires information from accelerometers installed in the longitudinal direction as signals obtained from the longitudinal direction have proven effective in capturing early-stage characteristics of defects [134]. Additionally, the information is collected from both the left and right wheels of all axles. The obtained measurements contain various rail dynamics, including healthy rails, welds, insulated joints, switches, and rail surface defects. This chapter assumes that the locations of insulated joints and switches are known. Hence, the signals at these locations are excluded from the analysis.

In this chapter, the ABA signals are aggregated into smaller segments, each containing 2000 datapoints, resulting in a total of 583 rail segments. With a hard threshold set to 60 m/s^2, we identify rail segments with ABA responses lower than the specified threshold for representation learning. These segments are assigned into a class of samples representing normal conditions, referred to as Class 0, containing 362 samples. Using information from fieldwork, we identify the defective samples containing rails with visible defects. These comprise 85 defective rail segments, referred to as Class 1. This leaves 136 ABA samples whose classification is ambiguous under the hard threshold, and they are grouped into Class U. A summary of the ABA

dataset is presented in Table 4.1.

4.5.2. CASE 2: MONITORING RAIL FASTENERS WITH TRAIN-BORNE LDV

While ABA monitors rails indirectly through train vibrations, in contrast, train-borne LDV is an innovative technology that offers the ability to measure track vibrations from a moving train directly by emitting a laser beam downward onto the track [244–246]. As illustrated in Fig. 4.5(a), an LDV is mounted on a train emitting a laser beam downward onto the track. As the train moves, the laser spot scans the track surface and measures its vibration velocity contactlessly. Different track components can be targeted, such as rails [245, 246] and sleepers [244]. In this case study, LDV is exploited to target rail fasteners, which are critical components in railway tracks to provide connection, constraint, and vibration reduction between rails and sleepers or track slabs.

The open-path scanning of a train-borne LDV may provide invalid measurements on some fasteners due to the lateral shift of the laser spot out of the fastener surface (see Fig. 4.6) or due to poor surface quality. An example of such an invalid measurement is shown in the second example of Fig. 4.2. Considering the large number of rail fasteners in a rail network, it is impractical to manually check the signal segment of each fastener and label it as valid or invalid. Meanwhile, the diversity of fastener vibrations and the presence of speckle noise induce significant fuzziness in distinguishing between valid and invalid signal segments, especially for those with small vibration amplitude, such as the third example in Fig. 4.2. Therefore, the developed unsupervised learning method is applied in this case study to extract useful features that characterize the rail fastener vibrations autonomously.

The LDV data considered in this case study are obtained from the rail fasteners of the same type on the slab tracks of seven bridges in the Rotterdam-Gouda line in the Netherlands, as shown in Fig. 4.6. On each bridge, the train-borne LDV scans these rail fasteners in a row and measures their vertical vibration individually. In total, 610 rail fasteners are scanned at the train speed of 45-75 km/h. The sampling frequency of the LDV is 102.4 kHz.

The mean of the FFT spectrum within the frequency range between 200 and 800 Hz is considered for class assignment. For LDV, two hard thresholds are used. We identify LDV data at rail fasteners as valid if the mean exceeds one threshold. These result in 211 samples that are assigned to Class 0. The other 258 samples are identified as invalid measurements, referred to as Class 1 if the mean is below the other threshold. The remaining 141 LDV samples are labeled to Class U due to uncertainties and fuzziness, as their mean is between the two thresholds. A summary of the LDV dataset is presented in Table 4.1.

4.6. RESULTS

4.6.1. IMPLEMENTATION DETAILS

Following the procedure depicted in Fig. 4.4, the vibration signals are first decomposed into IMFs by the EMD algorithm. In this chapter, various EMD levels up

Table 4.1: Summary of the datasets from the two case studies.

Cases	Target components	Length (datapoints)	No. of segments	Definition of (No. of samples)		
				Class 0	Class 1	Class U
ABA	Rail defects	2000	583	Normal rail (362)	Defective rail (85)	uncertain condition (136)
LDV	Rail fasteners	2048	610	Valid measurement (211)	Invalid measurement (285)	uncertain measurement (141)

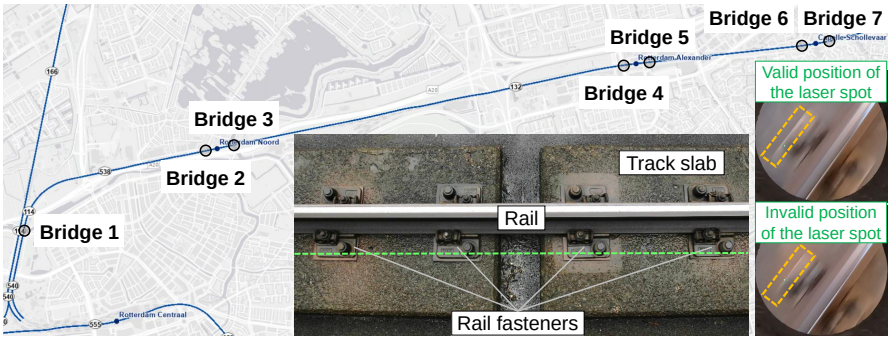

Figure 4.6: Targeted railway track sections on the Rotterdam-Gouda line in the Netherlands (Map: from ProRail).

to a maximum of five are explored. After decomposing the signal into different IMFs, the demodulated signal at each decomposition level is obtained by (4.9). The CAE structure considered in this chapter is symmetric, meaning that the same number of convolutional layers is designed for the encoder and decoder. We experiment with the number of convolutional layers used within the structures in which up to four layers are considered. Four different numbers of filters are used in the trial: 64, 32, 16, and 8. We also experiment with different filter sizes: 3×3, 5×5, 7×7, 9×9, and 11×11. Each convolutional layer in the encoder is followed by an activation layer in which the rectifier or ReLU activation function is used in the convolutional layers. A max-pooling layer with stride two is defined for downsampling at the end of the layer. Similarly, the upsampling steps use transposed convolutions with the ReLU function. At each upsampling step, the number of filters is doubled.

The demodulated signals from Class 0 are divided into training and test sets with a ratio of 75:25. Then, we employ signals from the training set to train the CAE while the test set is held out to validate the generalization of the proposed methodology. Five-fold cross-validation is performed in which 90% of the training set is used to train the models, and the other 10% is used for validating the trained model. The Adam with Nesterov momentum optimizer is exploited for the training, and the maximum number of epochs considered is 100. The early stopping is also applied when $\mathscr{L}_{\text{rec}}$ has stopped improving for more than five epochs.

To account for fuzziness and disturbance presented in data, all samples are included in binary clustering analysis, with the trained CAE generating representations serving as input to the GMM. The GMM is executed multiple times

with varying initializations, and the optimal result is selected based on within-cluster variance. Cluster separability is visualized to evaluate clustering results, including samples from Class U that exhibit more uncertainties and fuzziness. The report of clustering performance is based on the consideration of Class 0 and Class 1.

4.6.2. RESULTS OF DIFFERENT EMD LEVELS

This section investigates the impact of different EMD levels on the proposed method for representation learning, measured by reconstruction loss and average dissimilarity, and clustering performance, measured by F1-score. We showcase using LDV data as they contain more severe and complex noise components (speckle noise) than ABA data. In this analysis, the CAE architecture remains consistent as it learns representations from the demodulated signals at various EMD levels.

Fig. 4.7 shows the demodulated signals corresponding to various EMD levels obtained from rail fasteners with valid and invalid measurements. Specifically, analysis is conducted on demodulated signals for EMD levels up to 5. As the level of EMD increases, the demodulated signals become smoother, and the prominence of noise and high-frequency components is reduced. This enhances the signal reconstruction capability of the CAE, resulting in representations that can be used for a more accurate reconstruction for Class 0, as evidenced by the decreasing trend of the blue line in Fig. 4.8(a). This improvement is further shown by the consistency observed between the input signal and its corresponding reconstruction, as illustrated in Fig. 4.7(a). In contrast, Fig. 4.7(b) exhibits that a sample from Class 1 is not as effectively reconstructed compared to the sample from Class 0 at the respective EMD level.

Despite the enhancement in signal reconstruction at higher EMD levels, the disparity between the representations of normal and abnormal samples does not proportionally improve. This becomes apparent when evaluating the learned representations at each EMD level through clustering analysis, as shown in Fig. 4.8(b). It is suggested that the demodulated signal at EMD level 2 demonstrates optimal clustering efficacy as its embedded features are effective at distinguishing between normal and abnormal samples, evident by a high value of F1-score for both Class 0 and 1. Additionally, the average dissimilarity at EMD level 2 is promising, ranking second among all five levels, as depicted by the red line in Fig. 4.8(a). This observation underscores a tradeoff. While increasing the level of EMD offers signal denoising, it simplifies vibration patterns, thus affecting the capability of CAE to discriminate between normal and abnormal samples. Achieving an optimal balance between denoising and representation learning capability is thus crucial for accurate anomaly detection.

In the subsequent sequels, we present the proposed methodology for monitoring rail surfaces with ABA and monitoring rail fasteners with train-borne LDV. For each case study, we provide a comparative analysis for representation learning considering four variants of autoencoder-based models: autoencoder (AE), long short-term memory (LSTM)-AE, gated recurrent unit (GRU)-AE, and CAE, in which suitable experimental configurations are adopted for their development. We also compare with the denoising sparse wavelet network (DeSpaWN) [258], in which the parameter

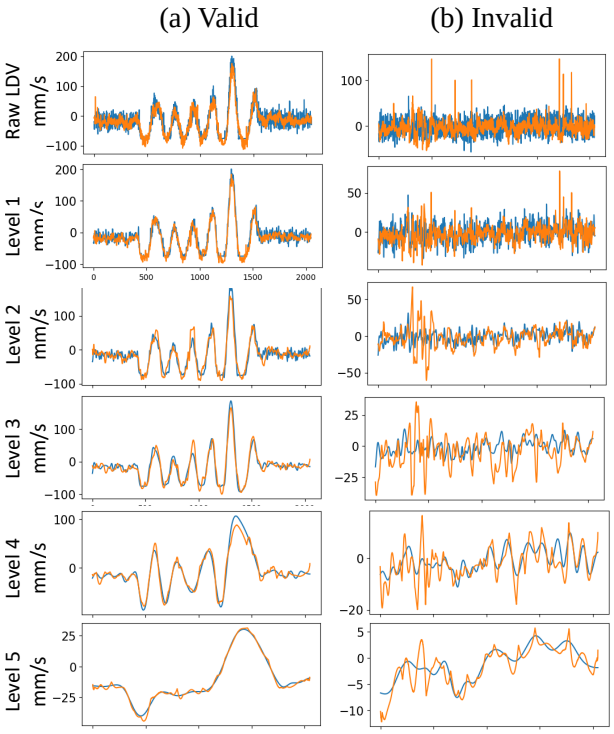

Figure 4.7: Examples of LDV signals from two different rail fasteners and their respective demodulated signal at different EMD levels.

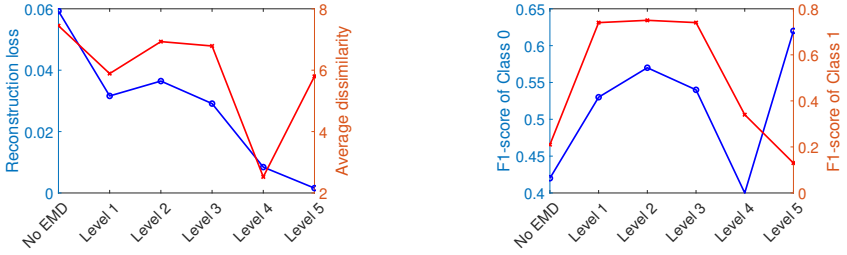

(a) (b)

Figure 4.8: (a) Effect of the EMD levels on the proposed method for the reconstruction loss and the ability to generate the discriminative features. (b) Effect of the EMD levels on the clustering results measured via F1-score.

setting and loss are followed from [258]. To be consistent with the development of our model, four maximum encoder and decoder layers are considered for all comparative models.

4.6.3. RESULTS OF RAIL SURFACE DEFECT DETECTION USING ABA

This section presents results from the representation learning considering the ABA data. It can be seen from Fig. 4.9(a) that different methods perform differently in signal reconstruction and differentiation of embedded representations between clusters. The GRU-AE method yields the lowest reconstruction loss. It also achieves the highest average dissimilarity, indicating that it generates embedded representations that discriminate between normal and abnormal samples better than the other methods. Our method provides the second-lowest reconstruction loss and average dissimilarity, reflecting its competitive capability for representation learning.

Fig. 4.10 presents clustering results obtained from using latent features extracted by different methods to train the GMM algorithm to provide two different clusters, considering all 583 ABA samples. The t-SNE [251, 252] using the perplexity of 200 is employed for a visualization of the 2D representations. Note that perplexity is related to the number of nearest neighbors each point considers in the t-SNE algorithm during the dimensionality reduction process. Lower values of perplexity make the algorithm focus on a very local structure, while higher values take into account a broader neighborhood. It is noticeable that the GRU-AE and our method provide better separability between two clusters with fewer overlaps than the others, reflecting their high average dissimilarity obtained. In contrast, the LSTM-AE exhibits more noticeable overlap, corresponding to its highest reconstruction loss and low average dissimilarity.

Next, the clustering results are evaluated using labeled data from Class 0 and Class 1 to investigate the informativeness of the learned representations obtained from each method. Table 4.2 presents a comparative study on the clustering tasks using different sets of latent features obtained from different methods. The results show that our method using the demodulated signals at EMD level 2 provides very competitive results. It correctly assigns 96% of Class 0 and correctly assigns 41% of Class 1. While the DeSpaWN exhibits cluster separability with more overlap than our method, it demonstrates the highest accuracy in correctly identifying samples of Class 1, yielding a 38% higher accuracy for this class. However, the DeSpaWN detects Class 0 with 63% lower accuracy compared to our method. Additionally, the GRU-AE method demonstrates the lowest reconstruction loss and exhibits good cluster separability owing to the high average dissimilarity obtained. Nevertheless, our method outperforms GRU-AE in terms of cluster performance. Furthermore, GRU-AE shows a lower precision for Class 1, indicating a higher misclassification rate where samples from Class 0 are incorrectly labeled as Class 1. The clustering performance of the proposed method demonstrates its efficacy in generating discriminative and informative representations of normal and abnormal rail surface conditions using ABA, attributed to the utilization of EMD.

It is noteworthy that the parameter configuration for the DeSpaWN can be further optimized to align with the characteristics of the problem, potentially resulting in improved performance. Furthermore, as the GRU-AE has a complex network (8 hidden layers are exploited), the model might have overfitted on the normal samples during training. Using a larger dataset can be considered to train the GRU-AE, potentially resulting in improved performance.

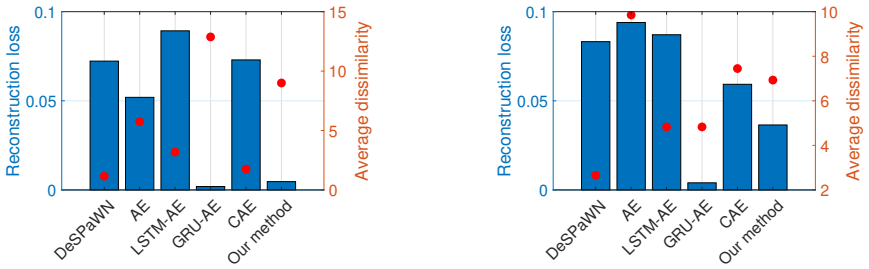

(a) ABA. (b) LDV.

Figure 4.9: Reconstruction loss and average dissimilarity between Class 0 and Class 1 obtained from different methods.

Next, we examine the effectiveness of our proposed method in handling uncertainties and fuzziness. Figs. 4.11(a) and 4.11(b) show two examples from Class U whose ABA responses display ambiguous abnormalities. Consequently, both examples are labeled as Class 1 by the hard threshold for clustering. According to the hard threshold labels, the method correctly identifies Fig. 4.11(a) to Class 1 and misidentifies Fig. 4.11(b) to Class 0. Validation against fieldwork information reveals that Fig. 4.11(a) represents a rail segment at a weld, while Fig. 4.11(b) is a rail segment at a small defect. However, it can be seen that the ABA signal of the rail at the weld in Fig. 4.11(a) shares similar characteristics with the ABA signal of the rail at squat in Fig. 4.11(c). This suggests that there might be some invisible rail defects located on this rail segment. Further experiments can be conducted to confirm their existence. Similarly, the ABA signal of the rail with a small defect in Fig. 4.11(b) resembles that of the normal rails shown in Fig. 4.11(d). These findings demonstrate that the latent features obtained from our method are informative for grouping rail dynamic responses with similar characteristics.

Table 4.2: Comparison results of clustering performance for ABA data.

Method	**Class 0**			**Class 1**		
	Precision	**Recall**	**F1-score**	**Precision**	**Recall**	**F1-score**
DeSpaWN [258]	0.87	0.33	0.48	0.22	**0.79**	0.34
AE	0.85	0.43	0.57	0.22	0.68	0.33
LSTM-AE	0.82	0.52	0.64	0.20	0.49	0.28
GRU-AE	0.84	0.52	0.65	0.22	0.56	0.31
CAE	0.81	0.62	0.70	0.19	0.36	0.25
Our method	**0.87**	**0.96**	**0.91**	**0.69**	0.41	**0.51**

NB: Better performances are highlighted in bold for each clustering algorithm.

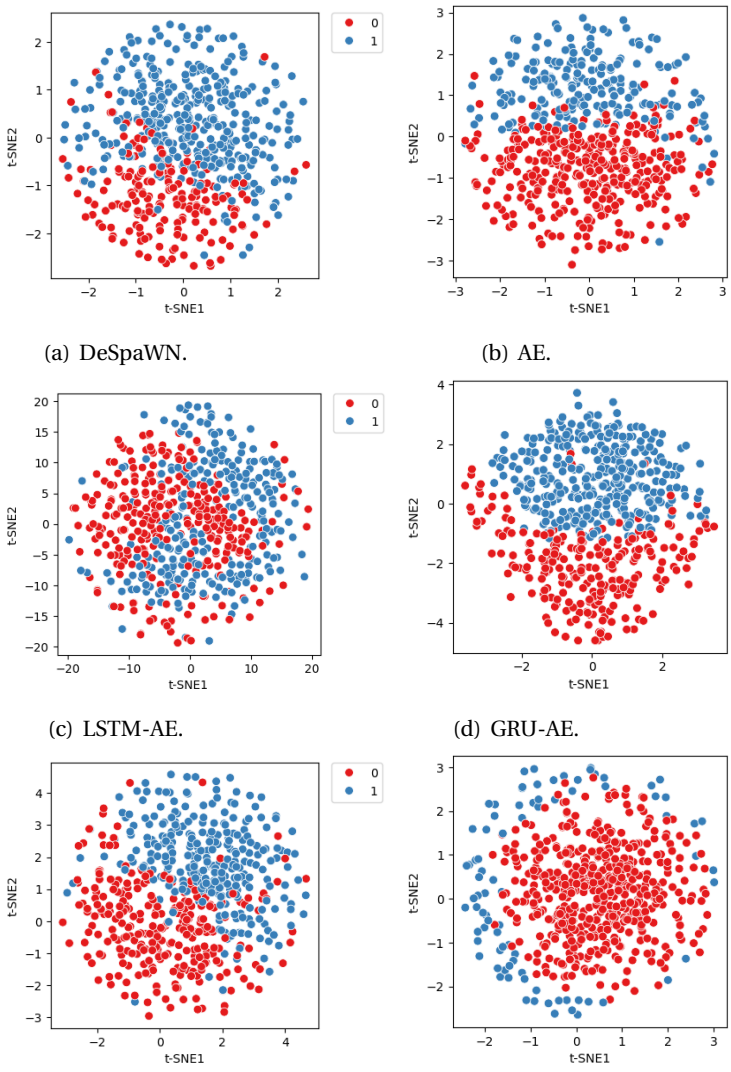

(a) DeSpaWN. (b) AE.

(c) LSTM-AE. (d) GRU-AE.

(e) CAE. (f) Our method.

Figure 4.10: Clustering results using latent features extracted from different models. The t-SNE with a perplexity of 200 is employed for visualizing clusters of two colors, from which red represents a cluster of Class 0 and blue represents a cluster of Class 1.

4.6.4. RESULTS OF MONITORING RAIL FASTENERS WITH LDV

This section presents results from the representation learning considering the LDV data. Similar to ABA, Fig. 4.9(b) shows that different methods perform differently in

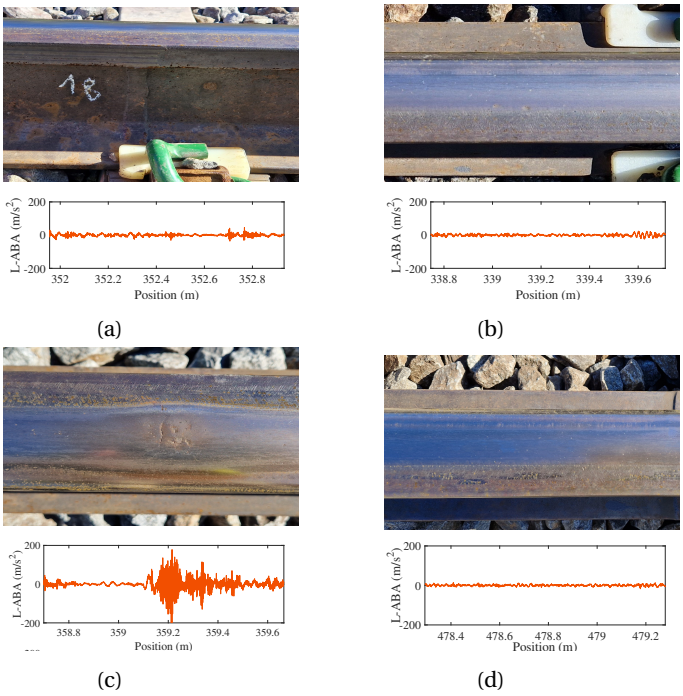

Figure 4.11: Examples of validated rail segments at (a) a weld, (b) a small defect, (c) a squat, and (d) a rail without visible defects.

signal reconstruction and generation of embedded features. The GRU-AE method yields the lowest reconstruction loss and generates the embedded representations that provide a good average dissimilarity between normal and abnormal samples. Our method provides the second-lowest reconstruction loss, reflecting its competitive capability for representation learning. Meanwhile, it has higher dissimilarity than the GRU-AE, reflecting its capability for clustering using the learned features. Similar to the ABA case study, this highlights the use of EMD in the proposed method.

Fig. 4.12 presents clustering results obtained from using latent features extracted by different methods. The t-SNE using the perplexity of 30 is employed for a visualization of the 2D representation of the encoded features obtained from each method. Despite different reconstruction loss and dissimilarity obtained, the latent features obtained from all methods provide a clear separation between a cluster of two colors representing a cluster of Class 0 and Class 1, with some minor overlaps seen more from the DeSpaWN than the other methods.

Evaluating against labeled data, Table 4.3 shows that our proposed methodology using the demodulated signals from the EMD level 2 demonstrates competitive results for both Class 0 and Class 1. It correctly assigns 47% of Class 0 and correctly assigns 90% of Class 1. Although the GRU-AE method yields the least reconstruction loss and provides good cluster separability due to high average dissimilarity, it

demonstrates a 43% lower accuracy in correctly identifying samples of Class 1 compared to our methodology. However, the GRU-AE achieves 18% higher detection accuracy for Class 0 than our method. The GRU-AE method also exhibits a higher rate of incorrectly identifying an LDV signal as invalid when it is valid. Mitigating these false positives is crucial as false positives impair the learning of actual trends and patterns in rail fastener health. By reducing false alarms, operators can identify issues early and proactively address them before they escalate.

Table 4.3: Comparison results of clustering performance for LDV data.

Method	**Class 0**			**Class 1**		
	Precision	**Recall**	**F1-score**	**Precision**	**Recall**	**F1-score**
DeSpaWN [258]	0.61	0.64	0.62	0.69	0.66	0.67
AE	0.37	0.40	0.38	0.47	0.44	0.46
LSTM-AE	0.39	0.41	0.40	0.49	0.47	0.48
GRU-AE	0.50	**0.65**	**0.57**	0.62	0.47	0.54
CAE	0.34	0.53	0.42	0.30	0.16	0.21
Our method	**0.71**	0.47	**0.57**	**0.65**	**0.90**	**0.75**

NB: Better performances are highlighted in bold for each clustering algorithm.

To examine the effectiveness of our proposed method in handling samples of Class U from LDV data, we compare the clustering results obtained from the latent features learned by our method with those obtained from a hand-crafted method. The hand-crafted method, as outlined in [276], involves the manual design of three features: the variations in the time and frequency domains as well as the power spectrum density entropy of each raw signal segment (without denoising). Various clustering algorithms are implemented, including k-means, k-medoids, and fuzzy c-means. For each algorithm, clustering with multiple clusters is used to handle the diverse patterns observed in the valid measurements and then merge them into a single group. The optimal number of clusters is tuned for each algorithm. More details of the feature design and clustering analysis can be found in [276].

Out of the 141 samples of Class U, 10 (or 20) samples are labeled as valid measurements, while 131 (or 121) samples are labeled as invalid measurements when using the hand-crafted method in [276] (or the proposed method). The ratio between the two labels is similar between the two methods despite their significant differences in the feature design as well as the clustering algorithm. The two methods consistently label 115 out of 141 samples (81.56%), whereas the remaining is labeled differently. Figs. 4.13 and 4.14 show several samples with inconsistent clustering results. The LDV samples shown in Fig. 4.13 are labeled as invalid using the hand-crafted method in [276] but as valid using the proposed method. It can be seen that these samples on top indeed carry vibration patterns (evident by the demodulated LDV), while the severe speckle noise makes them less pronounced. Owing to the use of EMD for denoising, the proposed method captures these vibration patterns more effectively, thus providing more reasonable labels compared to the hand-crafted method. The samples shown in Fig. 4.14 are labeled as valid

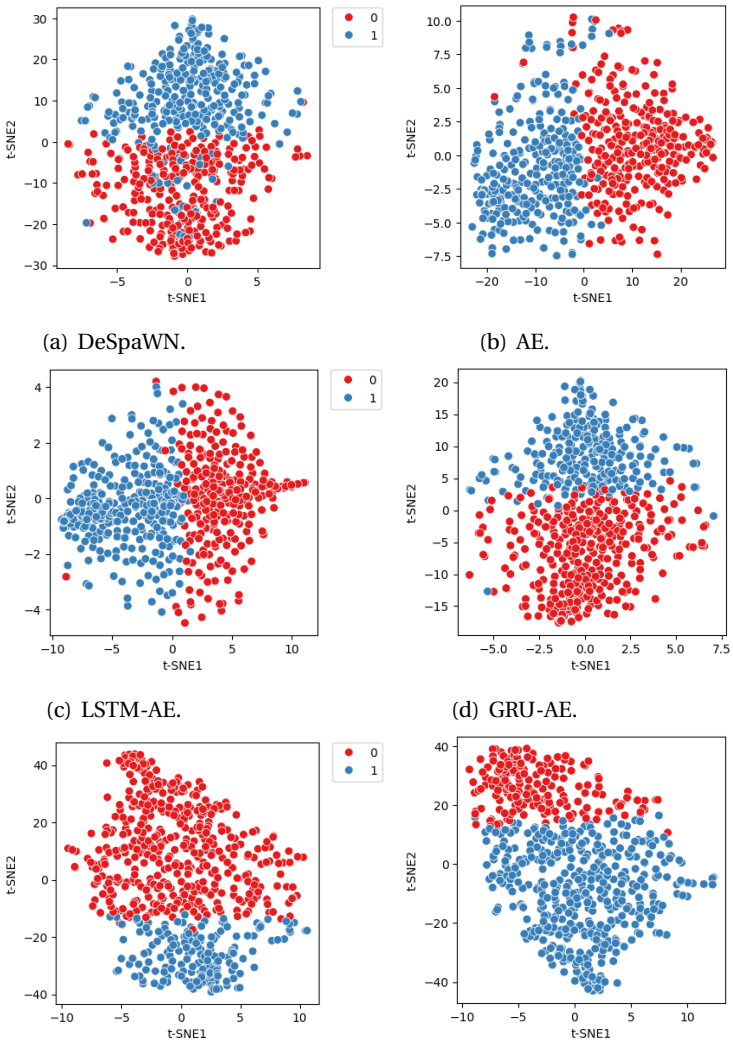

(a) DeSpaWN. (b) AE.

(c) LSTM-AE. (d) GRU-AE.

(e) CAE. (f) Our method.

Figure 4.12: Clustering results using latent features extracted from different models. The t-SNE with a perplexity of 30 is employed for visualizing clusters of two colors, from which red represents a cluster of Class 0 and blue represents a cluster of Class 1.

by the hand-crafted method, most likely due to the local and sudden variations in the signals, which are actually different from the targeted vibration patterns that are more stationary and continuous. The proposed method identifies such differences and avoids such signals being labeled as valid. These typical examples showcase the

effectiveness of the developed representation learning framework in capturing the targeted vibration pattern while reducing the disturbance of the noise.

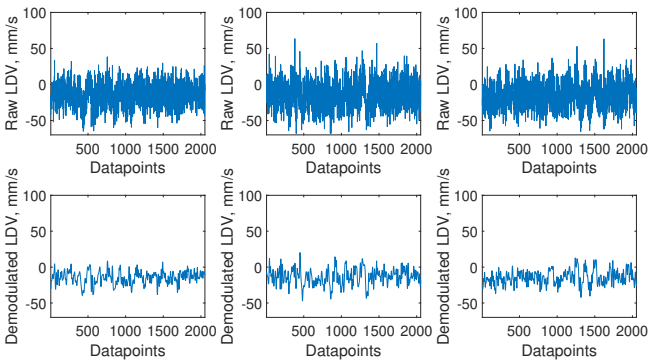

Figure 4.13: Examples of LDV measurements that are identified as valid measurements by our methodology but identified as invalid by the prediction using the handcrafted features.

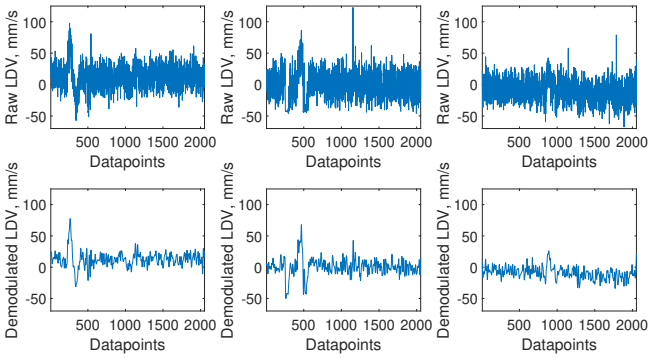

Figure 4.14: Examples of LDV measurements that are identified as invalid measurements by our methodology but identified as valid by the prediction using the handcrafted features.

4.7. CONCLUSIONS

This chapter presents an unsupervised representation learning methodology that synchronizes the empirical mode decomposition (EMD) with a convolutional autoencoder (CAE). By testing with the ABA measurements from the Swedish rail network and the LDV measurements from the Dutch rail network, the proposed methodology demonstrates a promising performance for unsupervised rail defect

and rail fastener analysis. Evaluating the obtained representations using the Gaussian mixture model clustering, cluster separability with minor overlaps is achieved for both application cases. This proves the effectiveness of the method in generating features that differentiate between normal and abnormal samples, even the inherent fuzziness and disturbance present in the ABA and LDV data. Verified against labels from a hard threshold, it demonstrates an improvement in detection accuracy compared to other variants of autoencoder-based models and the wavelet-based CAE. Furthermore, the latent features obtained from the proposed method have been proven to be informative. In the case of ABA data, clusters of rail segments with similar characteristics can be used to guide the inframanager about the locations of defects. For LDV data, clusters of rail segments with similar characteristics can be used to learn trends and patterns in rail fastener health. The success of the proposed method highlights the importance of EMD for denoising, enhancing representation learning of rail infrastructure characteristics and reducing noise interference.

Future research includes improving cluster separability through advanced clustering techniques and hybrid approaches to better distinguish between normal and abnormal samples. Incorporating additional data sources and measurements can be considered with a development of data fusion techniques to provide a comprehensive analysis and enhance accuracy and reliability of rail infrastructure conditions. Examining scalability and real-time processing capabilities can be considered for enabling real-time analysis of large-scale rail network data. Validating the methodology across different rail networks with varying environmental conditions and operational patterns is also essential to ensure its robustness and applicability.

5

A Hybrid Neural Model Approach for Health Assessment of Transition Zones with Multiple Data

This chapter proposes a framework that enables a more frequent evaluation of transition zone health by integrating multiple monitoring technologies, including track geometry measurements, interferometric synthetic aperture radar (InSAR), and axle box acceleration (ABA). Firstly, a spatio-temporal interpolation approach is employed to fill in missing InSAR data. Then, hybrid neural models are evaluated to predict missing track longitudinal levels, including a hybrid convolutional neural network (CNN) with gated recurrent units (GRU) network and a hybrid CNN with a long short-term memory (LSTM) network. The prediction relies on a fusion of historical and interpolated data from InSAR and the ABA measurements. As InSAR and ABA measurements can be obtained more frequently, a novel key performance index (KPI) is proposed using the predicted track longitudinal levels. To validate our framework, transition zones at a railway bridge between Dordrecht and Lage Zwaluwe station in the Netherlands are considered. A comparative analysis is conducted considering CNN, GRU, LSTM, hybrid CNN-GRU and CNN-LSTM models to assess their performance. The results show that CNN-LSTM and CNN-GRU exhibit superior capabilities in capturing spatial and temporal relationships between track longitudinal levels, InSAR, and ABA measurements. For one track, CNN-GRU emerges as the optimal choice, while for the other track, CNN-LSTM shows superiority. However, when considering overall performance, CNN-GRU yields the best on average. Furthermore, our framework demonstrates early detection capability for track irregularities, even before the next

This chapter has been submitted for publication as: Phusakulkajorn, W., Unsiwilai, S., Chang, L., Núñez, A., Li, Z., A Hybrid Neural Model Approach for Health Assessment of Railway Transition Zones with Multiple Data Sources.

measurement of track geometry profiles. This generates predictive results that can guide decisions regarding the time and locations for essential track maintenance.

5.1. INTRODUCTION

In railways, transition zones denote areas marked by structural discontinuities, leading to abrupt variations in track stiffness, damping, and track geometry. They are often observed at critical points like bridges, culverts, tunnels, transitions between ballasted and slab tracks, and road crossings. The abrupt changes in train dynamic responses significantly accelerate the degradation of transition zones, resulting in substantial maintenance costs to sustain smooth operation and safety. Hence, it is crucial to assess the structural health condition of transition zones more frequently to detect changes at an early stage. Correct health assessment allows prescriptive interventions to maintain operational efficiency and mitigate potential risks.

The health assessment of a railway transition zone includes various aspects. Examples are track geometry inspection to measure the track deviations from design specifications, condition monitoring of rail and other track components in areas of transition to examine wear, defects, and damage, dynamic response analysis to identify any irregularities or excessive forces that could affect safety and health, and embankment stability inspection where the transition zone is situated to prevent derailment, among others.

Information on the health of transition zones can be collected from track-side measurements, onboard measurements, and remote sensing technologies to perform the health assessment. Track-side measurements employ point-sensor technologies such as borehole inclinometers, geophones, linear variable differential transformers (LVDTs), and accelerometers [277–279]. Multidepth deflectometers and strain gauges were employed in [280] to assess conditions of railroad track transitions. Digital Image Correlation)-based device was used to evaluate track degradation in the embankment-bridge and bridge-embankment transitions [281]. Advanced fiber-optic technologies, including Rayleigh backscattered [282] and fiber Bragg grating [283], have also been employed for condition monitoring in transition zones. However, track-side measurements are typically installed at critical locations. This results in the local coverage of responses. The need for a broader perspective of train responses necessitates the installation of a greater number of sensors. This involves costs from not only devices but also expenses related to labour and power supplies.

In the case of onboard systems, they have been used in continuous monitoring frameworks related to transition zones. In [284], data collected from track geometry car measurements was used to predict long-term differential track settlement in a transition zone. In [285], an inertial measurement unit mounted on the bogie of the suspended train was used to detect track irregularities. In [286], a digital image correlation system was mounted on railcars to assess the conditions of ballast support. In [239], acceleration measurements recorded by in-service high-speed vehicles were exploited to monitor rail track conditions. In [250, 287, 288], measurement systems based on accelerometers installed at the axle box of a train were employed to assess the railway transition zone conditions. Some challenges that onboard monitoring techniques face include their integration with existing systems, the need for efficient data processing and analysis due to vast amounts of generated data, and their adaptations to make them robust and implementable in,

for instance, passenger trains.

Remote sensing technologies, particularly satellite measurements, have been employed in the literature for monitoring railway infrastructures and transition zones. Examples of remote sensing technologies include using satellite signals with GNSS technology for real-time displacement monitoring of a railway cable bridge [289] and satellite images for detecting potential landslides along high-speed railways [290]. Current dedicated Radar satellite missions, such as Sentinel-1, deliver radar images on a biweekly basis, with (tens of) meter-level spatial resolution. Interferometric synthetic aperture radar (InSAR) [291] is a specific technique used to process Radar images in several works to detect subtle ground movements with sub-centimetre precision, such as subsidence, uplift, and landslides. In [292, 293], railway irregularities were detected using InSAR. In [294], InSAR measurements were used for monitoring surface deformation over permafrost. In [295], InSAR time series measurements were used to study and characterise the deformation process resulting from subway-induced subsidence in the construction and operation periods. Despite its ability to provide valuable data, some railway applications require higher resolution and accuracy that are not currently possible to obtain from satellite data.

Assessing transition zone conditions heavily depends on the measurement frequency and the density of data gathered across a given area. A more frequent measurement is essential to enhance forecasts and insights into the evolution over time and assess severe events, allowing better maintenance strategic plans. High-density measurements over an area are essential for detecting track irregularities along transition zones. The more frequent measurements from satellites offer the advantage of tracking transition zone conditions over time and assessing significant events on a global scale. In a complementary manner, data obtained from ABA measurements excel at capturing local dynamic responses. Currently, ABA measurements occur less frequently because the system is still on the path towards standardisation, and it is required to be effectively installed in passenger trains. Additionally, track geometry is a standardised measurement used in various railway companies. While its quality is guaranteed with accuracy and resolution, track geometry does not capture locations with a poor dynamic train-track interaction. Recognising the complementary nature of these measurements, this chapter considers track geometry data, InSAR, and ABA measurements to predict conditions of transition zones.

Various machine learning models have been employed to predict railway transition zone conditions. Examples are support vector machine [296–298], random forests [298, 299], multi-layer perceptron [300], artificial neural networks [297, 301], and deep neural networks [302, 303]. As a prediction of railway transition zone conditions is regarded as a spatio-temporal dependency problem, models that are efficient in simultaneously capturing spatial and temporal data characteristics are needed. In the literature, convolutional neural networks (CNNs) have shown their capability to deal with spatial characteristics in various applications [304–306]. Recurrent neural networks (RNNs)-based models demonstrate their capability to learn the temporal dependencies of time series data [307]. However, these individual CNNs and RNNs

consider the spatial and temporal characteristics independently.

In railway applications, hybrid models integrating CNNs and RNNs have been presented to overcome this limitation [308–310]. Due to vanishing gradients, it is challenging for RNNs to capture long-term dependencies in time series data. The long short-term memory (LSTM) network model addresses the issue of RNNs by introducing additional gates and memory cells. In [308], a hybrid CNN and LSTM model was presented to account for spatial-temporal dependence with respect to track geometry change. In [309], a hybrid model of CNN-LSTM model was proposed to predict passenger flow. While effectively capturing long-term dependencies, LSTM has more parameters due to additional memory cells and gates. This makes them computationally expensive. The gated recurrent unit (GRU) is a type of RNN architecture also designed with gates and memory cells to address the vanishing gradient issue of RNNs. Compared to LSTM models, GRU models offer fewer parameters due to fewer gates and connections used [310]. Therefore, this chapter considers a hybrid CNN-LSTM and a hybrid CNN-LSTM model to solve a spatial and temporal dependency problem presented in track geometry changes.

This chapter proposes a framework that exploits track geometry measurements, InSAR measurements, and ABA measurements to assess transition zone conditions. This is with the objective of obtaining a more frequent evaluation when only track geometry is measured, typically once or twice per year in the Dutch railways. The proposed framework includes a spatio-temporal interpolation to fill in missing InSAR data, hybrid neural models to predict missing track longitudinal levels by integrating historical and interpolated data from InSAR and ABA measurements, and a key performance index (KPI) based on InSAR and ABA data to assess transition zone conditions. A case study from a transition zone at a railway bridge between Dordrecht and Lage Zwaluwe station in the Netherlands is used to validate our methodology. The following summarises our key contributions:

1. Multiple monitoring data, including track geometry measurements, InSAR measurements, and ABA measurements are used for assessing the health of railway transition zones.

2. A spatio-temporal interpolation approach is presented to impute missing InSAR data.

3. Hybrid neural models are proposed to fuse information from InSAR and ABA data and to predict missing track longitudinal levels.

4. A novel KPI is proposed by including InSAR and ABA data.

5. The method is tested at a transition zone of a railway bridge in the Netherlands.

The rest of this chapter comes in the following sequels. Section 5.2 introduces the measurement technologies considered. Section 5.3 presents problem formulation, while Section 5.4 discusses the proposed model and methodology used for a health assessment of railway transition zones. Section 5.5 describes a case study to evaluate the proposed methodology. A comparison of the proposed methodology with

different models from the literature and discussions are presented in Section 5.6. Section 5.7 concludes the chapter.

5.2. Measurement Technology

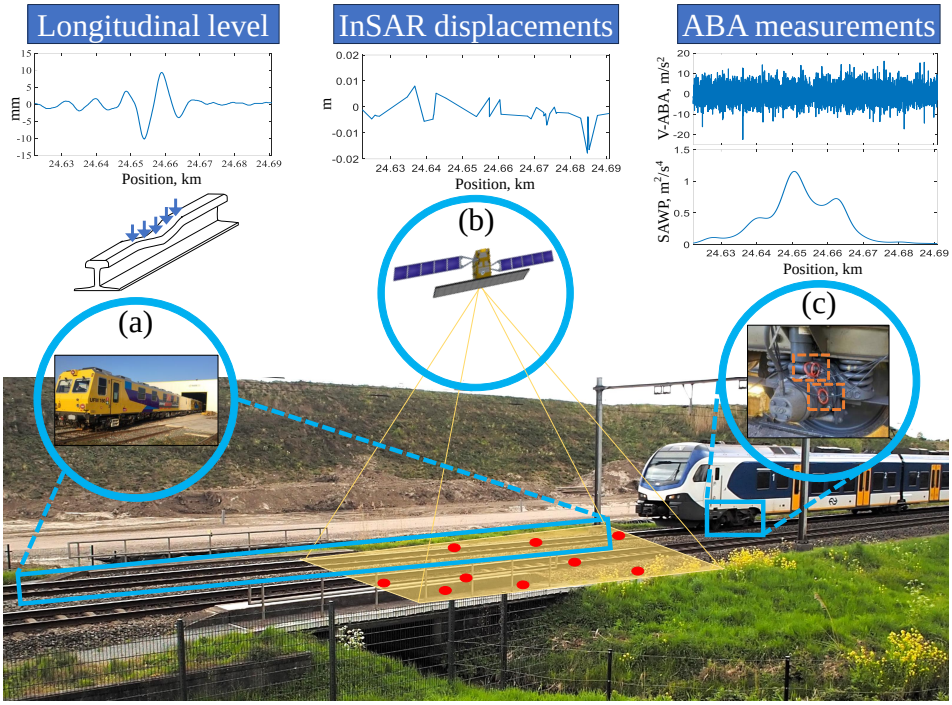

Figure 5.1: Illustration of the measurement technologies used in this chapter. (a) Track geometry measurement system, (b) InSAR, and (c) ABA system. Note that red points represent InSAR data points.

Fig. 5.1 illustrates an overview of three measurement technologies used in this chapter. The technologies include a track geometry measurement system, InSAR, and ABA measurement system.

5.2.1. Track Geometry Measurement

Track geometry measurement is often performed using measurement cars equipped with sensors and instruments. These cars move along the track and collect data on various parameters. Typically, the track geometry measurement includes the longitudinal level of both rails, alignment of both rails, gauge, and twist. The spatial resolution of track geometry measurements can be in the range of centimetres to decimetres. The frequency of track geometry measurements depends on several factors, including budget and the availability of measurement cars. The level of

train traffic and maintenance activities also affect the frequency of track geometry measurements due to track possession. Generally, track geometry measurements are performed regularly. In the Netherlands, for example, the measurement campaign is conducted once or twice per year.

5.2.2. INTERFEROMETRIC SYNTHETIC APERTURE RADAR

InSAR is a remote sensing technique that uses synthetic aperture radar (SAR) to measure and monitor surface changes of the Earth over time. SAR is an active sensing technique that emits electromagnetic pulses (in the microwave range) toward the surface of the earth and records the backscattered radar signal. The radar pulses are emitted along the satellite line-of-sight direction. Radar signals are composed of two main components: amplitude and phase. To derive the ground displacement that occurred between the two acquisitions, InSAR involves comparing the phase difference of radar signals acquired over the same area at different times, particularly for repeat-pass SAR satellites. A stack of radar signals over different times is used to get a time series of ground target movement [311]. InSAR data, namely InSAR displacements for our study, are collected every 5-12 days, and the spatial density of InSAR data varies depending on the studied area and processing strategy, which can be in the range of metres.

5.2.3. AXLE BOX ACCELERATION MEASUREMENT SYSTEM

Axle-box Acceleration (ABA) measurement system is an onboard measurement technique. It eliminates the need for dedicated measurement vehicles by mounting directly onto passenger trains. The fundamental concept of ABA measurement systems is to use a train as a moving load to excite the infrastructure and to detect defects and irregularities through an analysis of time-frequency characteristics. This analysis is derived from the dynamic response of the train-track interaction captured by accelerometers installed on the axle boxes.

In comparison to other measurement techniques that use dedicated measurement vehicles, ABA technology comes with the advantages of lower cost and easier maintenance. The ABA measurement system achieves high spatial resolution, typically within the millimetre range due to a high sampling frequency. While its technology readiness level is increasing [133, 275, 312], the ABA system still needs to evaluate its robustness and generalisation. This involves conducting extensive measurement and validation campaigns in different locations and under different measurement conditions. Once the technology advances and matures, more frequent ABA measurements are anticipated. This involves installing ABA systems on existing passenger trains or considering these systems already in the design of new generation trains with embedded smart sensors, offering real-time or near-real-time monitoring of track conditions. In this case study, ABA measurements are obtained yearly.

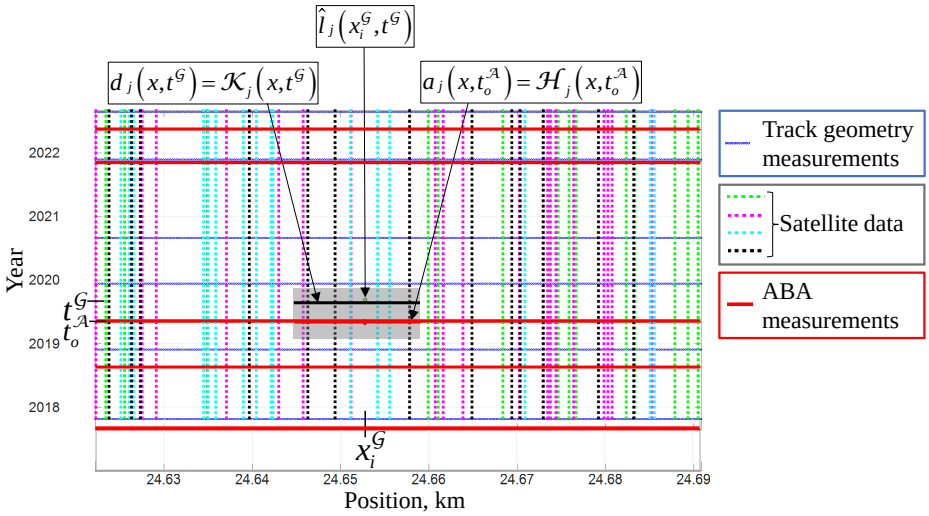

Figure 5.2: The availability of all measurement data in space and time obtained from the track geometry measurements (blue), InSAR measurements (other colors), and the ABA measurements (red). White spaces represent missing information, while the grey area defines the neighbouring measurements used for constructing the interpolation functions.

5.3. Problem Formulation

This chapter assumes the availability of datasets $\mathscr{D}_j^r=\left\{\mathscr{G}_j^r,\mathscr{S}_j^r,\mathscr{A}_j^r\right\}$ containing three different measurement technologies for a given railway track $j\in\mathbb{N}$ and rail $r\in\{\text{inner},\text{outer}\}$. The measurements include, firstly, a set of track geometry measurements, $\mathscr{G}_j^r$; secondly, a set of displacements derived from InSAR data $\mathscr{S}_j^r$; lastly, a set of ABA measurements $\mathscr{A}_j^r$. The measurements are collected from a transition zone at a position x within the kilometre range from x_b to x_e, and during the month t within time frame t_b and t_e. They are mathematically expressed as follows.

$$\mathscr{G}_j^r=\left\{l_j^r(x,t)\;\middle|\;x=x_1^{\mathscr{G}},\ldots,x_{\gamma_1}^{\mathscr{G}}\text{ and }t=t_1^{\mathscr{G}},\ldots,t_{\beta_1}^{\mathscr{G}}\right\},$$

$$\mathscr{S}_j^r=\left\{d_j^r(x,t)\;\middle|\;x=x_1^{\mathscr{S}},\ldots,x_{\gamma_2}^{\mathscr{S}}\text{ and }t=t_1^{\mathscr{S}},\ldots,t_{\beta_2}^{\mathscr{S}}\right\},$$

$$\mathscr{A}_j^r=\left\{a_j^r(x,t)\;\middle|\;x=x_1^{\mathscr{A}},\ldots,x_{\gamma_3}^{\mathscr{A}}\text{ and }t=t_1^{\mathscr{A}},\ldots,t_{\beta_3}^{\mathscr{A}}\right\},$$

where $l_j^r(x,t)$, $d_j^r(x,t)$, and $a_j^r(x,t)$ denote, respectively, the track longitudinal level, the displacement, and the ABA data collected at a position x and in month t. The variables γ_1, γ_2, and γ_3 represent the number of measurements in the spatial domain corresponding to track geometry, displacements, and ABA signals, respectively. Similarly, β_1, β_2, and β_3 represent the number of measurements in the temporal domain for each respective dataset. For all the measurements, missing

data can happen in which $l_j^r(x,t)$, $d_j^r(x,t)$, and $a_j^r(x,t)$ are represented by the Not-a-Number value.

The average spatial resolutions of the track geometry, ABA measurements, and displacements are defined as $\Delta x^{\mathscr{G}} = \frac{1}{\gamma_1 - 1}(x_{\gamma_1}^{\mathscr{G}} - x_1^{\mathscr{G}}), \Delta x^{\mathscr{S}} = \frac{1}{\gamma_2 - 1}(x_{\gamma_2}^{\mathscr{S}} - x_1^{\mathscr{S}}), \Delta x^{\mathscr{A}} = \frac{1}{\gamma_3 - 1}(x_{\gamma_3}^{\mathscr{A}} - x_1^{\mathscr{A}})$, respectively. Similarly, the average temporal resolutions of the track geometry, ABA measurements, and displacements are defined as $\Delta t^{\mathscr{G}} = \frac{1}{\beta_1 - 1}(t_{\beta_1}^{\mathscr{G}} - t_1^{\mathscr{G}}), \Delta t^{\mathscr{S}} = \frac{1}{\beta_2 - 1}(t_{\beta_2}^{\mathscr{S}} - t_1^{\mathscr{S}}), \Delta t^{\mathscr{A}} = \frac{1}{\beta_3 - 1}(t_{\beta_3}^{\mathscr{A}} - t_1^{\mathscr{A}})$, respectively. In this chapter, we assume that $\Delta t^{\mathscr{G}}$ and $\Delta t^{\mathscr{A}}$ are similar, but both are much less than $\Delta t^{\mathscr{S}}$. Conversely, $\Delta x^{\mathscr{A}}$ is significantly higher compared to both $\Delta x^{\mathscr{G}}$ and $\Delta x^{\mathscr{S}}$, with $\Delta x^{\mathscr{G}}$ being denser than $\Delta x^{\mathscr{S}}$. Fig. 5.2 shows which measurements were obtained across track positions and time. Track geometry measurements are in solid blue lines, InSAR in lines with other colours, and the ABA measurements with solid red lines. The spatial and temporal resolution of the different data sources can be estimated from such a diagram.

For track j and rail r, let $\mathscr{H}_j^r$ denote a 2D spatio-temporal function that provides the unobserved value of ABA data $\hat{a}_j^r(x, t^{\mathscr{A}})$ at position $x \in [x_b, x_e]$ and in the ABA measurement month $t^{\mathscr{A}} = t_1^{\mathscr{A}}, \ldots, t_{\beta_3}^{\mathscr{A}}$ such that:

$$\hat{a}_j^r(x, t^{\mathscr{A}}) = \mathscr{H}_j^r(x, t^{\mathscr{A}}). \tag{5.1}$$

Likewise, let $\mathscr{K}_j^r$ denote a 2D spatio-temporal function that provides the unobserved value of the displacements $\hat{d}_j(x,t)$ at position $x \in [x_b, x_e]$ and in month $t \in [t_b, t_e]$, such that:

$$\hat{d}_j^r(x,t) = \mathscr{K}_j^r(x,t). \tag{5.2}$$

To predict the track longitudinal level $\hat{l}_j^r(x^{\mathscr{G}}, t^{\mathscr{G}})$ at the observed position $x^{\mathscr{G}} = x_1^{\mathscr{G}}, \ldots, x_{\gamma_1}^{\mathscr{G}}$, and in the unobserved month $t^{\mathscr{G}}$, $t^{\mathscr{G}} \neq t_1^{\mathscr{G}}, \ldots, t_{\beta_1}^{\mathscr{G}}$, we exploit the interpolated values of InSAR an ABA data to construct a hybrid neural model $\mathscr{M}_j$ defined for all rails r such that:

$$\begin{aligned} \hat{l}_j^r(x^{\mathscr{G}}, t^{\mathscr{G}}) &= \mathscr{M}_j\left(\mathscr{H}_j^r(x^{\mathscr{G}}, t_o^{\mathscr{A}}), \mathscr{K}_j^r(x^{\mathscr{G}}, t^{\mathscr{G}})\right) \\ &= \mathscr{M}_j\left(\hat{a}_j^r\left(x^{\mathscr{G}}, t_o^{\mathscr{A}}\right), \hat{d}_j^r\left(x^{\mathscr{G}}, t^{\mathscr{G}}\right)\right), \end{aligned} \tag{5.3}$$

where $\mathscr{H}_j^r$ is derived from the closest available ABA measurement month $t_o^{\mathscr{A}}, o \in \left\{1, \ldots, \beta_3\right\}$, occurring prior to the measurement month $t^{\mathscr{G}}$ of the predicted track geometry. $\mathscr{K}_j^r$ is defined at the position $x^{\mathscr{G}}$ and the same month $t^{\mathscr{G}}$ of the predicted track longitudinal level. Then, a KPI is evaluated across unobserved months spanning the entire transition zone utilising the predicted track longitudinal level $\hat{l}_j^r(x^{\mathscr{G}}, t^{\mathscr{G}})$.

This chapter proposes a methodology that involves the identification of (1), (2), and (3) for an estimation of a KPI that aims at facilitating a more frequent assessment of transition zone health. The proposed methodology offers the capability to evaluate transition zone health prior to the next measurement of track geometry. With the

new available InSAR data that comes frequently, the KPI is updated to provide early warnings to support decision-making regarding the time and locations for maintenance interventions.

5.4. Methodology

Fig. 5.3 illustrates the framework of this chapter. It involves the development of two distinct 2D spatio-temporal interpolation functions to estimate values from InSAR and ABA data. Then, a hybrid neural model is developed to predict track longitudinal levels using these interpolated values. Finally, utilising the predicted track longitudinal levels, the KPI is evaluated across unobserved months spanning the entire transition zone.

5.4.1. Spatio-temporal interpolation

The railway track is a distributed system characterised by dynamic variations over time and locations. Temporal variation is due to continuous usage, degradation, and maintenance, while spatial variations arise from distinct dynamics at different locations, including transition zones. As performing an interpolation within a smaller region allows for addressing local variations over different locations and times, this work considers the development of spatio-temporal interpolation within smaller regions. Fig. 5.4 shows the workflow of the spatio-temporal interpolation. It involves domain discretisation, surface fitting for the displacements, and curve fitting for the ABA data within the subdomains.

Domain discretisation

This work predicts track longitudinal levels by utilising interpolated values derived from InSAR and ABA measurements. Subsequently, the domain is discretised to ensure that each subdomain contains displacements from at least two distinct locations and ABA values from at least one measurement. Based on these assumptions, a distance Δx can be defined for a spatial domain discretisation such that $\Delta x \geq \max\left\{\left(x_i^{\mathscr{S}} - x_{i-1}^{\mathscr{S}}\right), i = 2,\ldots,\gamma_2\right\}$. Likewise, Δt for a temporal domain discretisation can be defined such that $\Delta t \geq \max\left\{\left(t_i^{\mathscr{A}} - t_{i-1}^{\mathscr{A}}\right), i = 2,\ldots,\beta_3\right\}$.

Given Δx and Δt and a spatio-temporal domain $\mathscr{T} = \Big\{(x,t) \mid x \in [x_b, x_e]$ and $t \in [t_b, t_e]\Big\}$, we have that the spatial domain is uniformly discretised into M sub-spatial domains and the temporal domain is uniformly discretised into N sub-temporal domains. This results in a total of $M \times N$ subdomains. Mathematically, a subdomain $T_{m,n}$ is defined as:

$$T_{m,n} = \Big\{(x,t) \mid x \in \big[1 + (m-1)\cdot\Delta x, m\cdot\Delta x\big], \; t \in \big[1 + (n-1)\cdot\Delta t, n\cdot\Delta t\big]\Big\}, \tag{5.4}$$

where $m = 1,\ldots,M$ and $n = 1,\ldots N$.

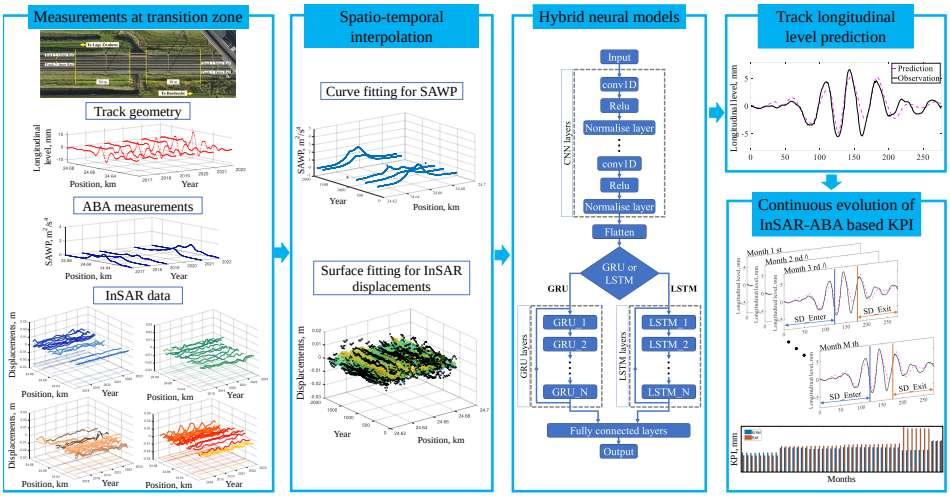

Figure 5.3: The proposed framework.

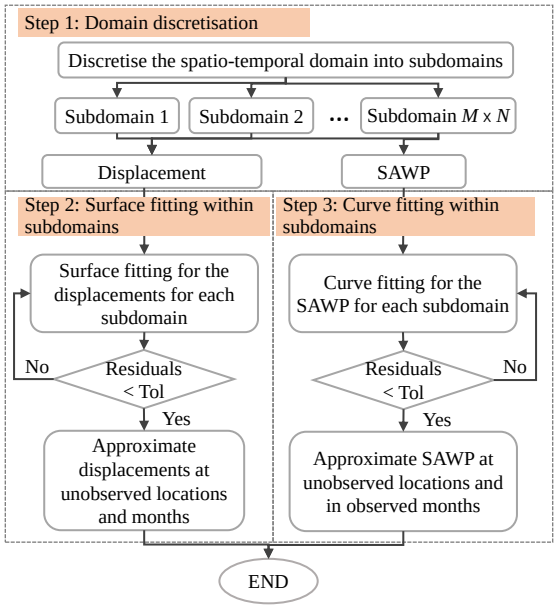

Figure 5.4: Workflow of the spatio-temporal interpolation.

The shaded region depicted in Fig. 5.2 provides an example of a subdomain where the interpolation functions are formulated based on the available InSAR and ABA measurements within that specific subdomain. Within this shaded region, ABA data

from the month $t_o^{\mathscr{A}}$ and InSAR data collected from positions and months confined by the spatial and temporal boundaries of the shaded area will be utilised to construct the interpolation functions.

Surface fitting for displacements

Given a subdomain $T_{m,n}$ and the displacements $d_j^{r,m,n}\left(x^{\mathscr{S}}, t^{\mathscr{S}}\right)$ collected from rail r of track j at position $x^{\mathscr{S}} \in \left[1+(m-1)\cdot\Delta x, m\cdot\Delta x\right]$ and in month $t^{\mathscr{S}} \in \left[1+(n-1)\cdot\Delta t, n\cdot\Delta t\right]$ that are available within $T_{m,n}$. This chapter considers two-dimensional polynomial interpolation to estimate values of displacements, $\hat{d}_j^{r,m,n}\left(x^{\mathscr{G}}, t^{\mathscr{G}}\right)$ at the position, $x^{\mathscr{G}}$, and in the month, $t^{\mathscr{G}}$, of the predicted track longitudinal level within a subdomain $T_{m,n}$. The two-dimensional polynomial interpolation $\mathscr{K}_j^{r,m,n}$ defined for rail r of track j within a subdomain $T_{m,n}$ is mathematically expressed as:

$$\mathscr{K}_j^{r,m,n}(x,t) = \sum_{p=0}^{P_j^{r,m,n}} \sum_{q=0}^{Q_j^{r,m,n}} c_{j,pq}^{r,m,n} x^p t^q, \tag{5.5}$$

where $P_j^{r,m,n}$ and $Q_j^{r,m,n}$ denote the degree of the polynomial used for interpolation in the spatial and temporal subdomain, respectively. The coefficients $c_{j,pq}^{r,m,n}, p = 0,\ldots,P_j^{r,m,n}$ and $q = 0,\ldots,Q_j^{r,m,n}$ are determined using the given data points in each corresponding subdomain, aiming at minimising the sum of the squared differences between the observed and predicted values. The degree of the polynomial defined in each subdomain is optimised to attain the lowest sum square error.

Curve fitting for the ABA signal

Given a subdomain $T_{m,n}$ and the ABA data $a_j^{r,m,n}\left(x^{\mathscr{A}}, t^{\mathscr{A}}\right)$ obtained from rail r of track j at position $x^{\mathscr{A}} \in \left[1+(m-1)\cdot\Delta x, m\cdot\Delta x\right]$ and in month $t^{\mathscr{A}} \in \left[1+(n-1)\cdot\Delta t, n\cdot\Delta t\right]$ that are available within $T_{m,n}$. Even though ABA data exhibits temporal variation, this chapter assumes a constant variation of the ABA values between two consecutive measurement months. This allows the formulation of 2D spatio-temporal interpolation to be simplified into 1D interpolation. To estimate the values of the ABA data $\hat{a}_j^{r,m,n}\left(x^{\mathscr{G}}, t_o^{\mathscr{A}}\right)$ at the position $x^{\mathscr{G}}$ from the closest ABA measurement month, $t_o^{\mathscr{A}}, o \in \left\{1,\ldots,\beta_3\right\}$, occurring prior to the measurement month $t^{\mathscr{G}}$, this chapter considers one-dimensional polynomial interpolation $\mathscr{H}_{j,t_o^{\mathscr{A}}}^{r,m,n}(x)$ defined for rail r of track j within a subdomain $T_{m,n}$ is mathematically expressed as:

$$\mathscr{H}_{j,t_o^{\mathscr{A}}}^{r,m,n}(x) = \sum_{\xi=0}^{R_j^{r,m,n}} b_{j,\xi}^{r,m,n} x^r, \tag{5.6}$$

where $R_j^{r,m,n}$ denotes the degree of the polynomial used for interpolation in the spatial subdomain $T_{m,n}$. The coefficients $b_{j,\xi}^{r,m,n}, \xi = 0,\ldots,R_j^{r,m,n}$ are determined using

the given data points in each corresponding subdomain, aiming at minimising the sum of the squared differences between the observed and predicted values of the ABA signals. The degree of the polynomial defined in each subdomain is optimised to attain the lowest sum square error.

5.4.2. HYBRID NEURAL MODEL

This chapter considers a hybrid CNN-LSTM and CNN-GRU model to predict the track longitudinal levels. Both hybrid models are designed to have CNN layers on top. Then, the LSTM or GRU structure is designed to follow the CNN layers, as seen in Fig. 5.3. The inputs to the CNN layers are the interpolated values of the displacements derived from the InSAR data and the ABA measurements. After the CNN layers, their output is fed into the LSTM or GRU layers and the fully connected layers, allowing for a prediction of the track longitudinal levels.

Given railway track j, rail r, and the interpolated values of the displacements $\hat{d}_j^{r,m,n}\left(x^{\mathcal{G}}, t^{\mathcal{G}}\right)$ and the ABA signals $\hat{a}_j^{r,m,n}\left(x^{\mathcal{G}}, t^{\mathcal{A}}\right)$, this chapter considers the input vector to a hybrid neural model as a concatenated vector denoted as $X = \left[\hat{d}_j^{r,m,n}\left(x^{\mathcal{G}}, t^{\mathcal{G}}\right), \hat{a}_j^{r,m,n}\left(x^{\mathcal{G}}, t^{\mathcal{A}}\right)\right]$. For the f^{th} convolutional layer, let denote its input as X_f, its filters as W_f, the bias term as b_f, and the activation function as ϕ. The output z_f of the f^{th} convolutional layer can be expressed mathematically as follow:

$$z_f = \phi\left(W_f * X_f + b_f\right) \tag{5.7}$$

where $*$ denotes the convolution operation, which involves sliding the filters W_f over the input X_f and computing the dot product at each position. The result is then passed through the activation function ϕ. The obtained output z_f represents the feature maps passed on to the next layers.

After the CNN layers, LSTM layers or GRU layers are considered. For the GRU layers, the core building blocks include hidden state (h), update gate (v), reset gate, (r), candidate hidden state ($\tilde{h}$), and hidden state update rule [313]. For a time step t, the hidden state h_t is the memory of the GRU that captures information from previous time steps. The update gate v_t determines how much of the previous hidden state h_{t-1} to retain and how much of the new candidate hidden state $\tilde{h}_t$ to incorporate. The update gate is computed using a sigmoid activation function (σ) as seen in (5.8). The reset gate determines how much of the previous hidden state h_{t-1} to forget. It is also computed using a sigmoid activation function (σ) as seen in (5.9). The candidate hidden state at the time step t represents the new information that could be added to the memory. It is computed by applying the hyperbolic tangent (tanh) activation function to the weighted sum of the reset-gated previous hidden state and the current input, as seen in (5.10). Then, the new hidden state h_t is computed by combining the previous hidden state h_{t-1} and the candidate hidden state $\tilde{h}_t$ using (5.11).

$$v_t = \sigma\left(W_v \cdot \left[h_{t-1}, z_t\right]\right), \tag{5.8}$$

$$r_t = \sigma\Big(W_r \cdot [h_{t-1}, z_t]\Big), \tag{5.9}$$

$$\tilde{h}_t = \tanh\Big(W_h \cdot [r_t \odot h_{t-1}, z_t]\Big), \tag{5.10}$$

$$h_t = \tanh\big((1 - v_t) \odot h_{t-1} + v_t \odot \tilde{h}_t\big), \tag{5.11}$$

where z_t is an input to the GRU layers obtained from the last convolution layer of the CNN layers, W_v is the weight matrix for the update gate, W_h is the weight matrix for the candidate hidden state, $\odot$ represents element-wise multiplication.

Similar to the GRU layers, the LSTM cell has three gates: the input gate, the forget gate, and the output gate. The forget gate determines what information from the previous cell state should be discarded. The input gate decides what new information to store, and the output gate controls how much of the current cell state should be revealed as the output. Additionally, there are a cell state update, $\tilde{c}_t$, and the actual cell state c_t designed for LSTM. Mathematically, they are expressed as follows:

$$f_t = \sigma\Big(W_f \cdot [h_{t-1}, z_t] + b_f\Big), \tag{5.12}$$

$$I_t = \sigma\Big(W_I \cdot [h_{t-1}, z_t] + b_I\Big), \tag{5.13}$$

$$\tilde{c}_t = \tanh\Big(W_c \cdot [h_{t-1}, z_t] + b_c\Big), \tag{5.14}$$

$$c_t = f_t \cdot c_{t-1} + I_t \cdot \tilde{c}_t, \tag{5.15}$$

$$o_t = \sigma\Big(W_o \cdot [h_{t-1}, z_t] + b_o\Big), \tag{5.16}$$

$$h_t = o_t \cdot \tanh\big(c_t\big), \tag{5.17}$$

where z_t is an input to the LSTM layers obtained from the last convolution layer of the CNN layers. f_t denotes forget gate, I_t is input gate, $\tilde{c}_t$ is cell state, c_t is update cell state, o_t is output gate, and h_t is hidden state update. The weight matrices are denoted as W_f, W_I, W_c, W_o, and the bias vectors are represented by b_f, b_I, b_c, b_o.

The final layer after the hybrid neural model consists of a fully connected layer. The output y_α^λ from the α^{th} node of the λ^{th} layer is mathematically expressed as:

$$y_\alpha^\lambda = \sum_j \omega_{\alpha\epsilon}^\lambda \Big(\phi(h_{t,\alpha}^\lambda) + b_\alpha^\lambda\Big), \tag{5.18}$$

where $\omega_{\alpha\epsilon}^\lambda$ represents the weight of the α^{th} and ϵ^{th} node for the layer λ and $\lambda - 1$, respectively, ϕ is an activation function, and b_α^λ is its bias.

5.4.3. EVALUATION OF KEY PERFORMANCE INDEX

Let the proposed KPI based on InSAR and ABA data denote as $\text{KPI}_{\text{InSAR+ABA}}$. To assess the health of transition zones, this work focuses on computing $\text{KPI}_{\text{InSAR+ABA}}$ for two track segments $k \in \{\text{Entrance}, \text{Exit}\}$. These segments cover a distance of 30 meters each, extending from the entrance and exit sides of the transition zones [250]. Specifically, the spatial boundaries are defined by x_b and $x_b + 30$ metres for the entrance side, while for the exit side, the spatial boundaries are defined by $x_e - 30$ metres and x_e. With a single value assigned to each segment k, two values of $\text{KPI}^{k,j}_{\text{InSAR+ABA}}$ are determined for a given track j. Their calculation involves determining the standard deviation of the predicted longitudinal levels, $\widehat{SD}_r$, at rail $r \in \{\text{inner}, \text{outer}\}$. The proposed $\text{KPI}^{k,j}_{\text{InSAR+ABA}}$ for a given segment k of track j is obtained as follows:

$$\text{KPI}^{k,j}_{\text{InSAR+ABA}} = \frac{\left(\widehat{SD}^{k,j}_{\text{inner}} + \widehat{SD}^{k,j}_{\text{outer}}\right)}{2}, \tag{5.19}$$

where

$$\widehat{SD}^{k,j}_{r} = \sqrt{\frac{\sum_{i=1}^{\gamma_1}\left(\hat{l}^r_j\left(x^{\mathscr{G}}, t^{\mathscr{G}}\right) - \bar{l}^r_j\right)^2}{\gamma_1}}, \tag{5.20}$$

and $\hat{l}^r_j(x^{\mathscr{G}}, t^{\mathscr{G}})$ is the predicted track longitudinal levels at a position $x^{\mathscr{G}}$ contained within the spatial boundaries of segment k and in a month $t^{\mathscr{G}}$, $\bar{l}^r_j$ is the mean of the predicted track longitudinal levels from rail r of track j, and γ_1 is the number of track geometry measurements in the spatial domain.

Following the European standard EN 13848–6 [314], the conventional TQI, referred to as CoSD, and the performance index based on the average between the standard deviation of the track longitudinal levels at the inner rail and that at the outer rail, referred to as avgSD, are considered baseline comparisons. Mathematically, the CoSD is expressed as in (5.21) and the avgSD can be obtained by considering the observed value of track longitudinal levels in (5.19) and (5.20).

$$\text{CoSD} = \sqrt{w_{\overline{AL}} SD^2_{\overline{AL}} + w_G SD^2_G + w_C SD^2_C + w_{\overline{LL}} SD^2_{\overline{LL}}}, \tag{5.21}$$

where for the individual geometry parameter i, SD_i is its standard deviation, w_i is its weighting factor. $\overline{AL}$ is the average alignment of the inner and outer rails, G is the track gauge, C is the cant, and $\overline{LL}$ is the average longitudinal level between 2 rails. This CoSD is calculated considering a track segment of the same distance.

5.4.4. EVALUATION METRICS

The CNN-LSTM and CNN-GRU models are trained to minimise the difference between the observed and the predicted track longitudinal level. In regression tasks, root mean square error (defined in (5.24)) is typically used as a loss function for model training. As typically conducted in CNN literature, including studies by [223, 308, 315], the following four statistics are utilised to evaluate model performance in this chapter:

- Mean absolute error (MAE) calculates the absolute differences between the actual and predicted values generated by the model and then averages these absolute differences. MAE gives equal weight to all errors without considering overestimation or underestimation. MAE is expressed as [223]:

$$\mathrm{MAE} = \frac{1}{N}\sum_{i=1}^{N}\left\{\left|y_i - \hat{y}_i\right|\right\}. \tag{5.22}$$

- Mean squared error (MSE) computes the squared differences between the actual and predicted values generated by the model and then averages these squared differences. By squaring the differences, MSE emphasises significant deviations in the model predictions. MSE is expressed as [315]:

$$\mathrm{MSE} = \frac{1}{N}\sum_{i=1}^{N}\left(y_i - \hat{y}_i\right)^2. \tag{5.23}$$

- Root mean square error (RMSE) is the square root of the average of the squared differences between the actual and predicted values generated by the model. RMSE is expressed as [223, 308, 315]:

$$\mathrm{RMSE} = \sqrt{\frac{1}{N}\sum_{i=1}^{N}\left(y_i - \hat{y}_i\right)^2}. \tag{5.24}$$

- R^2 measures the proportion of variance explained by the model and ranges from 0 to 1, with 1 indicating a perfect fit. R^2 is expressed as [315]:

$$R^2 = 1 - \frac{\sum_{i=1}^{N}\left(y_i - \hat{y}_i\right)^2}{\sum_{i=1}^{N}\left(y_i - \bar{y}\right)^2}. \tag{5.25}$$

where N is the number of samples, y_i indicates the predicted track longitudinal level value, $\hat{y}_i$ denotes the observed value, and $\bar{y}$ denotes the mean of the measurements.

5.5. Case Study

5.5.1. Description of the Case Study Site

This chapter selects transition zones at a railway bridge between Dordrecht and Lage Zwaluwe station as our case study. It is a 9-metre single-span bridge that crosses over a water channel. The bridge supports two tracks of a railway line with fixed travel directions. Fig. 5.5(a) shows photographs of the double-track railway bridge across a water channel from the side and top view, from which Fig. 5.5(b) shows aerial photographs obtained from different years. Track 1 is for trains travelling from Lage Zwaluwe to Dordrecht, and Track 2 is for trains from Dordrecht to Lage Zwaluwe. This transition zone features the entrance and exit sides on each of

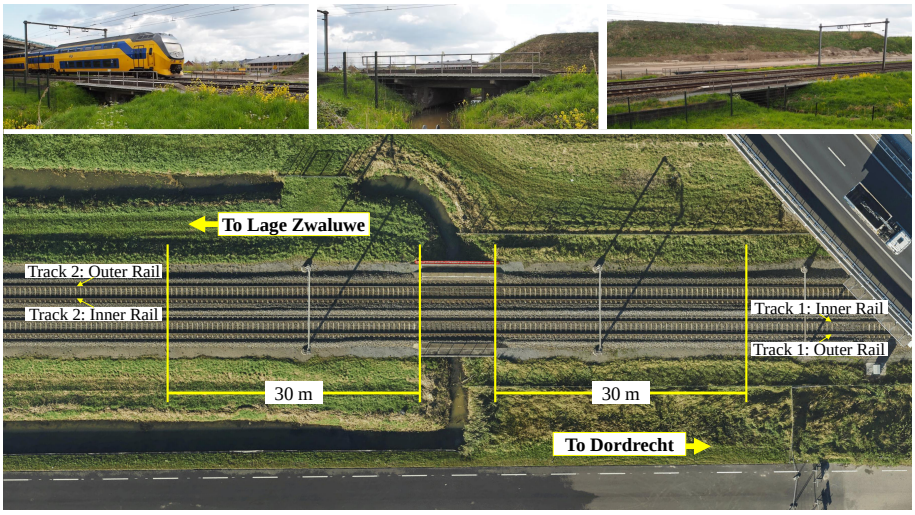

(a) Photographs at the double-track railway bridge across a water channel from the side and top view.

(b) Examples of aerial photographs showing the variability of the area near the railway track from 2014, 2015, 2016, and the most recent year (source: BBMS, ProRail)

Figure 5.5: Our study area of transition zones.

the two tracks, as well as the inner and outer rails. The entrance side marks the beginning of the transition in which trains move from the conventional track to the bridge. The exit side of a railway transition zone is the segment where the trains return back to the standard configuration of tracks.

5.5.2. DESCRIPTION OF THE MEASUREMENTS

All the measurement technologies are analysed at the track sections at both ends of the bridge, from 30 metres before the railway bridge on the entrance side to 30 metres after the bridge on the exit side and 30 metres away from both tracks. Therefore, the boundary area of our case study is defined to include measurements collected at positions x within the kilometre range from $x_b = \text{edge1} - 0.03$ km to $x_e = \text{edge2} + 0.03$ km. The transition zone of the bridge at the entrance side of Track 1, denoted as edge1, is marked at 24.652 km. The transition zone of the bridge at the exit side of Track 1, denoted as edge2, is marked at 24.661 km. The distance from x_b to x_e accounts for a total distance of 69 metres, including the bridge length of 9 metres.

Track geometry measurements

This chapter considers only track longitudinal levels from track geometry measurements conducted from a railway track $j \in \{1,2\}$ at rail $r \in \{\text{inner}, \text{outer}\}$. The measurements used are available yearly between November 2018 and August 2022. This accounts for five measurements in which $t_1^{\mathscr{G}}$ corresponds to November 2018, $t_2^{\mathscr{G}}$ corresponds to December 2019, $t_3^{\mathscr{G}}$ corresponds to August 2020, $t_4^{\mathscr{G}}$ corresponds to November 2021, and $t_5^{\mathscr{G}}$ corresponds to August 2022. The measurements are processed with a bandpass filter within a wavelength range of 3 metres to 25 metres, and the measurements are reported in the spatial domain with a resolution $\Delta x^{\mathscr{G}} =$ 0.25 metres [316]. This accounts for 276 datapoints within the boundary area. Hence, for this case study, a set of track longitudinal levels collected from a rail r of track j at position x and month t can be defined as:

$$\mathscr{G}_j^r = \left\{ l_j^r(x,t) \middle| x = x_1^{\mathscr{G}}, x_2^{\mathscr{G}}, \ldots, x_{276}^{\mathscr{G}} \text{ and } t = t_1^{\mathscr{G}}, \ldots, t_5^{\mathscr{G}} \right\}.$$

5

InSAR data

We use InSAR data that SkyGeo processed [317], and data were obtained from four satellites: west-1a, west-2a, midden-1, and midden-2. In this chapter, the data were collected by Sentinel-1 SAR satellites, with multi-track images, every 5-12 days from September 2018 to August 2022. Due to the temporal variations in InSAR data collection, this chapter considers representing InSAR data on a monthly basis to ensure a uniform measurement time across different satellites. We also perform a moving average technique to mitigate noise inherent in InSAR data, which can be due to temporal changes on the ground. Hence, the measurement month $t_1^{\mathscr{S}}$ aligns with September 2018. With subsequent measurement months determined at a monthly resolution, culminating in the final measurement month $t_{48}^{\mathscr{S}}$, which corresponds to August 2022. Within the boundary area, only 67 InSAR points were available. These InSAR points are spatially aligned by projecting their positions perpendicularly onto tracks 1 and 2. The projection yields InSAR data points spaced at an average interval of 1 meter, i.e., $\Delta x^{\mathscr{S}} = 1$ metre, with a maximum discrepancy between individual data points equals to 5.4 meters. For this chapter, we assume that the InSAR data for the inner rail are the same as those of the outer rail of the same track. Hence, a set of line-of-sight displacements collected from track j at position x and month t can be defined as:

$$\mathscr{S}_j = \left\{ d_j(x,t) \middle| x = x_1^{\mathscr{S}}, x_2^{\mathscr{S}}, \ldots, x_{67}^{\mathscr{S}} \text{ and } t = t_1^{\mathscr{S}}, \ldots, t_{48}^{\mathscr{S}} \right\}.$$

Axle box acceleration measurements

The ABA signals are collected from four wheelsets at a rail $r \in \{\text{inner}, \text{outer}\}$ and from a track $j \in \{1,2\}$. The measurements are available yearly between 2018-2019 and 2021-2022. This accounts for four measurements in which $t_1^{\mathscr{A}}$ corresponds to September 2018, $t_2^{\mathscr{A}}$ corresponds to June 2019, $t_3^{\mathscr{A}}$ corresponds to November 2021, and $t_4^{\mathscr{A}}$ corresponds to May 2022. In this chapter, the measurements come from the high sampling frequency of 25.6 kHz, e.g., local dynamic responses are measured

at every millimetre approximately for a measuring speed of 100 km/hr. Only the vertical ABA signals corresponding to the vertical train-track dynamic are considered in this work. A low pass filter at 100 Hz is applied to filter out high-frequency contents within the vertical ABA signals unrelated to transition zone conditions.

Then, the ABA signals in the time domain are transformed into the time-frequency domain using the Morlet wavelet. After the wavelet power spectrum (WPS) of the ABA signal is obtained, their corresponding scale average wavelet power (SAWP) is calculated to investigate characteristic frequency responses at the transition zones. Only the spatial frequency range between 0.04 m^{-1} and 0.33 m^{-1}, corresponding to track irregularities in the wavelength from 3 m to 25 m, are selected for our analysis as this is related to the condition of the substructure layer reported in [250]. This chapter considers the average SAWP from four ABA signals corresponding to the same rail to reduce uncertainty from the measurements, in which the SAWP is reported with a spatial resolution of 1 centimetre, i.e., $\Delta x^{\mathscr{A}} = 0.01$ metre. This accounts for 6900 data points within the boundaries of the spatial domain. Hence, a set of the average SAWP derived from the ABA measurements collected from rail r of track j at position x and month t can be defined as:

$$\mathscr{A}_j^r = \left\{ a_j^r(x,t) \middle| x = x_1^{\mathscr{A}}, x_2^{\mathscr{A}}, \ldots, x_{6900}^{\mathscr{A}} \text{ and } t = t_1^{\mathscr{A}}, \ldots, t_4^{\mathscr{A}} \right\}.$$

5.6. RESULTS

5.6.1. IMPLEMENTATION DETAILS

Due to limitations in the available measurement history, we discretise the temporal domain into five fixed subdomains. Then, we vary the number of subdomains in the spatial domain to assess their impact on the overall analysis. For a given subdomain, the degrees of polynomials used in the curve fitting for the SAWP and the surface fitting for displacements are experimented with. The polynomials up to the fifth degree are trials. The hybrid neural models are developed separately for Track 1 and Track 2, in which the same network architecture is used to predict the longitudinal levels from both the inner and outer rails of the respective track. We experiment with the number of hidden layers used within the CNN, GRU, and LSTM structures. For the CNN structure, up to three convolutional layers are considered, and four different numbers of filters are trial: 64, 32, 16, and 8. We also experiment with different filter sizes: 3×3, 5×5, 7×7, and 11×11. The rectifier or ReLU activation function is used in CNN. For the GRU and LSTM structure, up to two layers are considered, and six different numbers of hidden units are trial: 256, 128, 64, 32, 16, and 8. The hyperbolic tangent and sigmoid functions are exploited as the state and gate activation functions, respectively.

For the model training, the following parameter setting is specified: number of data in each batch (MiniBatchSize) = 10, the maximum number of epochs = 300, and the learning rate for parameter updates = 0.01. The dataset is divided into training and test sets with a ratio of 60:40, in which 90% of the training set is used to train the model, and the other 10% is used for validating the trained model. The trained model is then tested with the holdout test set to evaluate its performance for

the regression task. The models are trained with 5-fold cross-validation considering inner and outer rails data. The dropout layer and the L_2-regularisation are also considered to prevent overfitting.

5.6.2. Results of different interpolation functions

This section investigates the impact of using different interpolation functions on predictive performance. In this analysis, the hybrid CNN-GRU model is used to showcase the analysis and we consider uniformly discretising the domain into 35 subdomains. This is obtained by dividing the spatial and temporal domain uniformly into 7 and 5 subdomains, respectively. The tested interpolation functions include local linear regression, polynomial function, nearest interpolation, biharmonic interpolation, and cubic spline. We assess the performance in two aspects: interpolation performance and predictive performance. To assess the interpolation performance, the deviations of the estimates of the missing values from the actual values are measured, in which the evaluation metrics used are RMSE and R^2. To assess the predictive performance, RMSE, MSE, MAE, and R^2 are calculated.

Table 5.1 shows that the polynomial function yields the best predictive performance even though the nearest, biharmonic, and cubic spline interpolations demonstrate better fitting performance. Fig. 5.6 presents the results of the spatio-temporal interpolation obtained from the polynomials. The results are showcased from Track 1. It is observed from the experiments that the suitable degrees of the polynomials differ for different subdomains. This results from the variations in the distribution of the displacement data in different subdomains, as illustrated in Fig. 5.6(a). Fig. 5.6(b) presents the surface fitting results across the entire domain. Notably, the consistency between predicted and observed values are reasonable, evident by residuals shown in Fig. 5.6(c). The surface fitting of the displacements yields the average RMSE values of 0.0027 m and R^2 = 0.7731.

5.6.3. Results of different numbers of subdomains

Considering the polynomial functions obtained from Section 5.6.2 to estimate values of displacements, this section investigates the impact of discretising the domain into different numbers of subdomains. The hybrid CNN-GRU model is also used to showcase the analysis. It is observed in Table 5.2 that employing large subdomains for interpolation fails to capture local variations along the track. This leads to poor predictive performance, as indicated by a high error and a large R^2 value when discretising the domain into 5 subdomains. However, performing an interpolation with subdomains that are too small can result in overfitting, where the interpolation passes through all the data points. This is evident in the well-fitted performance with a small error and an R^2 value close to 1 when the domain is discretised into 50 subdomains. Analysing the results in Table 5.2 reveals that the best predictive performance is achieved through uniform discretisation into 35 subdomains.

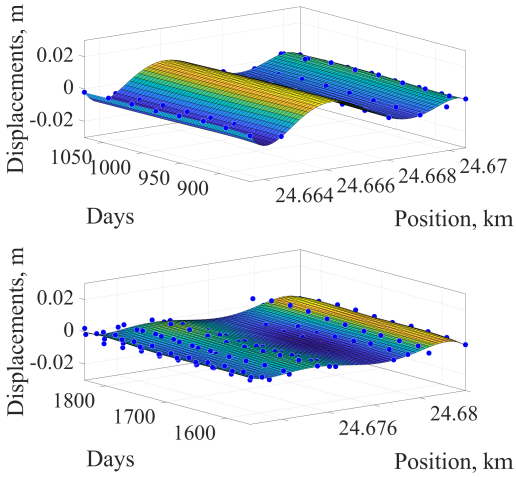

(a) Examples of surface fitting in subdomains.

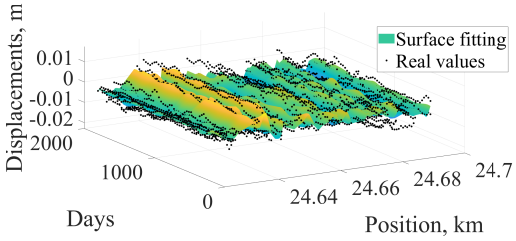

(b) Surface fitting for the displacements in the whole domain.

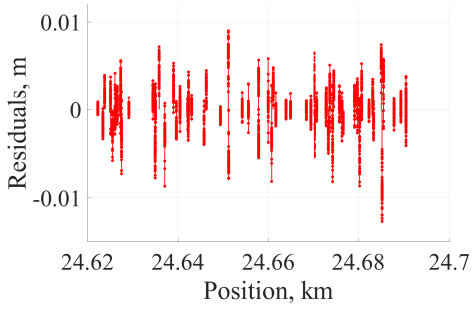

(c) Residuals.

Figure 5.6: Spatio-temporal interpolation, shown are from Track 1.

Table 5.1: Impact on the predictive performance when using different interpolation functions. Shown are the results obtained from the hybrid CNN-GRU of Track 1.

Interpolation function	**Interpolation performance**		**Predictive performance**			
	RMSE	**R^2**	**RMSE**	**MSE**	**MAE**	**R^2**
Local linear regression	0.0030	0.5547	0.0489	0.0033	0.0323	0.5061
Polynomial	0.0027	0.7731	**0.0403**	**0.0017**	**0.0275**	**0.8048**
Nearest interpolation	**0.0**	**1.0**	0.0472	0.0039	0.0303	0.7244
Biharmonic interpolation	**0.0**	**1.0**	0.0458	0.0022	0.0325	0.1959
Cubic spline	**0.0**	**1.0**	0.0862	0.0082	0.0600	-2.7106

Table 5.2: Impact on the predictive performance when discretising domain into different sizes of subdomains. Shown are the results from using a polynomial function in the interpolation and the hybrid CNN-GRU of Track 1 in the prediction.

No. of subdomains	**Interpolation performance**		**Predictive performance**			
	RMSE	**R^2**	**RMSE**	**MSE**	**MAE**	**R^2**
5	0.0042	0.1197	0.0649	0.0045	0.0447	-6.4755
15	0.0035	0.3690	0.1127	0.0130	0.0595	0.3451
35	0.0027	0.7731	**0.0403**	**0.0017**	**0.0275**	**0.8048**
45	0.0021	0.7996	0.0782	0.0062	0.0534	0.0563
50	0.0018	0.8466	0.0703	0.0058	0.0436	0.0344
55	0.0020	0.8020	0.0989	0.0105	0.0630	-37.2659

Table 5.3: Performance comparison among different predictive models. The reported performance is an average value between the inner and outer rail.

Model	**Track 1**				
	Architecture	**RMSE**	**MSE**	**MAE**	**R^2**
CNN	128-64	0.0828	0.0128	0.0579	0.5203
GRU	32-16-8	0.0477	0.0031	0.0327	0.5845
LSTM	128-64	0.0779	0.0069	0.0584	0.5829
CNN-LSTM	32-16-8-32-16	**0.0374**	**0.0015**	**0.0281**	**0.8149**
CNN-GRU	32-16-8-128-64	0.0403	0.0017	0.0275	0.8048
Model	**Track 2**				
	Architecture	**RMSE**	**MSE**	**MAE**	**R^2**
CNN	64-64	0.1045	0.0115	0.0744	0.5222
GRU	32-16-8	0.0558	0.0032	0.0396	0.5848
LSTM	64-32	0.0868	0.0080	0.0629	0.5436
CNN-LSTM	32-16-8-32-16	0.0553	0.0033	0.0395	0.7016
CNN-GRU	32-16-8-128-64	**0.0509**	**0.0031**	**0.0355**	**0.7539**

5.6.4. COMPARATIVE STUDY FOR TRACK LONGITUDINAL LEVEL PREDICTION

Following the results of Sections 5.6.2 and 5.6.3, we discretise the domain into 35 subdomains and using a polynomial for interpolation of displacements. For the

SAWP, the degrees of polynomials used in the interpolation are also experimented with. The results suggest the utilisation of a fifth-degree polynomial for the interpolation, in which the obtained interpolation performance is given with average RMSE values of 0.0012 m^2/s^4 and R^2 = 0.9999. To evaluate the effectiveness of the hybrid CNN-LSTM and CNN-GRU models, this chapter considers other models in the comparative study as benchmarks. The benchmark models include CNN, GRU, and LSTM. Each model employs the same parameter settings for the model training and undergoes the same experiments with different numbers of filters and sizes as described in Section 5.6.1.

Table 5.3 compares performance obtained from different predictive models developed using data obtained from railway Track 1 and 2. The reported performance is an average value between the inner and outer rail. Different network architectures are designed for different railway tracks, with those outlined in Table 5.3 exhibiting the lowest RMSE values. Notably, the GRU and LSTM models perform better than the CNN model. This is attributed to their ability to handle temporal characteristics. On average, their RMSE improves from that of the CNN model by 24.15%, and their R^2 improves by 12.19%. Within the comparison between the GRU and LSTM models, the GRU model, designed according to the network architecture specified in Table 5.3, exhibits higher performance than the LSTM model for the dataset from Track 1 and 2. Employing a hybrid model approach leads to enhanced performance. This is evident in both hybrid CNN-LSTM and CNN-GRU models. The CNN-GRU model outperforms all the individual models for Track 1 and 2, improving with an average RMSE of 32.88% and R^2 of 40.40%. Notably, the CNN-GRU model yields inferior performance to the CNN-LSTM model for Track 1, which is impaired by 7.75% for RMSE and 1.24% for R^2. Conversely, the hybrid CNN-GRU model yields superior performance for Track 2, surpassing the CNN-LSTM model with an improved RMSE of 7.96%, and R^2 of 7.45%.

Fig. 5.7 illustrates a comparison between the predicted track longitudinal levels obtained from different models in the years 2018-2022. These are the results obtained from the inner rail of Track 2. It can be seen that different models demonstrate different capabilities in capturing the spatial and temporal characteristics presented in the track longitudinal level changes over the years. This capability can be investigated through the spatial and temporal relationship between the predictions and measurements. In other words, a consistent trend between the predictions and measurements along the track positions and across the years should be observed. The predicted values obtained from the individual models, i.e., CNN, GRU, and LSTM, exhibit inconsistent trends with the real measurements. The inconsistency trend is more pronounced in 2022. This is evident by their smaller R^2 values, indicative of a less consistent trend with the observed track longitudinal levels. In contrast, the hybrid CNN-LSTM and CNN-GRU models exhibit more consistent trends, as evidenced by their higher R^2 values compared to the individual models. This suggests a superior ability to capture spatial characteristics. As time evolves, the increased errors in the predicted values from CNN, GRU, and LSTM models are observed. Also, the trend in their predictions shifts, failing to accurately capture peaks. While a slight drop in capturing peaks is observed in the hybrid CNN-GRU

model, it demonstrates an ability to adapt to the trends of the track longitudinal changing over time. This emphasises the effectiveness of the hybrid CNN-LSTM and CNN-GRU models in predicting track longitudinal levels.

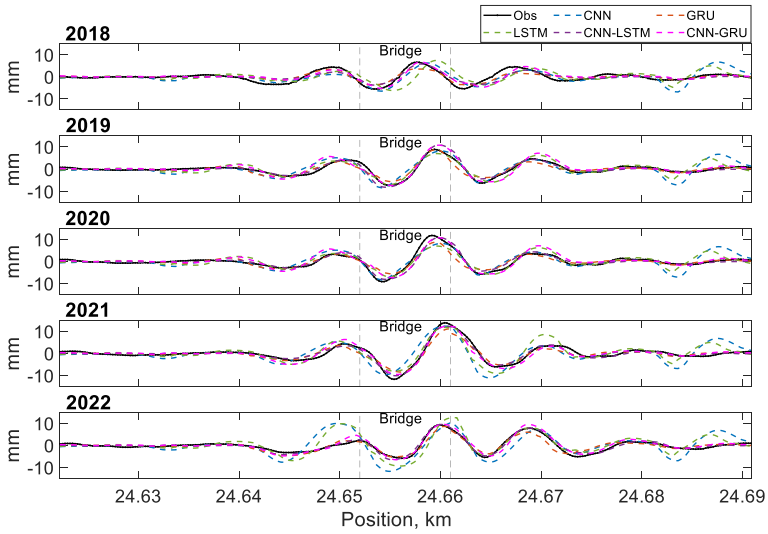

Figure 5.7: Predicted track longitudinal levels obtained from different models. Shown are the results from the inner rail of Track 2.

5.6.5. KPI based on InSAR and ABA data for the health assessment of railway transition zones

This section employs the results obtained from the hybrid CNN-GRU to showcase the evaluation of the proposed $KPI_{InSAR+ABA}$. Fig. 5.8 shows a continuous evolution of the proposed $KPI_{InSAR+ABA}$, at the entrance and exit side of the transition zones from September 2018, marked by month 1, to August 2022, marked by month 48. There were only five measurements of track geometry parameters within this period. Notably, the $KPI_{InSAR+ABA}$ provides consistent health conditions with the CoSD and the avgSD in the months highlighted in the black boxes for both Track 1 and 2. Specifically, from June 2019, marked by month 10, the $KPI_{InSAR+ABA}$ is similar to the trend of the CoSD and avgSD derived from the track geometry measurements. The transition zone at the exit side was more degraded than the entrance for Track 1, whereas the entrance side was more degraded than the exit for Track 2. Likewise, the CoSD, avgSD, and $KPI_{InSAR+ABA}$ consistently revealed that Track 2 was more degraded than Track 1, evident by their higher value.

In month 3, a contrasting trend is observed in Track 1, as highlighted by the red boxes. The $KPI_{InSAR+ABA}$ analysis for Track 1 uncovered that the entrance side of the transition zone exhibited greater degradation compared to the exit side. This is consistent with the information obtained from the ABA measurements depicted in

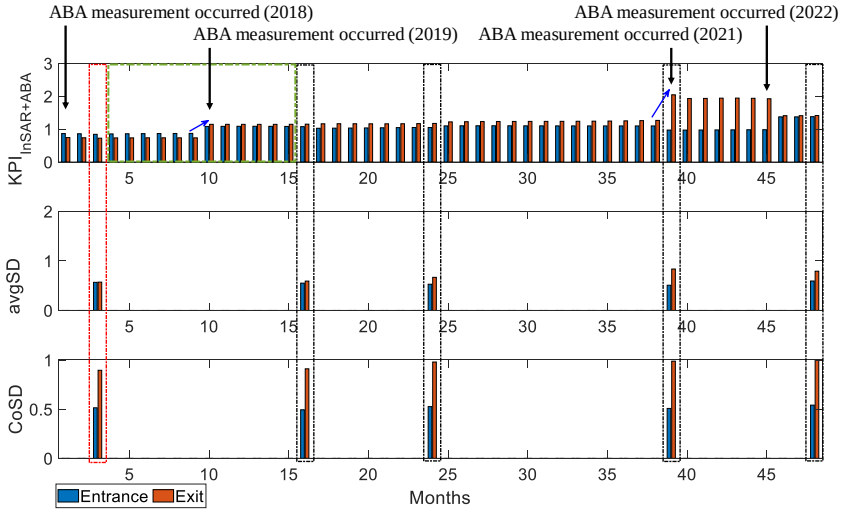

(a) Track 1.

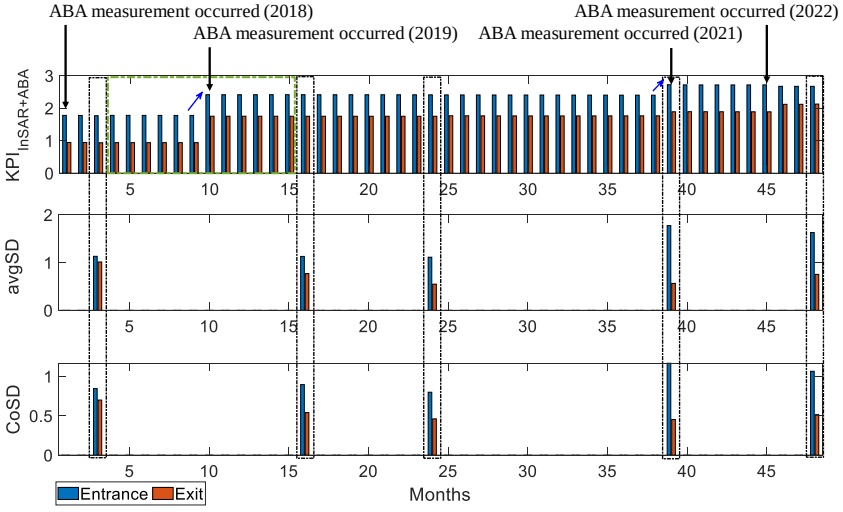

(b) Track 2.

Figure 5.8: Continuous evolution of the KPI at the entrance and exit side of the transition zones from September 2018, marked by month 1, to August 2022, marked by month 48.

Figs. 5.9(a), where the average values of SAWP on the entrance side of the transition zone surpass those on the exit side for Track 1. The inconsistency with the CoSD in Track 1 can be attributed to the inherent integration of ABA measurements in predicting track longitudinal levels. This integration enables the inclusion of

local changes within the substructure layers in the proposed KPI, a capability that traditional track geometry measurements may lack. This results from the consideration of the spatial frequency range of 0.04 m^{-1} to 0.33 m^{-1} (substructure related) in the SAWP calculation.

Furthermore, the track longitudinal levels at unobserved months can be obtained using our hybrid model. This results in a more frequent estimation of the KPI that can be used to facilitate regular assessments of transition zone health, owing to a high-frequency measurement of InSAR data. This approach can enhance the ability to detect changes in track irregularities early, even before obtaining the next measurement of track geometry profiles, as illustrated in the green box. In Fig. 5.8(a) and 5.8(b), abrupt changes of the $KPI_{InSAR+ABA}$ value are observed between months 9-10 and 38-39. This was when the track longitudinal levels were predicted from the ABA measurements of the most recent year. As seen in Fig. 5.9, the SAWP values for both Track 1 and 2 in 2019 increased from those of 2018, resulting in more degraded conditions of the transition zones in 2019 compared to 2018. This pattern is followed between months 38-39 as the increased SAWP values are observed in Figs. 5.9(c) and 5.9(f) for both Track 1 and 2 compared to those in 2019. Consequently, the $KPI_{InSAR+ABA}$ in month 10 is higher than in month 9, and similarly, the $KPI_{InSAR+ABA}$ in month 39 exceeds that of month 38. This consistent trend is observed for both tracks. Evaluating from the $KPI_{InSAR+ABA}$ values, in cases where the severity is classified as high, this proactive information allows for effective planning of maintenance actions.

5.6.6. Discussion

This section delves deeper into the analysis of predicted track longitudinal levels, providing insights into the physics. The investigation is showcased using data collected in 2020 from track 1. While consistency is evident between the prediction and observation in the time domain, depicted in Fig. 5.10a), a distinct variation in energy distribution within the frequency domain is noticeable. As seen in Figs. 5.10b) and 5.10c), differences are observed in the frequency content for wavelengths ranging from 3 to 25 metres when comparing observations to predictions. This is more pronounced, particularly when the wavelength is less than 5 metres for the entrance and exit sides of the inner and outer rails. The predicted track longitudinal levels at the railway bridge transition zones exhibit different characteristics, reflecting the limitation arising from the data-driven nature of the predictive models employed in this chapter. This comes from a lack of the incorporation of physical information from the track system.

5.7. Conclusions

This chapter presents a framework that enables a more frequent evaluation of transition zone health by integrating multiple monitoring technologies, including track geometry, InSAR, and ABA measurements. To illustrate its effectiveness, a case study at a railway bridge between Dordrecht and Lage Zwaluwe station in the Netherlands is used. Compared to individual models, i.e., CNN, GRU, and LSTM,

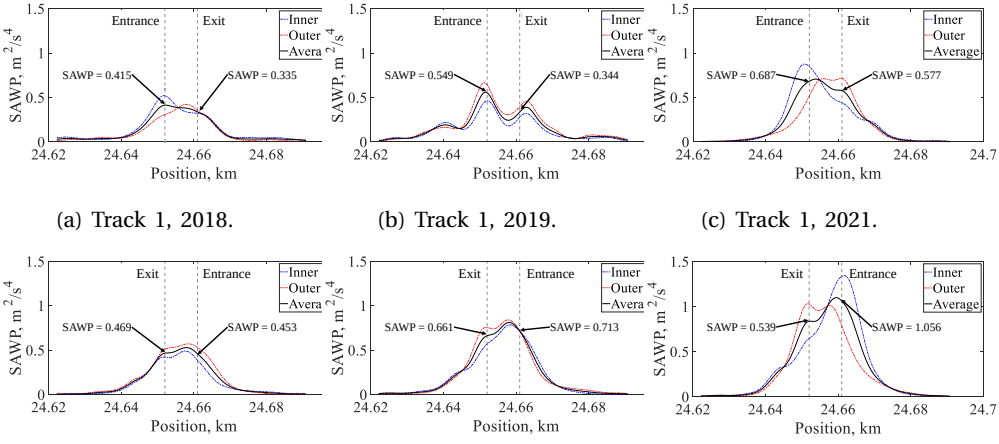

(a) Track 1, 2018. (b) Track 1, 2019. (c) Track 1, 2021.

(d) Track 2, 2018. (e) Track 2, 2019. (f) Track 2, 2021.

Figure 5.9: The interpolated SAWP for predicting the track longitudinal levels.

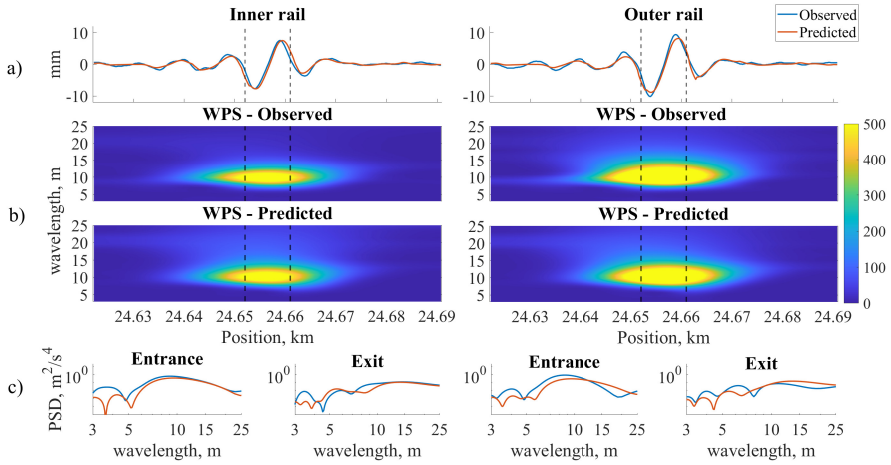

Figure 5.10: Comparison results between the predicted and observed track longitudinal levels in a) the time domain, and the frequency domain considering b) WPS and c) PSD at the transition zones from track 1.

hybrid CNN-LSTM and CNN-GRU exhibit a superior ability to capture the spatial and temporal relationships between the track longitudinal levels, InSAR, and ABA measurements. The hybrid models allow for more accurate predictions of track longitudinal levels during unobserved months, leading to a more frequent estimation of the KPI. This owes to a high-frequency measurement provided by InSAR data. As new measurements become available, the hybrid models facilitate the timely

estimation of KPI values. The proposed KPI proves effective in detecting changes in track irregularities, thereby enabling regular assessments of transition zone health.

Future research lines include evaluating the generalisation and robustness of the proposed methodology and the proposed KPI based on InSAR and ABA data for assessing the health of transition zones. This involves using a larger dataset containing diverse locations under varying transition zone conditions. Then, probabilistic models, e.g., the fuzzy-interval method and Bayesian networks, can be considered as predictive models to incorporate and quantify uncertainty in the data arising from diverse locations and conditions. The inclusion of physical variables and maintenance information in the predictions can also be considered via physics-informed machine learning to better capture the dynamic behaviour of transition zones. Given that ABA measurements depend on speed, a method to mitigate the impact of speed variations in measurements is needed to facilitate the broader application of the proposed framework.

6

Conclusions and Recommendations

At last, it comes to an end.

6.1. CONCLUSIONS

The comprehensive review of the development of AI methodologies in railway infrastructure allows us to gain insights into the challenges for successful implementation in the railway industry. Based on these, this PhD research considers AI solutions to address the selected challenges and provide support for maintenance decisions of railway infrastructure. The challenges covered are the detection of rail surface defects at early development stages based on ABA measurements, unsupervised representation learning from high-frequency moving vibration sensors, including ABA and LDV, and the fusion of information from different monitoring technologies. The research questions are addressed in the sequels.

RQ1: How successful are AI developments in addressing railway infrastructure problems?

Chapter 2 provides a comprehensive review of the development of AI methodologies in railway infrastructure. Our review primarily focuses on publications dealing with four selected groups of railway infrastructures: track system, catenary system, civil structures, and track substructures. The review highlights significant advances in addressing various problems within railway infrastructure. Examples of AI applications include monitoring the health status of railway components, detecting defects and failures, and planning maintenance activities. However, the distribution of AI methodologies across different railway components is uneven. While some components deploy AI methodologies extensively, others have only a limited number of AI applications. Despite its success, several challenges specific to railway infrastructure hinder the direct application of state-of-the-art AI methodologies. These challenges include insufficient and imbalanced data for model training, the complexity of railway data, and resistance to change within the industry. Therefore, to successfully apply AI in railway infrastructure, it is essential to design and develop methodologies that address its unique and challenging characteristics.

RQ2: Can an SNN-based methodology improve the detection accuracy of rail squats, particularly light squats, based on ABA measurements?

Chapter 3 provides the answer to this question. This chapter presents a spiking neural network with time-varying weights using no hidden layers, along with a training methodology that incorporates genetic algorithms, k-fold cross-validation, and multi-start backpropagation. As shown by real-field measurements from Dutch and Swedish railways, this approach improves the learning of complex spatio-temporal patterns presented in squats based on ABA measurements from the traditional methods, which are 78-85% to more than 93%. Our approach outperforms neural network-based models such as SVM, ANN, and GRU, as they detect only 60-68% of squats. Moreover, our SNN model has a simpler architecture without hidden layers. This success is primarily attributed to the use of time-varying weights, which allow the SNN to produce time-encoded outputs that simulate the continuous scanning of ABA measurements. Compared to constant weights, these time-varying weights enhance the ability of the model to handle temporal sequences and dynamic behaviours by 8.57%, which are crucial for accurate rail

squat detection. Furthermore, The method can be used to provide interpretability. The spike responses, postsynaptic potentials, and membrane potentials have offered an explainable way to analyse the ABA signals. These internal spike behaviours highlight a correspondency with high frequency band between 1000-2000 Hz of the detection problem of squats and offer an ability to capture subtle changes in the responses. However, the performance of our SNN-based method can be impaired by data quality such as class imbalance and noise. Variations in environmental conditions, infrastructure layouts, and operational characteristics may reduce signal prominence, further impacting the effectiveness of our SNN-based approach.

RQ3: How can we effectively extract, in an unsupervised manner and from high-frequency moving vibration sensing, representations that characterise dynamic behaviours of rail infrastructures?

Chapter 4 addresses this question by presenting an unsupervised representation learning methodology to characterise the dynamic behaviours of rail infrastructures using high-frequency moving vibration sensors. This methodology synchronises empirical mode decomposition (EMD) levels with the parameters of a convolutional autoencoder (CAE) to extract meaningful representations. Testing the proposed methodology with ABA measurements from the Swedish rail network and LDV measurements from the Dutch rail network demonstrated its effectiveness in distinguishing between normal and abnormal samples. Despite the inherent fuzziness and disturbances in ABA and LDV data, the method achieved clear cluster separability with minimal overlaps. Our method correctly assigns 96% of normal samples and correctly assigns 41% of abnormal samples for ABA data, and it correctly assigns 47% of normal samples and correctly assigns 90% of abnormal samples for LDV data. Compared to other variants of autoencoder-based models and the wavelet-based CAE, it achieves an improvement of 16% for ABA data and 21% for LDV data. Additionally, the latent features obtained from this method proved informative. For ABA data, clusters of rail segments with similar characteristics help guide infrastructure managers in terms of defect locations. For LDV data, clusters of rail segments with similar characteristics facilitate learning trends and patterns in rail fastener health. The success of the proposed method underscores the importance of EMD in denoising, enhancing the representation learning of rail infrastructure characteristics, and reducing noise interference.

RQ4: How can a hybrid neural model exploit information from track geometry measurements, InSAR measurements, and ABA measurements to assess transition zone conditions with a more frequent evaluation?

Chapter 5 addresses this question by presenting a framework incorporating spatio-temporal interpolation with a hybrid neural model. A spatio-temporal interpolation approach is employed to fill in missing InSAR data. The framework considers two hybrid neural models: a convolutional neural network (CNN) combined with gated recurrent units (GRU) and a CNN combined with a long short-term memory (LSTM) network. These hybrid models exploit the spatial and temporal characteristics inherent in the fusion of historical and interpolated data from InSAR and ABA measurements. The CNN layers extract spatial features from

the high-frequency vibration data. In contrast, the GRU and LSTM layers capture temporal dependencies from the InSAR. We employ a hybrid model approach to predict track longitudinal levels, and it achieves an averaged RMSE of 0.0459 and R^2 of 0.7788. Compared to individual models such as CNN, GRU, and LSTM, this approach reduces RMSE from 0.0759 by an average of 39.53% and increases R^2 from 0.5564 by 39.97%. This dual capability is crucial for understanding the dynamic behaviours of rail infrastructures over time and space. Then, this dissertation utilises the predicted track longitudinal levels to define a new key performance index, namely $KPI_{InSAR+ABA}$, to assess transition zone conditions. With this $KPI_{InSAR+ABA}$ combining InSAR and ABA data, transition zone conditions can be assessed more frequently as InSAR can be obtained every 5 to 12 days, and ABA data can be collected in real-time or near-real-time. Testing the proposed framework using data from a railway bridge between Dordrecht and Lage Zwaluwe station in the Netherlands demonstrates its capability to predict track longitudinal levels during unobserved months accurately. This leads to a more accurate and frequent estimation of the KPI that can be used to detect track irregularities early, even before the next measurement of track geometry profiles. Therefore, the proposed framework enables continuous monitoring and regular assessment of transition zone health. Although the $KPI_{InSAR+ABA}$ is updated more frequently, its accuracy is influenced by the quality of the InSAR data collected, with noise levels exceeding 10%. However, as ABA technology advances and enables real-time or near-real-time data collection, the $KPI_{InSAR+ABA}$ is expected to improve significantly with more ABA signals. This will allow infrastructure managers to monitor conditions more effectively via a dashboard, integrating all available information to better quantify the level of defects with increased flexibility.

The answers to these research questions conclude the dissertation and address the key research question:

"How can AI be adopted so that maintenance in a large-scale railway infrastructure is improved?"

The answers to RQ1, RQ2, RQ3, and RQ4 demonstrate the significant potential of AI-driven methodologies in enhancing rail transport through advanced technological solutions. This potential illuminates pathways for future advancements and the development of sustainable railway systems. By detecting defects at their early stages and enhancing the accuracy and frequency of condition assessments through data fusion, the safety and reliability of railway infrastructures are significantly enhanced. Consequently, delays and disruptions are minimised due to more reliable infrastructure supported by condition-based maintenance procedures on a large scale. Automatic condition monitoring and early anomaly detection, such as rail surface defects, improve the effectiveness of maintenance activities, enabling operators to adjust their schedules based on real-time data, thus reducing maintenance and operational costs. Furthermore, unsupervised learning allows exploratory analysis of high-frequency vibration signals when prior knowledge or reference information about infrastructure conditions is unavailable or very limited. Therefore, the maintenance of large-scale railway infrastructure is improved.

6.2. RECOMMENDATIONS

Despite their success in addressing the challenges outlined in the conclusions, the developed AI methodologies have certain limitations that hinder their successful implementation in the railway industry. To overcome these challenges, the following recommendations for future research are proposed.

- For the detection of defects at their early stages, future research should focus on techniques that address the issue of imbalanced datasets and adapt SNNs to incorporate multiple measurements from various sources and data types to minimise false alarms. Transformer models, for example, can be considered to tackle insufficient and imbalanced railway data. The integration of the metaverse and the Internet of Things (IoT) can also alleviate issues related to imbalanced data, as the metaverse can generate a wide range of virtual scenarios to create a more balanced dataset using information from sensors and IoT devices that collect real-time data from instrumented railway infrastructure. Exploring fuzzy interval methods can explicitly capture uncertainties during the training process, improving the understanding of SNN-based classifier behaviour when dealing with railway data. Advancements in machine learning, signal processing, and railway engineering can further enhance rail defect detection techniques. For instance, deep learning models, such as convolutional neural networks (CNNs), can enable autonomous feature extraction, reducing reliance on expert knowledge and improving detection accuracy. Transfer learning techniques can help models adapt to new conditions by leveraging knowledge from different railway networks, allowing for defect detection in untested environments. Implementing advanced denoising algorithms can improve the signal-to-noise ratio, making it easier to identify and address issues in their early stages. Deploying high-frequency sensors like ABAs on operational trains can enable continuous monitoring of rail infrastructure, enhancing detection capabilities and predictive maintenance.

- For the unsupervised representation learning from high-frequency moving vibration sensors, future research should aim to improve cluster separability through advanced clustering techniques and hybrid approaches to better distinguish between normal and abnormal samples. Incorporating additional data sources and developing data fusion techniques can provide a comprehensive analysis, enhancing the accuracy and reliability of rail infrastructure condition assessments. Examining scalability and real-time processing capabilities is crucial for enabling real-time analysis of large-scale rail network data. Validating the methodology across different rail networks with varying environmental conditions and operational patterns is essential to ensure robustness and applicability.

- For the fusion of information from different monitoring technologies, future research should evaluate the generalisation and robustness of the proposed methodology and KPI based on InSAR and ABA data for assessing the health

of transition zones. This involves using a larger dataset containing diverse locations under varying transition zone conditions. Probabilistic models, such as fuzzy-interval methods and Bayesian networks, can be considered as predictive models to incorporate and quantify uncertainty in the data arising from diverse locations and conditions. The inclusion of physical variables and maintenance information in the predictions can also be considered via physics-informed machine learning to better capture the dynamic behaviour of transition zones. Given that ABA measurements depend on speed, developing methods to mitigate the impact of speed variations in measurements is needed to facilitate the broader application of the proposed framework.

Beyond the challenges presented in this dissertation, the maintenance of railway infrastructures is pitted with a vast array of challenges, as discussed in Chapter 2. Current maintenance and operational protocols, which rely on predefined rule sets, will need adjustments to effectively integrate AI-driven solutions. Proper integration of a new AI-based system into the current operating system requires smooth integration without interrupting the service. The following recommendations outline examples of how the railway industry can realistically integrate AI for enhanced engineering and maintenance processes:

- Tailored cybersecurity policies should be introduced to protect sensitive data generated from AI systems and onboard monitoring. Without effective cybersecurity, rail operators cannot ensure the security of critical data and information. Consequently, business resources cannot be consolidated, and data are scarce with limited access.
- A data standard is required to enable the available interactions between heterogeneous formats and systems. This is because data interoperability presents a major challenge in deploying AI-based solutions in the railway industry. Its problem is how to convert and integrate the data across diverse systems, e.g., the data coming from the APIs of different customers. Each API has its way of working. Having compatibility among software is thus critical to facilitate the use of AI.
- The impact of AI-based maintenance solutions should be regularly evaluated to ensure safety. For example, risk assessments should accompany each AI recommendation to provide engineers with a clear understanding of the potential impacts on infrastructure safety.
- All AI-based solutions and recommendations should be logged and timestamped. This allows operators to track the sequence of AI recommendations and actions taken. This will facilitate the accountability and transparency of AI.
- The railway industry should promote the new way of work. This could include training railway staff to understand and interpret AI-driven insights. Improving knowledge of AI models will help them evaluate the results more effectively, improving confidence in AI recommendations.

Researchers in both academia and industry can leverage the insights from this dissertation to identify trends and develop benchmarks tailored to the specific challenges of railway infrastructure. The technological advancements in AI discussed here can serve as a foundation for generating even more innovative applications and use cases within the railway sector. Alongside the excitement about integrating AI into railway infrastructure, it is crucial to also consider economic efficiency and feasibility. Therefore, a comprehensive redesign of inspection, monitoring, and maintenance procedures is necessary to align with these technological advancements.

DISCLAIMER

This research was partly supported by ProRail and Europe's Rail Flagship Project IAM4RAIL - Holistic and Integrated Asset Management for Europe's RAIL System under Grant Agreement No 101101966.
Funded by the European Union. Views and opinion expressed are however those of the author(s) only and do not necessarily reflect those of the European Union or Europe's Rail Joint Undertaking. Neither the European Union nor the granting authority can be held responsible for them. The project FP3-IAM4Rail is supported by the Europe's Rail Joint Undertaking and its members.

BIBLIOGRAPHY

[1] Z. Li. “13 - Squats on railway rails”. In: *Wheel–Rail Interface Handbook*. Ed. by R. Lewis and U. Olofsson. Woodhead Publishing, 2009, pp. 409–436.

[2] X. Zhao, Z. Li, and R. Dollevoet. “The vertical and the longitudinal dynamic responses of the vehicle–track system to squat-type short wavelength irregularity”. In: *Vehicle Mechanics and Mobility* 51 (2013), pp. 1918–1937.

[3] Z. Li, M. Molodova, A. Núñez, and R. Dollevoet. “Improvements in Axle Box Acceleration Measurements for the Detection of Light Squats in Railway Infrastructure”. In: *IEEE Transactions on Industrial Electronics* 62 (2015), pp. 4385–4397.

[4] M. Naeimi, Z. Li, Z. Qian, Y. Zhou, J. Wu, R. H. Petrov, J. Sietsma, and R. Dollevoet. “Reconstruction of the rolling contact fatigue cracks in rails using X-ray computed tomography”. In: *NDT E International* 92 (2017), pp. 199–212.

[5] Y. Muhamedsalih, S. Hawksbee, G. Tucker, J. Stow, and M. Burstow. “Squats on the Great Britain rail network: Possible root causes and research recommendations”. In: *Fatigue* 149 (2021), p. 106267.

[6] Y. Zuo, F. Thiery, P. Chandran, J. Odelius, and M. Rantatalo. “Squat Detection of Railway Switches and Crossings Using Wavelets and Isolation Forest”. In: *Sensors* 22 (2022).

[7] I. Aydin, E. Akin, and M. Karakose. “Defect classification based on deep features for railway tracks in sustainable transportation”. In: *Applied Soft Computing* 111 (2021), p. 107706.

[8] X. Sun, F. Yang, J. Shi, Z. Ke, and Y. Zhou. “On-Board Detection of Longitudinal Track Irregularity Via Axle Box Acceleration in HSR”. In: *IEEE Access* 9 (2021), pp. 14025–14037.

[9] Q. Sun, C. Chen, A. H. Kemp, and P. Brooks. “An on-board detection framework for polygon wear of railway wheel based on vibration acceleration of axle-box”. In: *Mechanical Systems and Signal Processing* 153 (2021). 107540.

[10] J. Ćetković, S. Lakić, P. Bogdanović, R. Vujadinović, and M. Žarković. “Assessing Environmental Benefits from Investment in Railway Infrastructure”. In: *Polish Journal of Environmental Studies* 29.3 (2020), pp. 2125–2137.

[11] X. Guo, W. Sun, S. Yao, and S. Zheng. “Does high-speed railway reduce air pollution along highways? – Evidence from China”. In: *Transportation Research Part D: Transport and Environment* 89 (2020). 102607.

[12] E. N. Martey and N. Attoh-Okine. “Analysis of train derailment severity using vine copula quantile regression modeling”. In: *Transportation Research Part C: Emerging Technologies* 105 (2019), pp. 485–503.

[13] Y. Chang, S. Lei, J. Teng, J. Zhang, L. Zhang, and X. Xu. “The energy use and environmental emissions of high-speed rail transportation in China: A bottom-up modeling”. In: *Energy* 182 (2019), pp. 1193–1201.

[14] F. Ghofrani, Q. He, R. Goverde, and X. Liu. “Recent applications of big data analytics in railway transportation systems: A survey”. In: *Transportation Research Part C: Emerging Technologies* 90 (2018), pp. 226–246.

[15] N. Bešinović, L. De Donato, F. Flammini, R. M. P. Goverde, Z. Lin, R. Liu, S. Marrone, R. Nardone, T. Tang, and V. Vittorini. “Artificial Intelligence in Railway Transport: Taxonomy, Regulations, and Applications”. In: *IEEE Transactions on Intelligent Transportation Systems* 23 (2022), pp. 14011–14024.

[16] R. Tang, L. De Donato, N. Besinovic, F. Flammini, R. M. P. Goverde, Z. Lin, R. Liu, T. Tang, V. Vittorini, and Z. Wang. “A literature review of Artificial Intelligence applications in railway systems”. In: *Transportation Research Part C-Emerging Technologies* 140 (2022). 103679.

[17] A. Peinado Gonzalo, R. Horridge, H. Steele, E. Stewart, and M. Entezami. “Review of Data Analytics for Condition Monitoring of Railway Track Geometry”. In: *IEEE Transactions on Intelligent Transportation Systems* 23 (2022), pp. 22737–22754.

[18] A. Núñez, A. Jamshidi, and H. Wang. “Pareto-Based Maintenance Decisions for Regional Railways With Uncertain Weld Conditions Using the Hilbert Spectrum of Axle Box Acceleration”. In: *IEEE Transactions on Industrial Informatics* 15.3 (2019), pp. 1496–1507.

[19] Z. Su, A. Jamshidi, A. Núñez, S. Baldi, and B. De Schutter. “Multi-level condition-based maintenance planning for railway infrastructures – A scenario-based chance-constrained approach”. In: *Transportation Research Part C: Emerging Technologies* 84 (2017), pp. 92–123.

[20] J. Zhang. “Application of remote monitoring and management of high-speed rail transportation based on ZigBee sensor network”. In: *Journal on Wireless Communications and Networking* 2019.1 (2019). 40.

[21] Z. A. Bukhsh, A. Saeed, I. Stipanovic, and A. G. Doree. “Predictive maintenance using tree-based classification techniques: A case of railway switches”. In: *Transportation Research Part C: Emerging Technologies* 101 (2019), pp. 35–54.

[22] H. Khajehei, A. Ahmadi, I. Soleimanmeigouni, and A. Nissen. “Allocation of effective maintenance limit for railway track geometry”. In: *Structure and Infrastructure Engineering* 15.12 (2019), pp. 1597–1612.

[23] V. Sangiorgio, A. M. Mangini, and I. Precchiazzi. “A new index to evaluate the safety performance level of railway transportation systems”. In: *Safety Science* 131 (2020). 104921.

[24] Y. Long, W. Guo, N. Yang, C. Dong, M. Liu, Y. Cai, and Z. Zhang. “Research progress of intelligent operation and maintenance of high-speed railway bridges”. In: *Intelligent Transportation Infrastructure* 1 (2022). liac015.

[25] P. McMahon, T. Zhang, and R. Dwight. “Requirements for Big Data Adoption for Railway Asset Management”. In: *IEEE Access* 8 (2020), pp. 15543–15564.

[26] J. C. Cheng, W. Chen, K. Chen, and Q. Wang. “Data-driven predictive maintenance planning framework for MEP components based on BIM and IoT using machine learning algorithms”. In: *Automation in Construction* 112 (2020). 103087.

[27] O. Pokusaev, A. Klimov, V. Kupriyanovsky, P. Morhat, and D. Namiot. “Europe’s digital railway-from ERTMS to artificial intelligence”. In: *International Journal of Open Information Technologies* 7.7 (2019), pp. 90–119.

[28] B. Arslan and H. Tiryaki. “Prediction of railway switch point failures by artificial intelligence methods”. In: *Turkish Journal of Electrical Engineering and Computer Sciences* 28.2 (2020), pp. 1044–1058.

[29] D. Tokody and F. Flammini. “The intelligent railway system theory”. In: *International Transportation* 69 (2017), pp. 38–40.

[30] H. E. Johnson Jr. and P. P. Bonissone. “EXPERT SYSTEM FOR DIESEL ELECTRIC LOCOMOTIVE REPAIR”. In: *Journal of Forth Application and Research* 1.1 (1983), pp. 7–16.

[31] J. C. Hoag. “EXPERT SYSTEM FOR FINDING THE CAUSES OF TRAIN DERAILMENTS”. In: *IEEE 1985 Proceedings of the International Conference on Cybernetics and Society, Tucson, Arizona* (1985), pp. 12–15.

[32] J. F. Gilmore, K. J. Elibiary, and R. J. Peterson. “A neural network system for traffic flow management”. In: *Proceedings of SPIE - The International Society for Optical Engineering* 1709 (1992), pp. 558–571.

[33] P. McKenzie and M. Alder. “Syntactic pattern recognition by quadratic neural nets. A case study: Rail flaw classification”. In: *Proceedings of the International Conference on Neural Networks (IJCNN-93-Nagoya, Japan* 3 (1993), pp. 2101–2104.

[34] J. Schmidhuber. “Deep Learning in neural networks: An overview”. In: *Neural Networks* 61 (2015), pp. 85–117.

[35] L. Alzubaidi, J. Zhang, A. J. Humaidi, A. Al-Dujaili, Y. Duan, O. Al-Shamma, J. Santamaría, M. A. Fadhel, M. Al-Amidie, and L. Farhan. “Review of deep learning: concepts, CNN architectures, challenges, applications, future directions”. In: *Journal of Big Data* 8.1 (2021). 53.

[36] S. Abadal, A. Jain, R. Guirado, J. López-Alonso, and E. Alarcón. “Computing Graph Neural Networks: A Survey from Algorithms to Accelerators”. In: *ACM Computing Surveys* 54.9 (2021). 191, pp. 1–38.

[37] A. Telikani, A. Tahmassebi, W. Banzhaf, and A. H. Gandomi. “Evolutionary Machine Learning: A Survey”. In: *ACM Computing Surveys* 54.8 (2021). 161, pp. 1–35.

[38] Y. Han, G. Huang, S. Song, L. Yang, H. Wang, and Y. Wang. “Dynamic Neural Networks: A Survey”. In: *IEEE Transactions on Pattern Analysis and Machine Intelligence* 44 (2022), pp. 7436–7456.

[39] A. Jamshidi, S. Hajizadeh, Z. Su, M. Naeimi, A. Núñez, R. Dollevoet, B. De Schutter, and Z. Li. “A decision support approach for condition-based maintenance of rails based on big data analysis”. In: *Transportation Research Part C: Emerging Technologies* 95 (2018), pp. 185–206.

[40] G. Kang, S. Gao, L. Yu, and D. Zhang. “Deep Architecture for High-Speed Railway Insulator Surface Defect Detection: Denoising Autoencoder With Multitask Learning”. In: *IEEE Transactions on Instrumentation and Measurement* 68.8 (2019), pp. 2679–2690.

[41] J. Zhong, Z. Liu, Z. Han, Y. Han, and W. Zhang. “A CNN-Based Defect Inspection Method for Catenary Split Pins in High-Speed Railway”. In: *IEEE Transactions on Instrumentation and Measurement* 68.8 (2019), pp. 2849–2860.

[42] X. Gibert, V. Patel, and R. Chellappa. “Deep Multitask Learning for Railway Track Inspection”. In: *IEEE Transactions on Intelligent Transportation Systems* 18.1 (2017). 7506117, pp. 153–164.

[43] L. Oukhellou, A. Debiolles, T. Denœux, and P. Aknin. “Fault diagnosis in railway track circuits using Dempster-Shafer classifier fusion”. In: *Engineering Applications of Artificial Intelligence* 23.1 (2010), pp. 117–128.

[44] H. Zhang, J. Yang, W. Tao, and H. Zhao. “Vision method of inspecting missing fastening components in high-speed railway”. In: *Applied Optics* 50.20 (2011), pp. 3658–3665.

[45] H. Guler. “Prediction of railway track geometry deterioration using artificial neural networks: A case study for Turkish state railways”. In: *Structure and Infrastructure Engineering* 10.5 (2014), pp. 614–626.

[46] P. Galvín, D. Mendoza, D. Connolly, G. Degrande, G. Lombaert, and A. Romero. “Scoping assessment of free-field vibrations due to railway traffic”. In: *Soil Dynamics and Earthquake Engineering* 114 (2018), pp. 598–614.

[47] J. Chen, Z. Liu, H. Wang, A. Nunez, and Z. Han. “Automatic defect detection of fasteners on the catenary support device using deep convolutional neural network”. In: *IEEE Transactions on Instrumentation and Measurement* 67 (2018), pp. 257–269.

[48] A. C. Adoko, Y. Y. Jiao, L. Wu, H. Wang, and Z. H. Wang. “Predicting tunnel convergence using Multivariate Adaptive Regression Spline and Artificial Neural Network”. In: *Tunnelling and Underground Space Technology* 38 (2013), pp. 368–376.

[49] O. Fink, E. Zio, and U. Weidmann. “Predicting component reliability and level of degradation with complex-valued neural networks”. In: *Reliability Engineering and System Safety* 121 (2014), pp. 198–206.

[50] J. Shu, Z. Zhang, I. Gonzalez, and R. Karoumi. “The application of a damage detection method using Artificial Neural Network and train-induced vibrations on a simplified railway bridge model”. In: *Engineering Structures* 52 (2013), pp. 408–421.

[51] G. Krummenacher, C. S. Ong, S. Koller, S. Kobayashi, and J. M. Buhmann. “Wheel Defect Detection With Machine Learning”. In: *IEEE Transactions on Intelligent Transportation Systems* 19.4 (2018), pp. 1176–1187.

[52] J. Hegde and B. Rokseth. “Applications of machine learning methods for engineering risk assessment – A review”. In: *Safety Science* 122 (2020). 104492.

[53] K.-R. Müller, S. Mika, G. Rätsch, K. Tsuda, and B. Schölkopf. “An introduction to kernel-based learning algorithms”. In: *IEEE Transactions on Neural Networks* 12.2 (2001), pp. 181–201.

[54] A. J. Smola and B. Schölkopf. “A tutorial on support vector regression”. In: *Statistics and Computing* 14.3 (2004), pp. 199–222.

[55] J. Wang, X.-Z. Liu, and Y.-Q. Ni. “A Bayesian Probabilistic Approach for Acoustic Emission-Based Rail Condition Assessment”. In: *Computer-Aided Civil and Infrastructure Engineering* 1 (2018), pp. 21–34.

[56] I. Cárdenas-Gallo, C. Sarmiento, G. Morales, M. Bolivar, and R. Akhavan-Tabatabaei. “An ensemble classifier to predict track geometry degradation”. In: *Reliability Engineering and System Safety* (2017), pp. 53–60.

[57] C. Chen, T. Xu, G. Wang, and B. Li. “Railway turnout system RUL prediction based on feature fusion and genetic programming”. In: *Measurement* 151 (2020). 107162.

[58] M. Sysyn, U. Gerber, O. Nabochenko, Y. Li, and V. Kovalchuk. “Indicators for common crossing structural health monitoring with track-side inertial measurements”. In: *Acta Polytechnica* 52.2 (2019), pp. 170–181.

[59] S. Eftekhar Azam, A. Rageh, and D. Linzell. “Damage detection in structural systems utilizing artificial neural networks and proper orthogonal decomposition”. In: *Structural Control and Health Monitoring* 26.2 (2019). e2288.

[60] D. Yazdani, R. Cheng, D. Yazdani, J. Branke, Y. Jin, and X. Yao. “A Survey of Evolutionary Continuous Dynamic Optimization Over Two Decades—Part A”. In: *IEEE Transactions on Evolutionary Computation* 25.4 (2021), pp. 609–629.

[61] D. Yazdani, R. Cheng, D. Yazdani, J. Branke, Y. Jin, and X. Yao. “A Survey of Evolutionary Continuous Dynamic Optimization Over Two Decades—Part B”. In: *IEEE Transactions on Evolutionary Computation* 25.4 (2021), pp. 630–650.

[62] C. He, Y. Zhang, D. Gong, and X. Ji. “A review of surrogate-assisted evolutionary algorithms for expensive optimization problems”. In: *Expert Systems with Applications* 217.1 (2023). 119495.

[63] H. Tran-Ngoc, S. Khatir, G. De Roeck, T. Bui-Tien, L. Nguyen-Ngoc, and M. Abdel Wahab. “Model updating for Nam O bridge using particle swarm optimization algorithm and genetic algorithm”. In: *Sensors* 18.12 (2018). 4131.

[64] L. Sgambi, K. Gkoumas, and F. Bontempi. “Genetic Algorithms for the Dependability Assurance in the Design of a Long-Span Suspension Bridge”. In: *Computer-Aided Civil and Infrastructure Engineering* 27.9 (2012), pp. 655–675.

[65] D. Ribeiro, R. Calçada, R. Delgado, M. Brehm, and V. Zabel. “Finite element model updating of a bowstring-arch railway bridge based on experimental modal parameters”. In: *Engineering Structures* 40 (2012), pp. 413–435.

[66] S. Qin, Y. Zhang, Y.-L. Zhou, and J. Kang. “Dynamic model updating for bridge structures using the kriging model and PSO algorithm ensemble with higher vibration modes”. In: *Sensors* 18.6 (2018). 1879.

[67] C. Costa, D. Ribeiro, P. Jorge, R. Silva, A. Arêde, and R. Calçada. “Calibration of the numerical model of a stone masonry railway bridge based on experimentally identified modal parameters”. In: *Engineering Structures* 123 (2016), pp. 354–371.

[68] T. Zhang, J. Andrews, and R. Wang. “Optimal scheduling of track maintenance on a railway network”. In: *Quality and Reliability Engineering International* 29.2 (2013), pp. 285–297.

[69] C. Shen, R. Dollevoet, and Z. Li. “Fast and robust identification of railway track stiffness from simple field measurement”. In: *Mechanical Systems and Signal Processing* 152 (2021). 107431.

[70] L. F. Caetano and P. F. Teixeira. “Availability Approach to Optimizing Railway Track Renewal Operations”. In: *Journal of Transportation Engineering* 139.9 (2013), pp. 941–948.

[71] H. Y. Choi, D. H. Lee, and J. Lee. “Optimization of a railway wheel profile to minimize flange wear and surface fatigue”. In: *Wear* 300.1 (2013), pp. 225–233.

[72] I. Persson, R. Nilsson, U. Bik, M. Lundgren, and S. Iwnicki. “Use of a genetic algorithm to improve the rail profile on Stockholm underground”. In: *Vehicle System Dynamics* 48.1 (2010), pp. 89–104.

[73] W. Li, H. Pu, P. Schonfeld, J. Yang, H. Zhang, L. Wang, and J. Xiong. “Mountain Railway Alignment Optimization with Bidirectional Distance Transform and Genetic Algorithm”. In: *Computer-Aided Civil and Infrastructure Engineering* 32.8 (2017), pp. 691–709.

[74] J. H. Lee, Y. G. Kim, J. S. Paik, and T. W. Park. “Performance evaluation and design optimization using differential evolutionary algorithm of the pantograph for the high-speed train”. In: *Journal of Mechanical Science and Technology* 26.10 (2012), pp. 3253–3260.

[75] C. Sanchez-Rebollo, J. R. Jimenez-Octavio, and A. Carnicero. “Active control strategy on a catenary–pantograph validated model”. In: *Vehicle System Dynamics* 51.4 (2013), pp. 554–569.

[76] M. F. Gorman and J. J. Kanet. “Formulation and Solution Approaches to the Rail Maintenance Production Gang Scheduling Problem”. In: *Journal of Transportation Engineering* 136.8 (2010), pp. 701–708.

[77] M. Simarro, S. Postigo, M. Prado-Novoa, A. Pérez-Blanca, and J. Castillo. “Analysis of contact forces between the pantograph and the overhead conductor rail using a validated finite element model”. In: *Engineering Structures* 225 (2020). 111265.

[78] C. Chellaswamy, M. Krishnasamy, L. Balaji, A. Dhanalakshmi, and R. Ramesh. “Optimized railway track health monitoring system based on dynamic differential evolution algorithm”. In: *Measurement* 152 (2020). 107332.

[79] A. Bardhan, N. Kardani, A. K. Alzo’ubi, B. Roy, P. Samui, and A. H. Gandomi. “Novel integration of extreme learning machine and improved Harris hawks optimization with particle swarm optimization-based mutation for predicting soil consolidation parameter”. In: *Journal of Rock Mechanics and Geotechnical Engineering* 14.5 (2022), pp. 1588–1608.

[80] T. Dahoe. “Estimation of Railway Track Parameters Using Evolutionary Algorithms (Bachelor thesis, TU Delft Civil Engineering and Geosciences)”. In: *Retrieved from http://resolver.tudelft.nl/uuid:9b0154eb-ccbe-4b5e-9985-f7a9212e8d89* (2021).

[81] V. S. Tseng, J. Jia-Ching Ying, S. T. C. Wong, D. J. Cook, and J. Liu. “Computational Intelligence Techniques for Combating COVID-19: A Survey”. In: *IEEE Computational Intelligence Magazine* 15.4 (2020), pp. 10–22.

[82] Y. Lei, B. Yang, X. Jiang, F. Jia, N. Li, and A. K. Nandi. “Applications of machine learning to machine fault diagnosis: A review and roadmap”. In: *Mechanical Systems and Signal Processing* 138 (2020). 106587.

[83] J. Mena, O. Pujol, and J. Vitrià. “A Survey on Uncertainty Estimation in Deep Learning Classification Systems from a Bayesian Perspective”. In: *ACM Computing Surveys* 54.9 (2022). 193, pp. 1–35.

[84] B. Shahriari, K. Swersky, Z. Wang, R. P. Adams, and N. De Freitas. “Taking the human out of the loop: A review of Bayesian optimization”. In: *Proceedings of the IEEE* 104 (2016), pp. 148–175.

[85] M. Rafiq, M. Chryssanthopoulos, and S. Sathananthan. “Bridge condition modelling and prediction using dynamic Bayesian belief networks”. In: *Structure and Infrastructure Engineering* 11.1 (2015), pp. 38–50.

[86] I. Gonzales, M. Ülker-Kaustell, and R. Karoumi. “Seasonal effects on the stiffness properties of a ballasted railway bridge”. In: *Engineering Structures* 57 (2013), pp. 63–72.

[87] A. Neves, I. González, J. Leander, and R. Karoumi. “Structural health monitoring of bridges: A model-free ANN-based approach to damage detection”. In: *Journal of Civil Structural Health Monitoring* 7.5 (2017), pp. 689–702.

[88] Z. Liu, L. Wang, C. Li, and Z. Han. “A High-Precision Loose Strands Diagnosis Approach for Isoelectric Line in High-Speed Railway”. In: *IEEE Transactions on Industrial Informatics* 14.3 (2018), pp. 1067–1077.

[89] G. Wang, T. Xu, T. Tang, T. Yuan, and H. Wang. “A Bayesian network model for prediction of weather-related failures in railway turnout systems”. In: *Expert Systems With Applications* 69 (2017), pp. 247–256.

[90] S. Dindar, S. Kaewunruen, M. An, and J. Sussman. “Bayesian Network-based probability analysis of train derailments caused by various extreme weather patterns on railway turnouts”. In: *Safety Science* 110 (2018), pp. 20–30.

[91] A. Andrade and P. Teixeira. “Statistical modelling of railway track geometry degradation using Hierarchical Bayesian models”. In: *Reliability Engineering and System Safety* 142 (2015), pp. 169–183.

[92] J. M. Mendel. “Type-2 fuzzy sets and systems: An overview”. In: *IEEE Computational Intelligence Magazine* 2.1 (2007), pp. 20–29.

[93] Z. A. Sosnowski and L. Gadomer. “Fuzzy trees and forests—Review”. In: *Wiley Interdisciplinary Reviews: Data Mining and Knowledge Discovery* 9.3 (2019). e1316.

[94] R. Das, S. Sen, and U. Maulik. “A Survey on Fuzzy Deep Neural Networks”. In: *ACM Computing Surveys* 53.3 (2020). 54, pp. 1–25.

[95] R. Kumar, J. Khepar, K. Yadav, E. Kareri, S. D. Alotaibi, W. Viriyasitavat, K. Gulati, K. Kotecha, and G. Dhiman. “A Systematic Review on Generalized Fuzzy Numbers and Its Applications: Past, Present and Future”. In: *Archives of Computational Methods in Engineering* 29 (2022), pp. 5213–5236.

[96] J. García, J. Ureña, Á. Hernández, M. Mazo, J. Jiménez, F. Álvarez, C. De Marziani, A. Jiménez, M. Díaz, C. Losada, and E. García. “Efficient multisensory barrier for obstacle detection on railways”. In: *IEEE Transactions on Intelligent Transportation Systems* 11.3 (2010), pp. 702–713.

[97] A. Jamshidi, A. Núñez, R. Dollevoet, and Z. Li. “Robust and predictive fuzzy key performance indicators for condition-based treatment of squats in railway infrastructures”. In: *Journal of Infrastructure Systems* 23.3 (2017). 04017006.

[98] M. Metin and R. Guclu. “Active vibration control with comparative algorithms of half rail vehicle model under various track irregularities”. In: *Journal of Vibration and Control* 17.10 (2011), pp. 1525–1539.

[99] I. Hussain, T. Mei, and R. Ritchings. “Estimation of wheel-rail contact conditions and adhesion using the multiple model approach”. In: *International Journal of Vehicle Mechanics and Mobility* 51.1 (2013), pp. 32–53.

[100] L. Li, T. Lei, S. Li, Z. Xu, Y. Xue, and S. Shi. “Dynamic risk assessment of water inrush in tunnelling and software development”. In: *Geomechanics and Engineering* 9.1 (2015), pp. 57–81.

[101] L. Yi, J. Zhao, W. Yu, G. Long, H. Sun, and W. Li. “Health Status Evaluation of Catenary Based on Normal Fuzzy Matter-Element and Game Theory”. In: *Journal of Electrical Engineering and Technology* 15 (2020), pp. 2373–2385.

[102] M. Karakose and O. Yaman. “Complex Fuzzy System Based Predictive Maintenance Approach in Railways”. In: *IEEE Transactions on Industrial Informatics* 16.9 (2020). 8993841, pp. 6023–6032.

[103] E. Karakose, M. Gencoglu, M. Karakose, O. Yaman, I. Aydin, and E. Akin. “A new arc detection method based on fuzzy logic using S-transform for pantograph–catenary systems”. In: *Journal of Intelligent Manufacturing* 29.4 (2018), pp. 839–856.

[104] I. Aydin, S. Celebi, S. Barmada, and M. Tucci. “Fuzzy integral-based multi-sensor fusion for arc detection in the pantograph-catenary system”. In: *Proceedings of the Institution of Mechanical Engineers, Part F: Journal of Rail and Rapid Transit* 232 (2018), pp. 159–170.

[105] I. Aydin, M. Karakose, and E. Akin. “Anomaly detection using a modified kernel-based tracking in the pantograph-catenary system”. In: *Expert Systems with Applications* 42 (2015), pp. 938–948.

[106] R. Xu and D. Wunsch II. “Survey of clustering algorithms”. In: *IEEE Transactions on Neural Networks* 16.3 (2005), pp. 645–678.

[107] P. D. McNicholas. “Model-Based Clustering”. In: *Journal of Classification* 33.3 (2016), pp. 331–373.

[108] W. Qu, X. Xiu, H. Chen, and L. Kong. “A Survey on High-Dimensional Subspace Clustering”. In: *Mathematics* 11.2 (2023). 436.

[109] R. Cardoso, A. Cury, and F. Barbosa. “A robust methodology for modal parameters estimation applied to SHM”. In: *Mechanical Systems and Signal Processing* 95 (2017), pp. 24–41.

[110] A. Cury, C. Cremona, and E. Diday. “Application of symbolic data analysis for structural modification assessment”. In: *Engineering Structures* 32.03 (2010), pp. 762–775.

[111] G. Ćirović and D. Pamučar. “Decision support model for prioritizing railway level crossings for safety improvements: Application of the adaptive neuro-fuzzy system”. In: *Expert Systems with Applications* 40.6 (2013), pp. 2208–2223.

[112] F. Peng and Y. Ouyang. “Optimal Clustering of Railroad Track Maintenance Jobs”. In: *Computer-Aided Civil and Infrastructure Engineering* 29.4 (2014), pp. 235–247.

[113] F. Zhuang, Z. Qi, K. Duan, D. Xi, Y. Zhu, H. Zhu, H. Xiong, and Q. He. “A Comprehensive Survey on Transfer Learning”. In: *Proceedings of the IEEE* 109 (2021), pp. 43–76.

[114] W. M. Kouw and M. Loog. “A Review of Domain Adaptation without Target Labels”. In: *IEEE Transactions on Pattern Analysis and Machine Intelligence* 43 (2021), pp. 766–785.

[115] J. Zhong, Z. Liu, C. Yang, H. Wang, S. Gao, and A. Núñez. “Adversarial Reconstruction Based on Tighter Oriented Localization for Catenary Insulator Defect Detection in High-Speed Railways”. In: *IEEE Transactions on Intelligent Transportation Systems* 23.2 (2022), pp. 1109–1120.

[116] S. X. Chen, L. Zhou, Y. Q. Ni, and X. Z. Liu. “An acoustic-homologous transfer learning approach for acoustic emission–based rail condition evaluation”. In: *Structural Health Monitoring* 20.4 (2021), pp. 2161–2181.

[117] D. Yao, Q. Sun, J. Yang, H. Liu, and J. Zhang. “Railway Fastener Fault Diagnosis Based on Generative Adversarial Network and Residual Network Model”. In: *Shock and Vibration* 2020 (2020). 8823050.

[118] L. Zhuang, L. Wang, Z. Zhang, and K. Tsui. “Automated vision inspection of rail surface cracks: A double-layer data-driven framework”. In: *Transportation Research Part C: Emerging Technologies* 92 (2018), pp. 258–277.

[119] S. Lin, Q. Yu, Z. Wang, D. Feng, and S. Gao. “A fault prediction method for catenary of high-speed rails based on meteorological conditions”. In: *Journal of Modern Transportation* 27.3 (2019), pp. 211–221.

[120] L. Chen, W. Chen, L. Wang, C. Zhai, X. Hu, L. Sun, Y. Tian, X. Huang, and L. Jiang. “Convolutional neural networks (CNNs)-based multi-category damage detection and recognition of high-speed rail (HSR) reinforced concrete (RC) bridges using test images”. In: *Engineering Structures* 276 (2023). 115306.

[121] D. Zhang, M. Xie, J. Yang, and T. Wen. “Multi-Sensor Graph Transfer Network for Health Assessment of High-Speed Rail Suspension Systems”. In: *IEEE Transactions on Intelligent Transportation Systems* (2023), pp. 1–10.

[122] E. Hovad, H. Hansen, A. F. da Silva Rodrigues, and V. A. Dahl. *Automatic Detection of Rail Defects from Images*. In: Intelligent Quality Assessment of Railway Switches and Crossings. Springer Series in Reliability Engineering. Springer, 2021, pp. 187–205.

[123] Q. Zhou. “A Detection System for Rail Defects Based on Machine Vision”. In: *IOP Conference Series: Physics* 1748.2 (2021). 022012.

[124] X. Ni, H. Liu, Z. Ma, C. Wang, and J. Liu. “Detection for Rail Surface Defects via Partitioned Edge Feature”. In: *IEEE Transactions on Intelligent Transportation Systems* 23.6 (2022), pp. 5806–5822.

[125] D. Pham, M. Ha, and C. Xiao. “A novel visual inspection system for rail surface spalling detection”. In: *IOP Conference Series: Materials Science and Engineering* 1048 (2021). 012015.

[126] P. Dai, X. Du, S. Wang, Z. Gu, and Y. Ma. “Rail fastener automatic recognition method in complex background”. In: *Tenth International Conference on Digital Image Processing (ICDIP 2018)*. Aug. 2018, p. 314.

[127] M. Guerrieri, G. Parla, and C. Celauro. “Digital image analysis technique for measuring railway track defects and ballast gradation”. In: *Measurement* 113 (2018), pp. 137–147.

[128] A. Sabato and C. Niezrecki. “Feasibility of digital image correlation for railroad tie inspection and ballast support assessment”. In: *Measurement* 103 (2017), pp. 93–105.

[129] S. A. H. Tabatabaei, A. Delforouzi, M. H. Khan, T. Wesener, and M. Grzegorzek. “Automatic Detection of the Cracks on the Concrete Railway Sleepers”. In: *International Journal of Pattern Recognition and Artificial Intelligence* 33.9 (2019). 1955010.

[130] A. S. Franca and R. F. Vassallo. “A method of classifying railway sleepers and surface defects in real environment”. In: *IEEE Sensors Journal* 21.10 (2021), pp. 11301–11309.

[131] V. Skrickij, E. Šabanovič, D. Shi, S. Ricci, L. Rizzetto, and G. Bureika. “Visual Measurement System for Wheel–Rail Lateral Position Evaluation”. In: *Sensors* 21.4 (2021). 1297.

[132] W. Phusakulkajorn, A. Núñez, H. Wang, A. Jamshidi, A. Zoeteman, B. Ripke, R. Dollevoet, B. D. Schutter, and Z. Li. “Artificial Intelligence in Railway Infrastructure: Current Research, Challenges, and Future Opportunities”. In: *Intelligent Transportation Infrastructure* liad016 (2023), pp. 1–24.

[133] W. Phusakulkajorn, J. M. Hendriks, J. Moraal, R. P. B. J. Dollevoet, Z. Li, and A. Nunez. “A multiple spiking neural network architecture based on fuzzy intervals for anomaly detection: a case study of rail defects”. In: *IEEE International Conference on Fuzzy Systems (FUZZ-IEEE)* 2022 (2022), p. 1292.

[134] M. Molodova, Z. Li, A. Núñez, and R. Dollevoet. “Automatic Detection of Squats in Railway Infrastructure”. In: *IEEE Transactions on Intelligent Transportation Systems* 15 (2014), pp. 1980–1990.

[135] S. X. Chen, Y. Q. Ni, and L. Zhou. “A deep learning framework for adaptive compressive sensing of high-speed train vibration responses”. In: *Structural Control and Health Monitoring* 29.8 (2022), e2979.

[136] P. Xu, R. Liu, Q. Sun, and L. Jiang. “Dynamic-Time-Warping-Based Measurement Data Alignment Model for Condition-Based Railroad Track Maintenance”. In: *IEEE Transactions on Intelligent Transportation Systems* 16.2 (2015), pp. 799–812.

[137] G. Ashley and N. Attoh-Okine. “Approximate Bayesian computation for railway track geometry parameter estimation”. In: *Proceedings of the Institution of Mechanical Engineers, Part F: Journal of Rail and Rapid Transit* 235.8 (2021), pp. 1013–1021.

[138] Y. K. Luo, S. X. Chen, L. Zhou, and Y. Q. Ni. “Evaluating railway noise sources using distributed microphone array and graph neural networks”. In: *Transportation Research Part D: Transport and Environment* 107 (2022). 103315.

[139] A. Lasisi and N. Attoh-Okine. “Machine Learning Ensembles and Rail Defects Prediction: Multilayer Stacking Methodology”. In: *ASCE-ASME Journal of Risk and Uncertainty in Engineering Systems, Part A: Civil Engineering* 5.4 (2019). 04019016.

[140] K. Aboudolas, M. Papageorgiou, A. Kouvelas, and E. Kosmatopoulos. “A rolling-horizon quadratic-programming approach to the signal control problem in large-scale congested urban road networks”. In: *Transportation Research Part C: Emerging Technologies* 18 (2010), pp. 680–694.

[141] D. Peralta, C. Bergmeir, M. Krone, M. Galende, M. Menéndez, G. I. Sainz-Palmero, C. M. Bertrand, F. Klawonn, and J. M. Benitez. “Multiobjective Optimization for Railway Maintenance Plans”. In: *Computing in Civil Engineering* 32 (2018). 04018014.

[142] Z. Liu, Y. Song, Y. Han, H. Wang, J. Zhang, and Z. Han. “Advances of research on high-speed railway catenary”. In: *Journal of Modern Transportation* 26 (2018).

[143] H. Wang, A. Núñez, Z. Liu, D. Zhang, and R. Dollevoet. “A Bayesian Network Approach for Condition Monitoring of High-Speed Railway Catenaries”. In: *IEEE Transactions on Intelligent Transportation Systems* 21 (2020), pp. 4037–4051.

[144] W. Liu, Z. Liu, A. Núñez, and Z. Han. “Unified Deep Learning Architecture for the Detection of All Catenary Support Components”. In: *IEEE Access* 8 (2020). 8963687, pp. 17049–17059.

[145] F. Duan, Z. Liu, D. Zhai, and A. Rønnquist. “A Siamese network-based non-contact measurement method for railway catenary uplift trained in a free vibration test”. In: *Sensors* 20.14 (2020). 3984, pp. 1–17.

[146] S. Lin, C. Xu, L. Chen, S. Li, and X. Tu. “LiDAR point cloud recognition of overhead catenary system with deep learning”. In: *Sensors* 20 (2020). 2212.

[147] X. Wei, S. Jiang, Y. Li, C. Li, L. Jia, and Y. Li. “Defect detection of pantograph slide based on deep learning and image processing technology”. In: *IEEE Transactions on Intelligent Transportation Systems* 21.3 (2020), pp. 947–958.

[148] Y. Luo, Q. Yang, and S. Liu. “Novel Vision-Based Abnormal Behavior Localization of Pantograph-Catenary for High-Speed Trains”. In: *IEEE Access* 7 (2019). 8913549, pp. 180935–180946.

[149] Z. Liu, Y. Lyu, L. Wang, and Z. Han. “Detection approach based on an improved faster RCNN for brace sleeve screws in high-speed railways”. In: *IEEE Transactions on Instrumentation and Measurement* 69.7 (2020). 8836624, pp. 4395–4403.

[150] Y. Lyu, Z. Han, J. Zhong, C. Li, and Z. Liu. “A Generic Anomaly Detection of Catenary Support Components Based on Generative Adversarial Networks”. In: *IEEE Transactions on Instrumentation and Measurement* 69.5 (2020), pp. 2439–2448.

[151] S. Huang, Y. Zhai, M. Zhang, and X. Hou. “Arc detection and recognition in pantograph–catenary system based on convolutional neural network”. In: *Information Sciences* 501 (2019), pp. 363–376.

[152] W. Liu, Z. Liu, H. Wang, and Z. Han. “An Automated Defect Detection Approach for Catenary Rod-Insulator Textured Surfaces Using Unsupervised Learning”. In: *IEEE Transactions on Instrumentation and Measurement* 69 (2020), pp. 8411–8423.

[153] Z. Liu, K. Liu, J. Zhong, Z. Han, and W. Zhang. “A High-Precision Positioning Approach for Catenary Support Components with Multiscale Difference”. In: *IEEE Transactions on Instrumentation and Measurement* 69.3 (2020), pp. 700–711.

[154] Z. Qu, S. Yuan, R. Chi, L. Chang, and L. Zhao. “Genetic optimization method of pantograph and catenary comprehensive monitor status prediction model based on adadelta deep neural network”. In: *IEEE Access* 7 (2019). 8641278, pp. 23210–23221.

[155] M. Raissi, P. Perdikaris, and G. E. Karniadakis. “Physics-informed neural networks: A deep learning framework for solving forward and inverse problems involving nonlinear partial differential equations”. In: *Journal of Computational physics* 378 (2019), pp. 686–707.

[156] T. Kapoor, H. Wang, A. Núñez, and R. Dollevoet. “Physics-informed neural networks for solving forward and inverse problems in complex beam systems”. In: *arXiv preprint arXiv:2303.01055* (2023).

[157] Y. W. Wang, Y. Q. Ni, and S. M. Wang. “Structural health monitoring of railway bridges using innovative sensing technologies and machine learning algorithms: a concise review”. In: *Intelligent Transportation Infrastructure* 1 (2022). liac009, pp. 1–11.

[158] G. Michau and O. Fink. “Unsupervised transfer learning for anomaly detection: Application to complementary operating condition transfer”. In: *Knowledge-Based Systems* 216 (2021). 106816, pp. 1–9.

[159] Q. Wang, G. Michau, and O. Fink. “Domain adaptive transfer learning for fault diagnosis”. In: *In: 2019 Prognostics and System Health Management Conference* (2019).

[160] S. X. Chen, L. Zhou, and Y. Q. Ni. “Wheel condition assessment of high-speed trains under various operational conditions using semi-supervised adversarial domain adaptation”. In: *Mechanical Systems and Signal Processing* 170 (2022). 108853.

[161] V. Mnih, K. Kavukcuoglu, D. Silver, A. A. Rusu, J. Veness, M. G. Bellemare, A. Graves, M. Riedmiller, A. K. Fidjeland, G. Ostrovski, S. Petersen, C. Beattie, A. Sadik, I. Antonoglou, H. King, D. Kumaran, D. Wierstra, S. Legg, and D. Hassabis. “Human-level control through deep reinforcement learning”. In: *Nature* 518 (2015), pp. 529–533.

[162] J. Zhong, Z. Liu, H. Wang, W. Liu, C. Yang, Z. Han, and A. Núñez. “A looseness detection method for railway catenary fasteners based on reinforcement learning refined localization”. In: *IEEE Transactions on Instrumentation and Measurements* 70 (2021), pp. 1–13.

[163] R. Mohammadi and Q. He. “A deep reinforcement learning approach for rail renewal and maintenance planning”. In: *Reliability Engineering System Safety* 225 (2022). 108615.

[164] A. Thelen, X. Zhang, O. Fink, Y. Lu, S. Ghosh, B. D. Youn, M. D. Todd, S. Mahadevan, C. Hu, and Z. Hu. “A comprehensive review of digital twin - part 1: modeling and twinning enabling technologies”. In: *Structural and Multidisciplinary Optimization* 65 (12 2022). 354.

[165] N. M. Levine, Y. Narazaki, and B. F. Spencer. “Development of a building information model-guided post-earthquake building inspection framework using 3D synthetic environments”. In: *Earthquake Engineering and Engineering Vibration* (2023).

[166] M. Kor, I. Yitmen, and S. Alizadehsalehi. “An investigation for integration of deep learning and digital twins towards Construction 4.0”. In: *Smart and Sustainable Built Environment* 12.3 (2023), pp. 461–487.

[167] N. O. Attoh-Okine. *Big Data and Differential Privacy: Analysis Strategies for Railway Track Engineering*. John Wiley & Sons, 2017.

[168] S. Gulcimen, E. K. Aydogan, and N. Uzal. “Life cycle sustainability assessment of a light rail transit system: Integration of environmental, economic, and social impacts”. In: *Integrated Environmental Assessment and Management* 17.5 (2021), pp. 1070–1082.

[169] D. Yurlov, A. M. Zarembski, N. Attoh-Okine, J. W. Palese, and H. Thompson. “Probabilistic Approach for Development of Track Geometry Defects as a Function of Ground Penetrating Radar Measurements”. In: *Transportation Infrastructure Geotechnology* 6 (2019), pp. 1–20.

[170] M. O. Adeagbo, H.-F. Lam, and Y. Q. Ni. “A Bayesian methodology for detection of railway ballast damage using the modified Ludwik nonlinear model”. In: *Engineering Structures* 236 (2021). 112047.

[171] A. Vaswani, N. Shazeer, N. Parmar, J. Uszkoreit, L. Jones, A. N. Gomez, L. Kaiser, and I. Polosukhin. “Attention Is All You Need”. In: *arXiv preprint arXiv:1706.03762* (2017).

[172] Y. Bai, J. Mei, A. Yuille, and C. Xie. “Are transformers more robust than CNNs?” In: *arXiv preprint arXiv:2111.05464* (2021).

[173] W. Fedus, B. Zoph, and N. Shazeer. “Switch Transformers: Scaling to Trillion Parameter Models with Simple and Efficient Sparsity”. In: *Journal of Machine Learning Research* 23 (2022), pp. 1–40.

[174] Z. Su, A. Jamshidi, A. Núñez, S. Baldi, and B. D. Schutter. “Multi-level condition-based maintenance planning for railway infrastructures – A scenario-based chance-constrained approach”. In: *Transportation Research Part C: Emerging technologies* 84 (2017), pp. 92–123.

[175] Z. Su, A. Jamshidi, A. Núñez, S. Baldi, and B. D. Schutter. “Integrated condition-based track maintenance planning and crew scheduling of railway networks”. In: *Transportation Research Part C: Emerging technologies* 105 (2019), pp. 359–384.

[176] H. Zhu, H. Li, A. Al-Juboori, D. Wexler, C. Lu, A. McCusker, J. McLeod, S. Pannila, and J. Barnes. “Understanding and treatment of squat defects in a railway network”. In: *Wear* 442-443 (2020), p. 203139.

[177] Z. Song, T. Yamada, H. Shitara, and Y. Takemura. “Detection of damage and crack in railhead by using eddy current testing”. In: *Electromagnetic Analysis and Applications* 3 (2011), pp. 546–550.

[178] P. Liu, S. Liu, C. Yu, L. Gu, Y. Zhou, C. Zhao, and Z. Huang. “Quantitative evaluation of the rotational stiffness of rail cracks based on the reflection of guided waves”. In: *Intelligent Transportation Infrastructure* 1 (2022). liac008.

[179] S. Faghih-Roohi, S. Hajizadeh, A. Núñez, R. Babuska, and B. D. Schutter. “Deep Convolutional Neural Networks for Detection of Rail Surface Defects”. In: *In Proceedings of the international joint conference on neural networks* 2016 (2016), pp. 2584–2589.

[180] A. Jamshidi, S. Hajizadeh, Z. Su, M. Naeimi, A. Núñez, R. Dollevoet, B. D. Schutter, and Z. Li. “A decision support approach for condition-based maintenance of rails based on big data analysis”. In: *Transportation Research Part C: Emerging Technologies* 95 (2018), pp. 185–206.

[181] Z. Yuan, S. Zhu, C. Chang, X. Yuan, Q. Zhang, and W. Zhai. “An unsupervised method based on convolutional variational auto-encoder and anomaly detection algorithms for light rail squat localization”. In: *Construction and Building Materials* 313 (2021), p. 125563.

[182] W. Maass. “Networks of spiking neurons: The third generation of neural network models”. In: *Neural Networks* 10 (1997), pp. 1659–1671.

[183] B. Chandra and K. Naresh Babu. “Classification of gene expression data using Spiking Wavelet Radial Basis Neural Network”. In: *Expert Systems with Applications* 41 (2014), pp. 1326–1330.

[184] H. Shao, H. Jiang, H. Zhang, W. Duan, T. Liang, and S. Wu. “Rolling bearing fault feature learning using improved convolutional deep belief network with compressed sensing”. In: *Mechanical Systems and Signal Processing* 100 (2018), pp. 743–765.

[185] C. D. Virgilio G., J. H. Sossa A., J. M. Antelis, and L. E. Falcón. “Spiking Neural Networks applied to the classification of motor tasks in EEG signals”. In: *Neural Networks* 122 (2020), pp. 130–143.

[186] C. Tan, M. Šarlija, and N. Kasabov. “NeuroSense: Short-term emotion recognition and understanding based on spiking neural network modelling of spatio-temporal EEG patterns”. In: *Neurocomputing* 434 (2021), pp. 137–148.

[187] Z. Yan, J. Zhou, and W. F. Wong. “Energy efficient ECG classification with spiking neural network”. In: *Biomedical Signal Processing and Control* 63 (2021), p. 102170.

[188] L. Zuo, L. Zhang, Z. H. Zhang, X. L. Luo, and Y. Liu. “A spiking neural network-based approach to bearing fault diagnosis”. In: *Manufacturing Systems* 61 (2021), pp. 714–724.

[189] R. E. Turkson, H. Qu, C. B. Mawuli, and M. J. Eghan. “Classifcation of Alzheimer’s Disease Using Deep Convolutional Spiking Neural Network”. In: *Neural Processing Letters* 53 (2021), pp. 2649–2663.

[190] L. Guo, Q. Zhao, Y. Wu, and G. Xu. “Small-world spiking neural network with anti-interference ability based on speech recognition under interference”. In: *Applied Soft Computing* 130 (2022), p. 109645.

[191] A. Solairaj, G. Sugitha, and G. Kavitha. “Enhanced Elman spike neural network based sentiment analysis of online product recommendation”. In: *Applied Soft Computing* 132 (2023), p. 109789.

[192] S. M. Bohte, J. N. Kok, and H. L. Poutré. “Error-backpropagation in temporally encoded networks of spiking neurons”. In: *Neurocomputing* 48 (2002), pp. 17–37.

[193] O. Booij and H. T. Nguyen. “A gradient descent rule for multiple spiking neurons emitting multiple spikes”. In: *Information Processing Letters* 95 (2005), pp. 552–558.

[194] R. Gütig and H. Sompolinsky. “The tempotron: a neuron that learns spike timing-based decisions”. In: *Nature Neuroscience* 9 (2006), pp. 420–428.

[195] S. Ghosh-Dastidar and H. Adeli. “A new supervised learning algorithm for multiple spiking neural networks with application in epilepsy and seizure detection”. In: *Neural Networks* 22 (2009), pp. 1419–1431.

[196] J. J. Wade, L. J. McDaid, J. A. Santos, and H. M. Sayers. “SWAT: A Spiking Neural Network Training Algorithm for Classification Problems”. In: *IEEE Transactions on neural networks* 21 (2010), pp. 1817–1830.

[197] F. Ponulak and A. Kasiński. “Supervised learning in spiking neural networks with ReSuMe: sequence learning, classification, and spike shifting”. In: *Neural Computing* 22 (2010), pp. 467–510.

[198] A. Jeyasothy, S. Sundaram, and N. Sundararajan. “SEFRON: A New Spiking Neuron Model With Time-Varying Synaptic Efficacy Function for Pattern Classification”. In: *IEEE Transactions on Neural Networks and Learning Systems* 30 (2019), pp. 1231–1240.

[199] I. Hussain and D. M. Thounaojam. “WOLIF: An efficiently tuned classifier that learns to classify non-linear temporal patterns without hidden layers”. In: *Applied Intelligence* 51 (2021), pp. 2173–2187.

[200] Z. Li, X. Zhaoa, C. Esvelda, R. Dollevoet, and M. Molodova. “An investigation into the causes of squats—Correlation analysis and numerical modeling”. In: *Wear* 265 (2008), pp. 1349–1355.

[201] F. Ponulak and A. Kasinski. “Introduction to spiking neural networks: Information processing, learning and applications”. In: *Acta Neurobiologiae Experimentalis* 71 (2011), pp. 409–433.

[202] E. M. Izhikevich. “Which Model to Use for Cortical Spiking Neurons?” In: *IEEE Transactions on Neural Networks* 15 (2004), pp. 1–8.

[203] G. Indiveri and S.-C. Liu. “Memory and Information Processing in Neuromorphic Systems”. In: *Proceedings of the IEEE* 103 (2015), pp. 1379–1397.

[204] P. A. Merolla, J. V. Arthur, R. Alvarez-Icaza, A. S. Cassidy, J. Sawada, F. Akopyan, B. L. Jackson, N. Imam, C. Guo, Y. Nakamura, B. Brezzo, I. Vo, S. K. Esser, R. Appuswamy, B. Taba, A. Amir, M. D. Flickner, W. P. Risk, R. Manohar, and D. S. Modha. “A million spiking-neuron integrated circuit with a scalable communication network and interface”. In: *Science* 345 (2014), pp. 668–673.

[205] S. Dora, S. Sundaram, and N. Sundararajan. “An Interclass Margin Maximization Learning Algorithm for Evolving Spiking Neural Network”. In: *IEEE Transaction on Cybernetics* 49 (2019), pp. 989–999.

[206] Q. Zhou, C. Ren, and S. Qi. “An Imbalanced R-STDP Learning Rule in Spiking Neural Networks for Medical Image Classification”. In: *IEEE Access* 8 (2020), pp. 224162–224177.

[207] P. Werbos. “Backpropagation through time: what it does and how to do it”. In: *Proceedings of the IEEE* 78 (1990), pp. 1550–1560.

[208] B. Schrauwen and J. Van Campenhout. “Extending SpikeProp”. In: *2004 IEEE International Joint Conference on Neural Networks (IEEE Cat. No.04CH37541)*. Vol. 1. 2004, pp. 471–475.

[209] S. M. Silva and A. E. Ruano. “Application of Levenberg-Marquardt method to the training of spiking neural networks”. In: *2005 International Conference on Neural Networks and Brain*. Vol. 3. 2005, pp. 1354–1358.

[210] S. McKennoch, D. Liu, and L. G. Bushnell. “Fast modifications of the SpikeProp algorithm.” In: *In Proceedings of the international joint conference on neural networks* (2006), pp. 3970–3977.

[211] S. Ghosh-Dastidar and H. Adeli. “Improved spiking neural networks for EEG classification and epilepsy and seizure detection”. In: *Integrated Computer-Aided Engineering* 14 (2007), pp. 187–212.

[212] J. Lee, T. Delbruck, and M. Pfeiffer. “Training Deep Spiking Neural Networks Using Backpropagation”. In: *Frontiers in Neuroscience* 10 (2016), p. 508.

[213] H. A. Mallot. *Coding and representation*. Vol. 2, Berlin, Germany: Springer. 2013, pp. 743–765.

[214] C. Koch and I. Segev. *Methods in neuronal modeling: from ions to networks*. MIT press, 1998.

[215] J. Ceccarini, H. Liu, K. Van Laere, E. D. Morris, and C. Y. Sander. “Methods for Quantifying Neurotransmitter Dynamics in the Living Brain With PET Imaging”. In: *Frontiers in Physiology* 11 (2020), pp. 1–8.

[216] T. Wang, L. Yin, X. Zou, Y. Shu, M. J. Rasch, and S. Wu. “A Phenomenological Synapse Model for Asynchronous Neurotransmitter Release”. In: *Frontiers in Computational Neuroscience* 9 (2016), pp. 1–15.

[217] D. Dua and C. Graff. *UCI Machine Learning Repository*. 2017. URL: http://archive.ics.uci.edu/ml.

[218] A. Jeyasothy, S. Ramasamy, and S. Sundaram. “Meta-neuron learning based spiking neural classifier with time-varying weight model for credit scoring problem”. In: *Expert Systems With Applications* 178 (2021). 114985, pp. 1–12.

[219] X. Zhang, D. Jiang, T. Han, N. Wang, W. Yang, and Y. Yang. “Rotating Machinery Fault Diagnosis for Imbalanced Data Based on Fast Clustering Algorithm and Support Vector Machine”. In: *Sensors* 2017 (2017), p. 8092691.

[220] W. Jianan, H. Haisong, Y. Liguo, H. Yao, F. Qingsong, and H. Dong. “New imbalanced fault diagnosis framework based on Cluster-MWMOTE and MFO-optimized LS-SVM using limited and complex bearing data”. In: *Engineering Applications of Artificial Intelligence* 96 (2021), p. 103966.

[221] M. Li, Y. Wang, and C. Wei. “Intelligent Fault Diagnosis of Machines Based on Adaptive Transfer Density Peaks Search Clustering”. In: *Shock and Vibration* 2021 (2021), p. 9936080.

[222] Y. Wang, M. Han, and Y. Wu. “Semi-supervised Fault Diagnosis Model Based on Improved Fuzzy C-means Clustering and Convolutional Neural Network”. In: *IOP Conf. Series: Materials Science and Engineering* 1043 (2021), p. 052043.

[223] A. Islam, S. B. Belhaouari, A. U. Rehman, and H. Bensmail. “KNNOR: An oversampling technique for imbalanced datasets”. In: *Applied Soft Computing* 115 (2022), p. 108288.

[224] S. Maldonado, J. López, and C. Vairetti. “An alternative SMOTE oversampling strategy for high-dimensional datasets”. In: *Applied Soft Computing* 76 (2019), pp. 380–389.

[225] L. Han, C. Yu, C. Liu, Y. Qin, and S. Cui. “Fault diagnosis of rolling bearings in rail train based on exponential smoothing predictive segmentation and improved ensemble learning algorithm”. In: *Applied Sciences* 9.15 (2019), p. 3143.

[226] Y. Cao, Z. Zhou, C. Hu, W. He, and S. Tang. “On the Interpretability of Belief Rule-Based Expert Systems”. In: *IEEE Transactions on Fuzzy Systems* 29 (2021), pp. 3489–3503.

[227] A. Jeyasothy, S. Suresh, S. Ramasamy, and N. Sundararajan. “Development of a Novel Transformation of Spiking Neural Classifier to an Interpretable Classifier”. In: *IEEE Transactions on Cybernetics* (2022), pp. 1–10.

[228] S. Buijsman. *Defining Explanation and Explanatory Depth in XAI*. Minds Machines 32, 2022, pp. 563–584.

[229] J. Brownjohn, A. De Stefano, Y. Xu, H. Wenzel, and A. Aktan. “Vibration-based monitoring of civil infrastructure: challenges and successes”. In: *Journal of Civil Structural Health Monitoring* 1 (2011), pp. 79–95.

[230] D. Goyal and B. S. Pabla. “The vibration monitoring methods and signal processing techniques for structural health monitoring: a review”. In: *Archives of Computational Methods in Engineering* 23 (2016), pp. 585–594.

[231] S. Khan, S. Atamturktur, M. Chowdhury, and M. Rahman. “Integration of Structural Health Monitoring and Intelligent Transportation Systems for Bridge Condition Assessment: Current Status and Future Direction”. In: *IEEE Transactions on Intelligent Transportation Systems* 17 (2016), pp. 2107–2122.

[232] C.-H. Ho, M. Snyder, and D. Zhang. “Application of vehicle-based sensing technology in monitoring vibration response of pavement conditions”. In: *Journal of Transportation Engineering, Part B: Pavements* 146 (2020).

[233] I. Celiński, R. Burdzik, J. Młyńczak, and M. Kłaczyński. “Research on the applicability of vibration signals for real-time train and track condition monitoring”. In: *Sensors* 22 (2022).

[234] J. Castillo-Mingorance, M. Sol-Sánchez, F. Moreno-Navarro, and M. Rubio-Gámez. “A critical review of sensors for the continuous monitoring of smart and sustainable railway infrastructures”. In: *Sustainability* 12 (2020).

[235] V. Hodge, S. O’Keefe, M. Weeks, and A. Moulds. “Wireless sensor networks for condition monitoring in the railway industry: A survey”. In: *IEEE Transactions on intelligent transportation systems* 16 (2014), pp. 1088–1106.

[236] Y. Zeng, C. Shen, A. Núñez, R. Dollevoet, W. Zhang, and Z. Li. “An interpretable method for operational modal analysis in time-frequency representation and its applications to railway sleepers”. In: *Structural Control and Health Monitoring* (2023).

[237] J. Zhang, W. Huang, W. Zhang, F. Li, and Y. Du. “Train-induced vibration monitoring of track slab under long-term temperature load using fiber-optic accelerometers”. In: *Sensors* 21 (2021).

[238] G. Guo, X. Cui, and B. Du. “Random-forest machine learning approach for high-speed railway track slab deformation identification using track-side vibration monitoring”. In: *Applied Sciences* 11 (2021).

[239] I. La Paglia, M. Carnevale, R. Corradi, E. Di Gialleonardo, A. Facchinetti, and S. Lisi. “Condition monitoring of vertical track alignment by bogie acceleration measurements on commercial high-speed vehicles”. In: *Mechanical Systems and Signal Processing* 186 (2023), p. 109869.

[240] H. Jiang and J. Lin. “Fault Diagnosis of Wheel Flat Using Empirical Mode Decomposition-Hilbert Envelope Spectrum”. In: *Mathematical Problems in Engineering* 2018 (2018), pp. 1–16.

[241] C. Hoelzl, G. Arcieri, L. Ancu, S. Banaszak, A. Kollros, V. Dertimanis, and E. Chatzi. “Fusing Expert Knowledge with Monitoring Data for Condition Assessment of Railway Welds”. In: *Sensors* 23.5 (2023), pp. 1–31.

[242] N. Traquinho, C. Vale, D. Ribeiro, A. Meixedo, P. Montenegro, A. Mosleh, and R. Calçada. “Damage Identification for Railway Tracks Using Onboard Monitoring Systems in In-Service Vehicles and Data Science”. In: *Machines* 11.10 (2023).

[243] A. De Rosa, S. Alfi, and S. Bruni. “Estimation of lateral and cross alignment in a railway track based on vehicle dynamics measurements”. In: *Mechanical Systems and Signal Processing* 116 (2019), pp. 606–623.

[244] Y. Zeng, A. Núñez, and Z. Li. “Railway sleeper vibration measurement by train-borne laser Doppler vibrometer and its speed-dependent characteristics”. In: *Computer-Aided Civil and Infrastructure Engineering* (2024).

[245] C. Yang, K. Kaynardag, and S. Salamone. “Missing Rail Fastener Detection Based on Laser Doppler Vibrometer Measurements”. In: *Journal of Nondestructive Evaluation* (2023).

[246] K. Kaynardag, C. Yang, and S. Salamone. “A rail defect detection system based on laser Doppler vibrometer measurements”. In: *NDT and E International* (2023).

[247] A. Rodríguez, R. Sañudo, M. Miranda, A. Gómez, and J. Benavente. “Smartphones and tablets applications in railways, ride comfort and track quality. Transition zones analysis”. In: *Measurement* 182 (2021), p. 109644.

[248] A. Azzoug and S. Kaewunruen. “RideComfort: A Development of Crowdsourcing Smartphones in Measuring Train Ride Quality”. In: *Frontiers in Built Environment* 3 (2017).

[249] Y. Zeng, A. Núñez, and Z. Li. “Speckle noise reduction for structural vibration measurement with laser Doppler vibrometer on moving platform”. In: *Mechanical Systems and Signal Processing* 178 (2022). 109196, pp. 1–20.

[250] S. Unsiwilai, L. Wang, A. Núñez, and Z. Li. “Multiple-Axle Box Acceleration Measurements at Railway Transition Zones”. In: *Measurement* 213 (2023). 112688, pp. 1–21.

[251] S. Dong, W. Wu, K. He, and X. Mou. “Rolling bearing performance degradation assessment based on improved convolutional neural network with anti-interference”. In: *Measurement* 151 (2020), p. 107219.

[252] F. Jia, Y. Lei, S. Xing, and J. Lin. “A method of automatic feature extraction from massive vibration signals of machines”. In: *2016 IEEE International Instrumentation and Measurement Technology Conference Proceedings*. 2016, pp. 1–6.

[253] K. Maes, L. Van Meerbeeck, E. Reynders, and G. Lombaert. “Validation of vibration-based structural health monitoring on retrofitted railway bridge KW51”. In: *Mechanical Systems and Signal Processing* 165 (2022), p. 108380.

[254] Z. Wei, D. He, Z. Jin, B. Liu, S. Shan, Y. Chen, and J. Miao. “Density-Based Affinity Propagation Tensor Clustering for Intelligent Fault Diagnosis of Train Bogie Bearing”. In: *IEEE Transactions on Intelligent Transportation Systems* 24.6 (2023), pp. 6053–6064.

[255] R. Ghiasi, M. A. Khan, D. Sorrentino, C. Diaine, and A. Malekjafarian. “An unsupervised anomaly detection framework for onboard monitoring of railway track geometrical defects using one-class support vector machine”. In: *Engineering Applications of Artificial Intelligence* 133 (2024). 108167.

[256] Y. Tian, W. Du, and F. Qian. “High dimension feature extraction based visualized SOM fault diagnosis method and its application in p-xylene oxidation process”. In: *Chinese Journal of Chemical Engineering* 23.9 (2015), pp. 1509–1517.

[257] M. Chen, S. Zhu, W. Zhai, Y. Sun, and Q. Zhang. “Inversion and identification of vertical track irregularities considering the differential subgrade settlement based on fully convolutional encoder-decoder network”. In: *Construction and Building Materials* 367 (2023).

[258] G. Michau, G. Frusque, and O. Fink. “Fully learnable deep wavelet transform for unsupervised monitoring of high-frequency time series”. In: *PNAS* 119.8 (2022), pp. 1–10.

[259] S. Li, L. Jin, J. Jiang, H. Wang, Q. Nan, and L. Sun. “Looseness Identification of Track Fasteners Based on Ultra-Weak FBG Sensing Technology and Convolutional Autoencoder Network”. In: *Sensors* 22.15 (2022).

[260] D. Yang and K. Sun. “A CAE-Based Deep Learning Methodology for Rotating Machinery Fault Diagnosis”. In: *2021 7th International Conference on Control, Automation and Robotics (ICCAR)*. 2021, pp. 393–396.

[261] Z. Ye, S. Yue, P. Yang, R. Zhou, and J. Yu. “Deep Morphological Shrinkage Convolutional Autoencoder-Based Feature Learning of Vibration Signals for Gearbox Fault Diagnosis”. In: *IEEE Transactions on Instrumentation and Measurement* 73 (2024), pp. 1–12.

[262] T. Kim and S. Lee. “A Novel Unsupervised Clustering and Domain Adaptation Framework for Rotating Machinery Fault Diagnosis”. In: *IEEE Transactions on Industrial Informatics* 19.9 (2023), pp. 9404–9412.

[263] J. Yu and X. Zhou. “One-Dimensional Residual Convolutional Autoencoder Based Feature Learning for Gearbox Fault Diagnosis”. In: *IEEE Transactions on Industrial Informatics* 16.10 (2020), pp. 6347–6358.

[264] J. Dai, J. Wang, W. Huang, J. Shi, and Z. Zhu. “Machinery Health Monitoring Based on Unsupervised Feature Learning via Generative Adversarial Networks”. In: *IEEE/ASME Transactions on Mechatronics* 25.5 (2020), pp. 2252–2263.

[265] Y. Lei, F. Jia, J. Lin, S. Xing, and S. X. Ding. “An Intelligent Fault Diagnosis Method Using Unsupervised Feature Learning Towards Mechanical Big Data”. In: *IEEE Transactions on Industrial Electronics* 63.5 (2016), pp. 3137–3147.

[266] R. Wang, F. Liu, X. Hu, and J. Chen. “Unsupervised Mechanical Fault Feature Learning Based on Consistency Inference-Constrained Sparse Filtering”. In: *IEEE Access* 8 (2020), pp. 172021–172033.

[267] Q. He, J. Zhao, G. Jiang, and P. Xie. “An Unsupervised Multiview Sparse Filtering Approach for Current-Based Wind Turbine Gearbox Fault Diagnosis”. In: *IEEE Transactions on Instrumentation and Measurement* 69 (2020), pp. 5569–5578.

[268] Y. Ji, J. Zeng, W. Sun, and T. Mazilu. “Research on Wheel-Rail Local Impact Identification Based on Axle Box Acceleration”. In: *Shock and Vibration* 2022 (2022).

[269] N. E. Huang, Z. Shen, S. R. Long, M. L. Wu, H. H. Shih, Q. Zheng, N. C. Yen, C. C. Tung, and H. H. Liu. “The empirical Mode Decomposition and Hilbert spectrum for nonlinear and non-stationary time series analysis”. In: *Proc. Roy. Soc. London A* 454 (1998), pp. 903–995.

[270] P. Flandrin, G. Rilling, and P. Gonçalvés. “Empirical Mode Decomposition as a Filter Bank”. In: *IEEE Signal processing letters* 11.2 (2004), pp. 112–114.

[271] A. Ayenu-Prah, N. Attoh-Okine, and N. E. Huang. “Empirical mode decomposition and the hilbert-huang transform”. In: *Transforms and Applications Handbook, Third Edition* (2010), pp. 20-1-20–11.

[272] X. Wang and A. Gupta. “Unsupervised Learning of Visual Representations Using Videos”. In: *2015 IEEE International Conference on Computer Vision (ICCV)*. 2015, pp. 2794–2802.

[273] J. Masci, U. Meier, D. Cireşan, and t. C. A.-E. f. H. F. E. Schmidhuber Jürgen". In: *Artificial Neural Networks and Machine Learning – ICANN 2011*. Springer Berlin Heidelberg, 2011, pp. 52–59.

[274] R. Wang, S. Han, J. Zhou, Y. Chen, L. Wang, T. Du, K. Ji, Y.-o. Zhao, and K. Zhang. “Transfer-Learning-Based Gaussian Mixture Model for Distributed Clustering”. In: *IEEE Transactions on Cybernetics* 53.11 (2023), pp. 7058–7070.

[275] Z. Wei, A. Núñez, Z. Li, and R. Dollevoet. “Evaluating degradation at railway crossings using axle box acceleration measurements”. In: *Sensors* 17 (2017), p. 2236.

[276] Y. Zeng, A. Núñez, A. Zoeteman, R. Dollevoet, and Z. Li. “Direct Monitoring of In-situ Rail Fastener Vibrations from a Moving Train with Laser Doppler Vibrometer”. In: *under review* ().

[277] B. Coelho, P. Hölscher, J. Priest, W. Powrie, and F. Barends. “An Assessment of Transition Zone Performance”. In: *Proceedings of the Institution of Mechanical Engineers, Part F: Journal of Rail and Rapid Transit* 225.2 (2011), pp. 129–139.

[278] R. Sañudo, I. Jardí, J.-C. Martínez, F.-J. Sánchez, M. Miranda, B. Alonso, L. dell’Olio, and J.-L. Moura. “Monitoring Track Transition Zones in Railways”. In: *Sensors* 22.1 (2022), pp. 1–26.

[279] C. Alves Ribeiro, R. Calçada, and R. Delgado. “Experimental assessment of the dynamic behaviour of the train-track system at a culvert transition zone”. In: *Engineering Structures* 138 (2017), pp. 215–228.

[280] D. Mishra, E. Tutumluer, H. Boler, J. P. Hyslip, and T. R. Sussmann. “Railroad Track Transitions with Multidepth Deflectometers and Strain Gauges”. In: *Transportation Research Record* 2448 (2014), pp. 105–114.

[281] H. Wang, V. Markine, and X. Liu. “Experimental analysis of railway track settlement in transition zones”. In: *Proceedings of the Institution of Mechanical Engineers, Part F: Journal of Rail and Rapid Transit* 232 (2018), pp. 1774–1789.

[282] L. N. Wheeler, E. Pannese, N. A. Hoult, W. A. Take, and H. Le. “Measurement of distributed dynamic rail strains using a Rayleigh backscatter based fiber optic sensor: Lab and field evaluation”. In: *Transportation Geotechnics* 14 (2018), pp. 70–80.

[283] K. Nasrollahi, J. Dijkstra, and J. C. Nielsen. “Towards real-time condition monitoring of a transition zone in a railway structure using fibre Bragg grating sensors”. In: *Transportation Geotechnics* 44 (2024), p. 101166.

[284] K. Nasrollahi, J. C. Nielsen, E. Aggestam, J. Dijkstra, and M. Ekh. “Prediction of long-term differential track settlement in a transition zone using an iterative approach”. In: *Engineering Structures* 283 (2023), p. 115830.

[285] D. F. Hesser, K. Altun, and B. Markert. “Monitoring and tracking of a suspension railway based on data-driven methods applied to inertial measurements”. In: *Mechanical Systems and Signal Processing* 164 (2022), p. 108298.

[286] A. Sabato and C. Niezrecki. “Feasibility of digital image correlation for railroad tie inspection and ballast support assessment”. In: *Measurement* 103 (2017), pp. 93–105.

[287] C. Shen, P. Zhang, R. Dollevoet, A. Zoeteman, and Z. Li. “Evaluating railway track stiffness using axle box accelerations: A digital twin approach”. In: *Mechanical Systems and Signal Processing* 204 (2023). 110730, pp. 1–30.

[288] S. Unsiwilai, C. Shen, Y. Zeng, L. Wang, A. Núñez, and Z. Li. “Vertical dynamic measurements of a railway transition zone: a case study in Sweden”. In: *Journal of Civil Structural Health Monitoring* 236 (2024), pp. 1–18.

[289] Y. Zhu, M. Shuang, D. Sun, and H. Guo. “Algorithm and Application of Foundation Displacement Monitoring of Railway Cable Bridges Based on Satellite Observation Data”. In: *Applied Sciences* 13.5 (2023), pp. 1–16.

[290] Y. Zhu, H. Qiu, P. Cui, Z. Liu, B. Ye, D. Yang, and U. Kamp. “Early detection of potential landslides along high-speed railway lines: A pressing issue”. In: *Earth Surface Processes and Landforms* 48.15 (2023), pp. 3302–3314.

[291] R. Bamler and P. Hartl. “Synthetic aperture radar interferometry”. In: *Inverse Problems* 14.4 (Aug. 1998), R1.

[292] L. Chang, N. P. Sakpal, S. O. Elberink, and H. Wang. “Railway Infrastructure Classification and Instability Identification Using Sentinel-1 SAR and Laser Scanning Data”. In: *Sensors* 20.24 (2020), pp. 1–16.

[293] H. Wang, L. Chang, and V. Markine. “Structural Health Monitoring of Railway Transition Zones Using Satellite Radar Data”. In: *Sensors* 18 (2018).

[294] Y. Honglei, J. Qiao, H. Jianfeng, K. Ki-Yeob, and P. Junhuan. “InSAR measurements of surface deformation over permafrost on Fenghuoshan Mountains section, Qinghai-Tibet Plateau”. In: *Journal of Systems Engineering and Electronics* 32.6 (2021), pp. 1284–1303.

[295] X. Xu, D. Zhao, C. Ma, and D. Lian. “Monitoring Subsidence Deformation of Suzhou Subway Using InSAR Timeseries Analysis”. In: *IEEE Access* 9 (2021), pp. 3400–3416.

[296] M. N. Amir Falamarzi Sara Moridpour and S. Cheraghi. “Prediction of tram track gauge deviation using artificial neural network and support vector regression”. In: *Australian Journal of Civil Engineering* 17.1 (2019), pp. 63–71.

[297] J. S. Lee, S. H. Hwang, I. Y. Choi, and I. K. Kim. “Prediction of Track Deterioration Using Maintenance Data and Machine Learning Schemes”. In: *Journal of Transportation Engineering, Part A: Systems* 144.9 (2018), p. 04018045.

[298] A. Lasisi and N. Attoh-Okine. “Principal components analysis and track quality index: A machine learning approach”. In: *Transportation Research Part C: Emerging Technologies* 91 (2018), pp. 230–248.

[299] A. Falamarzi, S. Moridpour, M. Nazem, and S. Cheraghi. “Development of Random forests regression model to predict track degradation index: Melbourne case study”. In: *Australian transport research forum*. 2018, p. 12.

[300] H. Khajehei, A. Ahmadi, I. Soleimanmeigouni, M. Haddadzade, A. Nissen, and M. J. Latifi Jebelli. “Prediction of track geometry degradation using artificial neural network: A case study”. In: *International Journal of Rail Transportation* 10.1 (2022), pp. 24–43.

[301] S. Tian, L. Tang, T. Li, and X. Ling. “Artificial neural network-based investigation on high-speed train-induced embankment vibration in frozen regions”. In: *Soil Dynamics and Earthquake Engineering* 173 (2023), p. 108093.

[302] C. Li, Q. He, and P. Wang. “Estimation of railway track longitudinal irregularity using vehicle response with information compression and Bayesian deep learning”. In: *Computer-Aided Civil and Infrastructure Engineering* 37.10 (2022), pp. 1260–1276.

[303] L. Han, Y. Liao, H. Wang, and H. Zhang. “Long-term prediction for railway track geometry based on an optimised DNN method”. In: *Construction and Building Materials* 401 (2023), p. 132687.

[304] L. Wen, X. Li, L. Gao, and Y. Zhang. “A New Convolutional Neural Network-Based Data-Driven Fault Diagnosis Method”. In: *IEEE Transactions on Industrial Electronics* 65.7 (2018), pp. 5990–5998.

[305] X. Tang, Z. Chen, X. Cai, and Y. Wang. “Ballastless track arching recognition based on one-dimensional residual convolutional neural network and vehicle response”. In: *Construction and Building Materials* 408 (2023), p. 133624.

[306] S. Zhang, P. Huang, and W. Yan. “A data-driven approach for railway in-train forces monitoring”. In: *Advanced Engineering Informatics* 59 (2024), p. 102258.

[307] V. Shepelev, I. Slobodin, Z. Almetova, D. Nevolin, and A. Shvecov. “A Hybrid Traffic Forecasting Model for Urban Environments Based on Convolutional and Recurrent Neural Networks”. In: *Transportation Research Procedia* 68 (2023). XIII International Conference on Transport Infrastructure: Territory Development and Sustainability, pp. 441–446.

[308] X. Wang, Y. Bai, and X. Liu. “Prediction of railroad track geometry change using a hybrid CNN-LSTM spatial-temporal model”. In: *Advanced Engineering Informatics* 58 (2023), p. 102235.

[309] W. Yu, W. Zhifei, W. Hongye, Z. Junfeng, and F. Ruilong. “Prediction of Passenger Flow Based on CNN-LSTM Hybrid Model”. In: *2019 12th International Symposium on Computational Intelligence and Design (ISCID)*. Vol. 2. 2019, pp. 132–135.

[310] H. Xiao, Z. Chen, R. Cao, Y. Cao, L. Zhao, and Y. Zhao. “Prediction of shield machine posture using the GRU algorithm with adaptive boosting: A case study of Chengdu Subway project”. In: *Transportation Geotechnics* 37 (2022), p. 100837.

[311] J. Scoular. *THE ULTIMATE GUIDE TO USING INSAR*. https://skygeo.com/the-ultimate-guide-to-using-insar.

[312] M. Molodova, M. Oregui, A. Núñez, Z. Li, and R. Dollevoet. “Health condition monitoring of insulated joints based on axle box acceleration measurements”. In: *Engineering Structures* 123 (2016), pp. 225–235.

[313] K. Cho, B. van Merriënboer, C. Gulcehre, D. Bahdanau, F. Bougares, H. Schwenk, and Y. Bengio. “Learning Phrase Representations using RNN Encoder–Decoder for Statistical Machine Translation”. In: *Proceedings of the 2014 Conference on Empirical Methods in Natural Language Processing (EMNLP)*. Oct. 2014, pp. 1724–1734.

[314] *CEN, NEN-EN 13848-6:2014 (E) - Railway applications -Track - Track geometry quality - Part 6: Characterization of track geometry quality*. https://www.nen.nl/nen-en-13848-6-2014-en-194073.

[315] J. Hao and R. Liu. “Prediction for geometric degradation of track on machine learning”. In: *Society of Photo-Optical Instrumentation Engineers (SPIE) Conference Series*. Ed. by S. Easa and W. Wei. Vol. 12790. Society of Photo-Optical Instrumentation Engineers (SPIE) Conference Series. 2023, 127903U.

[316] *CEN, NEN-EN 13848-1:2019 (E) - Railway applications -Track - Track geometry quality - Part 1: Characterization of track geometry*. https://www.nen.nl/en/nen-en-13848-1-2019-en-257518.

[317] http://www.skygeo.com/.

ACKNOWLEDGEMENTS

The pandemic began in 2020, right at the start of my PhD journey. From the outset, it was challenging. Fortunately, I had the support of the following people.

Firstly, I am deeply grateful to my promotor, Prof. Zili Li, for his invaluable guidance and support. Thank you for your feedback, which has been crucial in ensuring the high quality of my work. Receiving compliments from you on my work always feels incredibly rewarding. I look forward to future opportunities to interact with and learn from you more, aspiring to achieve a higher level of success than I am today.

My deepest appreciation goes to my supervisor, Assoc. Prof. Alfredo Núñez Vicencio. I feel incredibly fortunate to have you as my supervisor. You are not only intelligent and extensively knowledgeable, but also kind and supportive. Your enthusiasm for research is truly inspiring. You are always full of ideas, and I thoroughly enjoy our research discussions. I deeply appreciate the time and effort you have invested in helping me navigate challenges and achieve my goals. You also care about my well-being, always checking to ensure I am doing well academically and emotionally. Working under your supervision has been an enriching experience, I look forward to future opportunities to work with you again.

I am grateful for the financial support provided by the Royal Thai government, and the Office of Educational Affairs, Royal Thai Embassy in Paris for their administrative support during my PhD. I would also like to express my gratitude to Dr. Ekkarat Viyanit for believing in me and offering me the opportunity to acquire advanced knowledge in rail and modern transportation technologies. With this support, I aim to improve and enhance Thailand's railway system. I look forward to applying the knowledge gained during my PhD to benefit and advance my home country.

I would like to thank my colleagues in the Railway Engineering section, Omid Hajizad, my very first friend in the Netherlands and former office mate, for the interesting and enjoyable conversations we shared. I am also grateful to my current office mates, Xinxin Yu and Pan Zhang, for the pleasant coffee and lunch breaks, knowledge sharing, and discussions. Thank you to Taniya Kapoor for the nice souvenirs from India, Siwarak Unsiwilai, Shashanka Katta, Nikhil Manakshya, Longge Su, and Chen Shen for the enjoyable coffee and lunch conversations. I appreciate Jurjen Hendriks, our ABA expert, and Yuanchen Zeng for their support and contributions to my research. Thank you, Jacqueline Barnhoorn and Ellard Groenewegen, for your assistance during my study. Also, I extend my thanks to all the other colleagues in the building with whom I have shared conversations in the corridor and at the coffee machine. Interactions with you have been a nice experience.

I would like to extend special thanks to Siwarak Unsiwilai and P'Malee for their

help before and after my departure to the Netherlands. I still remember our first day there – P'Malee had prepared lunch for us, knowing we'd be busy and hungry after shopping for essentials. Siwarak, your companionship and support have been indispensable throughout my study here. Thank you both for your kindness, support, and assistance.

My appreciation goes to two special friends, Masja and Termeh. Termeh, my dearest Iranian friend, you have transformed my Friday nights from dull to delightful. I enjoy our conversations and the moments we've shared over coffee and wine. I still cherish our nights in Cologne, enjoying each other's company and "the jazz club". Masja, my dearest Dutch friend, your warmth and generosity have made my time in the Netherlands truly unforgettable. You've introduced me to local/musical events, and you've been a constant source of support, especially during challenging times. The trip to Groningen with you was special to me. Spending time with both of you has been incredibly memorable and special, filled with fun, laughter, and joy.

I would like to express my heartfelt gratitude to my friends in Thailand, P'Punn, Top, May, P'Bee, P'Kaew, Kru Magmum, Pat, and P'Jig, for their emotional support. Even though we don't talk as often as we used to, you are always there when I need you. Special thanks to P'Bee, P'Kaew, Pat, and Kru Magmum for "kidnapping" me from time to time, allowing me to recharge my life battery. I am also deeply grateful to May and P'Punn for standing by me through all my ups and downs.

Lastly, and most importantly, I am deeply grateful to Martin, my beloved husband and the cornerstone of my success. Your sacrifices go far beyond what I ever imagined. Without you, this journey would be much more difficult. Floriana flower, my cherished daughter, you are the light of my life; your kisses rejuvenate me whenever I feel exhausted from work. To brother, thank you for taking good care of our parents while I'm away. To parents, thank you for your endless love and support.

Curriculum Vitæ

Wassamon Phusakulkajorn

08-10-1984 Born in Songkla, Thailand.

Education

2020 – 2024	Ph.D. (Railway Engineering) Delft University of Technology, The Netherlands
2010 – 2012	MPhil (Applied Mathematics) University of Manchester, UK
2007 – 2010	M.Sc. (Computational Science) Chulalongkorn University, Thailand
2004 – 2007	B.Sc. (Mathematics, First class honour) Prince of Songkla University, Thailand

Employment

2024 – present	Post-doctoral researcher (Railway Engineering) Delft University of Technology, The Netherlands
2018 – present	Senior research assistant National Metal and Materials Technology Center, Thailand
2013 – 2017	Research assistant National Metal and Materials Technology Center, Thailand

Awards

2024	Best Paper Award for "Artificial Intelligence in Railway Infrastructure: Current Research, Challenges, and Future Opportunities" from Intelligent Transportation Infrastructure, Oxford University Press
2010	Academic Excellence from the Professor Dr. Tab Nilanidhi Foundation, Thailand
2006	Outstanding Student with a High GPA from Prince of Songkla University, Thailand

LIST OF PUBLICATIONS

Thesis-related publications:

6. **Phusakulkajorn, W.**, Zeng, Y., Li, Z., Núñez, A., *Unsupervised Representation Learning for Monitoring Rail Infrastructures with High-Frequency Moving Vibration Sensors*, under review.

5. **Phusakulkajorn, W.**, Unsiwilai, S., Chang, L., Núñez, A., Li, Z., *A Hybrid Neural Model Approach for Health Assessment of Railway Transition Zones with Multiple Data Sources*, under review.

4. **Phusakulkajorn, W.**, Hendriks, J.M., Li, Z., Núñez, A., *Spiking Neural Network with Time-Varying Weights for Rail Squat Detection*, 2024, under review.

3. **Phusakulkajorn, W.**, Hendriks, J.M., Moraal, J., Shen, C., Zeng, Y., Unsiwilai, S., Bogojevic, B., Asplund, M., Zoeteman, A., Núñez, A., Dollevoet, R.P.B.J., Li, Z., *Detection of Rail Surface Defects based on Axle Box Acceleration Measurements: A Measurement Campaign in Sweden*, Transport Research Arena (TRA), Dublin, Ireland 2024, pp. 1–6, 2024.

2. **Phusakulkajorn, W.**, Núñez, A., Wang, H., Jamshidi, A., Zoeteman, A., Ripke, B., Dollevoet, R.P.B.J., Schutter, B.D., Li, Z., *Artificial intelligence in railway infrastructure: Current research, challenges, and future opportunities*, Intelligent Transportation Infrastructure, liad016, pp. 1–24, 2023.

1. **Phusakulkajorn, W.**, Hendriks, J.M., Moraal, J., Dollevoet, R.P.B.J., Li, Z., Núñez, A., *A multiple spiking neural network architecture based on fuzzy intervals for anomaly detection: a case study of rail defects*, IEEE International Conference on Fuzzy Systems (FUZZ-IEEE), Padua, Italy 2022, pp. 1–8, 2022.

Other publications:

9. **Phusakulkajorn, W.**, Hendriks, J.M., Moraal, J., Shen, C., Zeng, Y., Unsiwilai, S., Bogojevic, B., Asplund, M., Zoeteman, A., Núñez, A., Dollevoet, R.P.B.J., Li, Z., *Detection of Rail Surface Defects based on Axle Box Acceleration Measurements*, In2Track3: Concluding Technical Report. Edlund, P. & Ekberg, A. (eds.). In2Track3, pp. 167-169, 2024.

8. Unsiwilai, S., **Phusakulkajorn, W.**, Shen, C., Zoeteman, A., Dollevoet, R., Núñez, A., and Li, Z., *Enhanced Vertical Railway Track Quality Index with Dynamic Responses from Moving Trains*, Heliyon, p. e38670, 2024.

7. Wang, L., Shen, C., Unsiwilai, S., **Phusakulkajorn, W.**, Zeng, Y., Hendriks, J.M., Moraal, J., Núñez, A., Zoeteman, A., Dollevoet, R., and Li, Z., *Sleeper support condition monitoring using axle box acceleration measurement*, the 3rd International Conference on Rail Transportation (ICRT2024), 7-9 August, Shanghai, China, 2024.

6. **Phusakulkajorn, W.**, Tapracharoen, K., Otarawanna, S., *Suitable combination of a mean-stress correction method and a stress type for the fatigue analysis of aluminium alloy wheels under radial loading*, International Journal of Materials and Product Technology (IJMPT), Vol. 61, No. 1, 2020.

5. **Phusakulkajorn, W.**, Uttamung, P., Srisawat, F., Tanprayoon, D., and Palsson, N. S., *Corrosion Depth Prediction of an Onshore Gas Pipeline by Using Artificial Neural Network*, The 23rd International Annual Symposium on Computational Science and Engineering, 2019.

4. **Phusakulkajorn, W.**, Benyajati, C., Phraewphiphat, T., and Mongkoltanatas, J., *The Wavelet-based Artificial Neural Network for State of Charge Estimation in Lithium Ion Battery: its Reliability and Adaptability*, The 31st International Electric Vehicles Symposium & Exhibition (EVS 31) & International Electric Vehicle Technology Conference (EVTeC), pp. D3-3., 2018.

3. **Phusakulkajorn, W.**, Benyajati, C., Phraewphiphat, T., and Mongkoltanatas, J., *The Wavelet-based Artificial Neural Network for State of Charge Estimation in Lithium Ion Battery*, International Conference on Mechanical Engineering: conference series proceeding, pp. 363-375, 2017.

2. **Phusakulkajorn, W.**, Naewngerndee, R., Sucharitpwatskul, S., Malatip, A., and Otarawanna, S., *Fatigue Analysis of an Aluminium Alloy Wheel in the Dynamic Radial Fatigue Test by Using Finite Element Analysis*, International journal of fracture, fatigue, and wear: conference series proceeding, vol. 4, pp. 139 - 145, 2016.

1. **Phusakulkajorn, W.**, Lursinsap, C., Asavanant, J., *Wavelet-Transform Based Artificial Neural Network for Daily Rainfall Prediction in Southern Thailand*, IEEE conference proceeding on Communications and Information Technologies 2009 (ISCIT2009), pp. 432 - 437, September, 2009